THÈSE POUR OBTENIR LE GRADE DE DOCTEUR
DE L'UNIVERSITE DE MONTPELLIER

École doctorale : Information, Structures, Systèmes

Unités de recherche UMR AMAP, UMR PHIM

Interactions between pest attacks and plant growth using a model approach applied to Robusta coffee in Uganda. Effects on production

Présentée par Houssem TRIKI

Le 8 juillet 2025

Sous la direction de Marc Jaeger
Et l'encadrement de Fabienne Ribeyre et Fabrice Pinard

Devant le jury composé de

Jacques Gignoux, DR CNRS, Sorbonne Université, IEES Paris,	Rapporteur
Jean-Noël Aubertot, DR, INRAE - UMR AGIR,	Rapporteur
Véronique Letort Le Chevalier, MCF, Centrale-Supélec, MICS,	Examinatrice
David Hill, PR, Université Clermont Auvergne, CNRS, LIMOS,	Examinateur
Fabienne Ribeyre, CR, CIRAD/UMR PHIM,	Co-encadrante
Marc Jaeger, DR, CIRAD/ UMR AMAP,	Directeur de thèse

UNIVERSITÉ DE MONTPELLIER

Acknowledgements

Funding: This work is part of the EU (European Union) Desira Robust project, supported by EU FOOD/2021/427-759/DESIRA. It is also supported by a CIRAD Bios department PhD grant and French National Research Agency under the Investments for the Future Program, referred as ANR-16-CONV-0004/#DigitAg programs.

Table of contents

Acknowledgements ..... **II**

Résumé version française ..... **VII**

Summary: ..... **XIV**

Résumé: ..... **XV**

General Introduction **1**

1. Context 1
2. Modeling interactions with plant growth models 2
3. Modeling interactions on Coffea in the Uganda context 2
4. Modeling considerations 3

4.1. Coffee tree (and plant) growth modeling 3

4.2. The GreenLab model 4

4.3. Application on the coffee tree 4

4.4. Pest & disease modeling 6

5. Scientific Problematic and Modeling Challenges 7
6. Advancing Coffee P&D Modeling: From Isolated Processes to Coupled Interactions 8
7. References 10

Chapter 1: Coupling Plant and Pest Models: Conceptual Foundations and the MIMIC Framework **20**

1. Introduction 20

Chapter 2: Towards a Modular Framework for Pest and Disease Dynamics **37**

1. Introduction 37
2. Coffee Berry Borer (CBB) 39

2.1. Life Cycle 39

2.2. Dispersion 39

2.3. Economic Impact 39

2.4. Management 40

3. Black Coffee Twig Borer (BCTB) 40

3.1. Symptoms and Damage 40

3.2. Life Cycle 40

3.3. Dispersion 40

3.4. Economic Impact 41

3.5. Management 41

4. Red Blister Disease (RBD) 41

4.1. Symptoms and Damage 41

4.2. Life Cycle 42

4.3. Dispersion 42
4.4. Economic Impact 42
4.5. Management 42
5. Model-Oriented Similarities Among Pests 43
6. Modeling Principles 45
6.1. Knowledge base modeling 45
7. Disease 46
8. Generalised model (Plant's Pests) 47
9. Generalised Model for Coffee Berry Borer (CBB) 50
10. Pest Cohorts 53
11. Discussion and Conclusion 58
12. Implementation of the pest generalised model 61
13. References 64
Chapter 3: Plant Growth Modeling: A Cohort-Based GreenLab Approach 74
1. Plant architecture and notions of botany 74
2. Modeling and implementing the architectural concepts 77
3. Eco-physiological principles and structure for modeling 80
4. Crop and FSPM Models 82
5. Cohort-based models: the GreenLab example and its interest 82
6. Challenges and Issues in Integrating Plant Health 83
7. Our proposal 84
8. Plant structure and cohort 85
8.1. Reminder: phytomeres, automata, and organogenesis 86
8.2. Plant organogenesis 86
8.3. Limitations of this formalism 88
9. New phytomere (microstates) definition 89
10. New structural operators 90
11. Plant function 96
11.1. Reminders 96
12. Tuning GreenLab for wide-use interactions (Arts and Crafts for interaction) 99
13. Discussion 103
14. Implementation 104
15. References 109
Chapter 4: Field Protocols, Data Collection, and Model Parameterisation 119
1. Introduction 119
2. Field protocol 119

3. Data Overview, Dynamics and Analytical Insights 121
3.1. Pest Interaction Experiment (P&I) 121
3.2. Contamination and Physiology (C&P) 125
3.3. Tree Architecture (TA) 128
3.4. Harvest Weight Tracking (HWT) 129
4. Data-based parameter estimation for the CBB model 130
5. Discussion and conclusion 135
Chapter 5: Simulating Plant Pest Interactions: Evaluation and Validation 139
1. Introduction 139
2. Results of the Plant Model 139
2.1. Healthy plant (Stable case) 139
2.2. Non-healthy plant (Stable case) 144
3. Results of the generalised model CBB version 148
3.1. Predictions of the model 148
3.2. Validation of the simulation results 151
Discussion 160
Conclusion 168
Figures Table 170

Résumé version française

Introduction

Tout comme de nombreuses cultures pérennes, la production agronomique est confrontée à des enjeux multiples qui résultent de l'interaction entre la croissance des plantes et la pression des ravageurs et maladies, en particulier sous les tropiques, et c'est spécifiquement le cas pour le caféier (Gaitan et al, 2016a, 2016b, 2016c). Alors que la modélisation des plantes et cultures est devenue un outil incontournable pour la compréhension et la gestion des systèmes de production agronomiques, il subsiste une déconnexion forte entre les modèles de plante et les modèles de dynamiques de population de ravageurs, et ne peut estimer la production à moyen long terme. Cette dissociation empêche en effet de représenter correctement les effets réciproques entre le développement végétal et les attaques biotiques, rendant difficile toute prévision fiable ou la conception de stratégies de gestion durables.

Cette thèse, soutenue par le projet européen Désira ROBUST ("ROBUST | Capacity4dev," n.d.), s'inscrit dans cette problématique et propose une démarche de modélisation conjointe, permettant de simuler l'interaction dynamique entre un caféier et les ravageurs.

L'approche repose sur une structuration en trois volets : un cadre de couplage modulaire appelé MIMIC, deux modèles biologiques spécifiques (l'un pour la plante, l'autre pour le ravageur) et une base de données empiriques acquise sur le terrain au sein du dispositif CAFNET en Ouganda, complétée par des données externes collectées en Indonésie.

L'originalité de la démarche réside dans la possibilité de simuler des rétroactions mutuelles entre les deux populations : le développement des fruits ou des feuilles peut influencer la dynamique de colonisation du Coffee Berry Borer (CBB), tandis que les pertes causées par le ravageur peuvent modifier en retour la croissance de la plante. L'utilisation d'une logique de regroupement par cohortes permet de concilier précision biologique et efficacité computationnelle. Cette mécanique est développée dans le premier chapitre de la thèse.

Modélisation du couplage plante-ravageur : le cadre MIMIC

Le premier chapitre décrit les fondements conceptuels et informatiques d'un cadre de couplage de modèles. L'architecture proposée, appelée MIMIC (Modular Interactive Modeling for Integrated Coupling), a été conçue pour offrir une alternative souple et robuste aux systèmes fortement intégrés, souvent lourds et rigides. MIMIC permet de coupler des modèles hétérogènes sans en modifier la structure interne, grâce à l'introduction de composants d'interprétation mobilisant un fichier de configuration (UC User Configuration), un serveur d'états d'interactions (ISS), et un modèle d'interaction utilisateur (UIM).

L'efficacité de l'approche réside dans l'hypothèse que les dynamiques modélisées peuvent être abordées par cohortes (et non par individus indépendants). Le recours aux cohortes

permet de factoriser, simplifier, coordonner les l'échanges d'informations. Pour la plante, les feuilles, entre-nœuds et fruits sont regroupés selon leur date d'apparition et leur stade phénologique, permettant une représentation agrégée qui conserve la dynamique tout en réduisant la complexité. Pour les ravageurs, les individus sont regroupés en cohortes de ponte et évoluent selon un modèle déterministe ou probabiliste de maturation et d'interaction.

Sur le plan technique, la formalisation du système a été implémenté en Julia. Ce langage combine la vitesse de calcul du C avec la lisibilité et la flexibilité syntaxique de Python ou R, tout en permettant une métaprogrammation bien adaptée à la construction automatique de pseudo-modèles à partir de fichiers de configuration. Une attention particulière a été portée à la performance des simulations et à leur capacité à être mises à jour rapidement en cas de modification des paramètres.

Ce cadre permet un découplage conceptuel entre la définition des processus biologiques et leur articulation dans une chaîne de simulation, préfigurant une forme d'interopérabilité entre modèles complexes. Il a fait l'office d'une présentation en orale en congrès puis d'une publication dans le journal Plant Phenomics (Triki et al, 2023).

Construction du modèle générique de ravageur

Le deuxième chapitre s'intéresse à la formalisation du modèle de bioagresseur, en particulier celui du CBB. Plutôt que de construire un modèle spécifique, le choix a été fait de proposer une structure modulaire, qui distingue clairement les processus de maturation (croissance, reproduction, mortalité) de ceux d'interaction (choix de l'hôte, probabilité de colonisation, dispersion), ce qui en permet l'extension à d'autres scolytes.

Cette architecture permet par ailleurs de désactiver certains modules si les données sont manquantes, ou d'en remplacer d'autres selon les espèces à modéliser. Ainsi, le modèle devient un gabarit adaptable à différents contextes agronomiques.

Dans l'implémentation du cas du CBB, plusieurs hypothèses ont été posées : l'attractivité d'un fruit est fonction de son âge thermique depuis sa floraison, et permet de le classer dans des catégories (« attirant », « très attirant », etc.). La probabilité de colonisation est modélisée par un ratio dérivant d'un paramètre qui exprime un seuil de saturation à partir duquel l'augmentation de la charge fruitière ne conduit plus à plus d'infestation. Les mâles, dont le rôle dans le cycle du CBB est marginal, ne sont pas représentés.

Pour la calibration, deux jeux de données ont été utilisés. Le premier provient du site CAFNET (Uganda) et sert à estimer les probabilités d'attaque selon la proportion de fruits rouges, avec une attention portée à la dynamique temporelle. Le second provient de parcelles d'arabicas à Sumatra (Indonésie), où la production est continue toute l'année : cela permet de valider la robustesse du modèle sous climat équatorial, où les dynamiques saisonnières sont plus faibles voir absentes.

Ce modèle générique a donc la capacité d'être appliqué à d'autres espèces ou régions, à condition de recalibrer les paramètres comportementaux. Il constitue l'un des deux piliers du système couplé avec la plante, décrit dans le chapitre suivant.

Modélisation du développement du caféier

Le troisième chapitre est consacré à la représentation de la plante hôte, en l'occurrence le caféier. Pour cela, le formalisme GreenLab (de Reffye et al, 2021) a été utilisé et adapté afin de rendre compte à la fois de la dynamique architecturale de la plante et de son fonctionnement physiologique. La structuration de la plante repose sur la notion de cohortes de phytomères, portions d'axes feuillés regroupés par typologie et âge, ce qui permet d'identifier précisément la position et le développement dans le temps de chaque organe. L'un des apports majeurs de cette approche réside dans la possibilité à s'intéresser simultanément à des interactions globales et des interactions locales.

Les interactions globales sont relatives aux facteurs environnementaux qui affectent le comportement global de la plante. Ces facteurs incluent les ressources climatiques (rayonnement, température, etc.) ou édaphiques (nutriments disponibles), modélisés comme une influence globale sur la fonction de production de biomasse du modèle à chaque cycle de croissance. Nous avons donc introduit un facteur spécifique à cette échelle, que l'on pourrait qualifier de facteur de control global de la plante aux bio-agressions. Ces interactions s'approchent de la logique des modèles de culture classique.

En revanche, les interactions locales agissent à l'échelle des organes. Une attaque sur les feuilles, même localisée, entraîne une perte de surface foliaire, ce qui réduit la photosynthèse et affecte la production de biomasse. L'originalité du modèle GreenLab utilisé ici est de pouvoir remonter cette information du niveau organique vers l'échelle de la plante entière, via un système de régulations fondées sur la compétition entre les demandes des différents organes. Nous avons ici introduit la possibilité de jouer sur le fonctionnement de chaque type d'organe, ce qui permet à la fois un contrôle sur production (cas de feuilles attaquées), mais aussi sur la demande de la plante (cas d'organes en expansions attaqués).

La plante est modélisée sous forme de cohortes d'organes, ce qui permet une simulation détaillée mais économiquement viable en termes de ressources de calcul. Dans ce nouveau formalisme, les cohortes attaquées seront scindées en deux couvrant respectivement la part attaquée de celle ne l'étant pas.

Dans ce modèle nous avons aussi étendu le formalisme de la mise en place de la structure de la plante en introduisant explicitant la relation liant les axes dans les ramifications. Cela s'ajoute la notion d'historique structurel, qui permet de tenir compte des impacts passés sur les trajectoires futures de développement. Par exemple, si un entre-nœud est manquant, cela influence les futures branches susceptibles de se développer à cet endroit.

Enfin, sur les données terrain d'Ouganda, nous avons mesuré et calibré le modèle sur les deux clones de robusta utilisés (L2 et L3). Les différences de vigueur, de rendement et de réponse aux attaques sont bien capturées par les paramètres structurels et fonctionnels du modèle.

Le clone L3 présente une plus grande stabilité structurelle, tandis que L2, bien que plus productif en fruits, est plus vulnérable aux stress.

Protocoles de terrain et adaptations méthodologiques [Triki et al, 2025**]**

Le quatrième chapitre présente le travail de terrain mené sur le site CAFNET, situé en Ouganda. Ce site a été choisi pour sa représentativité des systèmes agroforestiers de caféiculture en Afrique de l'Est et pour la diversité de ses conditions de culture. L'objectif était de mettre en place un protocole d'observation capable d'alimenter les modèles précédents en données fiables sur la croissance du caféier et la dynamique des infestations.

La première version du protocole reposait sur des catégories clairement définies : arbres sains vs arbres infestés, conditions ombragées vs non ombragées. Cependant, dès les premières semaines de terrain, plusieurs ajustements ont dû être apportés pour faire face à la réalité écologique : la co-présence de plusieurs ravageurs (CBB, RBD, BTB, CLR) rendait difficile la catégorisation stricte ; l'ombrage était hétérogène et variait d'une parcelle à l'autre ; enfin, la présence d'agents humains (techniciens, agriculteurs) introduisait une variabilité supplémentaire dans les données (taille, récolte, élimination de branches malades). Face à cela, une approche plus souple a été adoptée. Les arbres ont été choisis selon des critères d'âge, de santé apparente, et de localisation dans des micro-environnements relativement homogènes. Des identifiants uniques ont été attribués, et les branches d'intérêt ont été balisées pour assurer un suivi dans le temps. Les mesures ont porté sur la croissance des entre-nœuds, la production de feuilles et de fruits, et l'apparition des symptômes de maladies.

Des mesures destructives ont été planifiées sur quelques arbres pour calibrer les relations allométriques et construire des équations de conversion biomasse/dimension organique. L'ensemble des données a permis de générer un corpus solide, notamment pour la classification des profils de fructification des arbres.

En complément, un jeu de données externe a été mobilisé : celui de plantations d'Arabica à Sumatra (Indonésie), sous climat équatorial. Ces données ont servi à calibrer certains paramètres du modèle CBB (en particulier les probabilités d'attaque selon la proportion de fruits rouges) et à valider la transférabilité du modèle dans des conditions de production très différentes de celles de CAFNET.

Simulation couplée et validation croisée

Le dernier chapitre présente des résultats de la simulation intégrée des dynamiques de croissance de la plante et les simulations de la dynamique du ravageur CBB. Les simulations de croissance de la plante ont été réalisée en utilisant les paramètres issus des campagnes précédentes et repose sur deux configurations principales : une simulation d'un arbre sain servant de base fonctionnelle, et une simulation stressée où un stress biotique a été introduit artificiellement pour évaluer la robustesse du modèle et sa capacité à restituer des perturbations localisées.

Dans le scénario sain, la simulation d'un arbre L3 montre une trajectoire stable de croissance avec une production de biomasse progressive, une expansion foliaire régulière et une répartition efficace entre croissance végétative et reproductive. La demande globale de la plante et les allocations se stabilisent au bout de quelques cycles, révélant un comportement équilibré propre aux arbres bien établis. Ce scénario constitue un point de référence pour comparer les effets d'une perturbation ciblée.

Dans le scénario stressé, une perte de surface foliaire de 0,75 % a été imposée sur douze feuilles localisées entre les entre-nœuds 10 à 24. Bien que la perte semble faible, les effets sur la physiologie de la plante sont tangibles : chute temporaire de la production de biomasse, réduction de l'expansion foliaire, et déviation dans la trajectoire de la surface foliaire cumulée. Ces perturbations initiales sont toutefois partiellement compensées par la plante dans les cycles suivants, grâce à l'émergence de nouvelles feuilles et à une régulation interne de la demande. Le modèle capture ainsi de manière crédible les mécanismes d'adaptation et de résilience du caféier.

Les simulations ont été renforcées par une visualisation schématique structurelle des cohortes. Dans l'exemple illustré, les feuilles attaquées apparaissent réduites, tandis que les fruits restent intacts, soulignant la capacité du modèle à localiser spatialement l'impact des stress sans compromettre la structure globale. Ce type de visualisation permet d'interpréter visuellement les conséquences fonctionnelles des attaques sur l'architecture de la plante.

En parallèle, le modèle du ravageur CBB a été confronté à des profils réels de production fruitière. Une classification des arbres en six classes (A à F) a permis d'évaluer la robustesse du modèle sur des profils contrastés en termes de charge fruitière. Pour chaque classe, une simulation a été confrontée aux observations de l'année suivante. L'indice d'accord moyen sur les fruits rouges colonisés atteint 0,74, avec une erreur absolue moyenne de 4,8 fruits, ce qui témoigne d'une bonne capacité prédictive. Toutefois, les scores R^2 sont plus hétérogènes et parfois négatifs, reflétant la sensibilité de cette métrique aux faibles variabilités intertemporelles.

En revanche, la prédiction du nombre total de fruits attaqués (rouges et verts) est plus incertaine. Les valeurs d'IA restent raisonnables (autour de 0,68), mais les erreurs absolues sont plus élevées, et les R^2 majoritairement négatifs. Ces écarts peuvent s'expliquer par une observation partielle des fruits, des attaques précoces non détectées, ou des facteurs exogènes non modélisés (microclimat, interventions humaines).

En somme, ces résultats démontrent que le couplage permet de simuler à la fois l'impact du ravageur sur la plante et la réponse adaptative de cette dernière. Le système reproduit de manière cohérente les dynamiques observées, tout en fournissant des indices quantitatifs sur la précision des prédictions.

Discussion générale et perspectives

La discussion s'articule autour de plusieurs axes. Le premier concerne la faisabilité technique et scientifique du couplage entre modèles de plante et de ravageur. L'approche par cohortes, bien que simplificatrice, s'avère efficace pour représenter les rétroactions complexes. Le choix du langage Julia et de l'infrastructure MIMIC permet une mise en œuvre souple et rapide, sans altérer les spécificités de chaque modèle. Cette approche modulaire constitue une réponse pertinente à la difficulté d'intégrer des modèles développés indépendamment.

Le deuxième axe de discussion touche à la pertinence du modèle à traduire les phénomènes biologiques. L'usage du formalisme GreenLab permet d'intégrer la structure de la plante dans sa dynamique fonctionnelle. Le modèle capture les effets locaux (perte foliaire, compétition entre organes) et leur propagation dans l'architecture entière. Du côté du ravageur, la modularité permet une calibration par composante (attractivité, colonisation, mortalité) et une adaptation à d'autres espèces ou systèmes. Toutefois, certaines hypothèses (absence d'ennemis naturels, spatialisation implicite, homogénéité de l'hôte) sont vraisemblablement limitantes et devraient être testées ultérieurement.

Le troisième axe concerne la qualité et la nature des données utilisées. Les données CAFNET, bien que riches, restent soumises à la variabilité des conditions réelles : Co-infestations, interventions humaines, conditions climatiques irrégulières. Cela renforce la valeur écologique des résultats, mais complexifie la validation. Dans notre cas, l'ajout de données issues d'autres contextes (ex. Sumatra) a permis de mieux contraindre le modèle et de tester sa généricité.

Enfin, le potentiel du système est discuté. Le couplage permettrait, à terme, de créer des outils d'aide à la décision capables de prédire des périodes critiques d'infestation, d'évaluer l'impact d'une attaque sur la productivité, ou d'optimiser la conduite culturale. Des extensions sont envisageables, notamment l'ajout de modèles climatiques à haute résolution ou de modules économiques pour simuler des scénarios de gestion.

Conclusion

Cette thèse propose une démarche pour modéliser de manière conjointe la dynamique de croissance d'un caféier et les attaques des ravageurs, en particulier celles du scolyte des baies (CBB). En s'appuyant sur un couplage par cohortes, une infrastructure de simulation modulaire (MIMIC) et deux modèles spécialisés plantes et ravageurs complémentaires, elle offre une représentation crédible des interactions plante-ravageur.

Les simulations illustrent que des stress localisés peuvent avoir des impacts mesurables sur la trajectoire physiologique de la plante, et que la dynamique des infestations peut être anticipée à partir de données de phénologie fruitière. Bien que des limites subsistent (absence de spatialisation explicite, simplification comportementale, variabilité non prise en compte), le cadre de modélisation est suffisamment flexible pour qu'il puisse évoluer.

Ce travail est une contribution pour des modélisations agroécologiques intégrées, capables de servir à la fois la recherche, l'enseignement et l'appui à la décision.

Références

De Reffye, P., Hu, B., Kang, M., Letort, V., Jaeger, M., 2021. Two decades of research with the GreenLab model in Agronomy. Annals of Botany 127, 281–295. https://doi.org/10.1093/aob/mcaa172

Gaitán, A.L., Cristancho, M.A., Castro Caicedo, B.L., Rivillas, C.A., Gómez, G.C., 2016a. PART I: Infectious Diseases, in: Bertha, L.C.C., Marco, A.C., Gabriel, C.G., Carlos, A.R., Alvaro, L.G. (Eds.), Compendium of Coffee Diseases and Pests, Diseases and Pests Compendium Series. The American Phytopathological Society, pp. 3–44. https://doi.org/10.1094/9780890544723.002

Gaitán, A.L., Cristancho, M.A., Castro Caicedo, B.L., Rivillas, C.A., Gómez, G.C., 2016b. PART II: Pests, in: Bertha, L.C.C., Carlos, A.R., Marco, A.C., Alvaro, L.G., Gabriel, C.G. (Eds.), Compendium of Coffee Diseases and Pests, Diseases and Pests Compendium Series. The American Phytopathological Society, pp. 45–60. https://doi.org/10.1094/9780890544723.003

Gaitán, A.L., Cristancho, M.A., Castro Caicedo, B.L., Rivillas, C.A., Gómez, G.C., 2016c. PART III: Abiotic and Physiological Disorders, in: Marco, A.C., Carlos, A.R., Gabriel, C.G., Bertha, L.C.C., Alvaro, L.G. (Eds.), Compendium of Coffee Diseases and Pests, Diseases and Pests Compendium Series. The American Phytopathological Society, pp. 61–66. https://doi.org/10.1094/9780890544723.004

Triki, H.E.M., Ribeyre, F., Pinard, F., Jaeger, M., 2023. Coupling Plant Growth Models and Pest and Disease Models: An Interaction Structure Proposal, MIMIC. Plant Phenomics 5, 0077. https://doi.org/10.34133/plantphenomics.0077

Triki, H.E.M., Ribeyre, F., Pinard, F., Jaeger, M., 2025. Uganda Field Protocol. https://github.com/Houssem-Triki/RobustaFieldProtocols

Summary:

The long-term impact of pest and disease attacks on plant growth and production remains a major issue for the prediction of agricultural production. In order to address this issue, a modeling-based approach is used, mobilising models of pest development, plant growth and their interactions.

In this thesis, we propose the development of a formalism enabling models to be coupled in order to integrate their interactions while minimising structural modifications to each model. The main application of this work concerns the evaluation of Robusta coffee production in Uganda, exposed to attacks by pests such as CBB (Coffee Berry Borer), BCTB (Black coffee Twig Borer) and RBD (Red Blister Disease).

Chapter One is devoted to formalising the coupling and implementing it in our context of biological population dynamics (plant organs, pests, pathogens). We adopt a cohort-based approach to structuring interactions between plants and pests. In this way, we limit the complexity that could arise from the unprecedented use of different types of models.

Chapter Two deals with the modeling of pest dynamics. It proposes a modular framework for describing the dynamics of bark beetle-type pests, insects that spend their entire life cycle within a plant organ (except for the dispersal phase). This framework is based on two distinct modules: (a) one describes the life cycle, integrating the different developmental stages and viability of the pest, (b) the other describes interactions with the environment, taking into account the biotic and abiotic factors influencing the development and viability of the pest.

Chapter three is devoted to the development of a plant growth model based on the GreenLab formalism. It models plant structure and function, and can be extended to the crop scale by factoring organs into cohorts. To take better account of interactions on plant structure, an extension of cohorts is introduced via a structural history. This development retains the advantages of factorisation while integrating the effects of pest attacks on new and existing cohorts. We introduce regulatory or control functions at the level of individual organs and the whole plant, enabling us to model a wide spectrum of plant responses to external effects.

The following chapters focus on the application of the approaches developed to the Ugandan study field. First, the parameterisation of the models is discussed, based on the literature and on specifically developed experimental protocols. The analytical basis for model calibration is then detailed, taking into account growing conditions.

Chapter Five uses simulations to analyse results and compare predictions with experimental data and literature. Emphasis is placed on the consequences of the modelled dynamics for the plant, in particular by assessing the effects of environmental and biotic constraints. Finally, a general discussion is offered on both the results obtained and the computational aspects. It also draws on the conclusions and partial discussions of the previous chapters.

Résumé :

L'impact à long terme des attaques de ravageurs et des maladies sur la croissance et la production des plantes demeure une problématique majeure pour la prédiction de la production agricole. Afin d'y répondre une approche basée sur la modélisation est utilisée, mobilisant des modèles de développement des bioagresseurs, de croissance des plantes et de leurs interactions.

Dans cette thèse, nous proposons le développement d'un formalisme permettant de coupler des modèles afin d'intégrer leurs interactions tout en minimisant les modifications structurelles sur chaque modèle. L'application principale de ce travail concerne l'évaluation de la production du caféier robusta en Ouganda, exposé à des attaques de bioagresseurs tels que le CBB (Coffee Berry Borer), le BCTB (Black coffee Twig Borer) et le RBD (Red Blister Disease) du caféier.

Le chapitre un est consacré à la formalisation du couplage et à son implémentation dans notre contexte relatif aux dynamiques de populations biologiques (organes de la plante, ravageurs, pathogènes). Nous adoptons une approche par cohortes pour structurer les interactions entre plantes et bioagresseurs. De ce fait, nous limitons la complexité qui pourrait apparaître en mobilisant sans a priori des modèles de diverses natures
.
Le chapitre deux concerne la modélisation des dynamiques des bioagresseurs. Il propose un cadre modulaire pour décrire la dynamique des ravageurs de type scolyte, insectes passant l'ensemble de leur cycle de vie au sein d'un organe de la plante (à l'exception de la phase de dispersion). Ce cadre repose sur deux modules distincts : (a) l'un décrit le cycle de vie, intégrant les différents stades de développement et la viabilité du ravageur, (b) et l'autre les interactions avec l'environnement, prenant en compte les facteurs biotiques et abiotiques influençant le développement et la viabilité du ravageur.

Le chapitre trois est consacré au développement d'un modèle de croissance des plantes basé sur le formalisme GreenLab. Il permet de modéliser la structure et le fonctionnement de la plante et peut être étendu à l'échelle de la culture en exploitant la factorisation des organes en cohortes. Afin de mieux prendre en compte les interactions sur la structure de la plante, une extension des cohortes est introduite, via un historique structurel. Cette évolution conserve les avantages de la factorisation tout en intégrant les effets d'attaques de bioagresseurs sur les nouvelles cohortes et sur celles déjà en place. Nous introduisons des fonctions de régulation ou contrôle à l'échelle des différents organes et de la plante entière, ce qui permet de modéliser un large spectre de réponses de la plante face à des effets externes.

Les chapitres suivants portent sur l'application des approches développées au terrain d'étude ougandais. On traite d'abord le paramétrage des modèles, en s'appuyant sur la littérature et sur des protocoles expérimentaux spécifiquement développés. Nous y détaillons les bases analytiques nécessaires à la calibration des modèles, en intégrant les conditions de culture. Le chapitre cinq met en œuvre des simulations dans le but d'analyser les résultats obtenus et confronter les prédictions aux données expérimentales et à celles issues de la littérature. L'accent est mis sur les conséquences des dynamiques modélisées pour la plante, en évaluant notamment les effets des contraintes environnementales et biotiques. Une discussion générale est enfin proposée, tant sur les résultats obtenus que sur les aspects calculatoires. Elle s'appuie aussi sur les conclusions et discussions partielles des chapitres précédents.

General Introduction

1. Context

In the last decade, Uganda has experienced a great resurgence of pests and diseases in coffee tree fields (Matovu et al., 2013; Wang et al., 2015), mainly on *coffea canephora*, known as Robusta coffee tree. Despite the important efforts of national institutes to create and disseminate resistant clones, especially for coffee wilt disease (CWD; *Fusarium xylarioides*). In addition to this, climate change induces new fluctuations in plant growth dynamics as well as in the dynamics of pathogens and insects. As a result, in Uganda, the coffee berry borer (CBB) and the coffee rust are present but generally at medium levels, while there are severe cases of Red Blister (RBD; *Cercospora coffeicola*), which infects leaves and berries, Black Twig Borer (BTB; *Xylosandrus compactus*) (Hultman, 2016), and coffee wilt disease (Rutherford, 2006). It was just until 2020 that Uganda was able to achieve the same export level as it had before the outbreak of CWD in the 1990s (Peck and Boa, 2024) Plant production estimation under P&D attacks

The production of a plant attacked by a pest or a disease (P&D) is generally evaluated in the short term, even for perennial crops. Production projections at mid and long term are seldom considered. This is partly due to the methods used to model and simulate plant growth, P&D dynamics and their interaction. There is a lack of mechanistic dynamic approaches (Louarn and Song, 2020) that go down to the level of the plant organ. As a result, feedback on the plant itself can hardly be taken into account.

P&D can damage one or more coffee plant organs, leading to direct damage. If the attacked organs include the fruits, there are direct yield losses. However, even if the fruits are not directly damaged, the yield and growth of the plant will be impacted due to the reduction of the biomass produced (**fig. 1**). In addition, mostly in the case of perennial plants, the attack may also induce a change in plant growth, favouring certain organ types over other or activating dormant buds. These feedback effects are rarely taken into account.

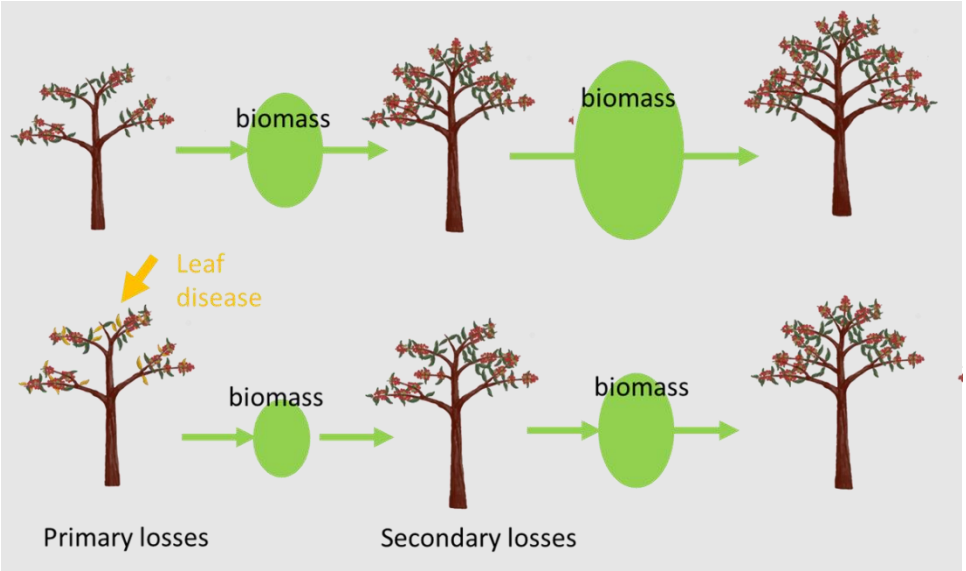


Figure 1: Interactions between P&D dynamics and coffee phenology. Case of a leaf disease impacting the biomass accumulation with a cumulative effect on long-term plant growth.

2. Modeling interactions with plant growth models

To address these limitations and better predict the dynamics of perennial crop production under pest, disease, and environmental stresses, developing new tools and methods that combine models and observations becomes essential. Such approaches are particularly useful for forecasting production under changing weather conditions and considering farmer interventions. To represent and simulate these feedbacks, especially on the yield.

Some studies have examined interactions between plant growth and environmental factors, such as climate (Gaudio et al., 2022) or pathogens (Qi et al., 2009b, 2009b). However, these models often focus on immediate, direct effects and lack the capacity to simulate longer-term feedbacks. Moreover, they tend to be tightly coupled to specific scenarios, limiting their generalizability. As noted by Louarn and Song (2020), few models simultaneously integrate both abiotic (e.g., climate) and biotic (e.g., pests, diseases, or management practices) influences.

A common approach is to test separate models against one another, but this remains highly case-specific and difficult to generalise (Garin et al., 2014).

3. Modeling interactions on Coffea in the Uganda context

Modeling crop losses in Uganda's coffee systems requires approaches tailored to the perennial nature of *Coffea canephora* and the diversity of stressors it faces. Long-term models must capture not only direct damage by pests and diseases (P&Ds), but also the feedback

between plant growth and organ-specific stress over time. These feedbacks influence yield dynamics beyond immediate impacts.

In the ROBUST project, we aim to develop a modeling framework that can simulate these complex interactions between the plant, its pests and pathogens, environmental conditions, and farmer practices—across the full life span of a Robusta coffee tree. Particular attention is given to the diversity of P&Ds that affect different organs, enabling us to disentangle their specific roles in altering plant development and productivity.

Yield forecasting actions will focus on modeling Robusta coffee tree and the locally available P&D (**fig. 4**), mostly the CBB, BTB and RB. Because each targets distinct plant organs—leaves, branches, or berries—they offer a unique opportunity to analyse how localised damage contributes to whole-plant performance, and to simulate outcomes under different scenarios of climate and management.

4. Modeling considerations

4.1. Coffee tree (and plant) growth modeling

Plant modeling

The main frameworks used to model plant growth in agronomy are the process-based models (PBMs) and the Functional Structural Plant Models (FSPM).

Crop models.

PBMs, usually called crop models, calculate the biomass produced from resources collected by roots and light interception by leaves (Tan et al., 2020). The different organs are clustered into separate compartments (**fig. 2**). The distribution of the biomass produced is differentiated for each compartment; this allows yield estimation per unit area (m2). However, this type of model ignores the structure of the plants, the dynamics of their establishment and lacks details on the mechanisms that occur in the plant. FSPM approaches, which address the dynamic and constructive setting up of the structure and the functioning of the organs, is then the alternative to be considered (Reffye and Hu, 2003).

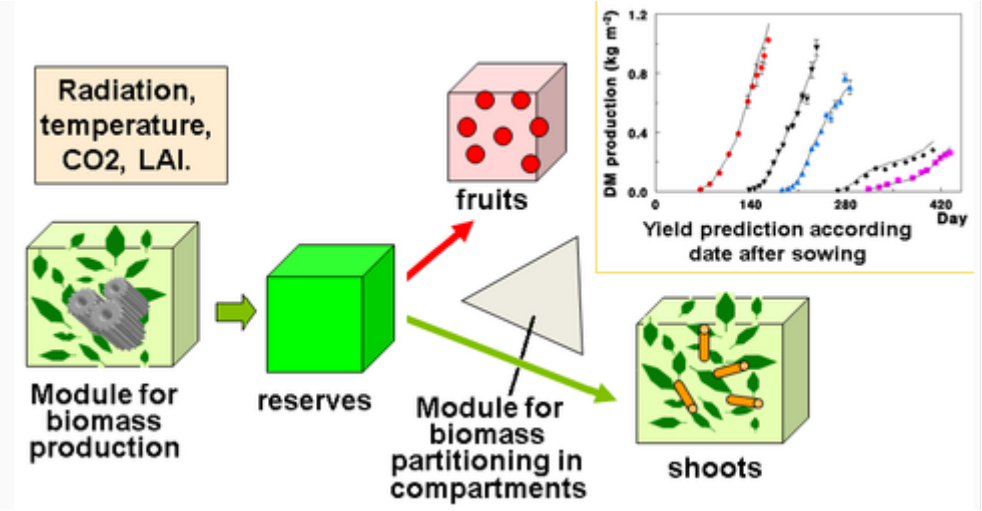


Figure 2: A typical process-based model application. The case of TomSim *Drawing and graph E. Heuvelink, WAGENINGEN UNIVERSITY (Heuvelink, 1999)*

FSPM

In an FSPM (Functional structural Plant model), the functioning and characteristics of each organ are taken into account (Reffye and Hu, 2003). In particular, the distribution of the biomass produced by the different organs and its distribution are tracked at the scale of each organ within the whole plant. With this type of model, focused on the individual plant, a geometric representation of the plant is generated explicitly, and it can be visualised in 3d. The use of an FSPM formalism is often cumbersome to implement and calibrate, since every organ and its functioning are simulated.

4.2. The GreenLab model

However, with a limited number of assumptions and by exploiting some PBM formalisms, one can factorise the processes according to organ structural criteria, properties and create a FSPM of reduced complexity. The GreenLab formalism is such a model; its positioning lies between the PBM and the FSPM (de Reffye et al., 2021). It applies the hypothesis of a common biomass pool, confirmed on several plants of agronomic interest (Heuvelink, 1996) and mobilises the classical PBM light interception model. Compared to crop models clustering all organs of the same nature in the same group, the GreenLab model operates with organ cohorts defined by their chronological and physiological ages (Barthélémy and Caraglio, 2007; Rivals, 1965). Moreover, this type of formalism enables scaling from the individual plant, characterised by its production surface, to the crop level, characterised by plant density.

4.3. Application on the coffee tree

The coffee tree holds a distinctive position in plant growth modeling due to its relatively simple and well-structured architecture. Both *Coffea arabica* and *Coffea canephora* (Robusta) exhibit a branching pattern that lends itself well to formal modeling.

Botanically, the coffee tree's structure is organised around two primary types of axes, which determine its overall form and development. Among the 27 architectural models described by (Hallé et al., 1978), coffee follows the Roux model (see Fig. 3), making it one of the more manageable species for architectural and functional growth modeling.

This predictable architecture makes the coffee tree particularly suitable for mechanistic models that simulate organ-level development and interactions with pests, diseases, and environmental factors over time.

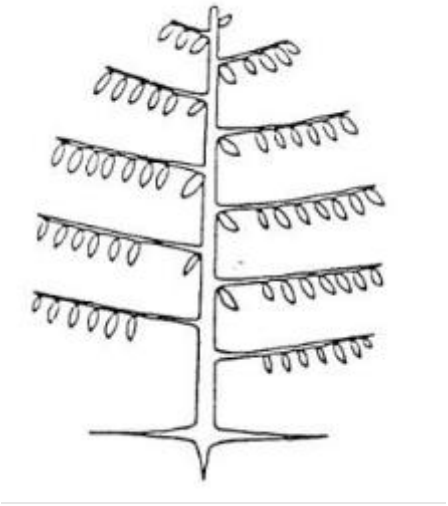


Figure 3: Roux architectural model representation (Hallé et al., 1978)

Modeling Coffea structure

In the Roux model, the orthotropic main stem grows vertically with radial symmetry, producing plagiotropic branches that grow horizontally with bilateral symmetry, typically in a single plane. The fundamental growth unit is the internode (De Reffye and Snoeck, 1976), and the tree exhibits non-rhythmic (i.e. continuous) growth throughout the year.

Growth can be tracked by the regular appearance of new internodes on both the main stem and the branches. This progression can be reproduced using statistical or analytical formulas, which may also be applied to simulate the development of organs such as leaves, buds, and flowers.

A complete model of the coffee tree's architecture can be constructed based on these growth rules. However, to ensure accuracy, it must be calibrated using observational data. This fitting process can rely on statistical analysis of internode distributions, enabling the estimation of growth parameters. For example, the crown analysis method, provides a means of estimating axis development patterns, relative growth rates, branching frequencies, and coupling between axes—key factors for capturing the tree's structural dynamics over time.

Modeling production

To simulate organ development and yield in the coffee tree, it is essential to incorporate functional aspects of plant growth. In particular, biomass production must first be estimated

using a leaf area-based light interception model, where leaves act as the source. The biomass generated is then allocated to various plant organs, each acting as a sink.

Biomass partitioning is a complex process because organ demands vary by type (e.g., stem vs. branch) and developmental stage. The ability of an organ to attract biomass for its growth and function is modelled using a sink function. These functions, often represented as beta distributions (Yin, 2003), describe the organ's capacity to absorb biomass during its expansion phase. Parameters for these functions must be calibrated using field data, typically derived from organ growth rates measured along plant axes, an approach known as "organic series" analysis (Rivals, 1965).

Such measurements usually involve determining organ weight and basic geometrical properties (e.g., length) along stem and branch sequences, which follow different growth rules. In our study, we adopt a low-effort, reliable approach using allometric relationships (Buis et al., 1987) applied to non-destructive measurements, as successfully tested on various *Coffea* species in Ivory Coast (Okoma et al., 2018).

Abiotic factors, particularly the availability of light, heat, and water, affect the total biomass that a plant can produce, and thus, the amount available for organ development and expansion. In our approach, we consider mid- and long-term yield under pest and disease (P&D) pressure as being primarily influenced by this feedback mechanism, without explicitly simulating structural damage.

However, plant architecture is also indirectly shaped by resource availability. Branching and the formation of new phytomeres depend partly on the balance between biomass supply and organ demand. This feedback can be modelled using the concept of "trophic pressure"—the ratio of available to requested biomass—as theoretically proposed by (Mathieu et al., 2009). While such models are difficult to validate, a recent study on young *Coffea canephora* trees in Ivory Coast (Letort et al., 2020) provides a framework for implementing and assessing stochastic feedback effects of biomass availability on structural development.

4.4. Pest & disease modeling

The design of pest and disease (P&D) models is closely tied to their intended application, with two primary approaches commonly employed: correlative models and mechanistic models. Correlative models rely on observational data to uncover statistical relationships between environmental or biological variables and P&D dynamics. These models, such as those used by Yates et al., (2018), can be powerful for prediction within the bounds of the data used for their development but often lack causal interpretation and struggle with extrapolation beyond their original context. In contrast, mechanistic models are grounded in biological knowledge, with parameters that carry explicit physiological meaning. They aim to reproduce key processes such as pest population growth (Bale et al., 2002), disease spread, and host impact (Daane et al., 2004), and though they typically begin simply, complexity is introduced only when justified (Royama, 1992). These models offer greater transferability across contexts but often require simplifications to remain computationally feasible (Bolker, 2008).

In terms of forecasting crop losses, correlative models often establish relationships between yield and P&D density or rely on comparisons with pest- and disease-free controls (Madden et al., 2007). Tools like RICEPEST (Willocquet et al., 2002) have operationalised such relationships for simulating yield losses in rice. Alternatively, mechanistic models may include damage functions that link physiological pest development, often temperature-dependent, to plant injury. These models are typically expressed through systems of differential or delay-differential equations that track transitions between susceptible, infected, sporulating, and dead tissues (Papastamati et al., 2001). Despite these advances, most current models focus on injury-driven yield reduction without accounting for the plant's dynamic responses to damage. As highlighted by (Savary et al., 2018), this omission overlooks important feedbacks, such as compensatory growth or altered development trajectories, which may significantly influence long-term outcomes. In response to these limitations, hybrid approaches are gaining traction—combining the predictive capabilities of data-driven models with the causal strength of mechanistic frameworks (Bouchet et al., 2019).

These assessments do not take into account feedback effects. The dynamics of the pest or disease induce injury that causes crop loss (Savary et al., 2018), but the plant response to the injury is not included.

5. Scientific Problematic and Modeling Challenges

Understanding and predicting the dynamics of pests and diseases (P&Ds) in perennial cropping systems like coffee remains a significant scientific challenge. While many existing studies focus on statistical or mechanistic models, they often treat plant development and pest/pathogen dynamics as separate, decoupled systems. This simplification limits the capacity of models to capture the feedback mechanisms that are central to real-world agroecosystems, such as how pest-induced injury alters plant growth and, in turn, how changes in plant physiology affect the success or suppression of pests and diseases.

The central scientific question of this thesis is: How can we develop a biologically grounded, modular framework that dynamically couples plant growth with pest and disease dynamics, capturing their mutual interactions over time and across scales?

This question brings with it a set of interrelated challenges:

- **Conceptual**: Formalising the coupling between plant development and P&D populations requires a coherent framework that can represent complex interactions while avoiding unnecessary model complexity.
- **Structural**: The integration of models representing different biological processes (plant growth, pest life cycles, pathogen infection) calls for a modular and scalable design, so that different components can interact without becoming computationally prohibitive.
- **Computational**: Directly coupling detailed sub models increases the computational burden, especially when scaling up to the crop level or simulating long time horizons.

Cohort-based modeling is proposed as a strategy to control this complexity while preserving biological realism.

- **Empirical**: Calibrating and validating such a coupled model demands detailed field data, particularly on both plant responses and P&D development under varied environmental and agronomic conditions. Existing data are often incomplete or incompatible, making targeted experimentation and methodological innovation necessary.
- **Applicability**: For the framework to be useful in practice, it must perform under real-world constraints and variable environments. This includes the ability to parameterise the model using available data and to adapt it to different cropping systems, such as Robusta coffee grown in East Africa.

With these challenges in view, the thesis adopts a multi-level approach to modeling plant–P&D interactions. It starts with the design of a flexible coupling framework, proceeds with the construction of pest and plant models, and culminates in a fully integrated system evaluated under real agroecological conditions.

In parallel with these efforts, developments in ecological simulation platforms such as *3Worlds* (Gignoux et al., 2022) reinforce the need for modular and ecosystem-aware architectures. By representing systems as dynamic interaction networks and supporting multi-paradigm simulation, *3Worlds* illustrates how structural formalism and interoperability can promote model reuse, cross-scale consistency, and integration, goals that are closely aligned with the objectives of this thesis.

6. Advancing Coffee P&D Modeling: From Isolated Processes to Coupled Interactions

Building on the modeling approaches discussed earlier, much of the existing research on coffee pests and diseases has predominantly relied on statistical methods. These studies often draw relationships from observational data and field monitoring. For example, (Avelino et al., 2005) used correspondence analysis to link specific production conditions to the intensity of coffee rust epidemics. More recently, machine learning approaches have gained traction; (Motisi et al., 2019), for instance, employed a data-driven regression tree model to predict coffee berry disease dynamics.

In parallel, some researchers have adopted more mechanistic, knowledge-based models. These approaches incorporate expert knowledge or findings from the literature to construct functional laws that capture pest or disease behaviour (Lasso et al., 2021). Mechanistic models have been developed for several major coffee pests and diseases, including the coffee berry borer (Rodríguez et al., 2011, 2013a), coffee leaf rust (Merle et al., 2020), and coffee berry disease (Motisi et al., 2022). However, most of these efforts have focused on *Coffea arabica* and typically treat plant phenology as independent from pest dynamics. For example, the

coffee tree's developmental stages are often modelled separately from pest models, without accounting for potential feedbacks between the host and the pathogen.

In contrast, this thesis aims to address that gap. Chapter One lays the groundwork by formalising the concept of coupling between plant and P&D dynamics. To manage the complexity that arises from integrating diverse models, a cohort-based framework is introduced. This approach structures the interactions at the level of plant organs, pests, and pathogens, offering a scalable method to capture feedbacks without unnecessary computational overhead.

Chapter One lays the foundation by formalising the concept of coupling and detailing its implementation within the context of biological population dynamics, specifically those involving plant organs, pests, and pathogens. To structure the interactions between plants and P&Ds, a cohort-based approach is adopted. This choice helps manage and reduce the complexity that would otherwise arise from indiscriminately combining models of different types.

Building on this formal foundation, Chapter Two turns to the modeling of P&Ds dynamics. A modular framework is proposed to describe the behaviour of bark beetle-type pests, insects whose life cycles occur almost entirely within a plant organ, apart from their dispersal phase. This framework comprises two complementary modules: the first captures the life cycle, including developmental stages and viability, while the second model's interactions with the environment, considering both biotic and abiotic factors that influence pest development and survival.

With the pest dynamics framework in place, Chapter Three introduces a plant growth model based on the GreenLab formalism. This model enables detailed representation of both plant structure and function, and it can be scaled up to the crop level by grouping organs into cohorts. To better reflect structural changes in the plant over time, an extension to the cohort concept is introduced through a structural history. This enhancement retains the benefits of organ grouping while also accounting for the effects of P&Ds attacks on both emerging and existing cohorts. The model incorporates regulatory functions at the level of individual organs and the whole plant, allowing for the simulation of a wide range of plant responses to external stressors.

The methodology developed in the earlier chapters is then applied in the context of a Ugandan field study. This begins with the parameterisation of the models, which draws upon existing literature and specifically designed experimental protocols. The chapter provides the analytical framework required for calibrating the models, taking into account growing conditions such as climatic parameters and agricultural practices.

Finally, Chapter Five presents the implementation of simulations aimed at evaluating the models' performance. The results are analysed and compared with both experimental data and findings from the literature. Special attention is given to the implications of the simulated dynamics on plant health, particularly under varying environmental and biotic stresses. The chapter concludes with a general discussion that synthesises the results, reflects on computational aspects, and builds on the insights from preceding chapters.

7. References

Abel, D.J., Kilby, P.J., Davis, J.R., 1994. The systems integration problem. Int. J. Geogr. Inf. Syst. 8, 1–12. https://doi.org/10.1080/02693799408901984

Aggarwal, P.K., Kalra, N., Chander, S., Pathak, H., 2006. InfoCrop: A dynamic simulation model for the assessment of crop yields, losses due to pests, and environmental impact of agro-ecosystems in tropical environments. I. Model description. Agric. Syst. 89, 1–25. https://doi.org/10.1016/j.agsy.2005.08.001

Argent, R.M., Voinov, A., Maxwell, T., Cuddy, S.M., Rahman, J.M., Seaton, S., Vertessy, R.A., Braddock, R.D., 2006. Comparing modeling frameworks – A workshop approach. Environ. Model. Softw. 21, 895–910. https://doi.org/10.1016/j.envsoft.2005.05.004

Aristizábal, L.F., Jiménez, M., Bustillo, A.E., Trujillo, H.I., Arthurs, S.P., 2015. Monitoring Coffee Berry Borer, *Hypothenemus hampei* (Coleoptera: Curculionidae), Populations with Alcoholbaited Funnel Traps in Coffee Farms in Colombia. Fla. Entomol. 98, 381–383. https://doi.org/10.1653/024.098.0165

Avelino, J., Barboza, B., Araya, J., Fonseca, C., Davrieux, F., Guyot, B., Cilas, C., 2005. Effects of slope exposure, altitude and yield on coffee quality in two altitude terroirs of Costa Rica, Orosi and Santa María de Dota. J. Sci. Food Agric. 85, 1869–1876. https://doi.org/10.1002/jsfa.2188

Bale, J., Masters, G., Hodkinson, I., Awmack, C., Bezemer, T. m, Brown, V., Butterfield, J., Buse, A., Coulson, J., Farrar, J., Good, J., Harrington, R., Hartley, S., Jones, T., Lindroth, R., Press, M., Symrnioudis, I., Watt, A., Whittaker, J., 2002. Herbivory in global climate change research: Direct effects of rising temperature on insect herbivores. Glob. Change Biol. 8, 1–16. https://doi.org/10.1046/j.1365-2486.2002.00451.x

Barthélémy, D., Caraglio, Y., 2007. Plant Architecture: A Dynamic, Multilevel and Comprehensive Approach to Plant Form, Structure and Ontogeny. Ann. Bot. 99, 375–407. https://doi.org/10.1093/aob/mcl260

Bar-Yam, Y., 2002. General Features of Complex Systems. UNESCO Encycl. Life Support Syst.

Ben-Kiki, O., Evans, C., n.d. YAML Ain't Markup Language (YAML™) Version 1.2.

Bergez, J.-E., Chabrier, P., Gary, C., Jeuffroy, M.H., Makowski, D., Quesnel, G., Ramat, E., Raynal, H., Rousse, N., Wallach, D., Debaeke, P., Durand, P., Duru, M., Dury, J., Faverdin, P., Gascuel-Odoux, C., Garcia, F., 2013. An open platform to build, evaluate and simulate integrated models of farming and agro-ecosystems. Environ. Model. Softw., Thematic Issue on the Future of Integrated Modeling Science and Technology 39, 39–49. https://doi.org/10.1016/j.envsoft.2012.03.011

Bezanson, J., Edelman, A., Karpinski, S., Shah, V.B., 2017. Julia: A Fresh Approach to Numerical Computing. SIAM Rev. 59, 65–98. https://doi.org/10.1137/141000671

Bolker, B.M., 2008. Ecological Models and Data in R. Princeton University Press. https://doi.org/10.2307/j.ctvcm4g37

Bondad, J., Harrison, M.T., Whish, J., Sprague, S., Barry, K., 2023. Integrated crop-disease models: New frontiers in systems thinking. Farming Syst. 1, 100004. https://doi.org/10.1016/j.farsys.2023.100004

Bouchet, P.J., Peterson, A.T., Zurell, D., Dormann, C.F., Schoeman, D., Ross, R.E., Snelgrove, P., Sequeira, A.M.M., Whittingham, M.J., Wang, L., Rapacciuolo, G., Oppel, S., Mellin, C., Lauria, V., Krishnakumar, P.K., Jones, A.R., Heinänen, S., Heikkinen, R.K., Gregr, E.J., Fielding, A.H., Caley, M.J., Barbosa, A.M., Bamford, A.J., Lozano-Montes, H.,

Parnell, S., Wenger, S., Yates, K.L., 2019. Better Model Transfers Require Knowledge of Mechanisms. Trends Ecol. Evol. 34, 489–490. https://doi.org/10.1016/j.tree.2019.04.006

Bouman, B.A.M., van Keulen, H., van Laar, H.H., Rabbinge, R., 1996. The 'School of de Wit' crop growth simulation models: A pedigree and historical overview. Agric. Syst. 52, 171–198. https://doi.org/10.1016/0308-521X(96)00011-X

Brandmeyer, J.E., Karimi, H.A., 2000. Coupling methodologies for environmental models. Environ. Model. Softw. 15, 479–488. https://doi.org/10.1016/S1364-8152(00)00027-X

Buddie, A.G., Crozier, J., Rutherford, M.A., Flood, J., Bridge, P.D., 2015. Population development within the coffee wilt pathogen Gibberella xylarioides reflects host-related divergence. Eur. J. Plant Pathol. 142, 291–304. https://doi.org/10.1007/s10658-015-0613-z

Buis, R., Barthou, H., Frezouls, M., 1987. Relations dimensionnelles inter-feuilles: Mise en évidence d'actions locales et à distance. Bull. Société Bot. Fr. Lett. Bot. 134, 107–114. https://doi.org/10.1080/01811797.1987.10824734

Cerda, R., Avelino, J., Gary, C., Tixier, P., Lechevallier, E., Allinne, C., 2017. Primary and Secondary Yield Losses Caused by Pests and Diseases: Assessment and Modeling in Coffee. PLOS ONE 12, e0169133. https://doi.org/10.1371/journal.pone.0169133

Chabrier, P., Garcia, F., Martin-Clouaire, R., Quesnel, G., Raynal, H., 2007. Toward a simulation modeling platform for studying cropping systems management: the record project, in: International Congress on Modeling and Simulation, International Society for Computer Simulation. Citeseer, pp. 10–13.

Cournède, P.-H., Guyard, T., Bayol, B., Griffon, S., de Coligny, F., Borianne, P., Jaeger, M., de Reffye, P., 2009. A Forest Growth Simulator Based on Functional-Structural Modeling of Individual Trees, in: 2009 Third International Symposium on Plant Growth Modeling, Simulation, Visualization and Applications. Presented at the 2009 Third International Symposium on Plant Growth Modeling, Simulation, Visualization and Applications, pp. 34–41. https://doi.org/10.1109/PMA.2009.55

Cournède, P.-H., Kang, M.-Z., Mathieu, A., Barczi, J.-F., Yan, H.-P., Hu, B.-G., de Reffye, P., 2006. Structural Factorization of Plants to Compute Their Functional and Architectural Growth. SIMULATION 82, 427–438. https://doi.org/10.1177/0037549706069341

Daane, K.M., Malakar-Kuenen, R.D., Walton, V.M., 2004. Temperature-dependent development of *Anagyrus pseudococci* (Hymenoptera: Encyrtidae) as a parasitoid of the vine mealybug, *Planococcus ficus* (Homoptera: Pseudococcidae). Biol. Control 31, 123–132. https://doi.org/10.1016/j.biocontrol.2004.04.010

Damon, A., 2000. A review of the biology and control of the coffee berry borer, *Hypothenemus hampei* (Coleoptera: Scolytidae). Bull. Entomol. Res. 90, 453–465. https://doi.org/10.1017/S0007485300000584

de REFFYE, P., n.d. Etude du fonctionnement des méristèmes et de la croissance des axes végétatifs.

de Reffye, P., Heuvelink, E., Guo, Y., Hu, B.-G., Zhang, B.-G., 2009. Coupling Process-Based Models and Plant Architectural Models: A Key Issue for Simulating Crop Production, in: Cao, W., White, J.W., Wang, E. (Eds.), Crop Modeling and Decision Support. Springer, Berlin, Heidelberg, pp. 130–147. https://doi.org/10.1007/978-3-642-01132-0_15

de Reffye, P., Hu, B., Kang, M., Letort, V., Jaeger, M., 2021. Two decades of research with the GreenLab model in Agronomy. Ann. Bot. 127, 281–295. https://doi.org/10.1093/aob/mcaa172

De Reffye, P., Jaeger, M., 2013. Modèles mathématiques du développement et de la croissance de l'architecture des plantes. Le cas du modèle GreenLab - Agritrop, in: Modéliser & Simuler. pp. 625–658.

De Reffye, P., Snoeck, J., 1976. Modèle mathématique de base pour l'étude et la simulation de la croissance et de l'architecture du Coffea robusta. Café Cacao Thé.

Donatelli, M., Magarey, R.D., Bregaglio, S., Willocquet, L., Whish, J.P.M., Savary, S., 2017. Modeling the impacts of pests and diseases on agricultural systems. Agric. Syst. 155, 213–224. https://doi.org/10.1016/j.agsy.2017.01.019

Dufour, B.P., Diman, C., De San Mateo, A., Mouttet, R., 2022. Le scolyte des fruits du caféier, *Hypothenemus hampei* (Ferr.) détecté en Guadeloupe. Cah. Agric. 31, 10. https://doi.org/10.1051/cagri/2022008

Dufour, B.P., Frérot, B., 2008. Optimization of coffee berry borer, *Hypothenemus hampei* Ferrari (Col., Scolytidae), mass trapping with an attractant mixture. J. Appl. Entomol. 132, 591–600. https://doi.org/10.1111/j.1439-0418.2008.01291.x

Dufour, B.P., Kerana, I.W., Ribeyre, F., 2021. Population dynamics of Hypothenemus hampei (Ferrari) according to the phenology of Coffea arabica L. in equatorial conditions of North Sumatra. Crop Prot. 146, 105639. https://doi.org/10.1016/j.cropro.2021.105639

Gaitán, A.L., Cristancho, M.A., Castro Caicedo, B.L., Rivillas, C.A., Gómez, G.C., 2016a. PART I: Infectious Diseases, in: Bertha, L.C.C., Marco, A.C., Gabriel, C.G., Carlos, A.R., Alvaro, L.G. (Eds.), Compendium of Coffee Diseases and Pests, Diseases and Pests Compendium Series. The American Phytopathological Society, pp. 3–44. https://doi.org/10.1094/9780890544723.002

Gaitán, A.L., Cristancho, M.A., Castro Caicedo, B.L., Rivillas, C.A., Gómez, G.C., 2016b. PART II: Pests, in: Bertha, L.C.C., Carlos, A.R., Marco, A.C., Alvaro, L.G., Gabriel, C.G. (Eds.), Compendium of Coffee Diseases and Pests, Diseases and Pests Compendium Series. The American Phytopathological Society, pp. 45–60. https://doi.org/10.1094/9780890544723.003

Gaitán, A.L., Cristancho, M.A., Castro Caicedo, B.L., Rivillas, C.A., Gómez, G.C., 2016c. PART III: Abiotic and Physiological Disorders, in: Marco, A.C., Carlos, A.R., Gabriel, C.G., Bertha, L.C.C., Alvaro, L.G. (Eds.), Compendium of Coffee Diseases and Pests, Diseases and Pests Compendium Series. The American Phytopathological Society, pp. 61–66. https://doi.org/10.1094/9780890544723.004

Gamma, E., Helm, R., Johnson, R., Vlissides, J., 1994. Design Patterns: Elements of Reusable Object-Oriented Software. Pearson Education.

Garin, G., Fournier, C., Andrieu, B., Houlès, V., Robert, C., Pradal, C., 2014. A modeling framework to simulate foliar fungal epidemics using functional–structural plant models. Ann. Bot. 114, 795–812. https://doi.org/10.1093/aob/mcu101

Gaudio, N., Louarn, G., Barillot, R., Meunier, C., Vezy, R., Launay, M., 2022. Exploring complementarities between modeling approaches that enable upscaling from plant community functioning to ecosystem services as a way to support agroecological transition. Silico Plants 4, diab037. https://doi.org/10.1093/insilicoplants/diab037

Gaunt, R.E., 1995. The Relationship Between Plant Disease Severity and Yield. Annu. Rev. Phytopathol. 33, 119–144. https://doi.org/10.1146/annurev.py.33.090195.001003

Gignoux, J., Davies, I.D., Flint, S.R., 2022. 3Worlds, a simulation platform for ecosystem modeling. Ecol. Model. 473, 110121. https://doi.org/10.1016/j.ecolmodel.2022.110121

Giordanengo, P., Brun, L.O., Frerot, B., 1993. Evidence for allelochemical attraction of the coffee berry borer,Hypothenemus hampei, by coffee berries. J. Chem. Ecol. 19, 763–769. https://doi.org/10.1007/BF00985007

Greco, E.B., Wright, M.G., 2015. Ecology, Biology, and Management of Xylosandrus compactus (Coleoptera: Curculionidae: Scolytinae) with Emphasis on Coffee in Hawaii. J. Integr. Pest Manag. 6, 7–7. https://doi.org/10.1093/jipm/pmv007

Guo, Y., Fourcaud, T., Jaeger, M., Zhang, X., Li, B., 2011. Plant growth and architectural modeling and its applications. Ann. Bot. 107, 723–727. https://doi.org/10.1093/aob/mcr073

Hallé, F., 2017. Des données récentes sur les arbres 48.

Hallé, F., Oldeman, R., 1970. Essai sur l'architecture et la dynamique de croissance des arbres tropicaux, Collection de monographies de botanique et de biologie végétale. Masson et Cie, Paris.

Hallé, F., Oldeman, R.A.A., Tomlinson, P.B., 1978. Tropical Trees and Forests. Springer, Berlin, Heidelberg. https://doi.org/10.1007/978-3-642-81190-6

Hamilton, L.J., Hollingsworth, R.G., Sabado-Halpern, M., Manoukis, N.C., Follett, P.A., Johnson, M.A., 2019. Coffee berry borer (Hypothenemus hampei) (Coleoptera: Curculionidae) development across an elevational gradient on Hawai'i Island: Applying laboratory degree-day predictions to natural field populations. PLoS ONE 14, e0218321. https://doi.org/10.1371/journal.pone.0218321

Henke, M., Kurth, W., Buck-Sorlin, G.H., 2016. FSPM-P: towards a general functional-structural plant model for robust and comprehensive model development. Front. Comput. Sci. 10, 1103–1117. https://doi.org/10.1007/s11704-015-4472-8

Heuvelink, E., 1996. Dry Matter Partitioning in Tomato: Validation of a Dynamic Simulation Model. Ann. Bot. 77, 71–80. https://doi.org/10.1006/anbo.1996.0009

Hultman, C., 2016. Black coffee twig borer, Xylosandrus compactus (Eichhoff) on robusta coffee in Uganda [WWW Document]. URL https://stud.epsilon.slu.se/9580/ (accessed 5.5.25).

Jaramillo, J., Chabi-olaye, A., Borgemeister, C., 2010. Temperature-Dependent Development and Emergence Pattern of <I>Hypothenemus hampei</I> (Coleoptera: Curculionidae: Scolytinae) From Coffee Berries. J. Econ. Entomol. 103, 1159–1165. https://doi.org/10.1603/EC09408

Jaramillo, J., Chabi-Olaye, A., Kamonjo, C., Jaramillo, A., Vega, F.E., Poehling, H.-M., Borgemeister, C., 2009. Thermal Tolerance of the Coffee Berry Borer Hypothenemus hampei: Predictions of Climate Change Impact on a Tropical Insect Pest. PLoS ONE 4, e6487. https://doi.org/10.1371/journal.pone.0006487

Johnson, M.A., Manoukis, N.C., 2021. Influence of seasonal and climatic variables on coffee berry borer (Hypothenemus hampei Ferrari) flight activity in Hawaii. PLOS ONE 16, e0257861. https://doi.org/10.1371/journal.pone.0257861

Kagezi, G., Kucel, P., Egonyu, J.P., Kyamanywa, S., Karungi, J.T., Pinard, F., Jaramillo, J., Van Asten, P.J.A., Wagoire, W.W., Ngabirano, H., 2015. A review of the status and progress in management research of the black coffee twig borer, Xylosandrus compactus (Eichhoff) in Uganda [WWW Document]. Proc. 25th Int. Conf. Coffee Sci. URL https://agritrop.cirad.fr/579968/ (accessed 2.27.23).

Kang, M., Hua, J., de Reffye, P., Jaeger, M., 2016. Parameter identification of plant growth models with stochastic development, in: 2016 IEEE International Conference on Functional-Structural Plant Growth Modeling, Simulation, Visualization and Applications (FSPMA). Presented at the 2016 IEEE International Conference on Functional-Structural Plant Growth Modeling, Simulation, Visualization and Applications (FSPMA), pp. 98–105. https://doi.org/10.1109/FSPMA.2016.7818294

Kang, M., Hua, J., Wang, X., de Reffye, P., Jaeger, M., Akaffou, S., 2018. Estimating Sink Parameters of Stochastic Functional-Structural Plant Models Using Organic Series-Continuous and Rhythmic Development. Front. Plant Sci. 9, 1688. https://doi.org/10.3389/fpls.2018.01688

Kang, M.Z., Cournède, P.H., de Reffye, P., Auclair, D., Hu, B.G., 2008. Analytical study of a stochastic plant growth model: Application to the GreenLab model. Math. Comput. Simul. 78, 57–75. https://doi.org/10.1016/j.matcom.2007.06.003

Khan, J., Rio, L.E.D., Nelson, R., Rivera-Varas, V., Secor, G.A., Khan, M.F.R., 2008. Survival, Dispersal, and Primary Infection Site for Cercospora beticola in Sugar Beet. Plant Dis. 92, 741–745. https://doi.org/10.1094/PDIS-92-5-0741

Kirkeby, C., Brookes, V.J., Ward, M.P., Dürr, S., Halasa, T., 2021. A Practical Introduction to Mechanistic Modeling of Disease Transmission in Veterinary Science. Front. Vet. Sci. 7, 546651. https://doi.org/10.3389/fvets.2020.546651

Kropff, M.J., Teng, P.S., Rabbinge, R., 1995. The challenge of linking pest and crop models. Agric. Syst., Agricultural Systems Applications Through an International Consortium, ICASA 49, 413–434. https://doi.org/10.1016/0308-521X(95)00034-3

Lasso, E., Motisi, N., Avelino, J., Corrales, J.C., 2021. FramePests: A Comprehensive Framework for Crop Pests Modeling and Forecasting. IEEE Access 9, 115579–115598. https://doi.org/10.1109/ACCESS.2021.3104537

Le Chevalier, V., Jaeger, M., Mei, X., Cournède, P.-H., 2007. Simulation and Visualisation of Functional Landscapes: Effects of the Water Resource Competition Between Plants. J. Comput. Sci. Technol. 22, 835–845. https://doi.org/10.1007/s11390-007-9105-8

Leclerc, G., Bommel, P., Motisi, N., Vezy, R., Treminio, E., Avelino, J., 2021. Coffee leaf rust (Hemeleia vastatrix) risk management in Central America: contribution of remote interactive simulations. Agron. Environ. Sociétés 11. https://doi.org/10.54800/roc535

Lessler, J., Cummings, D.A.T., 2016. Mechanistic Models of Infectious Disease and Their Impact on Public Health. Am. J. Epidemiol. 183, 415–422. https://doi.org/10.1093/aje/kww021

Letort, V., Sabatier, S., Okoma, M.P., Jaeger, M., de Reffye, P., 2020. Internal trophic pressure, a regulator of plant development? Insights from a stochastic functional–structural plant growth model applied to Coffea trees. Ann. Bot. 126, 687–699. https://doi.org/10.1093/aob/mcaa023

Loi, C., Cournède, P., Françon, J., 2010. A symbolic method to compute the probability distribution of the number of pattern occurences in random texts generated by stochastic 0L-systems. Discrete Math. Theor. Comput. Sci.

Loi, C., Cournède, P.-H., Françon, J., 2014. A Symbolic Method to Analyse Patterns in Plant Structure. Comb. Probab. Comput. 23, 842–860. https://doi.org/10.1017/S0963548314000108

Lorenz, E.N., 1963. Deterministic Nonperiodic Flow. J. Atmospheric Sci. 20, 130–141. https://doi.org/10.1175/1520-0469(1963)020<0130:DNF>2.0.CO;2

Louarn, G., Song, Y., 2020. Two decades of functional–structural plant modeling: now addressing fundamental questions in systems biology and predictive ecology. Ann. Bot. 126, 501–509. https://doi.org/10.1093/aob/mcaa143

Luzinda, H., Nelima, M., Wabomba, A., Kangire, A., Musoli, P., Musebe, R., 2016. Farmer awareness, coping mechanisms and economic implications of coffee leaf rust disease in Uganda. Uganda J. Agric. Sci. 16, 207. https://doi.org/10.4314/ujas.v16i2.6

Ma, Y., Li, B., Zhan, Z., Guo, Y., Luquet, D., de Reffye, P., Dingkuhn, M., 2007. Parameter Stability of the Functional–Structural Plant Model GREENLAB as Affected by Variation within Populations, among Seasons and among Growth Stages. Ann. Bot. 99, 61–73. https://doi.org/10.1093/aob/mcl245

Mathieu, A., Cournède, P.H., Letort, V., Barthélémy, D., de Reffye, P., 2009. A dynamic model of plant growth with interactions between development and functional mechanisms to study plant structural plasticity related to trophic competition. Ann. Bot. 103, 1173–1186. https://doi.org/10.1093/aob/mcp054

Matovu, R., Kangire, A., Phiri, N., Hakiza, G., Kagezi, G., Musoli, P., 2013. Ecological factors influencing incidence and severity of Coffee Leaf Rust and Coffee Berry Disease in major Arabica coffee growing districts of Uganda. Uganda J. Agric. Sci.

Merle, I., Tixier, P., Virginio Filho, E. de M., Cilas, C., Avelino, J., 2020. Forecast models of coffee leaf rust symptoms and signs based on identified microclimatic combinations in coffee-based agroforestry systems in Costa Rica. Crop Prot. 130, 105046. https://doi.org/10.1016/j.cropro.2019.105046

Mora, J.R.M., n.d. Resposta Da Broca - Do - Cafe, Hypothenemus hampel, A Estimulos Visuais E Semioquimicos. INIAP Archivo Historico.

Motisi, N., Bommel, P., Leclerc, G., Robin, M.-H., Aubertot, J.-N., Butron, A.A., Merle, I., Treminio, E., Avelino, J., 2022. Improved forecasting of coffee leaf rust by qualitative modeling: Design and expert validation of the ExpeRoya model. Agric. Syst. 197, 103352. https://doi.org/10.1016/j.agsy.2021.103352

Motisi, N., Ribeyre, F., Poggi, S., 2019. Coffee tree architecture and its interactions with microclimates drive the dynamics of coffee berry disease in coffee trees. Sci. Rep. 9, 2544. https://doi.org/10.1038/s41598-019-38775-5

Nanjego, W., Kagezi, G., Kyamanywa, S., Ronald, S., Kobusinge, J., Arinaitwe, G., 2024. Population Dynamics of the Black Coffee Twig Borer Xylosandrus compactus (Eichhoff) in Robusta Coffee Coffea canephora. Indian J. Entomol. https://doi.org/10.55446/IJE.2024.2046

Nelson, S.C., 2008. Cercospora Leaf Spot and Berry Blotch of Coffee.

Okoma, P., Akaffou, S., De Reffye, P., Hamon, P., Hamon, S., Konan, O., Kouassi, K.H., Legnate, H., Letort, V., Sabatier, S., 2018. Estimation of stem and leaf dry biomass using a non-destructive method applied to African Coffea species. Agrofor. Syst. 92, 667–675. https://doi.org/10.1007/s10457-016-0031-z

Papastamati, K., Welham, S.J., Fitt, B.D.L., Gladders, P., 2001. Modeling the progress of light leaf spot (Pyrenopeziza brassicae) on winter oilseed rape (Brassica napus) in relation to leaf wetness and temperature. Plant Pathol. 50, 154–164. https://doi.org/10.1046/j.1365-3059.2001.00551.x

Parmesan, C., Hanley, M.E., 2015. Plants and climate change: complexities and surprises. Ann. Bot. 116, 849–864. https://doi.org/10.1093/aob/mcv169

Peck, L.D., Boa, E., 2024. Coffee wilt disease: The forgotten threat to coffee. Plant Pathol. 73, 506–521. https://doi.org/10.1111/ppa.13833

Perkel, J.M., 2019. Julia: come for the syntax, stay for the speed. Nature 572, 141–142. https://doi.org/10.1038/d41586-019-02310-3

Pham, Y., Reardon-Smith, K., Mushtaq, S., Cockfield, G., 2019. The impact of climate change and variability on coffee production: a systematic review. Clim. Change 156, 609–630. https://doi.org/10.1007/s10584-019-02538-y

Piao, S., Liu, Q., Chen, A., Janssens, I.A., Fu, Y., Dai, J., Liu, L., Lian, X., Shen, M., Zhu, X., 2019. Plant phenology and global climate change: Current progresses and challenges. Glob. Change Biol. 25, 1922–1940. https://doi.org/10.1111/gcb.14619

Pinard, F., Makune, S.E., Campagne, P., Mwangi, J., 2016. Spatial Distribution of Coffee Wilt Disease Under Roguing and Replanting Conditions: A Case Study from Kaweri Estate in Uganda. Phytopathology® 106, 1291–1299. https://doi.org/10.1094/PHYTO-04-15-0097-R

Pradal, C., Dufour-Kowalski, S., Boudon, F., Donès, N., 2007. The architecture of OpenAlea: A visual programming and component based software for plant modeling.

Pradal, C., Dufour-Kowalski, S., Boudon, F., Fournier, C., Godin, C., 2008. OpenAlea: a visual programming and component-based software platform for plant modeling. Funct. Plant Biol. 35, 751–760. https://doi.org/10.1071/FP08084

Qi, R., Cournède, P.-H., de Reffye, P., 2009a. Tri-trophic Ecosystem Oil Palm-Pests-Auxiliaries: II. Sensitivity Analysis, Parameter Identification and Control, in: 2009 Third International Symposium on Plant Growth Modeling, Simulation, Visualization and Applications. Presented at the 2009 Third International Symposium on Plant Growth Modeling, Simulation, Visualization and Applications, pp. 327–333. https://doi.org/10.1109/PMA.2009.49

Qi, R., Cournède, P.-H., Lecoustre, R., de Reffye, P., 2009b. Tri-trophic Ecosystem Oil Palm-Pests-Auxiliaries: I. Modeling and Simulation, in: Proceedings of the 2009 Plant Growth Modeling, Simulation, Visualization, and Applications, PMA '09. IEEE Computer Society, USA, pp. 87–94. https://doi.org/10.1109/PMA.2009.48

Reffye, P. de, Hu, B.G., 2003. Relevant Qualitative and Quantitative choices for building an efficient dynamic plant growth model : Greenlab Case. Presented at the International Symposium on Plant Growth Modeling, Simulation, Visualization and their Applications - PMA'03, Springer and Tsinghua University Press, p. 87.

Ribeyre, F., Avelino, J., 2012. Impact of field pests and diseases on coffee quality. pp. 151–176.

Rivals, P., 1965. Essai sur la croissance des arbres et sur leurs systèmes de floraison (application aux espèces fruitières). J. Agric. Tradit. Bot. Appliquée 12, 655–686. https://doi.org/10.3406/jatba.1965.2856

ROBUST | Capacity4dev [WWW Document], n.d. URL https://capacity4dev.europa.eu/projects/desira/info/robust_en (accessed 5.13.25).

Rodríguez, D., Cure, J.R., Cotes, J.M., Gutierrez, A.P., Cantor, F., 2011. A coffee agroecosystem model: I. Growth and development of the coffee plant. Ecol. Model. 222, 3626–3639. https://doi.org/10.1016/j.ecolmodel.2011.08.003

Rodríguez, D., Cure, J.R., Gutierrez, A.P., Cotes, J.M., Cantor, F., 2013a. A coffee agroecosystem model: II. Dynamics of coffee berry borer. Ecol. Model. 248, 203–214. https://doi.org/10.1016/j.ecolmodel.2012.09.015

Rodríguez, D., Cure, J.R., Gutierrez, A.P., Cotes, J.M., Cantor, F., 2013b. A coffee agroecosystem model: II. Dynamics of coffee berry borer. Ecol. Model. 248, 203–214. https://doi.org/10.1016/j.ecolmodel.2012.09.015

Royama, T., 1992. Analytical population dynamics. London ; New York : Chapman & Hall.
Rutherford, M.A., 2006. Current Knowledge of Coffee Wilt Disease, a Major Constraint to Coffee Production in Africa. Phytopathology® 96, 663–666. https://doi.org/10.1094/PHYTO-96-0663
Savary, S., Nelson, A., Djurle, A., Esker, P.D., Sparks, A., Amorim, L., Filho, A.B., Caffi, T., Castilla, N., Garrett, K., Mcroberts, N., Rossi, V., Yuen, J., Willocquet, L., 2018. Concepts, approaches, and avenues for modeling crop health and crop losses. Eur. J. Agron. 15 p. https://doi.org/10.1016/j.eja.2018.04.003
Savary, S., Teng, P.S., Willocquet, L., Nutter, F.W., 2006. Quantification and Modeling of Crop Losses: A Review of Purposes. Annu. Rev. Phytopathol. 44, 89–112. https://doi.org/10.1146/annurev.phyto.44.070505.143342
Sedgwick, P., 2014. Retrospective cohort studies: advantages and disadvantages. BMJ 348, g1072. https://doi.org/10.1136/bmj.g1072
Siad, S.M., Iacobellis, V., Zdruli, P., Gioia, A., Stavi, I., Hoogenboom, G., 2019. A review of coupled hydrologic and crop growth models. Agric. Water Manag. 224, 105746. https://doi.org/10.1016/j.agwat.2019.105746
Sievänen, R., Perttunen, J., Nikinmaa, E., Posada, J.M., 2009. Invited Talk: Functional Structural Plant Models - Case LIGNUM, in: 2009 Third International Symposium on Plant Growth Modeling, Simulation, Visualization and Applications. Presented at the 2009 Third International Symposium on Plant Growth Modeling, Simulation, Visualization and Applications (PMA), IEEE, Beijing, China, pp. 3–9. https://doi.org/10.1109/PMA.2009.64
Soualiou, S., Wang, Z., Sun, W., de Reffye, P., Collins, B., Louarn, G., Song, Y., 2021. Functional–Structural Plant Models Mission in Advancing Crop Science: Opportunities and Prospects. Front. Plant Sci. 12, 747142. https://doi.org/10.3389/fpls.2021.747142
Souza, A.G.C., Rodrigues, F.Á., Maffia, L.A., Mizubuti, E.S.G., 2011. Infection Process of Cercospora coffeicola on Coffee Leaf: Infection Process of Cercospora coffeicola on Coffee Leaf. J. Phytopathol. 159, 6–11. https://doi.org/10.1111/j.1439-0434.2010.01710.x
Tan, M., Gou, F., Stomph, T.J., Wang, J., Yin, W., Zhang, L., Chai, Q., van der Werf, W., 2020. Dynamic process-based modeling of crop growth and competitive water extraction in relay strip intercropping: Model development and application to wheat-maize intercropping. Field Crops Res. 246, 107613. https://doi.org/10.1016/j.fcr.2019.107613
Tendeloo, Y.V., Vangheluwe, H., 2018. DISCRETE EVENT SYSTEM SPECIFICATION MODELING AND SIMULATION, in: 2018 Winter Simulation Conference (WSC). Presented at the 2018 Winter Simulation Conference (WSC), IEEE, Gothenburg, Sweden, pp. 162–176. https://doi.org/10.1109/WSC.2018.8632372
Túler, A., Valbon, W., de Souza Rodrigues, H., Noia, L., Santos, L., Fogaça, I., Rondelli, V., Filho, A., 2019. Black twig borer, Xylosandrus compactus (Eichhoff), a potential threat to coffee production. Rev. Cienc. Agríc. 36. https://doi.org/10.22267/rcia.1936E.102
Vezy, R., le Maire, G., Christina, M., Georgiou, S., Imbach, P., Hidalgo, H.G., Alfaro, E.J., Blitz-Frayret, C., Charbonnier, F., Lehner, P., Loustau, D., Roupsard, O., 2020. DynACof: A process-based model to study growth, yield and ecosystem services of coffee agroforestry systems. Environ. Model. Softw. 124, 104609. https://doi.org/10.1016/j.envsoft.2019.104609

Wang, N., Jassogne, L., van Asten, P.J.A., Mukasa, D., Wanyama, I., Kagezi, G., Giller, K.E., 2015. Evaluating coffee yield gaps and important biotic, abiotic, and management factors limiting coffee production in Uganda. Eur. J. Agron. 63, 1–11. https://doi.org/10.1016/j.eja.2014.11.003

Whish, J.P.M., Herrmann, N.I., White, N.A., Moore, A.D., Kriticos, D.J., 2015. Integrating pest population models with biophysical crop models to better represent the farming system. Environ. Model. Softw. 72, 418–425. https://doi.org/10.1016/j.envsoft.2014.10.010

Willmott, C.J., 1981. On the Validation of Models. Phys. Geogr. 2, 184–194. https://doi.org/10.1080/02723646.1981.10642213

Willocquet, L., Savary, S., Fernandez, L., Elazegui, F.A., Castilla, N., Zhu, D., Tang, Q., Huang, S., Lin, X., Singh, H.M., Srivastava, R.K., 2002. Structure and validation of RICEPEST, a production situation-driven, crop growth model simulating rice yield response to multiple pest injuries for tropical Asia. Ecol. Model. 153, 247–268. https://doi.org/10.1016/S0304-3800(02)00014-5

Wit, C.T. de, 1982. Simulation of living systems, in: Simulation of Plant Growth and Crop Production. Pudoc, pp. 3–8.

Wit, C.T. de, Vries, F.W.T.P. de, 1982. L'analyse des systemes de production primaire, in: La productivite des paturages Saheliens. Pudoc, pp. 20–23.

Yan, H., de Reffye, P., Pan, C., Hu, B., 2003. Fast construction of plant architectural models based on substructure decomposition. J. Comput. Sci. Technol. 18, 780–787. https://doi.org/10.1007/BF02945467

Yates, K.L., Bouchet, P.J., Caley, M.J., Mengersen, K., Randin, C.F., Parnell, S., Fielding, A.H., Bamford, A.J., Ban, S., Barbosa, A.M., Dormann, C.F., Elith, J., Embling, C.B., Ervin, G.N., Fisher, R., Gould, S., Graf, R.F., Gregr, E.J., Halpin, P.N., Heikkinen, R.K., Heinänen, S., Jones, A.R., Krishnakumar, P.K., Lauria, V., Lozano-Montes, H., Mannocci, L., Mellin, C., Mesgaran, M.B., Moreno-Amat, E., Mormede, S., Novaczek, E., Oppel, S., Ortuño Crespo, G., Peterson, A.T., Rapacciuolo, G., Roberts, J.J., Ross, R.E., Scales, K.L., Schoeman, D., Snelgrove, P., Sundblad, G., Thuiller, W., Torres, L.G., Verbruggen, H., Wang, L., Wenger, S., Whittingham, M.J., Zharikov, Y., Zurell, D., Sequeira, A.M.M., 2018. Outstanding Challenges in the Transferability of Ecological Models. Trends Ecol. Evol. 33, 790–802. https://doi.org/10.1016/j.tree.2018.08.001

Yin, X., 2003. A Flexible Sigmoid Function of Determinate Growth. Ann. Bot. 91, 361–371. https://doi.org/10.1093/aob/mcg029

Zeigler, B.P., 1989. DEVS representation of dynamical systems: event-based intelligent control. Proc. IEEE 77, 72–80. https://doi.org/10.1109/5.21071

Zeigler, B.P., Muzy, A., 2017. From Discrete Event Simulation to Discrete Event Specified Systems (DEVS). IFAC-Pap., 20th IFAC World Congress 50, 3039–3044. https://doi.org/10.1016/j.ifacol.2017.08.672

Zhao, X., De Reffye, P., Houllier, F., Hu, B.-G., 2003. Interactive simulation of plant architecture based on a dual-scale automaton model.

Chapter 1: Coupling Plant and Pest Models: Conceptual Foundations and the MIMIC Framework

1. Introduction

We aim to develop a formalism that explicitly captures all coupling effects on the dynamics of the integrated models over extended temporal scales, ideally spanning the entire lifespan of a perennial plant. The proposed implementation of inter-model interactions is designed around a modular architecture that manages interactions independently, inspired by the principles outlined in (Siad et al., 2019). In this framework, all models and components exchange information through standardized communication interfaces, facilitating the seamless integration of diverse pest and disease (P&D) models without necessitating modifications to the core interaction structure.

Such a coupling strategy promotes flexibility and extensibility but inherently introduces challenges related to temporal desynchronization and the heterogeneity of model time steps and dynamics. These issues must be addressed to ensure coherent and biologically realistic simulations across coupled components.

This chapter presents the article published in Plant Phenomics detailing the development and implementation of the coupling formalism, named MIMIC (Modular Interaction Model for Integrated Coupling).

Plant Phenomics
A SCIENCE PARTNER JOURNAL

DATABASE/SOFTWARE ARTICLE

Coupling Plant Growth Models and Pest and Disease Models: An Interaction Structure Proposal, MIMIC

Houssem E. M. Triki[1,2,3,4*], **Fabienne Ribeyre**[3,4], **Fabrice Pinard**[4,5], **and Marc Jaeger**[1,2]

[1]CIRAD, UMR AMAP, F-34398 Montpellier, France. [2]AMAP, University of Montpellier, CIRAD, CNRS, INRAE, IRD, Montpellier, France. [3]CIRAD, UMR PHIM, F-34398 Montpellier, France. [4]PHIM, University of Montpellier, CIRAD, INRAE, Institut Agro, IRD, Montpellier, France. [5]CIRAD, UMR PHIM, 00100 Nairobi, Kenya.

*Address correspondence to: houssem.triki@cirad.fr

Citation: Triki HEM, Ribeyre F, Pinard F, Jaeger M. Coupling Plant Growth Models and Pest and Disease Models: An Interaction Structure Proposal, MIMIC. *Plant Phenomics* 2023;5:Article 0077. https://doi.org/10.34133/plantphenomics.0077

Submitted 31 March 2023
Accepted 10 July 2023
Published 4 August 2023

Copyright © 2023 Houssem E. M. Triki et al. Exclusive licensee Nanjing Agricultural University. No claim to original U.S. Government Works. Distributed under a Creative Commons Attribution License 4.0 (CC BY 4.0).

Coupling plant growth model with pests and diseases (P&D) models, with consideration for the long-term feedback that occurs after the interaction, is still a challenging task nowadays. While a number of studies have examined various methodologies, none of them provides a generic frame able to host existing models and their codes without updating deeply their architecture. We developed MIMIC (Mediation Interface for Model Inner Coupling), an open-access framework/tool for this objective. MIMIC allows to couple plant growth and P&D models in a variety of ways. Users can experiment with various interaction configurations, ranging from a weak coupling that is mediated by the direct exchange of inputs and outputs between models to an advanced coupling that utilizes a third-party tool if the models' data or operating cycles do not align. The users decide how the interactions operate, and the platform offers powerful tools to design key features of the interactions, mobilizing metaprogramming techniques. The proposed framework is demonstrated, implementing coffee berry borers' attacks on *Coffea arabica* fruits. Observations conducted in a field in Sumatra (Indonesia) assess the coupled interaction model. Finally, we highlight the user-centric implementation characteristics of MIMIC, as a practical and convenient tool that requires minimal coding knowledge to use.

Introduction

Agroecological transition is an active research and development area, in which modeling agronomical system productions must be assessed from complex systems modeling in regard to the processes involved in and their interactions. As mentioned by Brandmeyer and Karimi [1], "complex environmental problems involve processes that occur both within and between environmental media"; thus, both aspects must be considered to build efficient model couplings.

The authors underline the difficulties in handling how the different models interact with each other. In each field of study, modeling communities developed their own techniques and frameworks for creating efficient simulation models of the processes they are interested in [2]. Nevertheless, certain problems and complications are not specific to one discipline.

In particular, the integration of the potential intertwined effects that the dynamics of certain models may have on each other and the compatibility of their architecture [3] focus our interest.

Indeed, we are interested in an application in the environmental domain, more specifically, in estimating plant production under certain conditions. In general, the productivity of a plant that has been attacked by a pest or a disease (pest and disease (P&D)) is assessed in the short term. P&D directly damages one or more organs of the plant by targeting them. If the infected organs encompass the fruits, then yield reductions are direct. Production projections at mid- and long term are seldom considered.

However, even if the fruits are not directly affected by the attack, the future yield and growth of the plant are usually affected because of the decrease in biomass production (e.g., an attack on the leaves reduces light interception). In addition, these effects alter plant growth by changing the balance between organs and potentially the distribution of resources; Fig. 1 illustrates such an effect.

These feedback effects are rarely taken into account when coupling descriptive models. This is, in part, due to the lack of mechanistic dynamic approaches reported at the organ level to model and simulate the interactions between plant growth and P&D attacks [4]. Therefore, feedback to the plant itself can hardly be assessed. Another critical point is that, even when mechanistic models are available, their coupling potential is not evaluated, both for computational cycles and for the data on which they interact with each other.

To determine more precisely the thresholds at which P&Ds are likely to have a important economic impact on production [5] and to make an appropriate treatment decision, a coupled model operating over the long term would be helpful.

Such a model could provide a more accurate estimation of the effects of climate change on plant phenology/biotic

Downloaded from https://spj.science.org at Cirad Dist on August 31, 2023

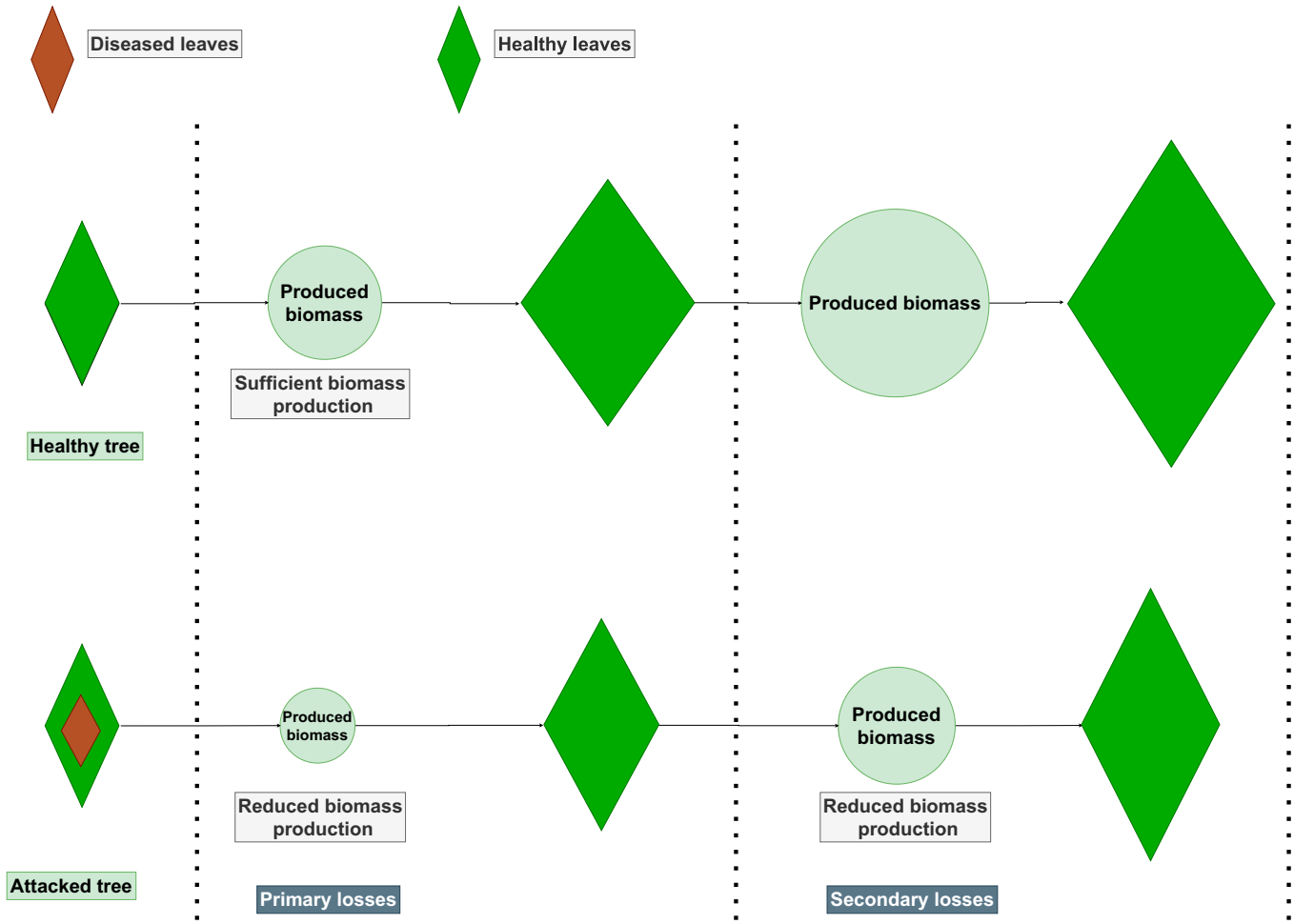


Fig. 1. Interactions between P&D dynamics and coffee phenology. Case of a leaf disease affecting the biomass accumulation with a cumulative effect on the long-term plant growth.

development. In the last decade, Uganda has experienced a great resurgence of P&Ds in coffee tree fields [6,7] despite the important efforts of national institutes to create resistant clones, especially for coffee wilt disease (*Fusarium xylarioides*). In addition to this, climate change induces new environmental conditions affecting plant growth dynamics and the dynamics of pathogens and insects [8–10]. Consequently, the coffee berry borer (CBB) (*Hypothenemus hampei*) and coffee leaf rust (CLR) (*Hemileia vastatrix*) are present in Uganda, although at moderate levels. However, severe cases of red blister (*Cercospora coffeicola*), which affects leaves and berries; of black twig borer (*Xylosandrus compactus*) [11]; and of coffee wilt disease [12–14] are now reported. This region combines multiple P&Ds that affect coffee trees at various organs and scales. Thus, we consider it as a good experimental field for an application of coupling framework.

Objectives and scope

Our overall goal is to assess variation in production linked to P&D and related mechanisms at the plant and crop scales, as well as the impact of crop practices. These elements can only be accessed through models. In other words, as suggested by Cerda et al. [15] and Gaunt [16], the estimated effects of P&D on plants are considered to result from interactions between dynamic models: the plant growth model (considered at least at the organ scale), the P&D model, and even a human intervention model (treatment, harvest, etc.). We are thus facing a complex system involving processes that interact at different levels, with the possibility of collective behaviors and relationships with the environment [17].

We propose here a specific coupling framework taking into account (a) the specific difficulties encountered when dealing with complex systems (cycle synchronization, data concurrency and sharing, etc.); (b) the specific difficulties related to the nature and type of models involved for plant growth and P&D dynamics models; (c) the limitation of technical complexity, as users are usually not specialized in automation and their convex domains; and (d) the possibility to add models without modifying other models already involved in the framework.

About plant growth models

In agronomy, process-based models (PBMs) and functional structural plant models (FSPMs) are 2 major frameworks to model plant growth dynamics.

PBMs, generally referred to as crop models, estimate the biomass produced mainly from the intercepted light by leaves per unit area (m^2)[18]. The different organs are grouped into distinct compartments. The distribution of produced biomass within each compartment is differentiated, allowing yield estimation. However, PBMs do not consider the organ typology

Downloaded from https://spj.science.org at Cirad Dist on August 31, 2023

resulting from the plant's structure, the plant phenology, nor the mechanisms that occur within the plant.

The FSPM aims at modeling the establishment of the plant structure and the functioning of the organs. In FSPM, the properties and functions of each organ are taken into account [19]. In particular, the distribution of biomass produced by the different organs is followed at the scale of each organ in the whole plant. Such models operate on the individual plant scale and generate an explicit 3D geometric representation of the plant. However, using FSPM formalism requires calibrations of the model parameters that are often cumbersome.

Nevertheless, with a limited number of assumptions and the use of certain PBM formalisms, it is possible to factorize the processes involved in FSPM, based on the attributes of the organ structural criterion, and generate a model with a reduced complexity [20]. Such a design is illustrated by the GreenLab formalism [21]. It applies the notion of a common biomass pool, assessed on several crops of interest [22]; uses the traditional light interception model of PBM; and operates with cohorts of organs defined from chronological and physiological ages [23,24]. Furthermore, this style of formalism allows to move from the individual plant level to the crop level.

About P&D models

There are numerous ways to design and qualify P&D models. We distinguish here 2 categories, statistical models and mechanistic models.

Statistical models are developed from data and statistical correlations between model variables. These models are capable of prediction but are difficult to transfer; they are difficult to project beyond the spatial and temporal boundaries of their underlying data [25].

Mechanistic P&D models include explicit hypothesis on biological mechanisms that influence the dynamics of the P&Ds. These models can be used to simulate the P&Ds on different scales (plots, regions, countries, etc.) [26,27]. Notions of cohorts are also often inherent in these approaches, quantifying populations of similar age and behavior.

Plant and P&D model coupling

Conceptually, coupling 2 or more processes together falls into one of the following categories, inspired by [28]:

1. Sequential coupling or loose coupling: Models are completely decoupled or models exchange data through inputs/outputs (I/O).
2. Shared coupling: (a) GUI (graphical user interface): Models share a common GUI or (b) Data: Models share the full I/O database.
3. Embedded or integrated: One model is fully contained within the other (usually as a subroutine) or model codes are merged into a single coherent model.
4. Framework coupling: Use of a global modeling framework, where the models are coupled using a third-party tool commonly called "Coupler," based on a combination of the previous methods.

The literature on coupling plant and P&D models to estimate plant production agrees that this is a challenge, requiring more physiological and field studies [29]. Studies are still scarce on the subject today. The most popular categories of coupling are loose coupling and integrated coupling.

The DynACof coffee plant model [30] is a dedicated PBM. In a recent study, it was linked to a rust model, with a loose coupling defined by the ratio of healthy to damaged leaf area [31].

Interaction through data is easy to manage, but this type of coupling requires some synergy between models. It is difficult to generalize to multiple models or interaction cases if the I/O do not match the requirements of each model. To circumvent this type of problem, a modeling environment may be mobilized such as OpenAlea [32]. This platform provides users an interface to create interactions between plant (sub)models and their environments. OpenAlea allows couplings ranging from simple sequential to shared coupling; users can simply define model sequences or build graphs to connect I/O models with a generic graphical interface: VisuAlea. The platform also provides multiple analysis and visualization tools. However, even if users are able to produce interacting models, this still requires coding to adjust or add other components [33].

The theoretical study conducted by Qi et al. [34] models the palm tree under pest attack, whose population is also constrained by auxiliary insects; the population dynamics and attack models of P&D integrate the plant growth model. This is a case of embedded and integrated coupling. Here, the feedback on biomass and plant populations is well evaluated over the long term, but while the plant model is generic, the insect models and interactions are not: Attacks are limited to leaf damage, and synchronization is implicit and climate conditions are supposed to be stable.

Recently, Motisi et al. [35] propose an integrated approach to such a system by decomposing the P&D model (leaf rust) and the growth model (coffee) into smaller models, acting as submodels embedded in each other, building an integrated coupling.

Le Chevalier et al. [36] developed a framework, inspired by the DEVS (Discrete Event System Specification) mathematical formalism [37], involving a simple big leaf implementation of the GreenLab model with a climate model (rainfall and temperature) and a water diffusion model (runoff, soil diffusion, and plant uptake); this framework allows modeling growth variability related to plant competition for water and local conditions such as altitude and orientation.

A common drawback of these examples is their lack of generality, especially regarding adding/changing P&D models or changing plant species. This is reflected in the limited literature that combines abiotic (climate) and biotic (P&D and/or farmer) influences on the plant [4]. Classically, model interactions are assessed by mutually coupling models together. However, this method is case specific and difficult to generalize even using a platform such as OpenAlea, as highlighted by Garin et al. [38].

The work presented here is part of a study focusing on P&D attacks on Robusta coffee in Uganda and, more specifically, on fruits with red blister and CBB; on leaves with CLR; and on young branches with black twig borer. We address modeling the interactions occurring at various levels of the plant with different P&D models over a large period (theoretically, the entire life span of the plant). To this end, our proposal is based on a "framework coupling" that encompasses the various coupling categories outlined previously [28].

In the following contribution, the rationales and components of the proposed model coupling framework are presented

Downloaded from https://spj.science.org at Cirad Dist on August 31, 2023

first. The framework's architecture and implementation are then explained. We then present a case study including the CBB and a fructification model. Before concluding, the framework structure genericity and assumptions are discussed.

Materials and Methods

Framework design assumptions

Although our applications are dedicated to the evaluation of coffee production under P&D attacks, we aim to develop a generic approach, adapted to many interactions mobilizing agronomical models, but not as generic as an implementation under DEVS (some arguments are given in the discussion) [37]. The latter would strongly put constrains on how to define the models and their inner mechanisms, particularly with regard to their synchronization procedure.

OpenMole could also be considered as an alternative [39]. However, OpenMole is not strictly a model coupling environment, and it does not provide an environment to design models from scratch. OpenMole shows high interest for analyzing existing interaction codes. It helps modelers to evaluate the sensitivity of their models' parameters and optimize them. Once finalized, at exploitation stage, OpenMole offers valuable upscaling deployment mobilizing cloud or HPC.

In MIMIC (Mediation Interface for Model Inner Coupling), our focus is to assist the user in the creation of the basic structures of the interaction. We may thus consider that an interaction model could be first created with MIMIC and then be integrated into management environments such as OpenMole.

Before describing our approach, we list here the founding assumptions of our framework.

Because we aim to integrate feedback on the plant growth model, we focus on developing the framework at the individual plant scale. This self-imposed condition allows us to implicit the spatial aspect involved in many P&D attacks.

Associating the effects of the dynamics of different models can be complicated, especially when considering models that work on different time scales or natures (chronological or thermal) and when considering feedback. The users must therefore be able to define a cycle correspondence between the third party and each model.

Among the different formalisms of plant growth models mentioned above, the adoption of a cohort-based formalism allows flexibility in the coupling of models by reducing the number of parameters required for calibration [40]. In addition, this formalism offers the advantage of incorporating plant growth feedback on organogenesis for the expression of plasticity in a competitive context [41] and provides practical means for parameter evaluation [42], including the case of functional feedback on the plant structure [43]. The structure calculation is implicit; calculations are factorized as defined by the number of organ types and cohorts (organ ages and physiological states), leading to short computation times [44] and, thus, minimizing interaction complexity. For P&D models, some correspondence with the type of plant model is necessary to reduce the complexity of the coupled system. For this reason, models using groups (cohorts) of populations are preferred.

Some P&D models are "individual-based" or based on age groups to take into consideration that various stages of development do not always react the same way to environmental factors (sometimes called cohort). In study of Rodríguez et al. [45], the term "cohort" designs a group of plants and CBB that are all the same age.

This assumption allows to take cohorts from each model and to create new ones with flexible criteria (see the discussion first section). Thus, the users can manipulate the outputs of the models and even add new interaction-related variables to define the new cohorts.

The proposed approach is framework based, which means that all models involved interact through a third party and do not interact directly with each other. The models involved must be able to initiate a computation at a given step, reading their inputs and providing outputs for the requested step. The models mobilized to interact should not be heavily modified, and their internal structure or operation must not be altered by the coupling.

MIMIC, a formal framework for interaction

In this study, the third-party tool is called MIMIC. MIMIC handles interactions between models in a flexible way, regardless of the number and types of models. In addition, while the development is based on the interplay between P&D and the plant growth model, this framework is not exclusive to P&D. MIMIC ensures coupling effects on the dynamics of all models on a long-term time scale.

MIMIC: Overview and principles

MIMIC manages the connection between models and their inputs and outputs. The fundamental assumption of the model is that each model operates and evaluates its own internal states in a finite amount of time, from one internal step to the next. MIMIC supervises the interaction through its own states and information, which are evaluated on the basis of the information collected from the connected models.

On the basis of the information obtained from the output of the models, MIMIC manages the underlying mechanics of the interaction between the components; there is no limit to the number of models that can be linked together. This reduces the expected complexity of such system combinations and allows for easy handling and independence of the models. Moreover, when developing a new application (adding elements and changing dynamics), no changes are required to MIMIC's kernel. This is an advantage from a development point of view because each component execution process is distinct and can be modified independently, which sustains the correct execution of the framework.

MIMIC: The components

MIMIC can be considered as a hyper model consisting of 3 main components, as shown in Fig. 2 in its central part. These components solve the problems classically encountered when coupling different and multiple dynamic systems, from desynchronization to feedback integration.

The first component schedules the simulations according to the temporalities of the connected models. The Cycle Synchronizer (CS) executes the connected models and starts the interaction process between the involved models. This component prioritizes multiple interacting models based on users' preferences. The second component, the Interaction System States Server (ISS), serves the communication protocols used to create the MIMIC state variables (variables used for interactions). Finally, the third component, the Interaction State and Data Recorder (ISDR), ensures the integrity of the interaction and the state variables of the coupling interface connecting the interacting models. It also manages data and other dynamics that are not required for interaction but can be requested by the users for observation purposes.

Cycle Synchronizer (CS)

Downloaded from https://spj.science.org at Cirad Dist on August 31, 2023

The CS component is built around a specific behavior design pattern called Mediator (Fig. 3), which describes how objects interact with each other. The Mediator promotes loose coupling by preventing objects from referring to each other explicitly and allows some independence between them [46]. A so-called "behavioral model" reduces chaotic dependencies between components. It forbids direct communication between them and requires them to collaborate only through the Mediator.

The activities of each model and component are scheduled using this Mediator-based component. Thus, it addresses the problems related to desynchronization. An essential point concerns the definition of scheduling. Typically, as defined in the DEVS formalism [47], a temporal base reference must be addressed to each connected model, and each model must be able to return its own cycle conversion step in the temporal reference.

For example, many P&D models operate by generations resulting from climate data (and other parameters), but plant models typically define their cycle from organogenesis (from a thermal calendar). In this case, an effective method is to have the users set the default time cycle in the interface based on the smallest cycle of the models available during the initialization phase and then mobilize a function (e.g., a function related to climate data) to retrieve the average daily temperature from which the interface calculates the date of the next plant growth stage.

Interaction System States Server (ISS)

When one of the models is active (running), its state variables pass through this component and are converted to MIMIC's state variables. This operation creates a state variable that can be understood by any other model involved in the interaction. The definition and translation of the ISS state variables are the responsibility of the users, based on their knowledge of the interacting models and the desired observations. State variables are of 3 types: (a) state variables considered as output copies of the connected models, (b) state variables specific to the internal operations of MIMIC, and (c) state variables defined by the users to encode the interaction between models and MIMIC.

Interaction State and Data Recorder (ISDR)

In this component, in addition to interaction-relevant states, data collected from connected models and internal data resulting from computations within the interface are recorded and stored at each event (when any model is executed) processed in the schedule. The storage of state variables and data from the coupling model interface makes stop-and-go simulation available. In a broader sense, storing interaction state and data allows users to access a simulation from a previous date in the scheduler, rerun it, and simulate different scenarios by dynamically adjusting the simulation parameters. The results of the interaction simulation are accessible directly from MIMIC, without going through the associated models. The results are adaptable, independent of the simulation itself, and can be read backward and forward (to the last event of the simulation).

To illustrate the MIMIC framework, a simple attack case is considered below.

A case study: The CBB and Arabica coffee

In this simple example, we consider the CBB that attacks coffee berries. We assume that, at the time scale considered, there is no visible effect on plant growth.

The CBB model

H. hampei (Ferrari) is a pest known as CBB, belonging to the order Coleoptera, family Curculionidae, and subfamily Scolytinae [48]. This small beetle originates from Central Africa and is present in all coffee-producing countries of the world.

A CBB hatches from an egg in the seed of a coffee berry. When the fertilized females leave the fruit, they colonize another

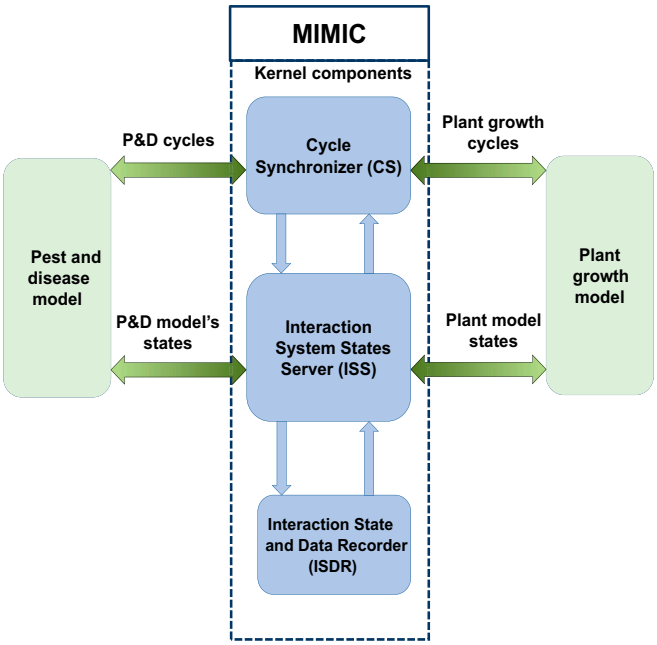


Fig. 2. The "Mediation Interface for Model Inner Coupling" (MIMIC) schematics, illustrating the kernel components (in blue) on a coupling example with a P&D model (left green box) and a plant growth model (right green box).

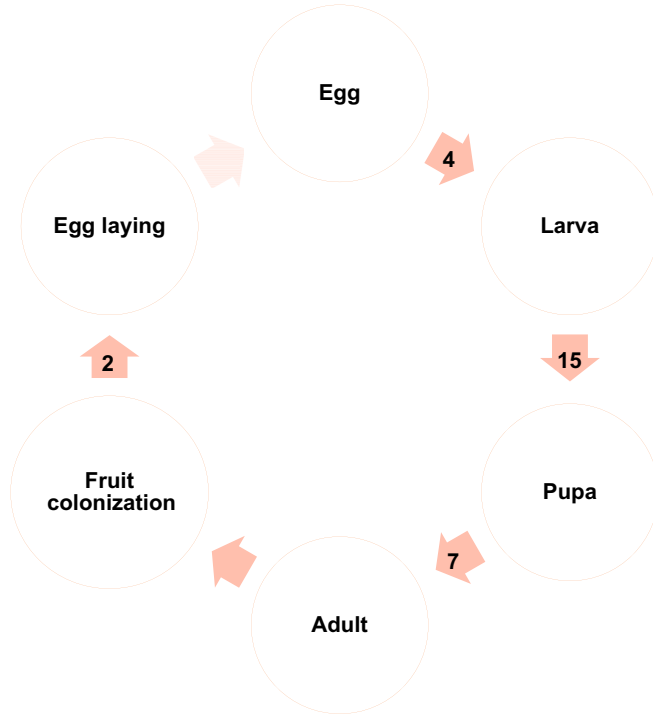


Fig. 3. Female CBB life cycle representation. Circles stand for the stages. Arrows stand for transitions with their average duration in days. Light-colored arrow means the restart of the cycle for another generation.

Downloaded from https://spj.science.org at Cirad Dist on August 31, 2023

one and start their own colony (Fig. 3). The factors triggering the exit from the fruit are the age of the insect and the climate (temperature, humidity, and rain). CBB is attracted to by red (ripe) fruits and green fruits (if they are large enough). The insect is more attracted by red than green fruits; however, if the number of attractive fruits is small, then CBB will colonize overripe fruits or fruits that have fallen to the ground. The average life span of a female CBB is nearby 45 d [49].

Fruits are grouped into 3 distinct categories. "Very attractive fruits" (VAp) are ripe fruits, from the moment they turn red. "Attractive fruits" (Ap) are well-developed green fruits. This category includes green fruits larger than 5 mm, with seeds capable of hosting the CBB, to fruits that turn yellow. "Ground fruits" (G) are all fruits fallen to the ground, whatever the former category they belonged to. In the proposed model, each of the above fruit categories has an attraction factor that influences whether CBB chooses to colonize a fruit or not.

Population monitoring is based on the grouping of different individuals within a population having the same oviposition day. Male CBBs are not considered in monitoring of populations as they do not play any role in the epidemic propagation (they represent only $\frac{1}{10}$ of the individuals in a colony and are not disseminated). As already mentioned, population dynamics depend on temperature, relative humidity, and precipitation.

The cohorts of the model are built by crossing the groups of individuals and the categories of fruits where these individuals live.

Table 1. CBB's cohort distribution based on population hatching day and colonized fruit category.

CBB population/fruit category	*Hatched the 1st day*	*Hatched the 2nd day*	...	*Hatched the nth day*
Very Appealing fruits	Cohort (1, VAp)	Cohort (2, VAp)	...	Cohort (n, VAp)
Appealing fruits	Cohort (1, Ap)	Cohort (2, Ap)	...	Cohort (n, Ap)
Fruits on the grounds	Cohort (1, G)	Cohort (2, G)	...	Cohort (n, G)

On each simulation step, the results of new attacks are grouped into 2 categories: population data and fruit data. The population data contain information about each population group for a given day. It contains the date when this group left its original fruit to colonize other fruits, the number of flying CBB, the number of dead CBB, and so on. The fruit data include the fruit categories presented above. In addition, they are divided into 2 subgroups, healthy and colonized fruit. The result is a cohort of fruit categories attacked by a quantity of CBB hatched on a given day.

The coffee fruit cohort model

In the Sumatra region of Indonesia, Arabica coffee trees produce coffee berries throughout the year. With the presence of rainfall throughout the year and an average daytime temperature between 22 and 30 °C, the equatorial climate provides the necessary conditions for the trees to flower. A plant growth model is created as a reduced model to simulate fruiting only. We designed a cohort fruit model inspired by the GreenLab cohort assumption: Fruits with the same parameters (chronological age, physiological age, and sink power) are merged into the same cohort. An automaton is created that build fruit cohorts on the basis of the obseved numbers of berries harvested. Then, the model estimates the age of the fruits according to the harvest frequencies and the climatic data.

Human intervention model

Human intervention is represented here as a simple harvest model. This model simulates harvesting of red berries at dates that correspond to observed data, which is useful for validation by comparing simulated data to actual data.

Integration of the coffee–CBB interaction

When CBB attacks a fruit on the tree, the inner seed is damaged, but the fruit continues to develop and the biomass is still distributed. We therefore consider that the feedback on the plant is negligible. Thus, in this case, the interaction focuses on the state of the fruits (attacked or healthy).

Interaction between the 2 models is achieved by converting the numbers of attacked fruits provided by the CBB model into the cohorts of the plant model An additional state variable ISS is created in MIMIC: the status of the cohort. This additional data is Boolean, indicating whether the cohort is colonized by the CBB.

Validation data

To validate the functioning of the interface, we used climatic, fruiting, and attack data on 2 coffee trees in Indonesia for almost a year [50]. The observations were not made daily but separated by slightly irregular periods of time (about 20 d between each observation). This implies a daily operation of the model and an estimated chronological age of the initial populations. The solution chosen was to consider maturation occured exactly between 2 observations. A CBB colony is established at the start of the simulation and begins its development. The number of colonized fruits is initialized by the observed data. Because there is no data for fruit on the ground, this category was discarded from the simulation.

The study case and simulation results are presented below, after detailing the overall implementation aspects.

Implementation and Results

We present here the implementation of MIMIC, starting with the architecture before detailing the components and some specific features and functions.

Architecture (kernel, pseudo-models, and models) of MIMIC

Using MIMIC, to integrate models into an interaction structure, results in a software architecture composed of 3 layers (Fig. 4). The first layer consists of the models involved in the coupling. These models are independent and external to MIMIC. They are only linked to MIMIC through the second layer: the pseudo-model's layer.

Downloaded from https://spj.science.org at Cirad Dist on August 31, 2023

The pseudo-models (red blocs in Figs. 4 and 5) are wrappers of the interacting models of the first layer. This association is unique and bijective. This layer is automatically created by MIMIC at the initialization stage. The pseudo-models provide all the information about the models, which are requested at run time. The third layer (blue blocs in Figs. 4 and 6) is the core of the MIMIC protocol. Composed of 3 components, it schedules, manages tasks, and manages data exchanges. The 3 specific components are described below.

Functioning of MIMIC's components

Models' layer

Models are independent of MIMIC. They exchange only data with MIMIC (state variables, cycles, etc.) each time an execution call is processed.

Pseudo-models' layer

Pseudo-models are automatically generated by MIMIC in an initialization process, from parameters and information related to the models, provided by the user (Fig. 5) filling a YAML file (see the User layer here under) [51]. The generated pseudo-model's variables host the data requested for simulation and interaction (state variables, arguments, step size, and path to the model code), as well as the current model cycle and state (running, pending, or unsolicited). The "mediator" field links the pseudo-model to the kernel.

MIMIC also generates the pseudo-models' functions. "Call model" refers to the function used to call the related model. The 2 other functions are the constructor of the link to the MIMIC kernel (using "Addmediator") and the constructor of the notifications to the kernel (using "Notifymediator").

MIMIC's kernel layer

The 3 components of the MIMIC's kernel (CS, ISS, and ISDR) are directly connected to one another through a shared communication bus (Fig. 6).

The CS controls how MIMIC manages and runs processes (Fig. 6, top). The function "UpdatesSchedule" is called each time a model or component is requested to close an event; it updates the list of scheduled tasks (Table 2), stored in the variable "Schedule." This type of dynamic scheduling allows interaction between models with different and varying step times or time natures, e.g., calendar and thermal time.

At each event, the "NotifyUser" function send messages to the console in a log file, allowing the user to follow the simulation step by step.

The ISDR stores interaction-relevant state variables and simulation data (task schedule, last model run, etc.) step by step. This simulation data logging is convenient for stop-and-go implementation. The ISDR is also appropriate when using a model with numerous outputs, from which a subset is requested to interact with variables in other coupled models. This component delivers the simulation results to the user.

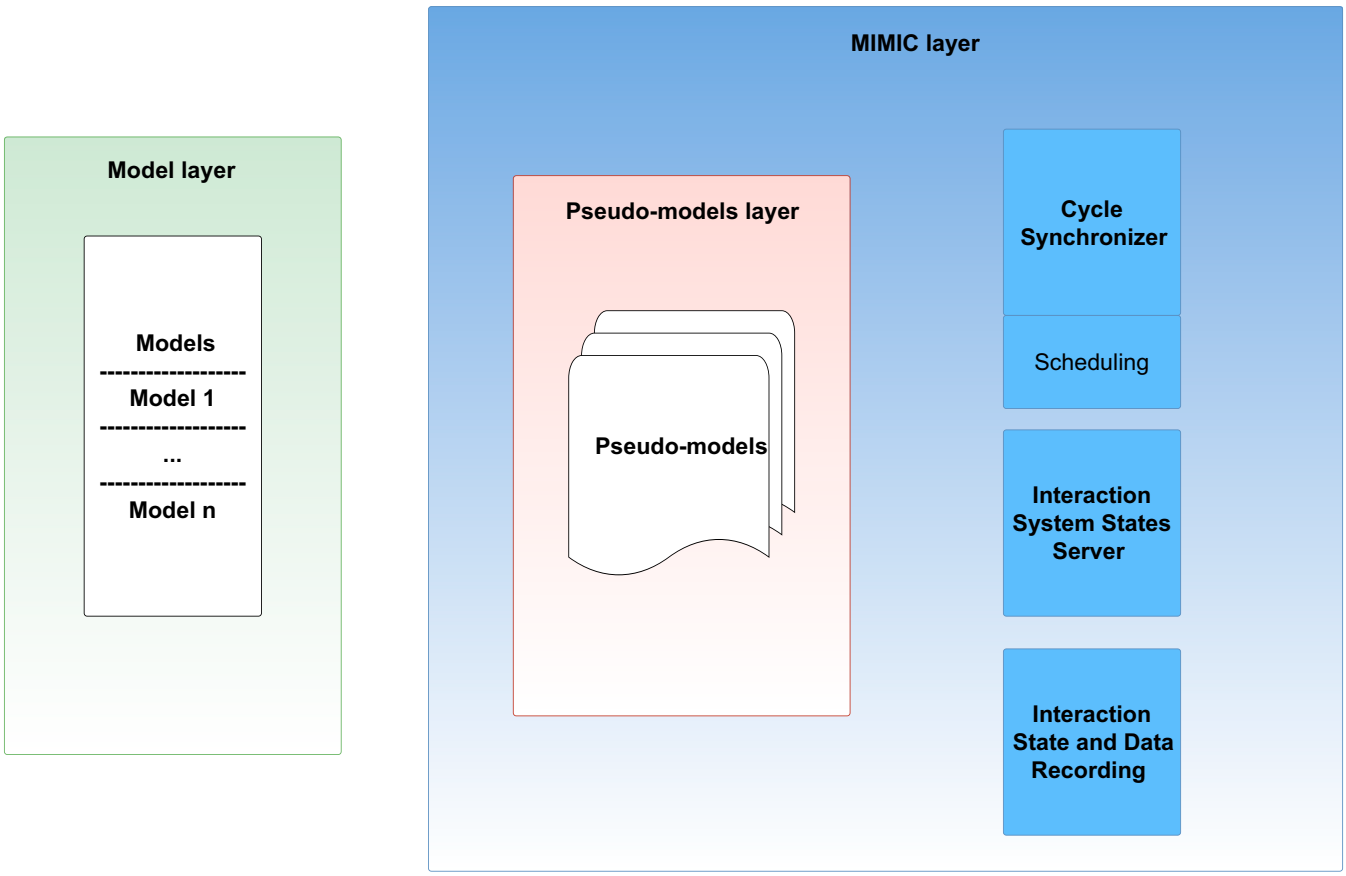


Fig. 4. MIMIC's and models' layer composition. The framework is composed of 3 layers: layer 1 (in green) stands for the external models, layer 2 bloc (in red) contains the pseudo-models, and layer 3 (in blue) contains MIMIC's functioning components.

Downloaded from https://spj.science.org at Cirad Dist on August 31, 2023

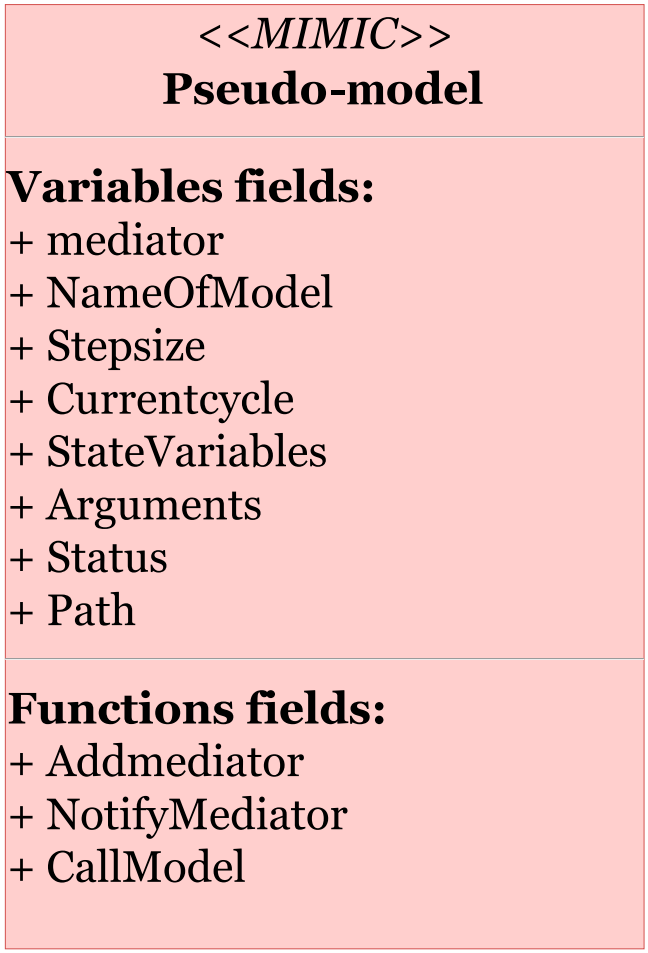


Fig. 5. Representation of pseudo-models as Unified Modeling Language (UML) (red bloc in Fig. 4). The structure of a pseudo-model (generated by MIMIC) with its variable and function fields. Mediator fields link the pseudo-model with the kernel, while the "CallModel" function links to its "external model." Note that in this UML diagram (and the following one), variables are values (input/output) used by the component, while functions are specific programs related to the component.

Each time a pseudo-model is executed, the ISS is solicited to convert or translate the state variables (the output) of the pseudo-model to MIMIC state variables (the ones used in the interaction codes). Thus, they can be used as inputs for the other pseudo-models.

The user's layer or how the users communicate with MIMIC

Interactions in MIMIC are generated from the users' instructions, covering the following 2 aspects: (a) the interaction code itself written by the user and so-called UIM (user interaction model) and (b) the control of the simulation, the so-called UC (user simulation control).

In both cases, the instructions are processed through the "User–MIMIC communication" component. Indeed, we want the kernel being untouched and safe from external process to guarantee the platform integrity.

In MIMIC, we consider the UIM and UC as pseudo-models. This offers numerous interests. It keeps the architecture consistent as a whole; the state variables of the interaction can be kept and made available easily; it gives the potential to build a hierarchical embedding of applications; the user can define active observers (acting as controllers operating according to results gained in the interaction code).

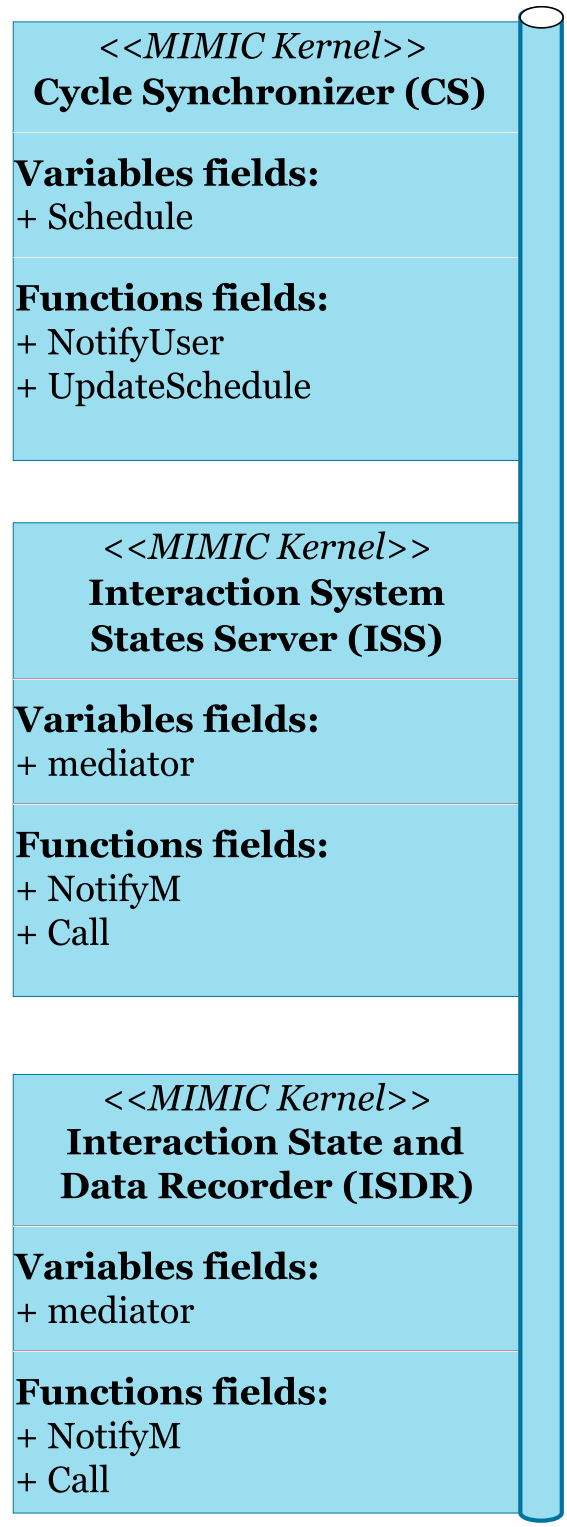


Fig. 6. MIMIC's kernel UML representation (blue bloc in Fig. 4), describing the data structure of MIMIC's main components (Cycle Synchronizer, Interaction State and Data Recorder, and Interaction System States Server) linked through a communication bus (blue cylinder).

Downloaded from https://spj.science.org at Cirad Dist on August 31, 2023

Table 2. The case study tasks list and the schedule after 10 simulation steps. (A) List of events submitted to the scheduler. (B) The events agenda of the scheduled tasks. On both lists, parameters are the following, from left to right: name of model (Model3 stands here for the human model), step size for the model, last time executed, next time to be executed, and status in the schedule.

A.Submitted event list

Rank	Process Id (name)	Step size	Order time	Exec time	Status
1	Tasks_Desk «CBB»	3.0	0.0	3.0	«Completed»
2	Tasks_Desk «Coffee_tree»	4.0	0.0	4.0	«Completed»
3	Tasks_Desk «CBB»	3.0	3.0	6.0	«Completed»
4	Tasks_Desk «Model3»	8.0	0.0	8.0	«Completed»
5	Tasks_Desk «Coffee_tree»	4.0	4.0	8.0	«Completed»
6	Tasks_Desk «CBB»	3.0	6.0	9.0	«Completed»
7	Tasks_Desk «Coffee_tree»	4.0	8.0	12.0	«In Queue»
8	Tasks_Desk «Model3»	8.0	8.0	16.0	«In Queue»
9	Tasks_Desk «CBB»	3.0	9.0	12.0	«In Queue»

B.Tasks scheduled at time 10

1	Tasks_Desk «Coffee_tree»	4.0	8.0	12.0	«In Queue»
2	Tasks_Desk «CBB»	3.0	9.0	12.0	«In Queue»
3	Tasks_Desk «Model3»	8.0	8.0	16.0	«In Queue»

The user–MIMIC communication component is, in fact, a parser that creates metadata for building the pseudo-models and the connections to the kernel (Fig. 7).

User interaction model (UIM)

Users write in Julia language, the code describing the interaction between the models, using the pseudo-model's state variables and pseudo-model's calls. However, using Julia to encode the UIM is not a requirement: (a) The interaction code can also be an "external" model, belonging to the model layer. This method leads to a higher level of complexity and lower performance since requesting to be wrapped in a pseudo-model. (b) Next, if the level of coupling is weak, operating only on the inputs and outputs of the models, forming a "shared coupling" as defined in [23], then the user is not requested to provide any UIM. The simulation starts directly from the initial schedule and runs from the explicit cycle input and output definitions described for the pseudo-model generation.

User simulation control (UC)

The UC defines the information related to the execution of models for simulation. These descriptions are presented in the form of a file in YAML format. The UC is used to parse the model metadata and create the variables to be mobilized during the interaction execution process. An example of such a file is given in Table 3. Some input fields are required, while others, left by the user, are filled with a default value. In the table, the name given to the model is "Tree." However, if no value was provided, then "model_n," where *n* is the rank of the model in the file,would have been the default value.

The model rank, i.e., the order in which the model is described, sets the model priority. The order of models is essential, because the models' priority is based on their location in the list definition. This priority is considered when several model calls must be processed on the same event date.

Executing MIMIC

MIMIC executes in a 2-step process. The first one, "MIMICinit," runs the initialization of MIMIC and generates the pseudo-model codes and the initial schedule. The second one, "MIMICmain," launches the schedule. MIMIC generates by default a CSV (comma-separated values) file containing the values of all variable states at each simulation step.

Development and dissemination

This framework is primarily aimed at scientists and engineers in the agricultural and environmental sectors looking to estimate P&D effects on plants on long term to assess possible resilience of plants. We intend that this implementation be a user-friendly tool, with an open access code for further development. The modular structure of the architecture should provide the flexibility to adjust and refine the interactions. Finally, its parameterization is easy to understand and is adapted to users who are not specialists in software development.

The tool was developed in Julia, an open-source high-level dynamic programming language [52]. It offers the advantage of calling scripts written in other languages popular in the plant science modeling community (MATLAB, R, etc.), and Julia remains close to them in its syntax. This choice is also

Downloaded from https://spj.science.org at Cirad Dist on August 31, 2023

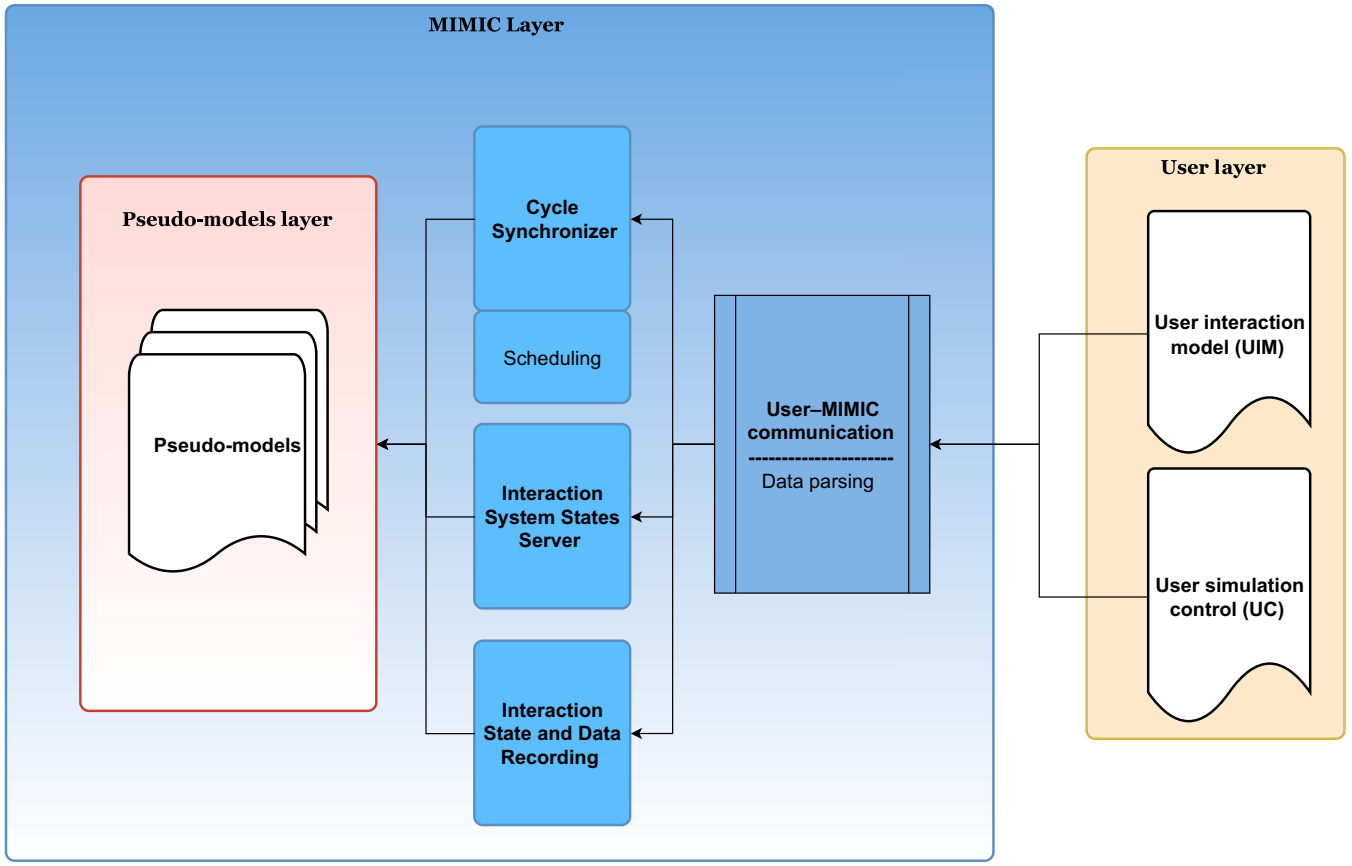


Fig. 7. Structure of the interaction between the MIMIC (functioning presented in Fig. 4) and the users. The data provided by the user are read and used to create metadata for the construction of the interaction in the "User–MIMIC communication." Then, the metadata is used in creating and filling the pseudo-models.

dictated (a) by the possibility to use existing codes (models) without direct rewriting; (b) by the performances, especially in terms of speed of the language; and (c) by a growing number of libraries produced by a growing community of contributors. This argument reflects concerns of many scientists in numerous fields [53].

In the user layer, translating variables from one model to another using variable manipulation with ISS or/and arithmetic operation is straightforward, even in Julia. The code is written in a file using a notepad, with a ".jl" extension or through a code editor. In the YAML file, the name of the functions and the path to the code are listed. The advantage of YAML over other file formats is its simplicity to be read. Writing instructions for this file type is simple and understandable for users of all professional backgrounds.

Access to the source code is free via GitHub: https://github.com/Houssem-Triki/MIMIC. The kernel code can be found there including the case study. The tool is coded as a package that can be downloaded using the Julia REPL command line. Users will find the templates for the YAML input files. These documents can be edited using notepad software or any code editor. The Git provides documentation on MIMIC and the case study example, for which a template sheet data file is provided for the fruiting data, allowing users to test different tree production and harvesting situations.

Study case: Sumatra, Indonesia (data used for simulation)

The case study example involving the CBB, fructification, and human models described in the previous section enables us to illustrate a simple application mobilizing MIMIC and its performances.

The models (CBB, coffee, and human) are loaded into MIMIC using a parameter template such as in Table 3. The complete template for this case study can be found on MIMIC's Git.

Parameters of the coupling

MIMIC's parameters used in the study case are shown in Table 4. The step time of the simulation will be determined from the parameters that are entered into the time data field of MIMIC's model parameters. For more details, each model and, thus, each pseudo-model are characterized by the simulation's step time (in cycles), the simulation's start time (start simulation), and the simulation's end time.

Users need to specify the models' state variables (CBB, coffee, and human) that are relevant to the interaction in MIMIC in the "variables data" field.

Results of the case study

The interaction between the coffee tree and the CBB models is constructed around the attraction of the pest on the type of fruits (from the CBB point of view). A specific detail concerns the way fruit maturity is considered in both human and fruit models.

Among the datasets, 2 trees were chosen (named C52 and C22), exhibiting dissimilar fruiting dynamics (Fig. 8, bars). Tree C52 produced ripe fruits for nearly the entire year, whereas tree C22 produced fruits for only the first one-third of the monitoring period.

Downloaded from https://spj.science.org at Cirad Dist on August 31, 2023

Table 3. YAML model definition pattern example on a plant model.

Field name	*Subfiled*	*Type of value*	*Value*
Is model active		Boolean	True
Name		String	Tree
Version		Any	a0.4
Language		String	R
Path to File		Path from root	D:/MyPrg/Plants/TreeSim.R
Time data	***Nature***	Keyword (*)	temperature
	Unit step size	Value	20
	End simulation	Value	2350
	Start simulation	Value	0
Variables data	***State variables***	Vector	[Yield, biomass]
	Inputs	Vector	[RelativeTempe]
	Outputs	Vector	[Yield]
Interaction data	***MyRefDir***	Path from root	/Fungus2Tree.jl
	Language	String	C

*Day, month, or temperature.

Table 4. Parameters used for interaction in the case study instancing the definition in Table 3.

Field name	*Subfiled*	*Value*
Is model active		*True*
Name		MIMIC
Version		0.9
Language		Julia
Path to File		*./MIMIC-main.jl*
Time data	***Nature***	*Day*
	Unit step size	1
	End simulation	355
	Start simulation	1
Variables data	***State variables***	[fruitsCohorts, Ag, Ar]
	Inputs	
	Outputs	[fruitsCohorts]
Interaction data	***MyRefDir***	*/Interaction.jl*
	Language	*Julia*

The proportion of infested fruits among harvested fruits for the 2 trees is the result of a MIMIC simulation in which an initial number of CBB was introduced. MIMIC simulated the attack dynamic accurately.

There was one significant peak in tree C22 and 2 less significant ones. The models succeeded in their task of fitting both the primary peak and one of the minor peaks, both in terms of amplitude and length. There was a minor shift in the position of the final weaker peak.

As for tree C52, there were 3 major and 2 secondary peaks. Two of the major peaks and one of the secondary peaks were well fitted by the model in amplitude. The last major peak was underestimated in intensity. The first peak at the beginning of the monitoring did not correspond to the observations, which is due to the initial conditions. Dynamic systems may be sensitive to initial conditions, and a small change can result in a different outcome [54].

Performances and coding key figures

The MIMIC code is compact, with reduced complexity. The complexity is linear as a function of the number of events. Table 5 shows its performance in the study case. Most of the simulation time is spent on initialization, which consists of interacting with the user layer. The rest of the run time is split between the MIMIC's kernel components and the external models.

Initialization clearly consumes the majority of simulation time. This is because Julia is executing a code for the first time. On the first run, Julia simulates a virtual machine to compile the algorithms. Hence,the second run requires less memory (3,720 GB with 28.9 s for the first run compared to a 727 MB with 3.81 s for the next one).

Discussion and Perspectives

In this paper, we introduced a methodology and tool for linking models, specifically plant and P&D models. Here, we discuss the underlying assumptions of our proposal and present some near-term perspectives.

Cohort assumption

Cohorts simplify the complexity of models and their associated data. Indeed, factorization makes it easier to manipulate the outputs/inputs of the various modeling formalisms to make them interact. Processes are no longer treated on an individual basis, but as homogenous sets with the same behaviors and parameters. Cohorts are commonly used in health sciences; their benefits are frequently addressed [55].

In our case, the usage of cohorts reduces the complexity of the interaction. Consequently, factoring into cohorts simplifies the handling of the outputs/inputs of multiple modeling formalisms during interaction, due to the unit of time that characterizes each cohort Assumedly, we suppose that the plant models organize organs by cohort [20]. This assumption cannot always be mobilized. However, in the case of FSPMs, factorizations can be performed post hoc by establishing cohorts clustering all organs of same physiological stages and appearance date (thus, sharing similar environmental conditions). Conversely, in crop models, the cohorts can also be defined subdividing the PBM organ compartments, gradually identifying the cohorts from the number of new organs appeared [56].

Downloaded from https://spj.science.org at Cirad Dist on August 31, 2023

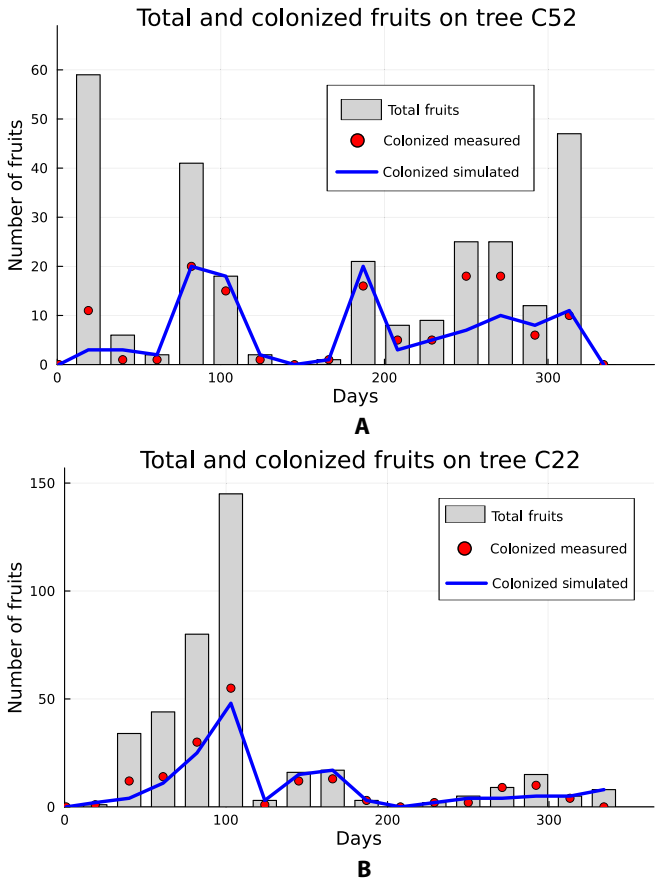


Fig. 8. Simulation results compared to field data on 2 coffee trees in Indonesia. (A) stands for tree C52 and (B) stands for the tree C22. Points represent the recorded number of harvested fruits colonized by CBBs on 6 fruiting branches of the tree. The line represents the results of the simulation by MIMIC at the same date than the observation. Bars represent the total observed harvested fruits (healthy and colonized).

Similarly, on P&D models, the cohorts can be defined from population dynamics from development stages. This allows compatibility between the interacting models.

About spatialization

In our proposal, we assume spatialization as an implicit aspect of the models. This point will not be detailed here. However, in some cases, geometrical (spatialization) can be related to aging (for instance, distance from soil or distance from crown). MIMIC may then be used for coupling spatialized models with ones that are not, providing the fact that the UIM can explicit the request spatialized inputs from the model implicit output ones.

Feedback and ISS

Pseudo-models' output transformation is performed by the ISS component that allows the manipulation of the variables directly without having to go through modifications on the intervening models. This discharges the users to ensure complete compatibility between models' outputs. It is up to them to handle the different levels of feedback of the interaction through the UIM. The users are given complete freedom on how to choose the principles of the interactions outside the models. This situation contrasts to other formalisms where inner modifications are requested, such as in DEVS [42], and where discrete time is driven by the models and events.

Despite DEVS formalism extensions, improvements, and adaptation to community needs [57], this problem is not solved including within the agronomy community [58], as illustrated in the Record project [59], an initiative stopped recently.

In MIMIC, the users can decide to make a shared coupling by not providing an UIM code, when the outputs between models are used as inputs. They only need to indicate these outputs/inputs in the UC file. Users can also explore different concepts on the interaction with the UIM code. They can make the interaction correspond to one of the other frameworks proposed by Siad et al. [28].

Table 5. Study case runtime performance and code complexity on the study case. User model and initialization; MIMIC's kernel; external models. The runtime and memory allocation columns contain information for a first and second execution (Intel Core i7-11850H @ 2.50 GHz, RAM 64 GB, Windows 10).

Task		Runtime (s)		# Calls	# Code lines	Ram (MiB)	
		First launch	Second launch			First launch	Second launch
Init tool		8.6	0.17	1	5	1250	13,1
Pseudo-code generation	Parsing	3.1	1.16	1	127	292	97.6
	Agenda	0.4	0.11	1	70	112	69.1
	Bit-compile	11.7	0.21	1		956	7.62
Total init		**23.8**	**1.65**	**1**		**2610**	**97.6**
MIMIC	CS	0.66	0.60	354	201	274	263
	ISS	0.07	0.06	354	48	3.4	3.4
	ISDR	0.53	0.08	1	47	67.4	8.4
	Others	0.55	0.17	1	24	154	26.1
Models	CBB	2.44	1.13	354	382	553	321
	Harvest	0.10	0.09	354	31	6.9	5.9
	Fruit	0.03	0.02	354	57	1.2	0.9
Total		**28.9**	**3.81**	**1**	**992**	**3720**	**727**

Choosing Julia, user-friendly meta programming

Julia is a fast, dynamic, easy to use, and open-source programming language; it is accessible to the modeling community. Its syntax bears a resemblance to the common program languages used by modelers (Python, R, and MATLAB). In addition, the UIM does not need to be written as a complex algorithm, as shown on our example.

When using dynamic programming (by requesting user–MIMIC parser to produce the pseudo-models), Julia's speed is advantageous because MIMIC's input (UC and UIM) is preprocessed and an optimized code is generated. The parser in MIMIC will take most of the time and resources at the first run of the program. However, after it, the simulations are swift (Table 5) and users can update the simulation parameters without losing performance.

The interaction complexity can be analyzed according to the number of models involved in the system and, more precisely, to the number of operations handled by the ISS, which translates variable sets between the pseudo-models and the kernel. Ignoring the initialization stage (that can be considered as a

Downloaded from https://spj.science.org at Cirad Dist on August 31, 2023

constant value plus a linear cost in terms of the number of models involved), the complexity related to the requested model exchanges is drastically limited in MIMIC compared to an embedded approach. With MIMIC, the number of set translations leads to a linear complexity with the number of models involved, because for n models, n translations are required. In the embedded case of an upfront coupling between each model and the other, the complexity is defined by the number of models mutually coupled. For n models, there are potentially n-1 variable set translations (to connect to the other models), which is, to say, up to n*(n-1) translations.

Perspectives

It is advantageous to have a modular structure for MIMIC when integrating additional components and adding extra capabilities. Additionally, it is designed to be compatible with other platforms, such as OpenAlea, even if not implemented yet [33]. We do not have a specific constraint on the type or nature of the involved models (except their ability to run in a stop and go way, and potentially input and output variables that can be expressed as cohort variables). Thus, the proposed approach is versatile and generic, which increases the coupling options.

We plan to design a generic plant model implementation within MIMIC. Users would then simply need to set plant-specific parameters and incorporate their other models (e.g., P&D).

Conclusion

The literature on the limitations of model coupling (plants and P&D) reveals that feedback is not taken into consideration and that it is challenging to find an appropriate framework without modifying the structures and logic of the models involved.

In this paper, the proposed framework was developed to address this issue and to provide a platform to couple prebuilt models. This framework is depicted by the tool MIMIC.

MIMIC provides the ability to couple models in a variety of ways, ranging from direct data transmission between models to more complex interaction principles that require a third-party tool to add a new element and modify the outputs of the interacting models. MIMIC's primary benefit is that it gives users the tools and freedom to construct their own interactions.

Given that all the coupled models and components of MIMIC are represented as pseudo-models, the implementation with Julia's high-speed metaprogramming enables rapid interaction outcomes.

The implementation of MIMIC in Julia provides a flexible and straightforward algorithmic environment for users with limited coding experience and a good trade-off with other modeling-oriented programming languages (R, Python, MATLAB, etc.).

The case study presented in this paper illustrates the MIMIC framework, coupling a coffee tree fructification model and a CBB model.

As a result, the proposed approach emphasizes the challenge on coupling plant growth and P&Ds interactions' models.

Acknowledgment

The authors want to address special thanks to T. Arsouze (Cirad-Amap) for help and advice on software development and to B. Dufour for help with the case study and for providing the validation data. **Funding:** This work is part of the EU (European Union) Desira Robust project, supported by EU FOOD/2021/427-759/DESIRA. It is also supported by a CIRAD Bios department PhD grant and French National Research Agency under the Investments for the Future Program, referred as ANR-16-CONV-0004/#DigitAg programs. H.E.M.T. and M.J. have been supported by the MaCS4Plants (Mathematics and Computer Sciences For Plants) CIRAD network, initiated from the AGAP Institute and AMAP joint research units. **Author contributions:** H.E.M.T.: Conceptualization, implementation, and writing. M.J.: Implementation, writing, and review. F.R.: Writing and review. F.P.: Robust project head and review. All authors have read and agreed to the published version of the manuscript. **Competing interests:** The authors declare that they have no competing interests.

Data Availability

The data and source code that support the findings of this study are openly available at https://github.com/Houssem-Triki/MIMIC.

References

1. Brandmeyer JE, Karimi HA. Coupling methodologies for environmental models. *Environ Model Softw*. 2000;15(5):479–488.
2. Argent RM, Voinov A, Maxwell T, Cuddy SM, Rahman JM, Seaton S, Vertessy RA, Braddock RD. Comparing modelling frameworks—A workshop approach. *Environ Model Softw*. 2006;21(7):895–910.
3. Abel DJ, Kilby PJ, Davis JR. The systems integration problem. *Int J Geogr Inf Syst*. 1994;8(1):1–12.
4. Louarn G, Song Y. Two decades of functional–structural plant modelling: Now addressing fundamental questions in systems biology and predictive ecology. *Ann Bot*. 2020;126(4):501–509.
5. Donatelli M, Magarey RD, Bregaglio S, Willocquet L, Whish JPM, Savary S. Modelling the impacts of pests and diseases on agricultural systems. *Agric Syst*. 2017;155:213–224.
6. Wang N, Jassogne L, van Asten PJA, Mukasa D, Wanyama I, Kagezi G, Giller KE. Evaluating coffee yield gaps and important biotic, abiotic, and management factors limiting coffee production in Uganda. *Eur J Agron*. 2015;63:1–11.
7. Matovu R, Kangire A, Phiri N, Hakiza G, Kagezi G, Musoli P. Ecological factors influencing incidence and severity of coffee leaf rust and coffee berry disease in major arabica coffee growing districts of Uganda. *Uganda J Agric Sci*. 2013;14:87–100.
8. Parmesan C, Hanley ME. Plants and climate change: Complexities and surprises. *Ann Bot*. 2015;116(6):849–864.
9. Pham Y, Reardon-Smith K, Mushtaq S, Cockfield G. The impact of climate change and variability on coffee production: A systematic review. *Clim Chang*. 2019;156(4):609–630.
10. Piao S, Liu Q, Chen A, Janssens IA, Fu Y, Dai J, Liu L, Lian X, Shen M, Zhu X. Plant phenology and global climate change: Current progresses and challenges. *Glob Change Biol*. 2019;25(6):1922–1940.
11. Kagezi G, Kucel P, Egonyu JP, Kyamanywa S, Karungi JT, Pinard F, Jaramillo J, Van Asten P, Wagoire WW, Ngabirano H. A review of the status and progress in management research of the black coffee twig borer, Xylosandrus compactus (Eichhoff) in Uganda. Paper presented at: ASIC 2014.

Downloaded from https://spj.science.org at Cirad Dist on August 31, 2023

Proceedings of the 25th International Conference on Coffee Science; 2014 Sep 8–13; Armenia, Colombia.
12. Pinard F, Makune SE, Campagne P, Mwangi J. Spatial distribution of coffee wilt disease under Roguing and replanting conditions: A case study from Kaweri Estate in Uganda. *Phytopathology*. 2016;106(11):1291–1299.
13. Luzinda H, Nelima M, Wabomba A, Kangire A, Musoli P, Musebe R. Farmer awareness, coping mechanisms and economic implications of coffee leaf rust disease in Uganda. *Uganda J Agric Sci*. 2016;16:207.
14. Buddie AG, Crozier J, Rutherford MA, Flood J, Bridge PD. Population development within the coffee wilt pathogen Gibberella xylarioides reflects host-related divergence. *Eur J Plant Pathol*. 2015;142(2):291–304.
15. Cerda R, Avelino J, Gary C, Tixier P, Lechevallier E, Allinne C. Primary and secondary yield losses caused by pests and diseases: Assessment and modeling in coffee. *PLoS One*. 2017;12(1):Article e0169133.
16. Gaunt RE. The relationship between plant disease severity and yield. *Annu Rev Phytopathol*. 1995;33(1):119–144.
17. Bar-Yam Y. *General features of complex systems: Encyclopedia of life support systems*. Oxford (UK): EOLSS UNESCO Publishers; 2002.
18. Tan M, Gou F, Stomph TJ, Wang J, Yin W, Zhang L, Chai Q, van der Werf W. Dynamic process-based modelling of crop growth and competitive water extraction in relay strip intercropping: Model development and application to wheat-maize intercropping. *Field Crops Res*. 2020;246:Article 107613.
19. Sievänen R, Perttunen J, Nikinmaa E, Posada JM. Invited talk: Functional structural plant models—Case LIGNUM. Paper presented at: PMA 2009. Proceedings of the 2009 Third International Symposium on Plant Growth Modeling, Simulation, Visualization and Applications; 2009 Nov 9–13; Beijing, China.
20. de Reffye P, Hu BG. Relevant qualitative and quantitative choices for building an efficient dynamic plant growth model: Greenlab case. Paper presented at: PMA 2003. Proceedings of the 2003 International Symposium on Plant Growth Modeling, Simulation, Visualization and their Application; 2003 Oct 13–16; Beijing, China.
21. Soualiou S, Wang Z, Sun W, de Reffye P, Collins B, Louarn G, Song Y. Functional–structural plant models mission in advancing crop science: Opportunities and prospects. *Front Plant Sci*. 2021;12:Article 747142.
22. Heuvelink E. Dry matter partitioning in tomato: Validation of a dynamic simulation model. *Ann Bot*. 1996;77(1):71–80.
23. Rivals P. Essai Sur la croissance des arbres et Sur leurs systèmes de floraison (application aux espèces fruitières). *J Agric Tradit Bot Appliquée*. 1965;12(12):655–686.
24. Barthélémy D, Caraglio Y. Plant architecture: A dynamic, multilevel and comprehensive approach to plant form, structure and ontogeny. *Ann Bot*. 2007;99(3):375–407.
25. Yates KL, Bouchet PJ, Caley MJ, Mengersen K, Randin CF, Parnell S, Fielding AH, Bamford AJ, Ban S, Barbosa AM, et al. Outstanding challenges in the transferability of ecological models. *Trends Ecol Evol*. 2018;33(10):790–802.
26. Lessler J, Cummings DAT. Mechanistic models of infectious disease and their impact on public health. *Am J Epidemiol*. 2016;183(5):415–422.
27. Kirkeby C, Brookes VJ, Ward MP, Dürr S, Halasa T. A practical introduction to mechanistic modeling of disease transmission in veterinary science. *Front Vet Sci*. 2021;7:Article 546651.
28. Siad SM, Iacobellis V, Zdruli P, Gioia A, Stavi I, Hoogenboom G. A review of coupled hydrologic and crop growth models. *Agric Water Manag*. 2019;224:Article 105746.
29. Kropff MJ, Teng PS, Rabbinge R. The challenge of linking pest and crop models. *Agric Syst*. 1995;49(4):413–434.
30. Vezy R, le Maire G, Christina M, Georgiou S, Imbach P, Hidalgo HG, Alfaro EJ, Blitz-Frayret C, Charbonnier F, Lehner P, et al. DynACof: A process-based model to study growth, yield and ecosystem services of coffee agroforestry systems. *Environ Model Softw*. 2020;124:Article 104609.
31. Leclerc G, Bommel P, Motisi N, Vezy R, Treminio E, Avelino J. Coffee leaf rust (Hemeleia vastatrix) risk management in Central America: Contribution of remote interactive simulations. *Agron Environ Sociétés*. 2021;11(2).
32. Pradal C, Dufour-Kowalski S, Boudon F, Donès N. The architecture of OpenAlea: A visual programming and component based software for plant modeling. Paper presented at: FSPM 2007. Proceedings of the 5th International Workshop on Functional-Structural Plant Models; 4–9 Nov 2007; Napier, New Zealand.
33. Pradal C, Dufour-Kowalski S, Boudon F, Fournier C, Godin C. OpenAlea: A visual programming and component-based software platform for plant modelling. *Funct Plant Biol*. 2008;35(10):751–760.
34. Qi R, Cournede P-H, Lecoustre R, de Reffye P. Tri-trophic ecosystem oil palm-pests-auxiliaries: I. Modeling and simulation. Paper presented at: PMA 2009. Proceedings of the 2009 Third Plant Growth Modeling, Simulation, Visualization, and Applications; 2009 Nov 9–13; Beijing, China.
35. Motisi N, Bommel P, Leclerc G, Robin MH, Aubertot JN, Butron AA, Merle I, Treminio E, Avelino J. Improved forecasting of coffee leaf rust by qualitative modeling: Design and expert validation of the ExpeRoya model. *Agric Syst*. 2022;197:Article 103352.
36. Le Chevalier V, Jaeger M, Mei X, Cournède P-H. Simulation and visualisation of functional landscapes: Effects of the water resource competition between plants. *J Comput Sci Technol*. 2007;22(6):835–845.
37. Zeigler BP. DEVS representation of dynamical systems: Event-based intelligent control. *Proc IEEE*. 1989;77(1):72–80.
38. Garin G, Fournier C, Andrieu B, Houlès V, Robert C, Pradal C. A modelling framework to simulate foliar fungal epidemics using functional–structural plant models. *Ann Bot*. 2014;114(4):795–812.
39. Reuillon R, Leclaire M, and Rey-Coyrehourcq S, OpenMOLE, a workflow engine specifically tailored for the distributed exploration of simulation models. *Future Gener Comp Syst*. 2013;29(8):1981–1990.
40. de Reffye P, Heuvelink E, Guo Y, Hu B-G, Zhang B-G. Coupling process-based models and plant architectural models: A key issue for simulating crop production. In: Cao W, White JW, Wang E, editors. *Crop modeling and decision support*. Berlin (Germany): Springer; 2009. p. 130–147.
41. Cournède P-H, Guyard T, Bayol B, Griffon S, de Coligny F, Borriane P, Jaeger M, de Reffye P. A forest growth simulator based on functional-structural modelling of individual trees. Paper presented at: PMA 2009. Proceedings of the 2009 Third International Symposium on Plant Growth Modeling, Simulation, Visualization and Applications; 2009 Nov 9–13; Beijing, China.

Downloaded from https://spj.science.org at Cirad Dist on August 31, 2023

42. Kang M, Hua J, Wang X, de Reffye P, Jaeger M, Akaffou S. Estimating sink parameters of stochastic functional-structural plant models using organic series-continuous and rhythmic development. *Front Plant Sci*. 2018;9:1688.
43. Letort V, Sabatier S, Okoma MP, Jaeger M, de Reffye P. Internal trophic pressure, a regulator of plant development? Insights from a stochastic functional–structural plant growth model applied to Coffea trees. *Ann Bot*. 2020;126(4):687–699.
44. Cournède P-H, Kang MZ, Mathieu A, Barczi JF, Yan HP, Hu BG, de Reffye P. Structural factorization of plants to compute their functional and architectural growth. *SIMULATION*. 2006;82(7):427–438.
45. Rodríguez D, Cure JR, Gutierrez AP, Cotes JM, Cantor F. A coffee agroecosystem model: II. Dynamics of coffee berry borer. *Ecol Model*. 2013;248:203–214.
46. Gamma E, Helm R, Johnson R, Vlissides J. *Design patterns: Elements of reusable object-oriented software*. London (UK): Pearson Education; 1994.
47. Tendeloo YV, Vangheluwe H. Discrete event system specification modeling and simulation. Paper presented at: WSC 2018. Proceedings of the 2018 Winter Simulation Conference; 2018 Dec 9–12; Gothenburg, Sweden.
48. Damon A. A review of the biology and control of the coffee berry borer, Hypothenemus hampei (Coleoptera: Scolytidae). *Bull Entomol Res*. 2000;90(6):453–465.
49. Jaramillo J, Chabi-Olaye A, Kamonjo C, Jaramillo A, Vega FE, Poehling HM, Borgemeister C. Thermal tolerance of the coffee berry borer Hypothenemus hampei: Predictions of climate change impact on a tropical insect pest. *PLoS One*. 2009;4(8):Article e6487.
50. Dufour BP, Kerana IW, Ribeyre F. Population dynamics of Hypothenemus hampei (Ferrari) according to the phenology of Coffea arabica L. in equatorial conditions of North Sumatra. *Crop Prot*. 2021;146:Article 105639.
51. Ben-Kiki O, Evans C. YAML Ain't Markup Language (YAMLTM) Version 1.2.
52. Bezanson J, Edelman A, Karpinski S, Shah VB. Julia: A fresh approach to numerical computing. *SIAM Rev*. 2017;59(1):65–98.
53. Perkel JM. Julia: Come for the syntax, stay for the speed. *Nature*. 2019;572(7767):141–142.
54. Lorenz EN. Deterministic nonperiodic flow. *J Atmos Sci*. 1963;20(2):130–141.
55. Sedgwick P. Retrospective cohort studies: Advantages and disadvantages. *BMJ*. 2014;348:Article g1072.
56. Whish JPM, Herrmann NI, White NA, Moore AD, Kriticos DJ. Integrating pest population models with biophysical crop models to better represent the farming system. *Environ Model Softw*. 2015;72:418–425.
57. Zeigler BP, Muzy A. From discrete event simulation to discrete event specified systems (DEVS). *IFAC-Pap*. 2017;50(1):3039–3044.
58. Bergez J-E, Chabrier P, Gary C, Jeuffroy MH, Makowski D, Quesnel G, Ramat E, Raynal H, Rousse N, Wallach D, et al. An open platform to build, evaluate and simulate integrated models of farming and agro-ecosystems. *Environ Model Softw*. 2013;39:39–49.
59. Chabrier P, Garcia F, Martin-Clouaire R, Quesnel G, Raynal H. Toward a simulation modeling platform for studying cropping systems management: The record project. Paper presented at: MODSIM 2007. Proceedings of the International Congress on Modelling and Simulation; 2007 Dec 10–13; Christchurch, New Zealand.

Downloaded from https://spj.science.org at Cirad Dist on August 31, 2023

Chapter 2: Towards a Modular Framework for Pest and Disease Dynamics

1. Introduction

Having established a formalism for integrating models, we now examine another critical factor influencing plant growth: the impact of pests and diseases (P&Ds). Coffee trees are susceptible to a wide range of P&Ds that can significantly impair their health and productivity. These effects manifest as damage across various plant organs, including roots, leaves, branches, and fruits. Understanding the diversity and pathology of these P&Ds provides essential insight into the biological stresses that coffee plants endure, as described in the compendium of coffee P&D (Gaitán et al., 2016a, 2016b, 2016c).

More than 50 species of mealybugs inhabit tropical regions and infest various crops, including coffee trees. Transported by ants, these insects weaken vegetation by inducing chlorosis (leaf yellowing) and forming a brownish, crusty sheath around the roots, which can suffocate the plant. Longicorn beetles, such as *Bixadus sierricola*, are another notable pest. Their larvae bore into tree bark, resulting in structural weakening, chlorosis, yield reduction, and, in severe cases, stem breakage. Other trunk and branch parasites, including various longicorn species, exacerbate this vulnerability by damaging the plant's supportive structures.

In terms of diseases, root rot, caused by fungi from the *Basidiomycetes* and *Ascomycetes* groups, attacks the root system and leads to foliar wilting and drying. *Phthiriose*, also associated with mealybugs, results in similar root suffocation due to crust formation. *Collar rot*, triggered by *Rhizoctonia bataticola*, causes necrosis at the base of the stem, compromising bark integrity and weakening the plant.

Tracheomycosis, a vascular wilt disease caused by *Fusarium xylarioides*, leads to yellowing leaves, drying branches, and dark vascular streaks under the bark. *Orange rust* (*Hemileia vastatrix*) appears as yellow-orange pustules on leaves of *Coffea arabica*, promoting premature defoliation. In contrast, *powdery rust* (*Hemileia coffeicola*) affects *Coffea canephora*, producing yellow, powdery lesions on leaf undersides in high-altitude regions. *American leaf disease* (*Omphalia flavida*) manifests as brown, necrotic leaf spots, reducing photosynthetic capacity.

Mancha Mantecosa, caused by *Colletotrichum* spp., is characterised by oily yellowish spots on leaves, which often precede defoliation. *Thread diseases*, involving white to grey fungal films, thrive under shaded and humid conditions. *Coffee leaf rust* (*Cephaleuros virescens*) forms reddish-brown lesions on leaves, contributing to foliage loss. *Sooty mould*, developing on the sugary excretions of mealybugs, creates blackish coatings that block sunlight and inhibit photosynthesis.

Pink disease (*Corticium salmonicolor*) presents as a pink fungal membrane on the bark, eventually leading to branch dieback. *Coffee berry disease* (CBD), caused by *Colletotrichum coffeanum*, affects immature fruits with yellowish lesions that expand and cause fruit loss.

Lastly, *powdery mildew* (*Trachysphaera fructigena*) targets both flowers and fruits, resulting in significant yield reductions.



Figure 2. 1: Pests and disease damage in coffee trees (C. canephora): Black coffee twig borer (upper left), Coffee berry borer (upper right), and Red blister disease (bottom).

Based on the observed diversity of P&Ds in coffee cultivation, four primary categories of damage can be distinguished: leaf damage, branch damage, fruit damage, and root damage. This work focuses on P&Ds affecting the above-ground parts of the coffee plant (leaves, branches, and fruits), excluding root-related issues. This focus is motivated by their more immediate and observable influence on plant growth and productivity.

This chapter highlights three major P&Ds with high prevalence and economic impact in East Africa: The Coffee Berry Borer, the Black Coffee Twig Borer, and Red Blister Disease. These pests and diseases are particularly detrimental to coffee yield and quality (Fig. 2.1). The following sections will explore their biological characteristics and the modeling approaches used to understand and predict their effects on coffee crops.

2. Coffee Berry Borer (CBB)

The Coffee Berry Borer (Hypothenemus hampei Ferrari), commonly known as the CBB, is a beetle belonging to the order Coleoptera, subfamily Scolytinae (Damon, 2000) . This pest is native to Central Africa but has since spread to all coffee-producing regions globally, making it one of the most economically significant pests in the coffee industry. Over recent years, CBB has also been detected on isolated islands, including Hawaii (Johnson and Manoukis, 2021) and, more recently, (Dufour et al., 2022).

Symptoms and Damage

CBB attacks coffee berries by boring into the fruit, where it lays its eggs. The larvae develop within the seeds, feeding on the endosperm, which damages the seeds and affects their viability. Typically, only one of the two seeds per fruit is affected. In addition to physical damage, infestation can also facilitate fungal contamination, further degrading the quality of the coffee beans.

2.1. Life Cycle

CBB's life cycle is highly adapted to its coffee berry habitat, in which it spends most of its life cycle. Female CBBs leave the berries to find new hosts, while males remain inside, fertilising the females. The female then begins a new colony in another berry. This cycle is repeated, with females laying an average of two eggs per day throughout their adult lives. The sex ratio is biased towards females. The average life cycle of a female CBB (from egg to adult) is approximately 45 days, depending on the environmental conditions (Jaramillo et al., 2010). The timing of the pest's movement from one berry to another is influenced by its age and climatic factors, such as temperature, humidity, and rainfall.

2.2. Dispersion

CBB is highly attracted to coffee berries, where it finds both food and a suitable reproductive habitat. The attraction is influenced by specific kairomones released by the berries and their colour. Studies (Aristizábal et al., 2015; Dufour and Frérot, 2008; Giordanengo et al., 1993; Mora, n.d.) have shown that CBB prefers red berries over yellow or green ones. This selective attraction plays a role in determining which fruits are colonised.

2.3. Economic Impact

In heavily infested berries, up to half of the seeds may be lost, leading to a substantial decline in overall yield. CBB damage further reduces bean weight. Beyond quantity, infestation also impairs bean quality by affecting sensory attributes and germination potential, ultimately lowering market value. These combined effects significantly reduce profitability for coffee producers, particularly in regions where coffee is a major source of income (Ribeyre and Avelino, 2012).

2.4. Management

Effective CBB management strategies combine several techniques (Greco and Wright, 2015). Traps using attractants like ethanol-methanol mixtures or coffee-based lures are used to capture adult beetles and monitor population levels. Biological control agents, such as entomopathogenic fungi (e.g., Beauveria bassiana), can help reduce CBB populations, although their efficacy may be influenced by environmental and field conditions. As with chemical insecticides, B. bassiana is most effective when applied during the brief window in which adult CBB are boring into the fruit. This necessitates multiple, precisely timed and spatially targeted applications to achieve optimal control. Integrated pest management (IPM) strategies that combine cultural practices, sanitation, trapping, and biological agents are the most effective means of controlling CBB while minimising environmental impacts.

3. Black Coffee Twig Borer (BCTB)

The Black Coffee Twig Borer (*Xylosandrus compactus Eichhoff*), commonly referred to as the BCTB, is an ambrosia beetle. As such, it carries with it ambrosia fungi, which serve as its primary food source (Hultman, 2016). It is considered invasive in Uganda.

3.1. Symptoms and Damage

BCTB infests the twigs and branches of a large variety of plants, including coffee, causing both mechanical damage from tunnelling and pathological damage from the introduction of ambrosia fungi into the plant tissues. Female beetles bore into small twigs, typically those with diameters less than 2 cm, where they create galleries and inoculate the wood with fungal spores. The fungi colonise the xylem tissue, disrupting vascular function and causing wilting, necrosis, and dieback in the affected branches.

Externally, infestations are indicated by small round entrance holes (often less than 1 mm in diameter) and the presence of fine dust around the entry points. Affected branches show signs of yellowing, wilting, and eventual death beyond the point of infestation.

3.2. Life Cycle

As for the CBB, the life cycle of the BCTB is relatively short and can occur multiple times within a single year, particularly under warm and humid conditions. Female beetles are the primary dispersal agents and initiate infestations by boring into suitable twigs. Once inside, they create a network of tunnels and inoculate the galleries with fungal spores. The ambrosia fungus serves as a food source for the larvae, and reproduction is characterised by a high sex ratio that is biased towards females. Most eggs develop into females, while males are rare, apterous, and remain within the natal gallery. After mating, fertilised females leave the natal gallery to infest new branches and repeat the cycle (Kagezi et al., 2015; Nanjego et al., 2024).

3.3. Dispersion

The BCTB disperses primarily through the movement of fertilised females, which emerge from the natal galleries and seek out new suitable twigs to infest. These beetles can rapidly colonise

new areas over significant distances, particularly under favourable environmental conditions. The dispersal of BCTB can be influenced by local weather conditions, such as temperature and humidity, as well as the availability of suitable host plants (With twigs meeting the selection criteria).

3.4. Economic Impact

BCTB infestation can cause substantial damage to coffee plants, primarily through branch dieback and a reduction in overall plant vigour. Affected branches often exhibit wilting and yellowing, which compromises the health of the entire tree and leads to a direct decline in coffee yield. The ambrosia fungus introduced by the beetle exacerbates the damage by further weakening the plant and increasing its susceptibility to secondary infections. The economic impact includes not only yield losses but also increased management costs, such as pruning and the removal of infested material. In some cases observed in Uganda, trees have reportedly ceased berry production altogether (Hultman, 2016; Túler et al., 2019).

3.5. Management

Management of BCTB is challenging due to its cryptic feeding habits and the protective nature of its gallery system. Integrated pest management (IPM) strategies are crucial in controlling BCTB populations. These strategies include regular monitoring to detect infestations early, pruning and destroying infested branches, and applying biological control agents. In some areas, entomopathogenic fungi or natural predators of the beetle may be used to help reduce BCTB populations (Hultman, 2016).

4. Red Blister Disease (RBD)

Cercospora coffeicola, the causative agent of Brown Eye Spot and known as Red Blister Disease in East Africa, is a pathogenic fungus that significantly threatens coffee crops worldwide. The fungus generally primarily infects the leaves and then the berries of coffee plants, causing severe damage to both the plants' vigour and coffee yield (Souza et al., 2011). However, in East Africa, the RBD version of the pathogen targets berries, causing direct yield losses.

4.1. Symptoms and Damage

RBD symptoms are easily identifiable in the field. On the leaves, initial lesions appear as small, circular spots ranging from chlorotic to reddish-brown or necrotic. As the infection progresses, the lesions develop greyish centres surrounded by a brown concentric halo. Over time, these lesions darken and become black and desiccated, often accompanied by surrounding chlorosis. On berries, the disease manifests as small, reddish lesions that expand as the fruit matures. Infected berries may ripen prematurely and fall off the tree before reaching full maturity. Severely infected berries show visible desiccation and darkening, resulting in a significant reduction in yield and quality (Nelson, 2008).

4.2. Life Cycle

The life cycle of Cercospora coffeicola comprises several distinct stages that contribute to its pathogenicity and persistence in coffee crops. Infection begins with the deposition of conidia, which are dispersed primarily by wind and rain splash onto susceptible tissues of the coffee plant, including leaves, stems, and berries. Under favourable environmental conditions, these spores germinate and produce germ tubes that penetrate the plant tissues, initiating the colonisation phase. This colonisation phase may persist for several days to weeks, during which the fungus progressively establishes itself within the host tissues. Following an incubation period, visible lesions begin to develop on the infected organs, gradually enlarging and darkening over time. Ultimately, these lesions enter a senescence phase, during which they dry out, turn black, and become necrotic. C. coffeicola is capable of completing multiple infection cycles within a single growing season, thereby maintaining its presence in the field and causing cumulative damage throughout the crop's development (Hultman, 2016; Nelson, 2008; Túler et al., 2019).

4.3. Dispersion

Cercospora coffeicola disperses at long distances, primarily through wind and rain. The pathogen can also defuse its spores at short distances in adjacent plants or plant' organs that were infected and fell, serving as a source of inoculum for future infections. Human activity also plays a role in spreading the pathogen as we transport the spores through our clothes and by touching sporulated areas in the plants. The spread of the disease is influenced by environmental conditions such as humidity and temperature, with wet, humid conditions being particularly conducive to spore germination and fungal growth (Khan et al., 2008).

4.4. Economic Impact

RBD leads to significant reductions in coffee yield and quality. Infected leaves drop prematurely, leading to a reduction in the plant's ability to photosynthesise, which weakens the overall health of the coffee tree. Infected berries may fall prematurely or fail to ripen properly, leading to the inclusion of immature fruits in the harvest. This results in yield losses and diminished coffee quality, both of which directly compromise the economic viability of coffee production. Additionally, the need for regular fungicide applications to control the disease increases production costs.

4.5. Management

Managing RBD involves a combination of cultural and chemical control measures. Key practices include removing infected plant material, improving field sanitation, and using fungicides to prevent spore germination. Early detection and regular monitoring are critical for controlling the disease. The development of resistant coffee plant varieties can be effective in mitigating the *Cercospora coffeicola* and other pathogens.

5. Model-Oriented Similarities Among Pests

The challenge of managing pests and diseases that impact crops is a persistent global issue. Understanding the dynamics of key P&Ds, such as the Coffee Berry Borer (CBB), Black Coffee Twig Borer (BCTB), and the fungal pathogen causing Red Blister Disease (RBD), is crucial for integrating them in an interaction study and implementing their impact on the host plant development and yield.

These P&Ds share many similar biological and ecological patterns, particularly in their life cycles and population behaviours. They all undergo stages such as infestation, reproduction, and development, which are influenced by environmental conditions, host availability, and management interventions. These common patterns are illustrated through life cycle diagrams for the CBB, BCTB, and RBD (Fig. 2.2), which demonstrate the shared structure of these organisms' life stages, from emergence and establishment to colonisation, reproduction, and dispersal.

Given these shared dynamics, a significant opportunity arises: the development of a unified modeling framework that can capture the essential mechanisms driving a wide range of P&Ds. This chapter aims to explore this opportunity by addressing the following problem: how can we create a flexible, modular model that integrates the common components of different pests and pathogens, while maintaining computational efficiency and adaptability to varying crop, climatic, and management contexts?

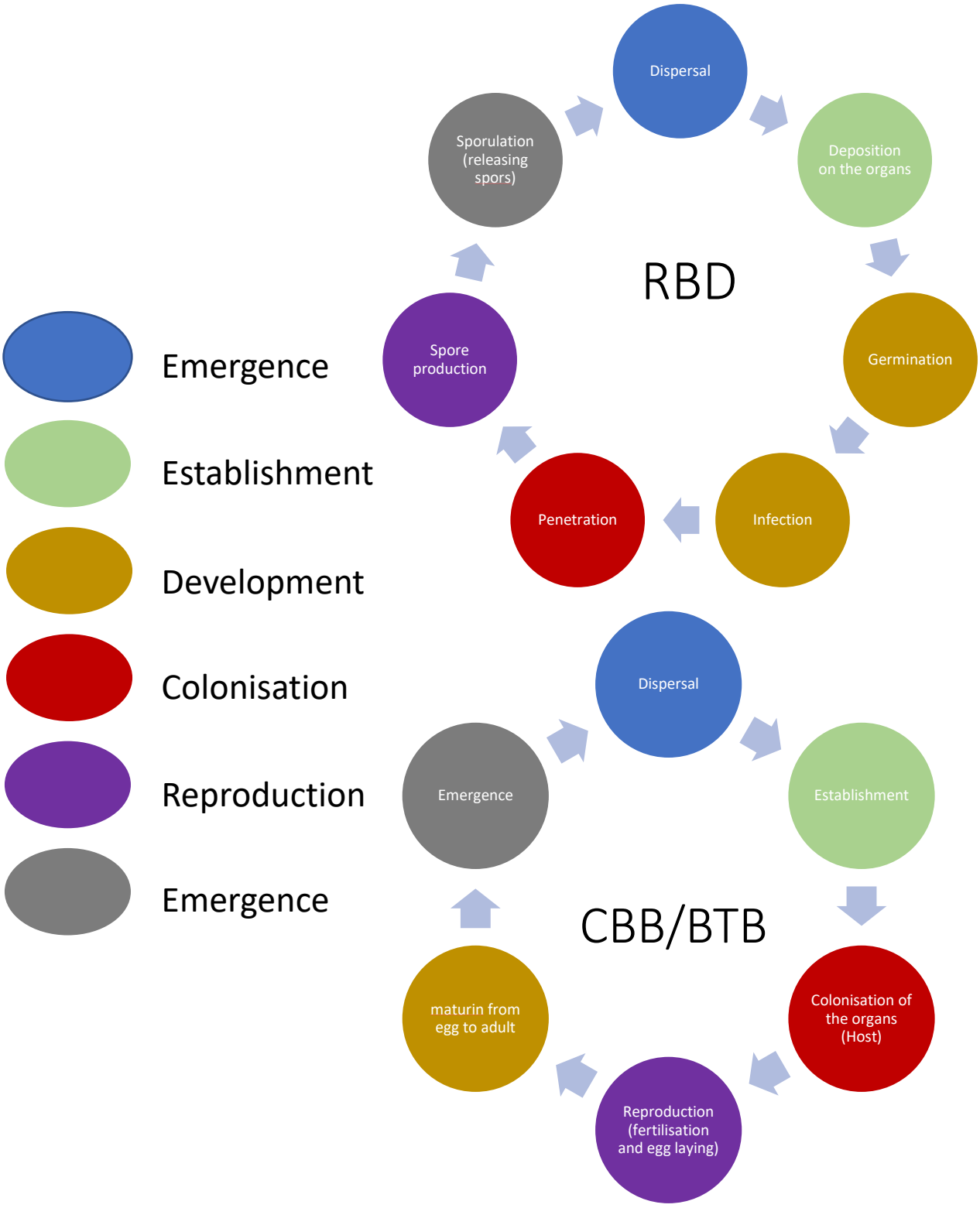


Figure 2. 2: Life cycles of the CBB/BTB (Bottom), and RBD (top), with colour codes indicating a generalised interpretation of their life stages from emergence (green) to establish/colonise (red), reproduction (purple), maturation (brown), leaving the plant (grey) and dispersal (blue).

6. Modeling Principles

6.1. Knowledge base modeling

A wide literature related to modeling the dynamics of the P&Ds, focusing on aspects that can predict and/or simulate their dynamics in a specific area, climate and conditions. Some models focus on predicting the level of dispersion of the P&D on a large scale, or in their development in a certain cultural plot (Aggarwal et al., 2006; Bondad et al., 2023; Donatelli et al., 2017; Merle et al., 2020; Rodríguez et al., 2013b, 2011).

Most models can be divided into three types of modeling techniques: descriptive, predictive, and conceptual. Descriptive models are used to test and apply hypotheses or experiments in a general manner. Predictive models are descriptive models aimed at providing outputs describing the severity and propagation of an epidemic. Conceptual models are mechanistic models that describe the behaviour and the dynamics of a P&D, thus reproducing it.

This part of the thesis aims to develop a model that can be applied to various circumstances. To achieve this, we need a model framework that can account for all P&D population dynamics without being limited to a particular area. Therefore, we have chosen to create a conceptual model that follows Knowledge-Based Model (KBM) principles (Lasso et al., 2021; Rodríguez et al., 2011).

The model will be created in a modular way to be able to adapt easily and to give the possibility to choose the different dynamics that are mobilised for a given situation or preferences.

The knowledge-based model formalism, as described in [Lasso], involves following a series of structured steps to build the model. These steps consist of:

- Gathering scientific and technical resources (scientific articles, reports) without omitting the grey literature.
- Creating data sets from these resources.
- Use one or more experts to validate and discuss these datasets.
- Formulating the data in the form of dynamics.
- Creating functioning laws of the Pest.
- Build a model with the desired outputs.

The advantage of using this modeling formalism is that it allows for the use of a diverse range of resources in creating the model. Additionally, experts can provide guidance on the legitimacy of the data and help in the modeling process.

While the steps outlined above provide a general idea of how to construct this type of model, the methodology can vary from one study to another (or a P&D and another). In the following section, we follow these steps to build our models.

7. Disease

Modeling plant diseases presents varying levels of complexity depending on the biology, life cycle, and transmission dynamics of the specific pathogen. A core objective of such models is to forecast the onset and progression of epidemics within a crop population. At the individual plant level, plant-pathogen models can simulate how infections spread across specific organs, such as leaves, branches, or fruits, and help estimate their physiological and agronomic consequences, including potential yield loss. This issue arises in the instance of *Cercospora coffeicola*. Traditionally known to infect mainly the leaves of coffee plants, recent outbreaks in Uganda have revealed an unusual and concerning epidemiological shift; this pathogen is now infecting primarily the coffee berries in East Africa. This novel behaviour suggests either a change in the pathogen's biology, an evolving interaction with the host plant and its environment or mistaking it for another pathogen, warranting urgent scientific investigation.

The objective is to develop a model for the spread and impact of Coffee Red Blister in Uganda at a tree scale. This work was conducted by students and supervised by us and their school

A major obstacle in modeling this disease is the scarcity of empirical and biological data, given its relatively recent emergence and atypical progression in the region. As a result, this study adopts a comparative modeling approach, drawing on knowledge and methodologies applied to similar coffee diseases, particularly the well-documented Coffee Berry Disease (CBD). These comparative insights will inform the structure, parameters, and assumptions of the Red Blister model.

The outcome is to propose a model structure tailored to the observed behaviour of *Cercospora coffeicola* in Uganda. This model is expected to serve as a foundational tool for future epidemiological studies, surveillance efforts, and disease management strategies aimed at protecting coffee production in the region.

To achieve this, a generalist model is developed to apply to both leaves and fruits, using available data from the literature as well as expert knowledge and insights.

The model will follow the following hypotheses. First, we assume that temperature does not prevent spore germination; rather, it modulates the rate at which lesions grow, slowing development under less favourable thermal conditions. Second, spore production is considered to cease entirely once a lesion has dried out, marking the end of its infectious period. Third, we assume that the durations of key pathogen life-cycle stages, namely deposition, germination, and maturation, are fixed and not influenced by climatic variables. Fourth, given the localised nature of rain splash dispersal, we hypothesise that spores are only transferred between branches of the same coffee plant, with no inter-plant dispersal occurring via this mechanism. Fifth, the effect of wind on spore dispersal is neglected, leading us to assume an isotropic spread pattern, one that is directionally uniform. Finally, while recognising that individual coffee plants vary in the number of leaves, we simplify the model by assuming each leaf has a uniform area, represented by a positive constant $\Gamma \in \mathbb{R}^+$. This allows for standardisation across calculations involving pathogen spread over leaf surfaces.

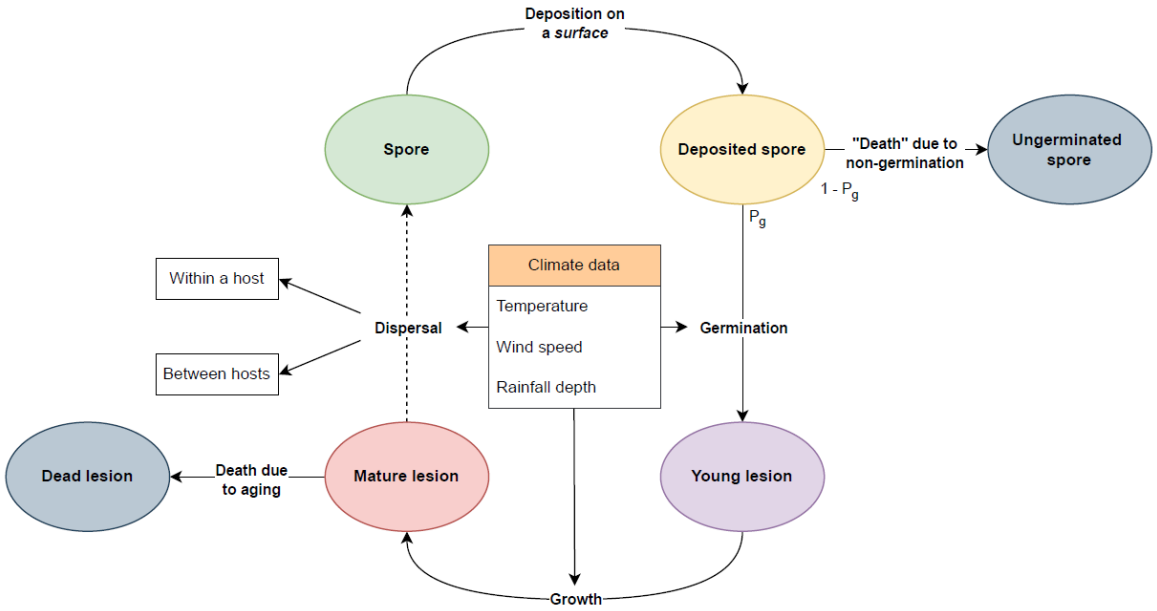


Figure 2. 3: Structure of the Cercospora pathogen model.

The resulting model (Fig. 2.3) corresponds to the cycle of the Red Blister presented in Fig. 2.2. The model is dependent on the climate data, temperature, wind speed and rainfall, making it able to be used in different contexts. Since it does not discriminate on the type of organ that it spreads, we can adapt it to the classical leaf contamination or our context in Uganda.

This part of the modeling was proposed as a project for a group of students. The two reports are included in the annex of this manuscript (A2.1 and A2.2).

8. Generalised model (Plant's Pests)

Current pest dynamics models are often tailored to specific pests or geographical regions, focusing on factors such as pest life cycles, crop susceptibility, and local climatic conditions [19]. For example, many models take into account temperature-dependent growth rates, dispersal patterns, and host-plant interactions of specific regions [20]. However, focusing on certain conditions and areas may limit their application beyond the original study contexts, making them less useful for broader agricultural or environmental scenarios or climate variation that occurs through time.

Several existing models integrate pest dynamics into broader frameworks such as Integrated Pest Management (IPM) [21] or Climate Smart Pest Management (CSPM) [22]. These approaches aim to manage pest populations sustainably, accounting for both ecological interactions and economic thresholds for intervention. Despite the progress achieved, the lack of a unified framework capable of taking into account a wide range of pest species and environmental variables remains a significant gap in this field.

Developing a generalised pest model presents several challenges, particularly in capturing the complex interactions between pests and their environment. Key factors to be integrated include:

- Climate variability: Climatic factors such as temperature, humidity, and extreme weather events significantly affect the development and dispersal patterns of pests. Models need to incorporate these variables dynamically to take account of future climate scenarios.
- Host factors: Host plants are crucial for pest survival, development, and reproduction. Pests rely on hosts as sources of energy, and their availability directly influences pest population dynamics.
- Ecological interactions: Pests interact not only with crops, but also with other species such as predators, parasitoids, and competitors. While modeling these interactions increases complexity, it is essential for realistic forecasts, as these relationships often regulate pest populations.
- Human and political factors: Human activities, such as land-use changes and pest control interventions, influence pest dynamics. Taking these factors into account in the models can improve their relevance for policy-makers and practitioners. Harvesting the crops can be a management tool for pests that depend on them (like the CBB). Good harvesting practices can help counter P&Ds dispersal and may reduce their activity.

Structure of the model

To manage the complexity of pest-environment interactions, the model distinguishes between two main aspects: intrinsic pest development ("Maturation") and interactions with the environment ("Interaction"). This modular design enhances both the clarity of the model structure and its adaptability to different systems or scenarios.

The model is structured into two interconnected modules:

Maturation: Refers to the pest's development in a relatively stable environment within the fruit, where external interactions are limited. This representation is informed by empirical studies, particularly on bark beetles [23], and general descriptions of pest life cycles [24], [25], [26]. Maturation dynamics, such as growth and reproductive readiness, are well-documented and can often be observed experimentally.

Interaction: Captures the pest's engagement with its environment after reaching adulthood. It encompasses attraction to plant organs, responses to natural enemies, and sensitivity to environmental factors. Unlike maturation, interaction dynamics are often based on assumptions derived from observed pest behaviour and the specific ecological context [27].

This division is motivated by both biological rationale and practical modeling considerations. Biologically, studied pests (beetles) undergo a clear transition from internal physiological development to external ecological interaction, typically marked by the onset of maturity. From a modeling perspective, separating these phases reduces complexity by allowing independent calibration of each module: the maturation component can be parameterised using laboratory or field studies, while the interaction component can be adapted to specific environmental scenarios or management strategies. Moreover, this modular structure enhances model flexibility, facilitating updates or extensions as new biological or ecological data become available.

An overview of the model's architecture and a summary of its component modules are provided in Table 2.1 and Figure 2.4. Each module corresponds to a specific biological or ecological process involved in pest dynamics. Depending on the availability and quality of data, each module can be selectively activated, allowing simulations to be tailored to the specific pest species, environmental conditions, and research objectives. Modules for which data or necessary information is lacking can be deactivated, ensuring that the model remains operational even when information is incomplete (in the condition that they are not essential).

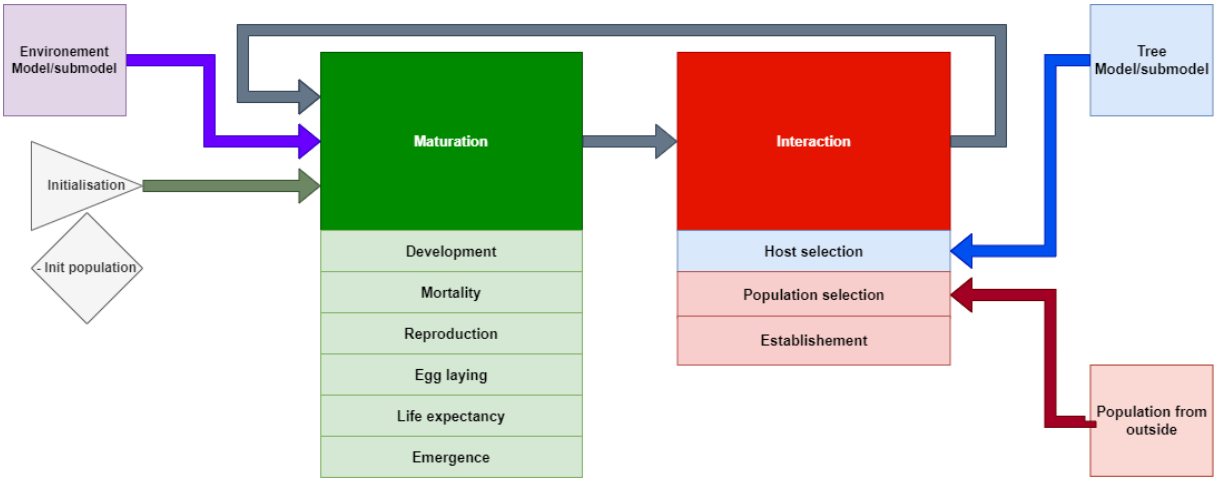


Figure 2. 4: Architecture of the generalised pest model, inspired by bark beetles' life cycle conceptualisation (CBB, BTB).

Table 2.1: Modules of the generalised pest model and their descriptions

Module	Module's description
Development	Developmental process of individuals from egg to adult
Mortality	Biological mortality of individuals following their development or/and reaching adulthood
Reproduction	Reproductive mechanisms
Egg laying	Egg-laying phase
Life Expectancy	Accumulated progression from birth to death (from 0 to 1, where 0 indicates the beginning of life as an egg and 1 marks its end).
Emergence	Emergence of pests from their initial colony
Host selection	Selection of potential hosts (organ, plant, etc.) by pests in search for a host
Population Selection	Selection of individuals that will attack the potential hosts
Establishment	Mechanisms for establishing new colonies within the selected hosts

This modular design offers several advantages. Since each component works as an independent unit, the sequence in which modules are applied can be adjusted flexibly according to the simulation needs and pest cycle. This flexibility enables researchers to reconstruct complex pest life cycles or interaction networks without being constrained by a fixed model structure. Moreover, individual modules can be invoked multiple times within a single simulation, if necessary, for example, to represent repeated multiple host interactions, or successive environmental challenges encountered by the pest during its life cycle.

The modular architecture thus enhances the model's adaptability, extensibility, and applicability across a wide range of pest–plant–environment systems. It supports both simple and highly detailed simulations, depending on the research question, available resources, and the biological complexity of the pest under study.

9. Generalised Model for Coffee Berry Borer (CBB)

In this section, we present the adaptation and development of the generalised pest model for the Coffee Berry Borer (CBB), focusing on the model-building process, structure, and parameter choices.

To construct the CBB-specific model framework, several assumptions and simplifications were made:

- **Fruit categorisation**: We hypothesise that fruit attractiveness to CBB is primarily determined by the number of days since flowering, estimated via accumulated temperature. Based on this, fruits are categorised into three distinct classes:

    1. **Very attractive fruits**: Ripe fruits that have turned red. We consider that at least 196 days have passed since the start of flowering.
    2. **Attractive fruits**: Well-developed green fruits, including those transitioning towards yellow. The upper threshold is 195 days, and the lower one is considered to be 95 days since the start of flowering.
    3. **Ground fruits**: Fruits from the above categories that have fallen to the ground. They are considered to be the two previous categories of fruits that have fallen; thus, we don't distinguish them in this category.

Small green fruits are excluded from the model, as they are not potential hosts for the CBB and thus play a negligible role in its life cycle.

- **Cohort structure**: We hypothesise that CBB populations can be represented as cohorts grouped by oviposition date. Each cohort is assumed to experience the same environmental conditions and follow uniform developmental dynamics.
- **Attraction factor**: We assume that each fruit category has a defined attraction coefficient (ranging between 0 and 1), which quantifies the likelihood of colonisation by a female CBB. This coefficient modulates host preference within the modelled space (i.e., the tree and its fruits).

- **Male exclusion and fertility**: We assume that males, which constitute approximately 10% of the population, can be excluded from the model without significantly compromising accuracy, as there are sufficient males within a fruit to ensure the fertilization of all females. Additionally, we assume that all females are fertile and capable of laying eggs.
- **Environmental effects**: We hypothesise that temperature is the dominant environmental variable controlling CBB development rate. Relative humidity and rainfall are incorporated as secondary modifiers, bounded by known physiological tolerance thresholds for the species.
- **Mortality mechanisms**: We assume two primary mechanisms of mortality: *Developmental mortality*, which occurs during the transformation from egg to adult and reflects physiological survival rates. *Post-emergence mortality*, which occurs after individuals leave the fruit, is largely due to predation, desiccation, or starvation.

  We assume that separating these two mortality types provides a more accurate representation of CBB population dynamics.

The life cycle of the CBB naturally divides into two distinct phases. The first phase occurs inside the coffee berry, where the CBB completes most of its development (green box in Fig. 2.4). The second phase begins when the adult female leaves the berry in search of new fruits to colonise, becoming highly exposed to external environmental factors (red box in Fig. 2.4).

The generalised model is structured to reflect the CBB's life cycle both within and outside the coffee berry (Fig. 2.5), with internal processes grounded in empirical data and external interactions modelled more conceptually due to data limitations.

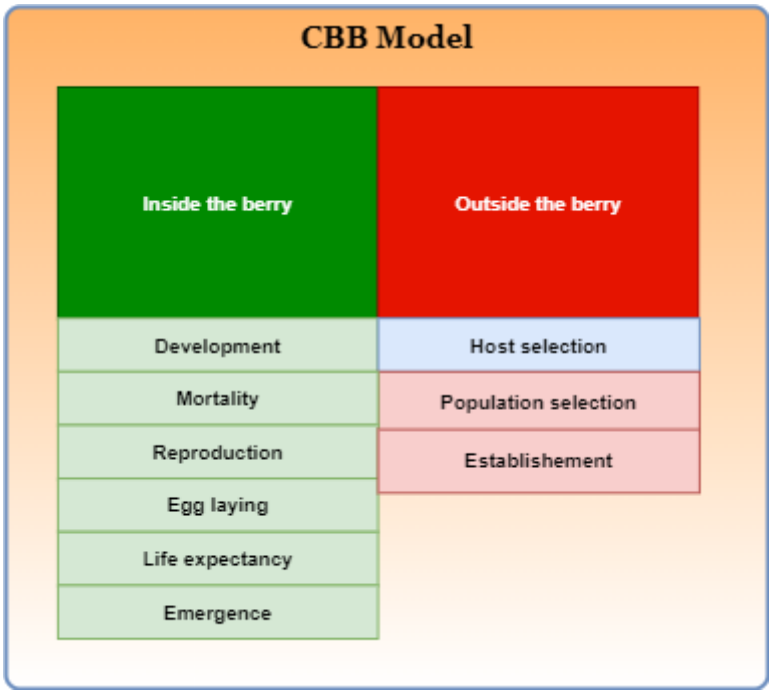


Figure 2. 5: CBB model modules, distributed between two main blocks.

The life cycle of the Coffee Berry Borer (CBB) inside a coffee berry involves the development of an egg into an adult, followed by biological mortality upon reaching adulthood. The model simulates this process through a series of stages:

- **Reproduction phase**: Upon reaching adulthood, each female is theoretically assessed for the presence of males to determine her reproductive potential. However, since we assume that males emerging from the same fruit (typically siblings) are always present and available for mating, this condition is considered to be systematically fulfilled for all adult females.
- **Life expectancy phase**: The lifespan of each adult individual is estimated, taking into account species-specific life history traits.
- **Exploration phase**: Following internal development, the model assesses whether individuals are capable of leaving the original berry to seek new hosts for colonisation.

Outside the berry, the model describes three key phases of CBB dispersal and colonisation:

1. **Host selection**: Individuals identify potential new fruits available for colonisation, as provided either by model simulations or input data.
2. **Population selection**: The model determines whether the simulated CBBs choose to colonise the offered fruits or disperse further in search of better options.
3. **Establishment**: The selected individuals and host fruits form new colonies, initiating a new reproductive cycle.

During these external phases, the CBB model dynamically interacts with the fruit module, which provides information about the availability and attractiveness of fruits for colonisation. It also accounts for interactions with CBB populations not explicitly tracked by the model: supplementary individuals may compete for the same fruits, while some modelled CBBs may disperse beyond the study area. Mortality during dispersal is also explicitly considered, influenced by climatic hazards (e.g., temperature extremes, humidity) and natural enemies.

From the perspective of the CBB model, any variable or parameter originating externally (from another model), for example, environmental conditions, is treated as an **input**. Each module within the model depends on specific inputs, although some inputs are common across multiple components (Fig. 2.4).

Using climate data as an external input ensures consistency across all modules, while allowing flexibility in the sequencing of modules and enabling the input format, such as temperature data presented daily, weekly, or otherwise, to be adapted to meet the specific temporal resolution required by each module.

For instance, in the first block of the model (the internal development phase illustrated in Fig. 2.5), temperature is a critical input required by all components to regulate developmental processes. Relative humidity serves as an additional key input, particularly influencing mortality rates and emergence dynamics. Furthermore, rainfall conditions are necessary for accurately modeling the timing and success of emergence from the berry.

The current model is composed of distinct, well-defined components, each informed by a combination of empirical data, established biological knowledge, and mathematical formulations. The internal biological dynamics, particularly those occurring within the coffee berry, are based on data extracted from existing literature, while the reproduction stage is included as a default value without explicit dynamic modeling. External dynamics, such as dispersal and host-seeking behaviour, are guided by selected scientific articles, expert input, and parameterised mathematical equations. Transitions between components are constructed in collaboration with domain experts, ensuring biological coherence. All procedures align with the knowledge-based modeling framework introduced earlier, reinforcing the consistency and scientific grounding of the model structure.

10.Pest Cohorts

The CBB model is structured around two primary state variables: the pest cohort and the fruits of interest. State variables represent observable properties of a system that define its current condition, such as population size, developmental stage distribution, or resource availability. Tracking these variables is essential for capturing the dynamic evolution of the pest population and its interactions with the environment.

The pest population is represented through cohorts, groups of individuals sharing key biological characteristics. Each cohort is described by a structured set of attributes, detailed in Table X1. The cohort description is defined as follows:

$$PestCohort(\text{Stage}, EggLayDay, NumberOfIndividuals, Reproduction, Development, LifeExpectancy, DeathDate, ReadyToAttack, SelectedForAttack, Matriarch, AttackDate)$$

Or, in a more mathematical formulation:

$$PCo\begin{pmatrix} Stage(K,V), t_0, N(t_0), Rep: \{0,1\}, D(t), L(t), tf, \\ ReA: \{0,1\}, SeA: \{0,1\}, Ma: \{0,1\}, t_a \end{pmatrix}$$

Table 2.2: Pest Cohort's description and expression

Cohort elements	Description of its function	Formulation	Expression
Stage	The current stage of the cohort	$"Stage"$	$Stage: K \rightarrow V$ K: Set of keys, V: Set of values
EggLayDate	The time of cohort initiation (e.g., the day the eggs were laid)	t_0	$t_0 = t_{cuurent}$, when a group of eggs are laid
NumberOfIndividuals	Number of individuals in the pest cohort	$N(t_0)$	$N(t_0) \sum new\ Pest\ eggs\ at\ t_0$
Reproduction	Egg-laying capacity of individuals in the cohort	$Rep: \{0, 1\}$	$Rep = \begin{cases} 1, & D = 1 \\ 0, & D < 1 \end{cases}$
Development	Egg-to-adult development rate	$D(t)$	$\sum_{t=t_0}^{t_{current}} \frac{1}{d(temperature, t)}$
LifeExpectancy	Normalised life progression index (0 = egg stage, 1 = death)	$L(t)$	$\sum_{t=t_0}^{t_{current}} \frac{1}{l(temperature, t)}$
DeathDate	The time of death for the cohort population	t_f	$t_f = t_{cuurent}$, when the $N(t_0)$ of the cohort are dead
ReadyToAttack	Readiness of the pest to disperse from its colony and establish elsewhere	$Rea: \{0, 1\}$	$Rea = \begin{cases} 1, & Stage = "Emergence" \\ 0, & Stage \neq "Emergence" \end{cases}$
SelectedForAttack	Readiness of the pest to colonise and establish a new colony, minus the cohorts that left for other trees	$SeA: \{0, 1\}$	$SeA = \begin{cases} 1, & Rea = 1 \\ 0, & Rea < 1 \end{cases}$
Matriarch	Pest's status as a new colony Founder	$Ma: \{0, 1\}$	$Ma = \begin{cases} 1, & Stage = "Establishement" \\ 0, & Stage \neq "Establishement" \end{cases}$
AttackDate	the time at which individuals leave their original fruit and colonise new ones.	t_a	$t_a = \begin{cases} t_{current}, & Ma = 1 \\ indef, & Ma \neq 1 \end{cases}$

The fruit population, representing the potential hosts, is managed separately through the fruits of interest state variable, allowing dynamic interaction with pest cohorts based on attraction factors, availability, and environmental conditions through the coupling platform MIMIC.

The Fruits of Interest state variable classifies fruits into two categories, colonised and healthy, establishing a clear distinction between fruits that can still be attacked and those that are no longer available for colonisation. Within each category, three subcategories are defined following the classification presented earlier in the hypothesis.

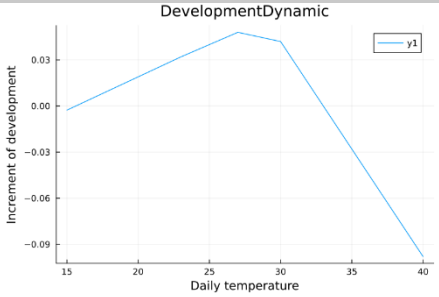
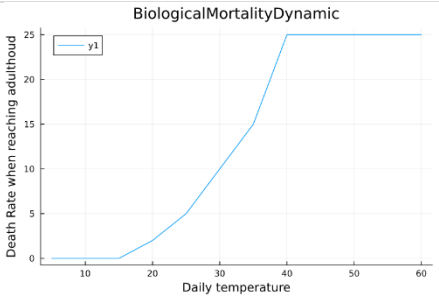
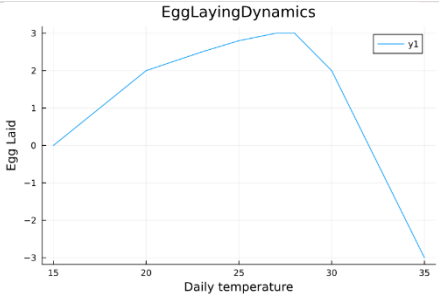
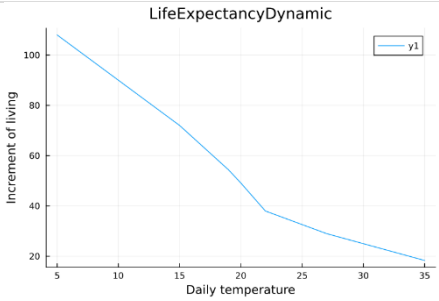
$$FruitsOfInterest = \begin{cases} Healthy \begin{cases} Very\ attractive \\ Attractive \\ Ground \end{cases} \\ Colonised \begin{cases} Very\ attractive \\ Attractive \\ Ground \end{cases} \end{cases}$$

Knowledge-based parametrisation of the CBB model, inside the berry

Several experimental studies have quantitatively linked Coffee Berry Borer population dynamics to external environmental factors, such as temperature, relative humidity, and rainfall, the key model inputs outlined earlier. From these sources, we extracted empirical relationships and trends that were further refined through expert discussions to ensure biological plausibility and contextual relevance.

The dynamics presented in Table 2.3 define each component of the model (its module).

Table 2.3: Data origin and representation for each module of the model

Module	Origin	Expression
Development	Literature	
Mortality	Literature	
Reproduction	Expert, Assumption	If Adult == can reproduce
Egg laying	Literature	
Life expectancy	Literature	
Emergence	Literature, Expert	Climatic conditions: Temperature >21°C < 31°C Rain = true (we consider it is true if it rains more than 2mm per day) Relative humidity > 40%

Knowledge-based parametrisation of CBB model, Outside the berry

The dynamics governing CBB behaviour outside the berry, particularly attraction to new host fruits, are complex and inherently difficult to quantify due to the multitude of environmental factors involved. Furthermore, expert opinions and empirical findings sometimes diverge on how specific elements influence pest behaviour.

To address these challenges, we developed mathematical relationships based on a combination of collected field data and expert consultations. These relationships incorporate **adjustable parameters**, allowing users to tailor the model to their specific conditions, expert knowledge, or calibration data.

In our case, the **Attraction factor** and **Mortality mechanisms** hypothesis are applied here. The mortality is integrated in the selection of the attacking population through a threshold ratio between the number of CBB and potential hosts. And the attraction factor is introduced in the calculation of the established colonies.

Host selection

Due to competition, not all healthy fruits may be attacked, even if there are enough CBB individuals. This may result from the difficulty in locating uncolonised fruits when their availability is low, as well as from competition among CBB individuals. The maximum number of healthy fruits that can be attacked is considered to be determined by an exponential relationship, where the likelihood of a fruit being colonised depends on both the number of healthy fruits available and the number of fruits already colonised on the same tree. The formulation is as follows:

$$\boldsymbol{Maximum\ of\ attacked\ fruits} = (\mathbf{1} - \boldsymbol{e}^{\left\{-\omega \frac{\boldsymbol{Healthy\ Fruits}}{\boldsymbol{Total\ Fruits}}\right\}}) * \boldsymbol{\ Healthy\ Fruits}$$

where the parameter ω regulates the curve's steepness, of the formula and can be adjusted to determine or consider the amount of the maximum attacked fruits. And the ***healthy fruits*** are the number of healthy fruits in each category.

Population selection

Once the maximum number of fruits available for colonisation is determined, the next step assess the **population of CBB** emerging from previously infested berries. A simple **population-to-host ratio** is calculated to estimate how many individuals will stay and attack fruits within the observed tree, while the remainder are assumed to migrate to surrounding trees:

$$\boldsymbol{RatioPestHost} = \frac{\boldsymbol{Emerged\ \ pest\ population}}{\boldsymbol{Maximum\ of\ attacked\ fruits}} < \boldsymbol{RatioThreshold}$$

The **RatioThreshold** is a flexible parameter defined by users, based on observations, expert assessments, or calibration against field data.

Establishment

Once both the susceptible fruit categories and the attacking pest population have been identified, the model proceeds to the establishment phase. This step simulates how pests successfully colonise new fruits, accounting for the varying attractiveness of different fruit types, very appealing, appealing, and ground fruits.

The model uses an Attractivity parameter for each fruit category, which reflects the influence of biological and chemical cues, particularly allelochemicals emitted by the host plant, that affect pest host preference. Because these factors are difficult to measure directly, Attractivity is treated as a normalised coefficient between 0 and 1 for each fruit class.

To calculate the number of fruits successfully attacked, the model weighs the attractiveness of each category against its availability. The establishment equation applied to each fruit class is:

$$\boldsymbol{AttackedFruits} = \boldsymbol{Attractivity} \times \boldsymbol{Emerged\ pest\ population} \times \boldsymbol{Proportions}$$

where:

- **Attractivity** is the vector of preference weights for each fruit category,
- **Emerged Pest Population** is the scalar value representing the total number of attacking pests
- **Proportions** vector representing the relative abundance of each fruit category.

This formulation ensures that the number of attacks is proportionally distributed according to both fruit availability and host preference, allowing a flexible and biologically interpretable representation of pest establishment dynamics.

The parameterisation of the CBB model outside the berry illustrates how empirical knowledge and expert assumptions can be systematically integrated, specifically through the parameters **ω**, **RatioThreshold**, **Attractivity**, and **Proportions**, into a modular framework, without requiring any changes to the algorithm itself. These formulations, covering host selection, population pressure and establishment, demonstrate the model's ability to represent key ecological interactions in a flexible and adaptable way. Together, these components provide the operational basis for simulating pest behaviour under a variety of field conditions and stay in under the scope of making it generic.

Now that the core dynamics are in place, it's important to reflect on what the model can and cannot do in its current form. The following discussion offers a practical look at its potential use in integrated pest management, while also outlining its current limitations and how it could be developed further.

11.Discussion and Conclusion

The model developed for the generic pest and disease (P&D) framework is designed to offer a flexible and adaptable approach for simulating pest population dynamics across a wide range

of agricultural systems. Its modular structure allows it to be tailored to specific pests, crop types, and geographical regions, making it applicable to various pest management scenarios. This flexibility enables adaptation to local environmental conditions, crop phenology, and pest pressure, factors that are crucial for effective and sustainable pest management practices.

A core advantage of the model lies in its modular architecture, which is designed to reflect the biological and ecological complexity of pest systems while maintaining conceptual clarity. The model separates pest behaviour into two major components: maturation (internal development in a relatively stable microenvironment) and interaction (external engagement with environmental factors, including host selection and colonisation). This separation is biologically justified, as certain pest species—such as the two studied—exhibit two distinct phases: a developmental phase and a reproductive–dispersal phase. This structure allows for a more accurate representation of their life cycle. It is also methodologically advantageous, as it enables the independent calibration and targeted application of each model component based on data availability or specific research objectives. Each biological process, such as development, reproduction, mortality, emergence, host selection, and establishment, is encapsulated in a dedicated module that can be selectively activated, parameterised, or modified. This structure is particularly helpful in addressing a common challenge in pest modeling: incomplete or uneven datasets. When empirical data for certain processes (e.g., dispersal, natural enemies) are limited or unavailable, the relevant modules can be temporarily disabled without compromising the integrity of the overall simulation. Conversely, detailed sub-models can be introduced as data becomes available, ensuring the model remains scalable and responsive to both simple and complex applications.

The generalised model also integrates both empirical data and expert knowledge, enabling robust calibration using historical datasets, field observations, and domain expertise. This hybrid capacity improves the model's predictive accuracy while preserving its general applicability across diverse cropping systems and agroecological contexts. Furthermore, the inclusion of host resource dynamics, such as fruit availability, quality, and status, allows the model to simulate key feedback loops between pest populations and host phenology. These dynamics are further shaped by environmental variability (e.g., temperature, humidity, rainfall), reinforcing the model's relevance under current and future climate scenarios.

The implementation of the generalised model for the Coffee Berry Borer (CBB) serves as a valuable case study, illustrating both the flexibility and current limitations of the framework.

The CBB-specific model is built upon a set of targeted hypotheses, each designed to simplify complex ecological interactions while retaining biological realism. One of the most central is the fruit categorisation hypothesis, which assumes that fruit attractiveness to the CBB is determined by thermal time since flowering. Fruits are thereby grouped into three operational categories: very attractive, attractive, and ground fruits, which structure the simulation of host selection and colonisation. This abstraction, while generalisable and useful, would benefit from more detailed biochemical validation across different cultivars and environments.

The cohort structure is another key feature, hypothesising that CBB populations can be grouped by oviposition time and shared developmental trajectory. This assumption supports computational efficiency while capturing the dominant trends in population behaviour, though it simplifies micro-scale variability such as spatial heterogeneity or asynchronous development.

Similarly, the attraction factor, defined per fruit category, enables a probabilistic but structured representation of host preference, providing a flexible way to integrate expert-derived knowledge where direct measurements are lacking. The exclusion of males, justified by their minimal role in population dynamics, is valid for CBB but might require revision in other pest models.

Environmental inputs such as temperature, humidity, and rainfall are treated as primary drivers of development, mortality, and emergence. While widely used and supported by existing literature (Hamilton et al., 2019; Johnson and Manoukis, 2021), their effects are currently modelled linearly or through threshold functions. Future work could incorporate non-linearities or cumulative stress effects, particularly in scenarios involving climate extremes or complex management regimes.

An essential aspect of the model is the initialisation phase, which sets biologically coherent starting conditions for simulations. Pest cohorts are created based on a defined egg-laying event and assigned values for life expectancy, development, and reproduction. Fruit populations are categorised by attractiveness and colonisation status. This structure allows the model to be easily configured for different cropping scenarios, infestation stages, or environmental settings, enhancing its operational flexibility and transferability.

Partitioning mortality into developmental and post-emergence phases adds biological precision, aligning well with observed patterns in CBB life cycles. Processes occurring after adult emergence—such as dispersal, host selection, and colony initiation—are represented through probabilistic mechanisms governed by adjustable parameters (e.g., ω, RatioThreshold, Attractivity), which facilitate both site-specific calibration and broader model portability. Although the modeling framework necessarily abstracts some biological complexity, the assumptions made are explicitly defined, empirically supported, and designed to balance interpretability with predictive utility.

The integration of the CBB model with MIMIC, a multi-model coupling framework, offers a powerful approach to extending the model's capabilities, enabling the simulation of complex agroecosystem interactions, including plant-pest dynamics and pest cohort interactions. MIMIC allows for in-memory, real-time coupling of independently developed simulation models, such as climate simulators, plant growth models, or economic decision tools, enabling synchronised, multi-directional data exchange.

Incorporating the CBB model into MIMIC offers several key advantages:

- **Dynamic feedback loops** between pest behaviour and plant physiology (e.g., changes in berry development or nutrient stress) can be explicitly simulated.

- **Climate responsiveness** can be enhanced by linking with weather generators or regional climate models, enabling more realistic forecasting under climate change scenarios.
- **Modular independence** is preserved, meaning that improvements to one model do not require reengineering of the entire system.

By leveraging MIMIC's infrastructure, the generalised P&D model, exemplified here through its CBB application, can be embedded within broader agroecological simulation platforms, making it an effective tool for research, extension services, and decision-support systems alike. It advances the model's relevance from a single-pest focus to a systems-level perspective, crucial for addressing the interdependent challenges of climate resilience, biodiversity, and agricultural productivity.

The generalised pest and disease (P&D) model developed in this study presents a robust and flexible framework for simulating pest dynamics across diverse agricultural systems. By adopting a modular, hypothesis-driven structure, the model successfully balances biological realism with computational efficiency. It enables the simulation of key life history processes, such as development, mortality, reproduction, and host colonisation, while allowing for adaptation to a wide range of pest species, host plants, and environmental conditions.

While the model does not represent the full complexity of agroecological systems, its modular and extensible structure offers a solid base for future development and adaptation. Current limitations, such as data scarcity, uncertainties in initial conditions, and simplified ecological assumptions, remain challenges, but the model is designed to accommodate gradual improvements. New datasets, biological insights, or external modules can be integrated without major structural changes.

The model's compatibility with coupling frameworks, MIMIC, further extends its potential by enabling integration with other systems, such as crop models or climate simulations. This makes it well-suited for exploring interactions between pest dynamics, environmental variability, and plant development in a coordinated way.

Overall, this work delivers a practical and adaptable modeling framework. It applies to individual pest cases like the Coffee Berry Borer but also serves more broadly as a tool for analysing pest–plant–environment interactions across diverse agricultural settings.

12.Implementation of the pest generalised model

This section presents the algorithmic implementation of the generalised pest model for the CBB case, with a specific focus on how the biological structure is translated into computational components. The model has been designed to simulate the life cycle and behaviour of pest populations at the cohort level, incorporating environmental dependencies, host dynamics, and biological processes in a modular and extensible architecture.

Object-Oriented Structure and Biological Entities

The simulation is grounded in a **cohort-based approach**, in which pest populations are grouped into units (PestCohort) sharing key biological traits: developmental stage, hatching date, individual count, energy accumulation, reproduction status, and lifecycle metrics. This object-oriented structure allows fine-grained tracking of cohort dynamics and facilitates scalable population modeling.

Each PestCohort object tracks:

- **Stage**: the current biological state (e.g., development, reproduction, emergence),
- **HatchingDate**: initiation date of the cohort,
- **Development**: progression through developmental phases (0 to 1),
- **LifeExpectancy**: normalised lifespan,
- **Reproduction, ReadyToAttack, Matriarch**: Boolean reflecting reproductive potential and colonisation status,
- **AttackDate, DateOfDeath**: temporal markers of key life events.

Fruits, the primary host resource, are managed through a FruitsOfInterest object, which dynamically tracks fruit availability and colonisation status across three categories: **very attractive**, **attractive**, and **ground fruits**. Percentages of healthy and attacked fruits in each category are calculated at every simulation step, enabling realistic host-pest interaction dynamics.

Biological Process Modules

Biological processes are encapsulated in the PestStages structure. This structure maps each stage of the pest life cycle to a corresponding function. These include:

- **Alimentation**: Sets the stage label to track active feeding.
- **Development**: Incremental development based on temperature-dependent functions; includes intra-fruit mortality due to unsuitable environmental conditions.
- **Reproduction and Egg Laying**: Governed by maturity and reproductive readiness; successful females lay new cohorts based on temperature-dependent egg production rates.
- **Life Expectancy**: Progresses individuals through life span dynamics, terminating cohorts that exceed biological limits.
- **Mortality**: Includes internal mortality (developmental failure) and external mortality (e.g., exposure, predation, desiccation).
- **Emergence**: Triggers transition from berry to external environment based on humidity, rain, and temperature.

- **Host Selection and Population Filtering**: Evaluates resource availability and determines the portion of individuals that attempt to colonise fruits.
- **Establishment**: Calculates fruit colonisation success based on attractiveness coefficients and pest pressure.

Each module is executed in an order specified by a ranked sequence (StageRank) to ensure that biological causality is respected. For instance, development precedes emergence, and reproduction occurs only once emergence and maturation conditions are met.

Simulation Cycle and Execution Flow

The simulation proceeds in **daily cycles**, orchestrated by a main function (MainGcbb). Each cycle performs the following steps:

1. **Ordering**: StageRank is sorted to enforce logical execution.
2. **Execution**: PestCycleExecution iterates through ordered stages and applies relevant functions to all cohorts.
3. **Updates**: Cohorts and fruit resources are updated after each biological stage.

The **PestCycleExecution** function ensures modular execution by dynamically evaluating the appropriate function for each stage, maintaining flexibility and extensibility. Daily execution reflects both cohort evolution and changes in fruit availability, enabling responsive simulations over extended periods.

Environmental Integration and Data processing

Environmental variables, **temperature, humidity, and rainfall**, are integrated into core biological functions via interpolated empirical functions. These include:

- **DevelopmentDynamic**: Calculates daily development rate based on temperature,
- **BiologicalMortalityDynamic**: Adjusts mortality according to combined temperature and humidity conditions,
- **EggLayingDynamics**: Computes daily fecundity as a function of temperature,
- **EmergenceDynamic**: Triggers emergence probability based on microclimatic thresholds,
- **LifeExpectancyDynamic**: Determines progression through the normalised lifespan based on temperature.

Linear interpolation ensures smooth and biologically plausible transitions between empirical data points. First-call caching is used to initialise interpolation functions efficiently on the first simulation step.

Host Interaction and Colonisation Logic

The model includes detailed logic for simulating **colonisation behaviour**, balancing pest pressure with host availability:

- **HostSelectionDynamic** estimates fruit availability by applying exponential response curves to observed fruit categories.
- **PopulationSelectionDynamic** calculates pest-to-host ratios and determines how many individuals colonise vs. disperse.
- **EstablishementDynamic** distributes successful attackers across fruit categories, weighted by attractiveness and proportional abundance.

Each of these modules uses parameters like Attractivity, ω, and RatioThreshold to regulate colonisation pressure, competitive exclusion, and dispersal.

13.References

Abel, D.J., Kilby, P.J., Davis, J.R., 1994. The systems integration problem. Int. J. Geogr. Inf. Syst. 8, 1–12. https://doi.org/10.1080/02693799408901984

Aggarwal, P.K., Kalra, N., Chander, S., Pathak, H., 2006. InfoCrop: A dynamic simulation model for the assessment of crop yields, losses due to pests, and environmental impact of agro-ecosystems in tropical environments. I. Model description. Agric. Syst. 89, 1–25. https://doi.org/10.1016/j.agsy.2005.08.001

Argent, R.M., Voinov, A., Maxwell, T., Cuddy, S.M., Rahman, J.M., Seaton, S., Vertessy, R.A., Braddock, R.D., 2006. Comparing modeling frameworks – A workshop approach. Environ. Model. Softw. 21, 895–910. https://doi.org/10.1016/j.envsoft.2005.05.004

Aristizábal, L.F., Jiménez, M., Bustillo, A.E., Trujillo, H.I., Arthurs, S.P., 2015. Monitoring Coffee Berry Borer, *Hypothenemus hampei* (Coleoptera: Curculionidae), Populations with Alcoholbaited Funnel Traps in Coffee Farms in Colombia. Fla. Entomol. 98, 381–383. https://doi.org/10.1653/024.098.0165

Avelino, J., Barboza, B., Araya, J., Fonseca, C., Davrieux, F., Guyot, B., Cilas, C., 2005. Effects of slope exposure, altitude and yield on coffee quality in two altitude terroirs of Costa Rica, Orosi and Santa María de Dota. J. Sci. Food Agric. 85, 1869–1876. https://doi.org/10.1002/jsfa.2188

Bale, J., Masters, G., Hodkinson, I., Awmack, C., Bezemer, T. m, Brown, V., Butterfield, J., Buse, A., Coulson, J., Farrar, J., Good, J., Harrington, R., Hartley, S., Jones, T., Lindroth, R., Press, M., Symrnioudis, I., Watt, A., Whittaker, J., 2002. Herbivory in global climate change research: Direct effects of rising temperature on insect herbivores. Glob. Change Biol. 8, 1–16. https://doi.org/10.1046/j.1365-2486.2002.00451.x

Barthélémy, D., Caraglio, Y., 2007. Plant Architecture: A Dynamic, Multilevel and Comprehensive Approach to Plant Form, Structure and Ontogeny. Ann. Bot. 99, 375–407. https://doi.org/10.1093/aob/mcl260

Bar-Yam, Y., 2002. General Features of Complex Systems. UNESCO Encycl. Life Support Syst.

Ben-Kiki, O., Evans, C., n.d. YAML Ain't Markup Language (YAML™) Version 1.2.

Bergez, J.-E., Chabrier, P., Gary, C., Jeuffroy, M.H., Makowski, D., Quesnel, G., Ramat, E., Raynal, H., Rousse, N., Wallach, D., Debaeke, P., Durand, P., Duru, M., Dury, J., Faverdin, P., Gascuel-Odoux, C., Garcia, F., 2013. An open platform to build, evaluate

and simulate integrated models of farming and agro-ecosystems. Environ. Model. Softw., Thematic Issue on the Future of Integrated Modeling Science and Technology 39, 39–49. https://doi.org/10.1016/j.envsoft.2012.03.011
Bezanson, J., Edelman, A., Karpinski, S., Shah, V.B., 2017. Julia: A Fresh Approach to Numerical Computing. SIAM Rev. 59, 65–98. https://doi.org/10.1137/141000671
Bolker, B.M., 2008. Ecological Models and Data in R. Princeton University Press. https://doi.org/10.2307/j.ctvcm4g37
Bondad, J., Harrison, M.T., Whish, J., Sprague, S., Barry, K., 2023. Integrated crop-disease models: New frontiers in systems thinking. Farming Syst. 1, 100004. https://doi.org/10.1016/j.farsys.2023.100004
Bouchet, P.J., Peterson, A.T., Zurell, D., Dormann, C.F., Schoeman, D., Ross, R.E., Snelgrove, P., Sequeira, A.M.M., Whittingham, M.J., Wang, L., Rapacciuolo, G., Oppel, S., Mellin, C., Lauria, V., Krishnakumar, P.K., Jones, A.R., Heinänen, S., Heikkinen, R.K., Gregr, E.J., Fielding, A.H., Caley, M.J., Barbosa, A.M., Bamford, A.J., Lozano-Montes, H., Parnell, S., Wenger, S., Yates, K.L., 2019. Better Model Transfers Require Knowledge of Mechanisms. Trends Ecol. Evol. 34, 489–490. https://doi.org/10.1016/j.tree.2019.04.006
Bouman, B.A.M., van Keulen, H., van Laar, H.H., Rabbinge, R., 1996. The 'School of de Wit' crop growth simulation models: A pedigree and historical overview. Agric. Syst. 52, 171–198. https://doi.org/10.1016/0308-521X(96)00011-X
Brandmeyer, J.E., Karimi, H.A., 2000. Coupling methodologies for environmental models. Environ. Model. Softw. 15, 479–488. https://doi.org/10.1016/S1364-8152(00)00027-X
Buddie, A.G., Crozier, J., Rutherford, M.A., Flood, J., Bridge, P.D., 2015. Population development within the coffee wilt pathogen Gibberella xylarioides reflects host-related divergence. Eur. J. Plant Pathol. 142, 291–304. https://doi.org/10.1007/s10658-015-0613-z
Buis, R., Barthou, H., Frezouls, M., 1987. Relations dimensionnelles inter-feuilles: Mise en évidence d'actions locales et à distance. Bull. Société Bot. Fr. Lett. Bot. 134, 107–114. https://doi.org/10.1080/01811797.1987.10824734
Cerda, R., Avelino, J., Gary, C., Tixier, P., Lechevallier, E., Allinne, C., 2017. Primary and Secondary Yield Losses Caused by Pests and Diseases: Assessment and Modeling in Coffee. PLOS ONE 12, e0169133. https://doi.org/10.1371/journal.pone.0169133
Chabrier, P., Garcia, F., Martin-Clouaire, R., Quesnel, G., Raynal, H., 2007. Toward a simulation modeling platform for studying cropping systems management: the record project, in: International Congress on Modeling and Simulation, International Society for Computer Simulation. Citeseer, pp. 10–13.
Cournède, P.-H., Guyard, T., Bayol, B., Griffon, S., de Coligny, F., Borianne, P., Jaeger, M., de Reffye, P., 2009. A Forest Growth Simulator Based on Functional-Structural Modeling of Individual Trees, in: 2009 Third International Symposium on Plant Growth Modeling, Simulation, Visualization and Applications. Presented at the 2009 Third International Symposium on Plant Growth Modeling, Simulation, Visualization and Applications, pp. 34–41. https://doi.org/10.1109/PMA.2009.55
Cournède, P.-H., Kang, M.-Z., Mathieu, A., Barczi, J.-F., Yan, H.-P., Hu, B.-G., de Reffye, P., 2006. Structural Factorization of Plants to Compute Their Functional and Architectural Growth. SIMULATION 82, 427–438. https://doi.org/10.1177/0037549706069341

Daane, K.M., Malakar-Kuenen, R.D., Walton, V.M., 2004. Temperature-dependent development of *Anagyrus pseudococci* (Hymenoptera: Encyrtidae) as a parasitoid of the vine mealybug, *Planococcus ficus* (Homoptera: Pseudococcidae). Biol. Control 31, 123–132. https://doi.org/10.1016/j.biocontrol.2004.04.010

Damon, A., 2000. A review of the biology and control of the coffee berry borer, *Hypothenemus hampei* (Coleoptera: Scolytidae). Bull. Entomol. Res. 90, 453–465. https://doi.org/10.1017/S0007485300000584

de REFFYE, P., n.d. Etude du fonctionnement des méristèmes et de la croissance des axes végétatifs.

de Reffye, P., Heuvelink, E., Guo, Y., Hu, B.-G., Zhang, B.-G., 2009. Coupling Process-Based Models and Plant Architectural Models: A Key Issue for Simulating Crop Production, in: Cao, W., White, J.W., Wang, E. (Eds.), Crop Modeling and Decision Support. Springer, Berlin, Heidelberg, pp. 130–147. https://doi.org/10.1007/978-3-642-01132-0_15

de Reffye, P., Hu, B., Kang, M., Letort, V., Jaeger, M., 2021. Two decades of research with the GreenLab model in Agronomy. Ann. Bot. 127, 281–295. https://doi.org/10.1093/aob/mcaa172

De Reffye, P., Jaeger, M., 2013. Modèles mathématiques du développement et de la croissance de l'architecture des plantes. Le cas du modèle GreenLab - Agritrop, in: Modéliser & Simuler. pp. 625–658.

De Reffye, P., Snoeck, J., 1976. Modèle mathématique de base pour l'étude et la simulation de la croissance et de l'architecture du Coffea robusta. Café Cacao Thé.

Donatelli, M., Magarey, R.D., Bregaglio, S., Willocquet, L., Whish, J.P.M., Savary, S., 2017. Modeling the impacts of pests and diseases on agricultural systems. Agric. Syst. 155, 213–224. https://doi.org/10.1016/j.agsy.2017.01.019

Dufour, B.P., Diman, C., De San Mateo, A., Mouttet, R., 2022. Le scolyte des fruits du caféier, *Hypothenemus hampei* (Ferr.) détecté en Guadeloupe. Cah. Agric. 31, 10. https://doi.org/10.1051/cagri/2022008

Dufour, B.P., Frérot, B., 2008. Optimization of coffee berry borer, *Hypothenemus hampei* Ferrari (Col., Scolytidae), mass trapping with an attractant mixture. J. Appl. Entomol. 132, 591–600. https://doi.org/10.1111/j.1439-0418.2008.01291.x

Dufour, B.P., Kerana, I.W., Ribeyre, F., 2021. Population dynamics of Hypothenemus hampei (Ferrari) according to the phenology of Coffea arabica L. in equatorial conditions of North Sumatra. Crop Prot. 146, 105639. https://doi.org/10.1016/j.cropro.2021.105639

Gaitán, A.L., Cristancho, M.A., Castro Caicedo, B.L., Rivillas, C.A., Gómez, G.C., 2016a. PART I: Infectious Diseases, in: Bertha, L.C.C., Marco, A.C., Gabriel, C.G., Carlos, A.R., Alvaro, L.G. (Eds.), Compendium of Coffee Diseases and Pests, Diseases and Pests Compendium Series. The American Phytopathological Society, pp. 3–44. https://doi.org/10.1094/9780890544723.002

Gaitán, A.L., Cristancho, M.A., Castro Caicedo, B.L., Rivillas, C.A., Gómez, G.C., 2016b. PART II: Pests, in: Bertha, L.C.C., Carlos, A.R., Marco, A.C., Alvaro, L.G., Gabriel, C.G. (Eds.), Compendium of Coffee Diseases and Pests, Diseases and Pests Compendium Series. The American Phytopathological Society, pp. 45–60. https://doi.org/10.1094/9780890544723.003

Gaitán, A.L., Cristancho, M.A., Castro Caicedo, B.L., Rivillas, C.A., Gómez, G.C., 2016c. PART III: Abiotic and Physiological Disorders, in: Marco, A.C., Carlos, A.R., Gabriel, C.G.,

Bertha, L.C.C., Alvaro, L.G. (Eds.), Compendium of Coffee Diseases and Pests, Diseases and Pests Compendium Series. The American Phytopathological Society, pp. 61–66. https://doi.org/10.1094/9780890544723.004
Gamma, E., Helm, R., Johnson, R., Vlissides, J., 1994. Design Patterns: Elements of Reusable Object-Oriented Software. Pearson Education.
Garin, G., Fournier, C., Andrieu, B., Houlès, V., Robert, C., Pradal, C., 2014. A modeling framework to simulate foliar fungal epidemics using functional–structural plant models. Ann. Bot. 114, 795–812. https://doi.org/10.1093/aob/mcu101
Gaudio, N., Louarn, G., Barillot, R., Meunier, C., Vezy, R., Launay, M., 2022. Exploring complementarities between modeling approaches that enable upscaling from plant community functioning to ecosystem services as a way to support agroecological transition. Silico Plants 4, diab037. https://doi.org/10.1093/insilicoplants/diab037
Gaunt, R.E., 1995. The Relationship Between Plant Disease Severity and Yield. Annu. Rev. Phytopathol. 33, 119–144. https://doi.org/10.1146/annurev.py.33.090195.001003
Gignoux, J., Davies, I.D., Flint, S.R., 2022. 3Worlds, a simulation platform for ecosystem modeling. Ecol. Model. 473, 110121. https://doi.org/10.1016/j.ecolmodel.2022.110121
Giordanengo, P., Brun, L.O., Frerot, B., 1993. Evidence for allelochemical attraction of the coffee berry borer,Hypothenemus hampei, by coffee berries. J. Chem. Ecol. 19, 763–769. https://doi.org/10.1007/BF00985007
Greco, E.B., Wright, M.G., 2015. Ecology, Biology, and Management of Xylosandrus compactus (Coleoptera: Curculionidae: Scolytinae) with Emphasis on Coffee in Hawaii. J. Integr. Pest Manag. 6, 7–7. https://doi.org/10.1093/jipm/pmv007
Guo, Y., Fourcaud, T., Jaeger, M., Zhang, X., Li, B., 2011. Plant growth and architectural modeling and its applications. Ann. Bot. 107, 723–727. https://doi.org/10.1093/aob/mcr073
Hallé, F., 2017. Des données récentes sur les arbres 48.
Hallé, F., Oldeman, R., 1970. Essai sur l'architecture et la dynamique de croissance des arbres tropicaux, Collection de monographies de botanique et de biologie végétale. Masson et Cie, Paris.
Hallé, F., Oldeman, R.A.A., Tomlinson, P.B., 1978. Tropical Trees and Forests. Springer, Berlin, Heidelberg. https://doi.org/10.1007/978-3-642-81190-6
Hamilton, L.J., Hollingsworth, R.G., Sabado-Halpern, M., Manoukis, N.C., Follett, P.A., Johnson, M.A., 2019. Coffee berry borer (Hypothenemus hampei) (Coleoptera: Curculionidae) development across an elevational gradient on Hawai'i Island: Applying laboratory degree-day predictions to natural field populations. PLoS ONE 14, e0218321. https://doi.org/10.1371/journal.pone.0218321
Henke, M., Kurth, W., Buck-Sorlin, G.H., 2016. FSPM-P: towards a general functional-structural plant model for robust and comprehensive model development. Front. Comput. Sci. 10, 1103–1117. https://doi.org/10.1007/s11704-015-4472-8
Heuvelink, E., 1996. Dry Matter Partitioning in Tomato: Validation of a Dynamic Simulation Model. Ann. Bot. 77, 71–80. https://doi.org/10.1006/anbo.1996.0009
Hultman, C., 2016. Black coffee twig borer, Xylosandrus compactus (Eichhoff) on robusta coffee in Uganda [WWW Document]. URL https://stud.epsilon.slu.se/9580/ (accessed 5.5.25).
Jaramillo, J., Chabi-olaye, A., Borgemeister, C., 2010. Temperature-Dependent Development and Emergence Pattern of <I>Hypothenemus hampei</I> (Coleoptera: Curculionidae:

Scolytinae) From Coffee Berries. J. Econ. Entomol. 103, 1159–1165. https://doi.org/10.1603/EC09408
Jaramillo, J., Chabi-Olaye, A., Kamonjo, C., Jaramillo, A., Vega, F.E., Poehling, H.-M., Borgemeister, C., 2009. Thermal Tolerance of the Coffee Berry Borer Hypothenemus hampei: Predictions of Climate Change Impact on a Tropical Insect Pest. PLoS ONE 4, e6487. https://doi.org/10.1371/journal.pone.0006487
Johnson, M.A., Manoukis, N.C., 2021. Influence of seasonal and climatic variables on coffee berry borer (Hypothenemus hampei Ferrari) flight activity in Hawaii. PLOS ONE 16, e0257861. https://doi.org/10.1371/journal.pone.0257861
Kagezi, G., Kucel, P., Egonyu, J.P., Kyamanywa, S., Karungi, J.T., Pinard, F., Jaramillo, J., Van Asten, P.J.A., Wagoire, W.W., Ngabirano, H., 2015. A review of the status and progress in management research of the black coffee twig borer, Xylosandrus compactus (Eichhoff) in Uganda [WWW Document]. Proc. 25th Int. Conf. Coffee Sci. URL https://agritrop.cirad.fr/579968/ (accessed 2.27.23).
Kang, M., Hua, J., de Reffye, P., Jaeger, M., 2016. Parameter identification of plant growth models with stochastic development, in: 2016 IEEE International Conference on Functional-Structural Plant Growth Modeling, Simulation, Visualization and Applications (FSPMA). Presented at the 2016 IEEE International Conference on Functional-Structural Plant Growth Modeling, Simulation, Visualization and Applications (FSPMA), pp. 98–105. https://doi.org/10.1109/FSPMA.2016.7818294
Kang, M., Hua, J., Wang, X., de Reffye, P., Jaeger, M., Akaffou, S., 2018. Estimating Sink Parameters of Stochastic Functional-Structural Plant Models Using Organic Series-Continuous and Rhythmic Development. Front. Plant Sci. 9, 1688. https://doi.org/10.3389/fpls.2018.01688
Kang, M.Z., Cournède, P.H., de Reffye, P., Auclair, D., Hu, B.G., 2008. Analytical study of a stochastic plant growth model: Application to the GreenLab model. Math. Comput. Simul. 78, 57–75. https://doi.org/10.1016/j.matcom.2007.06.003
Khan, J., Rio, L.E.D., Nelson, R., Rivera-Varas, V., Secor, G.A., Khan, M.F.R., 2008. Survival, Dispersal, and Primary Infection Site for Cercospora beticola in Sugar Beet. Plant Dis. 92, 741–745. https://doi.org/10.1094/PDIS-92-5-0741
Kirkeby, C., Brookes, V.J., Ward, M.P., Dürr, S., Halasa, T., 2021. A Practical Introduction to Mechanistic Modeling of Disease Transmission in Veterinary Science. Front. Vet. Sci. 7, 546651. https://doi.org/10.3389/fvets.2020.546651
Kropff, M.J., Teng, P.S., Rabbinge, R., 1995. The challenge of linking pest and crop models. Agric. Syst., Agricultural Systems Applications Through an International Consortium, ICASA 49, 413–434. https://doi.org/10.1016/0308-521X(95)00034-3
Lasso, E., Motisi, N., Avelino, J., Corrales, J.C., 2021. FramePests: A Comprehensive Framework for Crop Pests Modeling and Forecasting. IEEE Access 9, 115579–115598. https://doi.org/10.1109/ACCESS.2021.3104537
Le Chevalier, V., Jaeger, M., Mei, X., Cournède, P.-H., 2007. Simulation and Visualisation of Functional Landscapes: Effects of the Water Resource Competition Between Plants. J. Comput. Sci. Technol. 22, 835–845. https://doi.org/10.1007/s11390-007-9105-8
Leclerc, G., Bommel, P., Motisi, N., Vezy, R., Treminio, E., Avelino, J., 2021. Coffee leaf rust (Hemeleia vastatrix) risk management in Central America: contribution of remote interactive simulations. Agron. Environ. Sociétés 11. https://doi.org/10.54800/roc535

Lessler, J., Cummings, D.A.T., 2016. Mechanistic Models of Infectious Disease and Their Impact on Public Health. Am. J. Epidemiol. 183, 415–422. https://doi.org/10.1093/aje/kww021
Letort, V., Sabatier, S., Okoma, M.P., Jaeger, M., de Reffye, P., 2020. Internal trophic pressure, a regulator of plant development? Insights from a stochastic functional–structural plant growth model applied to Coffea trees. Ann. Bot. 126, 687–699. https://doi.org/10.1093/aob/mcaa023
Loi, C., Cournède, P., Françon, J., 2010. A symbolic method to compute the probability distribution of the number of pattern occurences in random texts generated by stochastic 0L-systems. Discrete Math. Theor. Comput. Sci.
Loi, C., Cournède, P.-H., Françon, J., 2014. A Symbolic Method to Analyse Patterns in Plant Structure. Comb. Probab. Comput. 23, 842–860. https://doi.org/10.1017/S0963548314000108
Lorenz, E.N., 1963. Deterministic Nonperiodic Flow. J. Atmospheric Sci. 20, 130–141. https://doi.org/10.1175/1520-0469(1963)020<0130:DNF>2.0.CO;2
Louarn, G., Song, Y., 2020. Two decades of functional–structural plant modeling: now addressing fundamental questions in systems biology and predictive ecology. Ann. Bot. 126, 501–509. https://doi.org/10.1093/aob/mcaa143
Luzinda, H., Nelima, M., Wabomba, A., Kangire, A., Musoli, P., Musebe, R., 2016. Farmer awareness, coping mechanisms and economic implications of coffee leaf rust disease in Uganda. Uganda J. Agric. Sci. 16, 207. https://doi.org/10.4314/ujas.v16i2.6
Ma, Y., Li, B., Zhan, Z., Guo, Y., Luquet, D., de Reffye, P., Dingkuhn, M., 2007. Parameter Stability of the Functional–Structural Plant Model GREENLAB as Affected by Variation within Populations, among Seasons and among Growth Stages. Ann. Bot. 99, 61–73. https://doi.org/10.1093/aob/mcl245
Mathieu, A., Cournède, P.H., Letort, V., Barthélémy, D., de Reffye, P., 2009. A dynamic model of plant growth with interactions between development and functional mechanisms to study plant structural plasticity related to trophic competition. Ann. Bot. 103, 1173–1186. https://doi.org/10.1093/aob/mcp054
Matovu, R., Kangire, A., Phiri, N., Hakiza, G., Kagezi, G., Musoli, P., 2013. Ecological factors influencing incidence and severity of Coffee Leaf Rust and Coffee Berry Disease in major Arabica coffee growing districts of Uganda. Uganda J. Agric. Sci.
Merle, I., Tixier, P., Virginio Filho, E. de M., Cilas, C., Avelino, J., 2020. Forecast models of coffee leaf rust symptoms and signs based on identified microclimatic combinations in coffee-based agroforestry systems in Costa Rica. Crop Prot. 130, 105046. https://doi.org/10.1016/j.cropro.2019.105046
Mora, J.R.M., n.d. Resposta Da Broca - Do - Cafe, Hypothenemus hampel, A Estimulos Visuais E Semioquimicos. INIAP Archivo Historico.
Motisi, N., Bommel, P., Leclerc, G., Robin, M.-H., Aubertot, J.-N., Butron, A.A., Merle, I., Treminio, E., Avelino, J., 2022. Improved forecasting of coffee leaf rust by qualitative modeling: Design and expert validation of the ExpeRoya model. Agric. Syst. 197, 103352. https://doi.org/10.1016/j.agsy.2021.103352
Motisi, N., Ribeyre, F., Poggi, S., 2019. Coffee tree architecture and its interactions with microclimates drive the dynamics of coffee berry disease in coffee trees. Sci. Rep. 9, 2544. https://doi.org/10.1038/s41598-019-38775-5
Nanjego, W., Kagezi, G., Kyamanywa, S., Ronald, S., Kobusinge, J., Arinaitwe, G., 2024. Population Dynamics of the Black Coffee Twig Borer Xylosandrus compactus

(Eichhoff) in Robusta Coffee Coffea canephora. Indian J. Entomol. https://doi.org/10.55446/IJE.2024.2046
Nelson, S.C., 2008. Cercospora Leaf Spot and Berry Blotch of Coffee.
Okoma, P., Akaffou, S., De Reffye, P., Hamon, P., Hamon, S., Konan, O., Kouassi, K.H., Legnate, H., Letort, V., Sabatier, S., 2018. Estimation of stem and leaf dry biomass using a non-destructive method applied to African Coffea species. Agrofor. Syst. 92, 667–675. https://doi.org/10.1007/s10457-016-0031-z
Papastamati, K., Welham, S.J., Fitt, B.D.L., Gladders, P., 2001. Modeling the progress of light leaf spot (Pyrenopeziza brassicae) on winter oilseed rape (Brassica napus) in relation to leaf wetness and temperature. Plant Pathol. 50, 154–164. https://doi.org/10.1046/j.1365-3059.2001.00551.x
Parmesan, C., Hanley, M.E., 2015. Plants and climate change: complexities and surprises. Ann. Bot. 116, 849–864. https://doi.org/10.1093/aob/mcv169
Peck, L.D., Boa, E., 2024. Coffee wilt disease: The forgotten threat to coffee. Plant Pathol. 73, 506–521. https://doi.org/10.1111/ppa.13833
Perkel, J.M., 2019. Julia: come for the syntax, stay for the speed. Nature 572, 141–142. https://doi.org/10.1038/d41586-019-02310-3
Pham, Y., Reardon-Smith, K., Mushtaq, S., Cockfield, G., 2019. The impact of climate change and variability on coffee production: a systematic review. Clim. Change 156, 609–630. https://doi.org/10.1007/s10584-019-02538-y
Piao, S., Liu, Q., Chen, A., Janssens, I.A., Fu, Y., Dai, J., Liu, L., Lian, X., Shen, M., Zhu, X., 2019. Plant phenology and global climate change: Current progresses and challenges. Glob. Change Biol. 25, 1922–1940. https://doi.org/10.1111/gcb.14619
Pinard, F., Makune, S.E., Campagne, P., Mwangi, J., 2016. Spatial Distribution of Coffee Wilt Disease Under Roguing and Replanting Conditions: A Case Study from Kaweri Estate in Uganda. Phytopathology® 106, 1291–1299. https://doi.org/10.1094/PHYTO-04-15-0097-R
Pradal, C., Dufour-Kowalski, S., Boudon, F., Donès, N., 2007. The architecture of OpenAlea: A visual programming and component based software for plant modeling.
Pradal, C., Dufour-Kowalski, S., Boudon, F., Fournier, C., Godin, C., 2008. OpenAlea: a visual programming and component-based software platform for plant modeling. Funct. Plant Biol. 35, 751–760. https://doi.org/10.1071/FP08084
Qi, R., Cournède, P.-H., de Reffye, P., 2009a. Tri-trophic Ecosystem Oil Palm-Pests-Auxiliaries: II. Sensitivity Analysis, Parameter Identification and Control, in: 2009 Third International Symposium on Plant Growth Modeling, Simulation, Visualization and Applications. Presented at the 2009 Third International Symposium on Plant Growth Modeling, Simulation, Visualization and Applications, pp. 327–333. https://doi.org/10.1109/PMA.2009.49
Qi, R., Cournède, P.-H., Lecoustre, R., de Reffye, P., 2009b. Tri-trophic Ecosystem Oil Palm-Pests-Auxiliaries: I. Modeling and Simulation, in: Proceedings of the 2009 Plant Growth Modeling, Simulation, Visualization, and Applications, PMA '09. IEEE Computer Society, USA, pp. 87–94. https://doi.org/10.1109/PMA.2009.48
Reffye, P. de, Hu, B.G., 2003. Relevant Qualitative and Quantitative choices for building an efficient dynamic plant growth model : Greenlab Case. Presented at the International Symposium on Plant Growth Modeling, Simulation, Visualization and their Applications - PMA'03, Springer and Tsinghua University Press, p. 87.

Ribeyre, F., Avelino, J., 2012. Impact of field pests and diseases on coffee quality. pp. 151–176.
Rivals, P., 1965. Essai sur la croissance des arbres et sur leurs systèmes de floraison (application aux espèces fruitières). J. Agric. Tradit. Bot. Appliquée 12, 655–686. https://doi.org/10.3406/jatba.1965.2856
ROBUST | Capacity4dev [WWW Document], n.d. URL https://capacity4dev.europa.eu/projects/desira/info/robust_en (accessed 5.13.25).
Rodríguez, D., Cure, J.R., Cotes, J.M., Gutierrez, A.P., Cantor, F., 2011. A coffee agroecosystem model: I. Growth and development of the coffee plant. Ecol. Model. 222, 3626–3639. https://doi.org/10.1016/j.ecolmodel.2011.08.003
Rodríguez, D., Cure, J.R., Gutierrez, A.P., Cotes, J.M., Cantor, F., 2013a. A coffee agroecosystem model: II. Dynamics of coffee berry borer. Ecol. Model. 248, 203–214. https://doi.org/10.1016/j.ecolmodel.2012.09.015
Rodríguez, D., Cure, J.R., Gutierrez, A.P., Cotes, J.M., Cantor, F., 2013b. A coffee agroecosystem model: II. Dynamics of coffee berry borer. Ecol. Model. 248, 203–214. https://doi.org/10.1016/j.ecolmodel.2012.09.015
Royama, T., 1992. Analytical population dynamics. London ; New York : Chapman & Hall.
Rutherford, M.A., 2006. Current Knowledge of Coffee Wilt Disease, a Major Constraint to Coffee Production in Africa. Phytopathology® 96, 663–666. https://doi.org/10.1094/PHYTO-96-0663
Savary, S., Nelson, A., Djurle, A., Esker, P.D., Sparks, A., Amorim, L., Filho, A.B., Caffi, T., Castilla, N., Garrett, K., Mcroberts, N., Rossi, V., Yuen, J., Willocquet, L., 2018. Concepts, approaches, and avenues for modeling crop health and crop losses. Eur. J. Agron. 15 p. https://doi.org/10.1016/j.eja.2018.04.003
Savary, S., Teng, P.S., Willocquet, L., Nutter, F.W., 2006. Quantification and Modeling of Crop Losses: A Review of Purposes. Annu. Rev. Phytopathol. 44, 89–112. https://doi.org/10.1146/annurev.phyto.44.070505.143342
Sedgwick, P., 2014. Retrospective cohort studies: advantages and disadvantages. BMJ 348, g1072. https://doi.org/10.1136/bmj.g1072
Siad, S.M., Iacobellis, V., Zdruli, P., Gioia, A., Stavi, I., Hoogenboom, G., 2019. A review of coupled hydrologic and crop growth models. Agric. Water Manag. 224, 105746. https://doi.org/10.1016/j.agwat.2019.105746
Sievänen, R., Perttunen, J., Nikinmaa, E., Posada, J.M., 2009. Invited Talk: Functional Structural Plant Models - Case LIGNUM, in: 2009 Third International Symposium on Plant Growth Modeling, Simulation, Visualization and Applications. Presented at the 2009 Third International Symposium on Plant Growth Modeling, Simulation, Visualization and Applications (PMA), IEEE, Beijing, China, pp. 3–9. https://doi.org/10.1109/PMA.2009.64
Soualiou, S., Wang, Z., Sun, W., de Reffye, P., Collins, B., Louarn, G., Song, Y., 2021. Functional–Structural Plant Models Mission in Advancing Crop Science: Opportunities and Prospects. Front. Plant Sci. 12, 747142. https://doi.org/10.3389/fpls.2021.747142
Souza, A.G.C., Rodrigues, F.Á., Maffia, L.A., Mizubuti, E.S.G., 2011. Infection Process of Cercospora coffeicola on Coffee Leaf: Infection Process of Cercospora coffeicola on Coffee Leaf. J. Phytopathol. 159, 6–11. https://doi.org/10.1111/j.1439-0434.2010.01710.x

Tan, M., Gou, F., Stomph, T.J., Wang, J., Yin, W., Zhang, L., Chai, Q., van der Werf, W., 2020. Dynamic process-based modeling of crop growth and competitive water extraction in relay strip intercropping: Model development and application to wheat-maize intercropping. Field Crops Res. 246, 107613. https://doi.org/10.1016/j.fcr.2019.107613

Tendeloo, Y.V., Vangheluwe, H., 2018. DISCRETE EVENT SYSTEM SPECIFICATION MODELING AND SIMULATION, in: 2018 Winter Simulation Conference (WSC). Presented at the 2018 Winter Simulation Conference (WSC), IEEE, Gothenburg, Sweden, pp. 162–176. https://doi.org/10.1109/WSC.2018.8632372

Túler, A., Valbon, W., de Souza Rodrigues, H., Noia, L., Santos, L., Fogaça, I., Rondelli, V., Filho, A., 2019. Black twig borer, Xylosandrus compactus (Eichhoff), a potential threat to coffee production. Rev. Cienc. Agríc. 36. https://doi.org/10.22267/rcia.1936E.102

Vezy, R., le Maire, G., Christina, M., Georgiou, S., Imbach, P., Hidalgo, H.G., Alfaro, E.J., Blitz-Frayret, C., Charbonnier, F., Lehner, P., Loustau, D., Roupsard, O., 2020. DynACof: A process-based model to study growth, yield and ecosystem services of coffee agroforestry systems. Environ. Model. Softw. 124, 104609. https://doi.org/10.1016/j.envsoft.2019.104609

Wang, N., Jassogne, L., van Asten, P.J.A., Mukasa, D., Wanyama, I., Kagezi, G., Giller, K.E., 2015. Evaluating coffee yield gaps and important biotic, abiotic, and management factors limiting coffee production in Uganda. Eur. J. Agron. 63, 1–11. https://doi.org/10.1016/j.eja.2014.11.003

Whish, J.P.M., Herrmann, N.I., White, N.A., Moore, A.D., Kriticos, D.J., 2015. Integrating pest population models with biophysical crop models to better represent the farming system. Environ. Model. Softw. 72, 418–425. https://doi.org/10.1016/j.envsoft.2014.10.010

Willmott, C.J., 1981. On the Validation of Models. Phys. Geogr. 2, 184–194. https://doi.org/10.1080/02723646.1981.10642213

Willocquet, L., Savary, S., Fernandez, L., Elazegui, F.A., Castilla, N., Zhu, D., Tang, Q., Huang, S., Lin, X., Singh, H.M., Srivastava, R.K., 2002. Structure and validation of RICEPEST, a production situation-driven, crop growth model simulating rice yield response to multiple pest injuries for tropical Asia. Ecol. Model. 153, 247–268. https://doi.org/10.1016/S0304-3800(02)00014-5

Wit, C.T. de, 1982. Simulation of living systems, in: Simulation of Plant Growth and Crop Production. Pudoc, pp. 3–8.

Wit, C.T. de, Vries, F.W.T.P. de, 1982. L'analyse des systemes de production primaire, in: La productivite des paturages Saheliens. Pudoc, pp. 20–23.

Yan, H., de Reffye, P., Pan, C., Hu, B., 2003. Fast construction of plant architectural models based on substructure decomposition. J. Comput. Sci. Technol. 18, 780–787. https://doi.org/10.1007/BF02945467

Yates, K.L., Bouchet, P.J., Caley, M.J., Mengersen, K., Randin, C.F., Parnell, S., Fielding, A.H., Bamford, A.J., Ban, S., Barbosa, A.M., Dormann, C.F., Elith, J., Embling, C.B., Ervin, G.N., Fisher, R., Gould, S., Graf, R.F., Gregr, E.J., Halpin, P.N., Heikkinen, R.K., Heinänen, S., Jones, A.R., Krishnakumar, P.K., Lauria, V., Lozano-Montes, H., Mannocci, L., Mellin, C., Mesgaran, M.B., Moreno-Amat, E., Mormede, S., Novaczek, E., Oppel, S., Ortuño Crespo, G., Peterson, A.T., Rapacciuolo, G., Roberts, J.J., Ross, R.E., Scales, K.L., Schoeman, D., Snelgrove, P., Sundblad, G., Thuiller, W., Torres, L.G., Verbruggen, H., Wang, L., Wenger, S., Whittingham, M.J., Zharikov, Y., Zurell, D.,

Sequeira, A.M.M., 2018. Outstanding Challenges in the Transferability of Ecological Models. Trends Ecol. Evol. 33, 790–802. https://doi.org/10.1016/j.tree.2018.08.001
Yin, X., 2003. A Flexible Sigmoid Function of Determinate Growth. Ann. Bot. 91, 361–371. https://doi.org/10.1093/aob/mcg029
Zeigler, B.P., 1989. DEVS representation of dynamical systems: event-based intelligent control. Proc. IEEE 77, 72–80. https://doi.org/10.1109/5.21071
Zeigler, B.P., Muzy, A., 2017. From Discrete Event Simulation to Discrete Event Specified Systems (DEVS). IFAC-Pap., 20th IFAC World Congress 50, 3039–3044. https://doi.org/10.1016/j.ifacol.2017.08.672
Zhao, X., De Reffye, P., Houllier, F., Hu, B.-G., 2003. Interactive simulation of plant architecture based on a dual-scale automaton model.

Chapter 3: Plant Growth Modeling: A Cohort-Based GreenLab Approach

1. Plant architecture and notions of botany

Francis Hallé and Roelof Oldeman (Hallé and Oldeman, 1970) developed the concept of plant architecture through their studies on the structure of tropical plants. They designed leafy axis typologies by observing how buds' function throughout their development, both vegetative and sexual. By integrating these axe typologies for both stems and first branching order axes, they establish architectural patterns describing the structural development of each plant. The authors identified 23 models that collectively define the architecture of all known plants (Hallé et al., 1978)

This typology is grounded in the morphological characteristics of the leafy axis, which serves as the architectural framework's foundational descriptive element.

The leafy axis

The leafy axis of a plant is composed of a series of elements known as phytomeres, which can be compared to the metamer in animal anatomy. Each phytomere consists of a node featuring one or more leaves, an internode, and auxiliary bud(s) located in the axil of each leaf carried by the internode. The development of a phytomere originates from a terminal bud (Barthélémy and Caraglio, 2007).

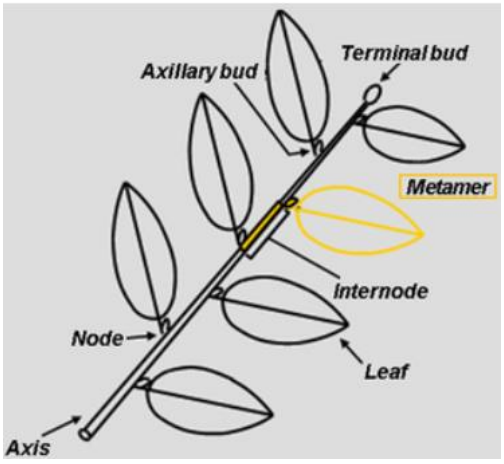


Figure 3. 1The leafy axis (Drawing D. Barthelemy, Cirad) (Barthélémy and Caraglio, 2007)

A thorough study and architectural analysis of a plant are essential to characterizing leafy axes effectively. This allows us to comprehend how internal (endogenous) factors influence plant growth while separating them from external (exogenous) influences. Observing the axes, particularly through growth processes, sexual positioning, branching, and orientation, is crucial for this analysis.

Leafy axis growth, branching, and orientation

Growth

In more detail, plant growth results first from an organogenesis stage in which stage a meristem (bud) forms the various components of a phytomere in their embryonic form, and, a next phase of development with the expansion of the organs (internode, leaves, …).

In leafy axes, the organogenesis can be rhythmic, creating growth units that are usually possible to identify distinct periods of growth (de REFFYE, n.d.). This is opposed to continuous growth, where the production of leaves or twigs occurs almost constantly and uniformly along the axis.

The growth of a leafy axis can be categorised as bounded or limited, respectively referring to: determinate growth (limited number of phytomeres on an axis), and indeterminate or continuous growth (when the formation of new phytomeres is not restricted over time). The plant's sexuality position may impact this character. If flowering remerges from the terminal meristem, the growth of the axis is interrupted and new phytomere may only occur via lateral branching leading to a determinate leafy axis growth; whereas flowering occurring at the level of the lateral meristems does not structurally restrict the leafy axis growth, thus allowing indeterminate (free).

Branching

Branching is the process by which a new leafy axis is formed from an axillary bud. Different types of branching can primarily be identified through observation, distinguishing continuous from rhythmic and diffuse branching according to the distribution of the axillary meristem along the leafy axis.

Axis orientation

Other criteria also characterize leafy axis typology. The axis orientation can usually be easily retrieved from observation, distinguishing orthotropic axes (so-called exploration axes with vertical orientation, radial symmetry with spiral leaves) from plagiotropic axes (so-called exploitation axis with a horizontal or even slightly inclined orientation, leaves arranged in a plane, in a bilateral symmetry).

Plant architectural models, and the architectural unit

The different types of leaf axis morphology seen so far can be combined to create representative plant growth models. (Hallé and Oldeman, 1970) has shown that a minimal set

of models is sufficient to describe the growth stages of plants on Earth (each model is named after a well-known botanist).

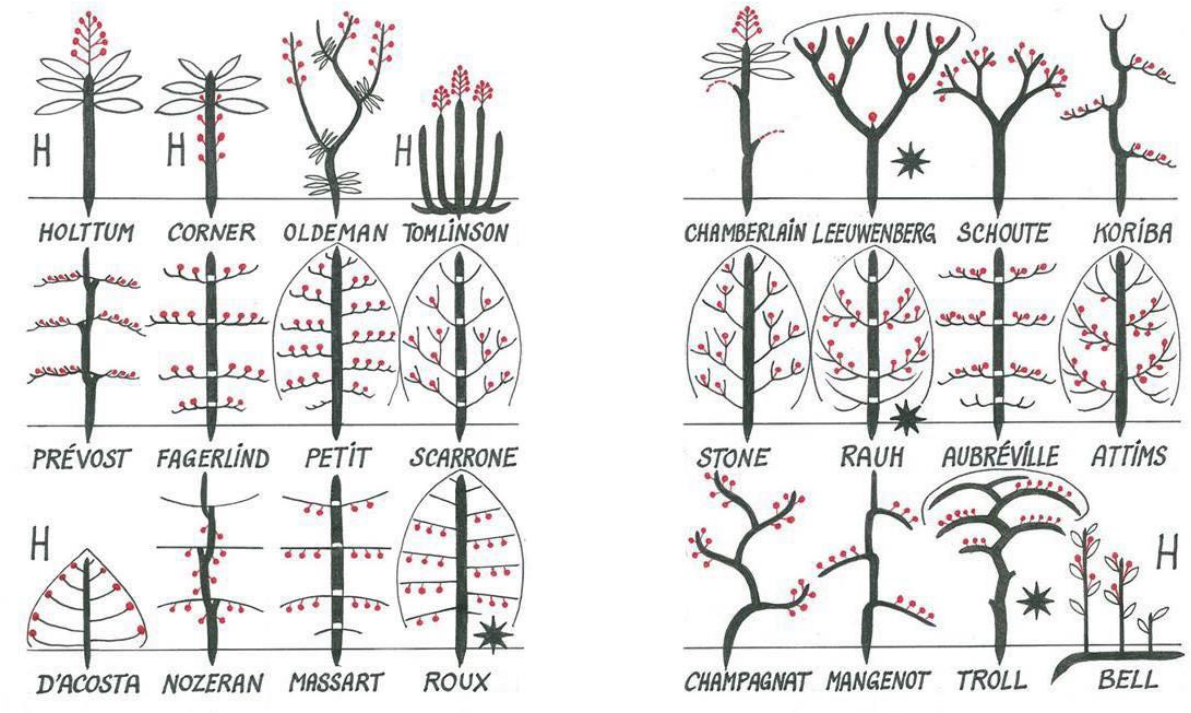


Figure 3. 2: The latest list of architectural models (Hallé, 2017).

Architectural unit

Many plant species share the same architectural model. However, the detailed growth strategy varies from one species to another. Especially, the number of different axis typologies is often greater than 2 (in practice, we are confronted with 4 or 5, such as stem, main axis, mid-length axis, twigs, and short axis), on which the analysis of architectural units can be carried out. This analysis of the species leads to the architectural unit. It is described in a table containing all the information from the architectural analysis (direction of growth, type of growth, sexuality, etc.) for each physiological age. It is completed by a diagram (drawing) showing the structure of the plant and the axes at key growth stages, summarising the sequence of development as described hereunder.

Plant sequence of development and reiteration process

From germination to death, a plant's development is like the expression of precise and ordered sequences of morphogenetic events.

The architectural sequence of development of the species summarises the main morphological stages of differentiation of plant ontogeny. The young tree develops following its architectural unit. Then, if the level of resources allows it, the adult tree gradually

duplicates (reiterates) the architectural unit, usually at the top of the main stem. This process of reiteration is sequential and gives rise to a more complex crown.

The reiteration process may be complete (the entire architectural unit is present in the reiteration), or partial (higher branching orders only are present in the reiteration)

2. Modeling and implementing the architectural concepts

From the modeling point of view, plant structural development modeling can straightforwardly be copied from the principles of architectural analysis.

The leafy axes modeling must be seen as a discrete process of the activity of terminal and axillary buds, building new phytomeres according to rules described in the architectural table and according to rules defining the level and date of reiteration occurrences. Geometrical characters may be involved in the process or post-added (such as insertion angles, biomechanics, lengths, …) to finalise faithful structural representations. Grammars are thus a natural mathematical way to implement and simulate such a modeling. In our approach, we mobilise the GreenLab dual-scale automate approach.

Before detailing the principles, we clarify the notions of ages we have to deal with since they relate to structural phytomere positions in axis typology and positions in time and space (rank in the leafy axis).

Branching order, physiological, chronological, and ontogenetic ages

Branching order is naturally introduced from the level of ramification. However, in the architectural approach, the order may be confusing according to the axis typology.

In the architectural unit, the typology of axes refers to the concept of physiological age, starting from 1 (usually the stem, up to 4 or 5 for twigs or short shoots). The physiological represents the degree of differentiation of the different plant's leafy axes. It depends on its precise level of differentiation in the plant's architecture. Besides the physiological age, we also have to consider two other ages in the modeling and simulation processes: the chronological age, corresponding to the observation time elapsed since the germination of the seed, and the ontogenetic age, corresponding to the time elapsed since the creation of the concerned phytomere.

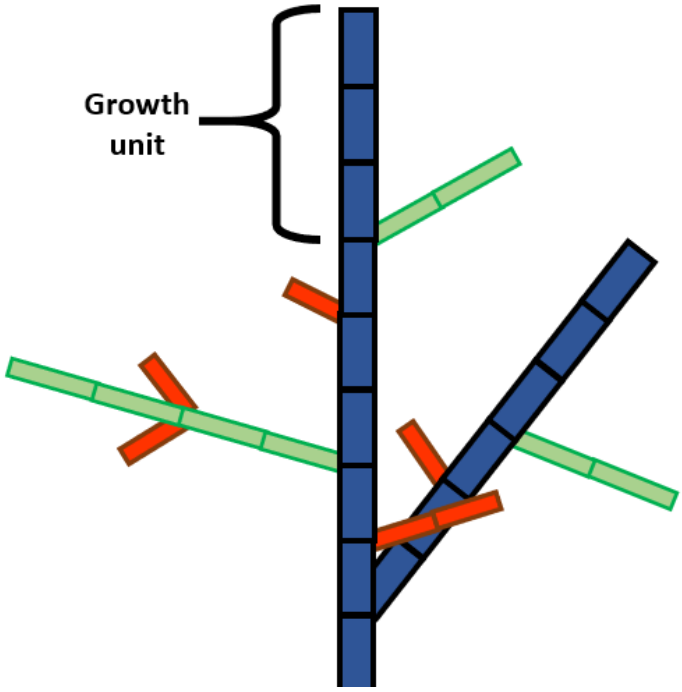


Figure 3. 3:Representation of a structural simulation of a rhythmic plant of chronological age 3. The architectural diagram consists of 3 physiological ages, respectively drawn in blue (physio 1), green (physio 2) and red (physio 3), standing for stem, branch and t

Physiological age	Type	Characteristic
1	Stem	3 phytomers per growth unit carry branches and possible reiteration
2	Branches	2 phytomers per growth unit carry a verticil of 2 twigs
3	Twigs	1 phytomer per growth unit

The plant model shows a total reiteration occurred with a slight delay on the first phytomere of the trunk in the first growth unit.

Dual-scale automaton

The plant's structural development can be seen as a succession of discrete events that an automated machine can simulate. This machine is called a state machine (Zhao et al., 2003).

The automaton is based on elementary elements standing for different phytomeres, here called microstates, as the basic unit for constructing the plant's architecture, as defined in the previous section.
A succession of microstates over a growth cycle (discrete time) is called a macrostate. In turn, successive macro-states construct an axis. The use of these two elements in the structure of the automaton is the reason for its being called a two-level automaton.



Figure 3. 4: A set of macro states standing for Figure 3.3. the blue micro states are for physiological 1, the green ones are for the physiological age 2 and the red one is for the physiological age 3

Growing rules are therefore explicated by the definition of phytomere microstates, indexed by their physiological ages, that define on one side
The branching properties (specified by the carried physiological age)
the sequence (deterministic or not) of successive micro-states
the sequence (deterministic or not) of successive macro-states
A formal mathematical definition, as well as a formal operator, is given in the next chapter, since this definition will be upgraded in our new modeling approach

Structure factorisation: phytomere and organ cohorts
From the dual-scale automaton, the formal numbering of phytomeres of the same characters (i.e. same physiological chronological and ontogenetic ages) can be assumed (Loi et al., 2014, 2010). Such phytomeres share the same fate (if micro-climate due to precise geometric location is neglected), and can thus be clustered in a single cohort, leading to factorising the plant structure components and its dynamics (Yan et al., 2003), including their functional aspect (Cournède et al., 2006).

The same rule applies to organs carried by phytomeres, since they inherit from phytomeres' age characters, leading to a model of the overall plant by a set of organ cohorts (leaves, internodes, fruits...) of the same physiological, chronological, and ontogenetic ages.

Organ series
Reversely, any leafy axis of the plant is, by definition, a succession of phytomeres belonging to different cohorts (since at least the ontogenetic age decreases along the axis). It may also change physiological age, as the terminal bud mutates to a higher physiological age. However, these successions may also be duplicated in the plant structure, verticils are an obvious example of it, and can also be factorised. According to (Rivals, 1965), the successive stages from top to bottom build an organic series, described in our case by the subsequent list of cohorts of decreasing chronological time. In practice, characters of organic series are the key point for plant measurements, since they link the model to the plant axis, from the youngest

phytomeres to the oldest, and allow efficient structural (and also functional) parameter identification and calibration (Kang et al., 2016).

The potential of such a structural modeling is huge, but still inoperable when considering the organ dimension (or weights), and therefore its production; even at the whole plant level, the yield cannot be assessed. Moreover, possible feedback coming from plant assimilation resources on the axis organogenesis cannot be considered. As a summary, the functional point of view is mandatory and thus considered in the next section.

3. Eco-physiological principles and structure for modeling

In agronomy, since the mid-past century (Wit, 1982; Wit and Vries, 1982), modeling plant production led to efficient models considering plant production in a homogeneous crop for a given area (usually per square meter). These models, based on eco-physiological principles, aim to predict the yield per square meter. The yield is the biomass allocated to the fruits, considered as a unique organ compartment (Savary et al., 2006).

Principals:
In a process-based crop model, an organ compartment represents a specific plant part, such as leaves, stems, roots, or fruits, serving as a distinct unit for modeling growth, biomass accumulation, and resource allocation. Such a model is built from multiple primitive processes that simulate fundamental physiological activities like photosynthesis, respiration, water uptake, and nutrient assimilation, all of which interact to drive plant development. A key component of this approach is the biomass production model, which calculates total biomass based on environmental factors such as solar radiation, CO_2 concentration, and water availability. Once biomass is produced, the biomass partitioning model determines its distribution among different organ compartments, influenced by the plant's growth stage and external conditions. These organ compartments function dynamically within the model, reflecting the plant's response to varying environmental conditions.

Thermal time

Thermal time is used in plant modeling due to its proportionality with the number of organogenesis cycles. It is calculated by summing up the daily accumulation of heat with consideration of the development threshold, where the development rate is zero.

Common pool

The modeling of the storage of the biomass produced and its reallocation is based on the following hypothesis: The biomass produced is stored in a common stock, and its reallocation is subject to competition between organs (Heuvelink, 1996)

Biomass production

When the leaves receive light, only part of it is absorbed and used for photosynthesis. The rest is reflected and transmitted through the leaf. The part that is absorbed is called photosynthetically active radiation (PAR). This is the useful spectral band of light captured by photosynthetic organisms.

There is a linear relationship between biomass production and the level of light absorbed by the leaves, known as the Light Use Efficiency (LUE) factor. In the case of a relationship with total radiation, Radiation Light Use Efficiency (RUE).
On a daily basis, dry biomass growth can be expressed as follows:

$$dW = LUE \,.\, PAR \,.\, (1 - e^{\{-k\, LAI\}})$$

Where:
dW is the biomass growth rate (in $g.m^{-2}.d^{-1}$),
LUE is the Light Use Efficiency (in $g.MJ^{-1}$),
k is the extinction coefficient,
LAI is the Leaf Area Index,
PAR is the Photosynthetic Active Radiation incident on the crop ($MJ.m^{-2}.d^{-1}$).

Biomass partitioning

In a process-based crop model, an organ compartment represents a set of organ types such as leaves, stems, and roots (potentially merged), and a fruit compartment serves as distinct units for modeling growth, biomass accumulation, and resource allocation. Such a model is built from multiple primitive processes that simulate fundamental physiological activities like photosynthesis, respiration, water uptake, and nutrient assimilation, all of which interact to drive plant development. A key component of this approach is the biomass production model, which calculates total biomass based on environmental factors such as solar radiation, CO_2 concentration, and water availability. Once biomass is produced, the biomass partitioning model distributes it among the different organ compartments, influenced by the plant's growth stage and external conditions. These organ compartments function dynamically within the model, reflecting the plant's response to varying environmental conditions.

Crop Model Pro & Cons

Process-based models are valuable in crop modeling due to their modular design and flexibility, enabling efficient crop growth simulation under various environmental conditions with minimal parameter requirements.
However, they have limitations, such as difficulty accurately simulating the leaf area index (LAI) and variations in the harvest index, which complicate the assessment of plant structure and external stresses. These models cannot also incorporate stochastic behaviour and implicitly model organogenesis, making predictions of organ differentiation and abortion challenging.
Structural limitations, like difficulties linking modules and neglecting secondary growth, also reduce their applicability, particularly across different crop species.

Despite these challenges, process-based models remain essential tools for understanding plant growth and productivity, with potential for further refinement (Bouman et al., 1996; Gaudio et al., 2022).

4. Crop and FSPM Models

In the field of agronomy, process-based models (PBMs) play a key role in simulating the dynamics of plant growth. Often referred to as crop models, these tools estimate biomass production by measuring the light intercepted by leaves per unit area (m^2). By categorising various plant organs into distinct compartments, PBMs facilitate a more precise distribution of biomass, thereby enhancing the accuracy of yield predictions, which is their primary function. However, they do not consider the plant structure, the typology of plant organs, phenological stages, or the physiological mechanisms occurring within the plant.

The Functional structural Plant models - FSPM (de Reffye et al., 2021), (Sievänen et al., 2009), in addition to the development of the plant structure (i.e., the emergence and dynamic spatial organisation of organs such as leaves, stems, and even roots), integrate the functional modeling of physiological processes such as photosynthesis, transpiration, and resource allocation to the plant's geometric architecture. Initially used to model individual tree growth (Sievänen et al., 2009), these models have been used on various plants of agronomical interest, including wheat, maize, and ornamental plants (Guo et al., 2011). The primary goal of these models is to predict the individual plant's final architecture and yield based on external environmental factors and internal interactions.

For instance, in our study context, (Pradal et al., 2008) proposed an extension of the FSPM model to simulate pathogen dispersion at the organ scale by adjusting growth parameters in response to infection intensity. However, incorporating health aspects into FSPMs remains complex due to the challenge of dynamically and accurately modeling interactions between plant growth and multiple stress factors. Another difficult point arises from the difficulty of scaling up from the individual plant level to the crop level.

For this reason, we chose to develop our approach using the GreenLab cohort-based model (de Reffye et al., 2021).

5. Cohort-based models: the GreenLab example and its interest

The GreenLab model employs a mathematical framework to simulate organogenesis through meristem production equations, which are defined based on the physiological age of the organs and derived from empirical observations. The growth, mortality, and branching processes are governed by probabilistic laws, allowing for a dynamic representation of plant development (Reffye and Hu, 2003).

In each growth cycle, the model simulates the emergence of new organ populations, referred to as cohorts. These cohorts consist of organs sharing the same developmental stage and physiological characteristics. Biomass allocation within the plant is regulated through a common biomass pool, from which each organ draws resources based on the strength of its

sink function. This sink function is not static; rather, it varies over time as the organ matures, influencing the overall distribution of biomass within the plant system.

A key computational advantage of the GreenLab model is its ability to apply efficient factorisation techniques. Since all organs within a given cohort and organ type exist in an identical physiological state, their collective biomass demand can be expressed as the sum of the individual demands of each cohort. This approach simplifies the computation of plant demand (D), enhancing the model's efficiency in simulating large-scale plant structures and growth dynamics.

Few applications mobilising this model with P&D. A theoretical case is held by (Qi et al., 2009b, 2009a), in which the P&D and its predator models and codes were fully embedded in the plant growth model. While this approach provides a tightly integrated framework, it significantly limits the model's genericity and applicability across diverse contexts. This limitation is particularly relevant when considering the broader challenges associated with coupling plant growth dynamics in a health-related context. Addressing these challenges requires a more flexible and modular approach, which we discuss in detail in the next section, where we examine the underlying issues and propose a novel framework to enhance adaptability while maintaining the integrity of the coupled system.

6. Challenges and Issues in Integrating Plant Health

Complexity of Plant-Environment Interactions

Biotic stresses (e.g., diseases, herbivory) and abiotic stresses (e.g., drought, salinity) affect plant growth dynamically and in complex ways. These interactions depend on various parameters, such as temperature, resource availability, and the plant's phenological stage. Integrating these aspects into the plant model requires a deep understanding of plant physiology (Kang et al., 2008) and defence mechanisms.

Parameterisation and Validation

Collecting precise data and developing algorithms to estimate parameters in changing environmental conditions remain significant challenges (Kang et al., 2018; Ma et al., 2007). Incorporating plant responses to stresses adds a level of complexity, requiring the parameterisation of numerous variables affected by interactions, which can make the model even more difficult to validate.

Objectives

To couple with a pest model, we need a plant growth model capable of:

- Facilitating the integration of complex interactions between plant physiological processes and environmental conditions (biotic and abiotic stresses) without causing computational overload.
- Modularising the modeling to enable independent calibration of different levels, simplifying implementation and validation.

- Allowing flexibility in managing organ cohorts and their influence on the overall plant's health while ensuring scalable simulation capabilities.

The model should have the following properties:

- Modular decomposition: Each level of the model should function independently but in coordination, reducing complexity at each step.
- Calibrability: Each level must be calibrated independently, allowing the model to be adjusted across different scales without requiring global recalibration.
- Computational simplicity: Calculations should be limited to specific levels, reducing complexity while maintaining coherent simulation.

7. Our proposal

Adopting a hierarchical structure makes the model flexible and capable of representing the morphological diversity of plants while facilitating the management of complex interactions among organs, resource flows, and environmental conditions, as described by (Henke et al., 2016), with a so-called FSPM-P model. In this approach, it is possible to model plant structure and function at different hierarchical scales, focusing on improving the robustness and flexibility of models for various plant species and environmental conditions. However, this model requires significant time and computational power for calibration and has a steep learning curve. Moreover, its capabilities to be operative at a crop level are not been considered so far.

Incorporating the hierarchical concept of FSPM-P into a cohort-based approach, as in GreenLab (Cournède et al., 2006; de Reffye et al., 2021), addresses the need for simplification and efficiency in modeling plant-environment interactions. A model capable of integrating different levels of complexity while remaining flexible and scalable is essential. The proposed model must manage plant-environment interactions effectively while minimising computational demands and ensuring independent calibration of the different levels.

We chose this approach for the following motivations:

- Modularity and Independence: Each level operates modularly, enabling independent calibration and intervention, reducing the overall model complexity, and facilitating validation.
- Reduction in Computational Complexity: Subdividing complex biological processes limits the need for intensive calculations while maintaining coherent interaction across levels.
- Adaptability: This architecture easily adjusts the model based on specific needs (environmental conditions, organ health) while reducing interdependencies.
- Dynamic Organ Management: Integrating cohort-based organ management at the organ level simplifies simulations while allowing local changes (e.g., senescence or stress) to affect the entire plant scale.

Therefore, we built a plant growth model structured in hierarchical modules, which allows a clear and organised representation of the various biological processes involved in growth (Fig. 3.5).

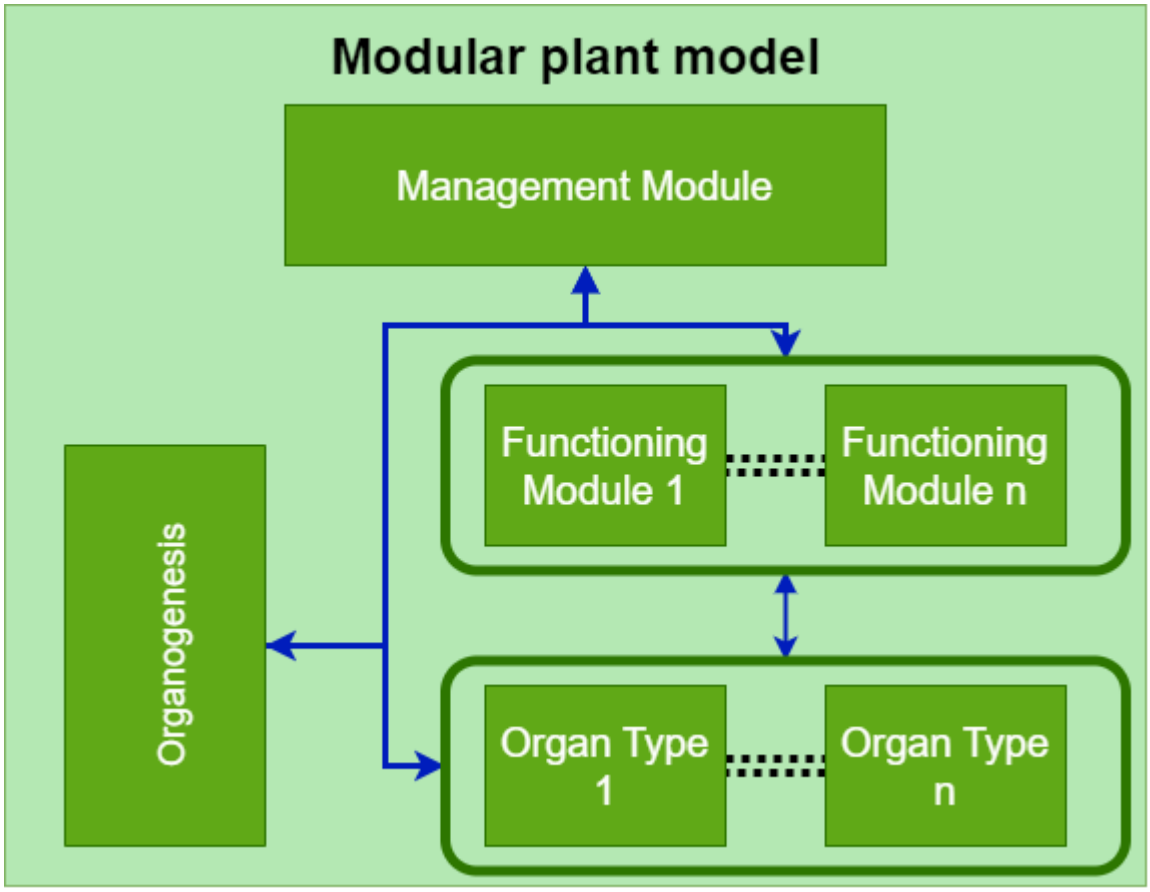


Figure 3. 5: The proposed frame structure of the plant model.

This approach's modules are differentiated and hierarchical, reflecting interaction complexities at different levels. At the hierarchy's base are structures representing individual plant organs (leaves, roots, fruits), modelled with specific characteristics such as age, biomass, and physiological function. The management module allows control of the components independently and provides a way to implement interactions, either between the modules (inner) or with other outside components.

(*A more detailed implementation is given in the implementation section.)*

8. Plant structure and cohort

In GreenLab formalism, cohort is defined as $C_o(p,t)$, where p is the physiological age of the organs, t is the chronological age of the given type of organ o in the cohort. The

chronological age is defined by the apparition cycle of the organ and the current cycle (subtraction gives this chronological age).

8.1. Reminder: phytomeres, automata, and organogenesis

From automaton theories, we can simulate the establishment of plant structures using phytomeres and their development and ramifications. Using the basic element of the dual scale automaton described in the previous section, we define the upper triangular matrix $\vec{S}(nxn)$n where n is the maximum physiological age of the plant. This matrix contains the structural elements of the plant (physiological age) at a certain chronological age. To express the development of the plant, we use operator matrices (De Reffye and Jaeger, 2013). These operators are: the development operator diagonal matrix $U(nxn)$, the upper triangular ramification matrix $M(nxn)$.

The elements of matrix S quantify the number of macro states at a given chronological age, representing the structural organisation of the plant over time. Each row corresponds to a physiological age, reflecting the distribution of phytomeres, branching structures, and organ differentiation. This allows for the analysis of growth patterns, structural stability, and the influence of branching on plant development.

The development operator

The development operator U contains the number of phytomeres that appear at each cycle for each of the physiological ages of the plant. If we have a plant with 3 physiological ages, the development operator takes the following form:

$$\vec{U} = \begin{vmatrix} u_1 & 0 & 0 \\ 0 & u_2 & 0 \\ 0 & 0 & u_3 \end{vmatrix}$$

The ramification operator

The ramification operator $\vec{M}$, contains the ramification number corresponding to each physiological age, along with the resulting physiological age it generates. For a plant with 3 physiological ages, the ramification operator will look like this:

$$\vec{M} = \begin{vmatrix} 1 & m_{12} & m_{13} \\ 0 & 1 & m_{23} \\ 0 & 0 & 1 \end{vmatrix}$$

Each row of the ramification operator corresponds to the ramification potential of each physiological age. For instance, the physiological age 1 has m_{12} ramifications for bearing a physiological age 2 and m_{13} for bearing a physiological age 3.

8.2. Plant organogenesis

Through the automaton, we can construct an algorithm that calculates the plant's phytomere production and thus gives a potential structure for it. It follows the evolution of the $\vec{S}$ matrix through different growth cycles.

At the initial cycle 1, the value of $\vec{S}$ is equal to the development matrix: $\overrightarrow{S_1} = \vec{U}$.

The evolution follows the following recursive formula:

$$\overrightarrow{S_t} = \vec{U} + \vec{M}.\overrightarrow{S_{t-1}}$$

An application

For the following values of $\vec{U}$ and $\vec{M}$, we get the following evolution:

$$\vec{U} = \begin{vmatrix} 3 & 0 & 0 \\ 0 & 2 & 0 \\ 0 & 0 & 1 \end{vmatrix}, \vec{M} = \begin{vmatrix} 1 & 1 & 1 \\ 0 & 1 & 1 \\ 0 & 0 & 1 \end{vmatrix}$$

$$\overrightarrow{S_1} = \vec{U} = \begin{vmatrix} 3 & 0 & 0 \\ 0 & 2 & 0 \\ 0 & 0 & 1 \end{vmatrix}$$

$$\overrightarrow{S_2} = \vec{U} + \vec{M}.\overrightarrow{S_1} = \begin{vmatrix} 3 & 0 & 0 \\ 0 & 2 & 0 \\ 0 & 0 & 1 \end{vmatrix} + \begin{vmatrix} 1 & 1 & 1 \\ 0 & 1 & 1 \\ 0 & 0 & 1 \end{vmatrix} . \begin{vmatrix} 3 & 0 & 0 \\ 0 & 2 & 0 \\ 0 & 0 & 1 \end{vmatrix} = \begin{vmatrix} 6 & 2 & 1 \\ 0 & 4 & 1 \\ 0 & 0 & 2 \end{vmatrix}$$

$$\overrightarrow{S_3} = \vec{U} + \vec{M}.\overrightarrow{S_2} = \begin{vmatrix} 9 & 6 & 4 \\ 0 & 6 & 3 \\ 0 & 0 & 3 \end{vmatrix}$$

$$\overrightarrow{S_4} = \vec{U} + \vec{M}.\overrightarrow{S_3} = \begin{vmatrix} 12 & 12 & 10 \\ 0 & 8 & 6 \\ 0 & 0 & 4 \end{vmatrix}$$

The result $\overrightarrow{S_4}$ can be described as a plant with a structure composed of:

- A principal structure containing 4 phytomeres of physiological age 1, 6 phytomeres of physiological age 2, and 10 phytomeres of physiological age 3 at chronological age 4
- A secondary structure containing 4 phytomeres of physiological age 2 and 6 phytomeres of physiological age 3
- A tertiary structure containing 4 phytomeres of physiological age 3

The evolution of the plant can be represented by the following figure:

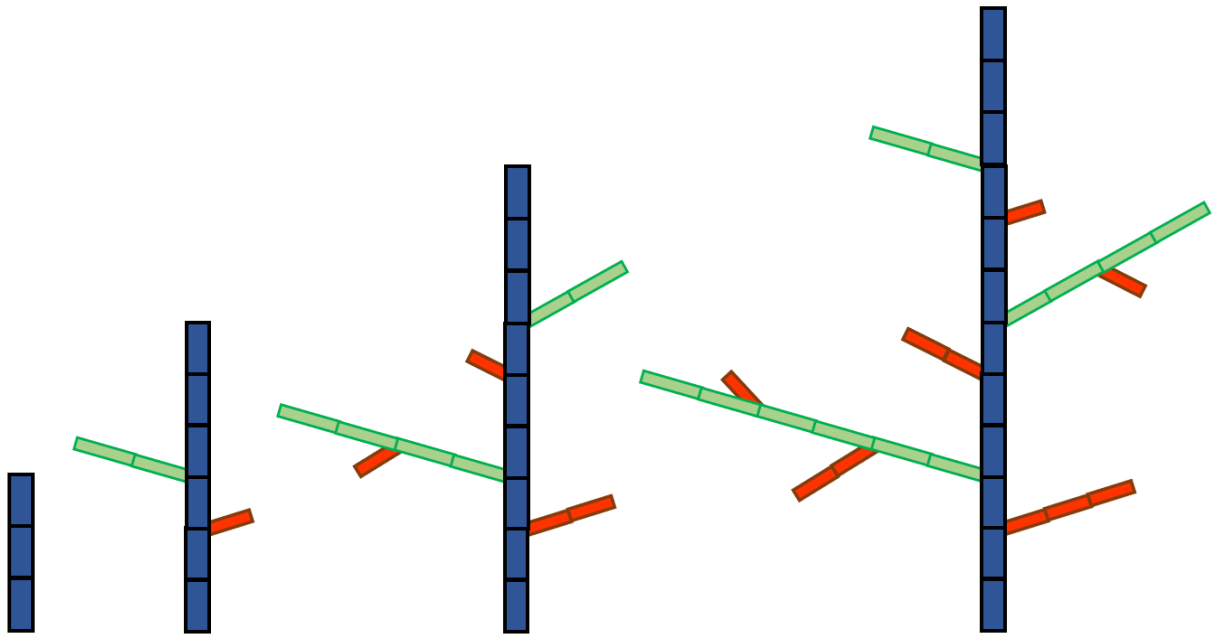


Figure 3. 6: Representation of the structure of the plant presented in the application after 4 growth cycles

8.3. Limitations of this formalism

These approaches for defining the plant cohort and the dual-scale automaton were initially conceived to model plant growth in isolation, without explicitly accounting for interactions or the spatial dynamics of individual plants. Consequently, when integrating these models with other P&D frameworks, the effects on the plant growth process are introduced indirectly. This indirect coupling may not only limit the accuracy of the representation but also reduce the overall effectiveness of the model in capturing the complex feedback mechanisms between plant growth and P&D dynamics.

In our approach, we propose refining the cohort definition to capture the structural aspects of the plant better while maintaining computational efficiency and avoiding unnecessary model complexity. Without compromising the phytomere and by exploiting its structural properties, we will modify the automaton's construction methodology and streamline the associated operators to enhance clarity and improve computational tractability, ensuring a more intuitive and effective modeling framework.

In the dual-scale automaton, macro states are represented by the S matrix. However, this representation can be ambiguous, as it considers each structural level independently without accounting for reiterations of physiological ages. Additionally, the current formulation contains mathematical inconsistencies, which require correction for greater accuracy in modeling plant development.

9. New phytomere (microstates) definition

We introduce here a formal phytomere description from the microstate definition that considers the historical progression of the units forming the plant's architecture. As previously (see section 1.5), a microstate is defined by the physiological age i of the phytomere's internode, and the physiological age j of the axillary bud carried by the internode.

Considering a phytomer of physiological age i, we introduce ψ_j as the number of axillaries of physiological age j carried by this phytomer. By convention, we note ψ_0 as the case where no axillary is present in the microstate. Example: on the coffee main stem, each phytomer may carry a couple of plagiotropic axes (of physiological age 2), we have thus ψ_2 = 2

The vector $\overrightarrow{\Psi_j}(1 \times \max\varphi + 1) = [\psi_0 \quad \psi_1 \quad \cdots \quad \psi_{max\varphi}]$ denotes all possible arrangement and patterns of physiological ages/Co-Physiological ages of a phytomere with a given physiological age φ_i, including the case of no Co-Physiological age attached to a physiological age (no axillary bud).

In other words, the $\overrightarrow{\Psi_j}$ defines all possible microstates of physiological age j.

Going back to the example, the microstate sets of a simple coffee structure is described as follows

$$\overrightarrow{\Psi_1} = [0 \quad 0 \quad 2 \quad 1], \overrightarrow{\Psi_2} = [1 \quad 0 \quad 1 \quad 0], \overrightarrow{\Psi_3} = [1 \quad 0 \quad 1 \quad 0]$$

From micro to macro state

A collection of microstates defines a macrostate, representing the plant's developmental progression within a growth cycle. Formally, the macrostate is represented as:

$$Macro = \{\psi_j\}, j \in [0, max\varphi]$$

Where each microstate ψ_j corresponds to a specific structural configuration at a given physiological age and developmental cycle.

Considering the different physiological ages i, the final representation of a microstate is expressed as:

$$Macro = \{\psi_{ij}\}, i \in [1, max\varphi], j \in [0, max\varphi]$$

Here, the microstate is defined by the indices i and j, where i stands for the physiological age of the phytomere, and j for the physiological age of the axillary bud associated with the phytomere. A microstate usually involves a subset of all possible microstates, and often involves several times some microstates. Example of a 2 physiological age plant on which the stem microstate of 5 phytomers, where the third phytomer reiterates and the fifth phytomer carries 3 branches:

$$MacroEx = \{\psi_{10,}\, \psi_{10,}\, \psi_{11,}\, \psi_{10,}\psi_{12}\} \; with\, \psi_{10} = 1, \psi_{11} = 1,\, \psi_{12} = 3$$

A factorisation process is utilised, as in the original formalism, to improve computational efficiency and minimise redundancy in representing plant structures.

This method consolidates repetitive microstate sequences into a factorised macrostate, which reduces complexity while maintaining essential structural information.

By ordering the microstate in the sequence and numbering their occurrences (retrieved by the function called Index hereunder), the factorised macrostate offers a more concise and computationally efficient representation of plant development.

$$FactorizedMacro = \{ Index(\psi_{ij}), 1 \leq i \leq max\varphi, 0 \leq j \leq max\varphi \} = \{ N\psi_{ij} \}$$

Note that for a given physiological age i, $\{ N\psi_{j} \}$ is a list of $max\psi$ terms, whatever the length of the macrostate is $max\psi + 1$.

On the previous example we have

$$FactorizedMacroEx = \{N\psi_{10,} N\psi_{11,} N\psi_{12}\} \; with \; N\psi_{10} = 3, N\psi_{11} = 1, \; N\psi_{12} = 1$$

This approach enhances the clarity of structural pattern analysis and allows the construction of new operators dedicated to computing the number of phytomers during growth (i.e., the number of organs per cohort)

10.New structural operators

We update the S matrix definition, standing for the number of phytomers in the plant structure, by the matrix $\overrightarrow{S_{HC}}$ build from the occurrences of the microstates$N\psi_{ij}$ and the sorted microstates ψ_{ij} that represents the number of branching for a microstate $N\psi_{ij}$.

For a phytomere of a physiological age i, we introduce its axillary in a matrix of vectors in the following form:

$$\overrightarrow{S_{HC_{\psi i}}} = \left| \begin{matrix} [N\psi_{i0} & N\psi_{i1} & \cdots & N\psi_{ij}] \\ [\ \psi_{i0} & \psi_{i1} & \cdots & \psi_{ij}] \end{matrix} \right|_{j \in 0:max\varphi}$$

We can represent all the physiological ages in one vector matrix $\overrightarrow{S_{HC}}$ as:

$$\overrightarrow{S_{HC}} = \left| \begin{array}{c|c|c|c} \overrightarrow{\Phi_1} & \overrightarrow{\Phi_2} & \cdots & \overrightarrow{\Phi_i} \\ \hline \overrightarrow{\Psi_1} & \overrightarrow{\Psi_2} & \cdots & \overrightarrow{\Psi_i} \end{array} \right| \quad i \in 1{:}\, max\varphi$$

With each vector inside the matrix corresponding to $\overrightarrow{\Phi_i}(1 \times (max\varphi + 1)) = [N\psi_{i0} \quad N\psi_{i1} \quad \dots \quad N\psi_{ij}]$ and $\overrightarrow{\Psi_i}(1 \times max\varphi + 1) = [\psi_{i0} \quad \psi_{i1} \quad \dots \quad \psi_{ij}]$.

Each matrix column holds information on the possible ramifications of each physiological age of the plant. By looking at this matrix and its value, we have a direct link to the plant's structure.

An example, given a physiological age 1 and three possible ramification, we obtain the following values for $\overrightarrow{S_{HC_{\psi 1}}}$: $\overrightarrow{\Phi_1}(1 \times 4) = [N\psi_{10} \quad N\psi_{11} \quad N\psi_{12} \quad N\psi_{13}] = [1 \quad 0 \quad 1 \quad 1]$ and $\overrightarrow{\Psi_1}(1 \times 4) = [\psi_{10} \quad \psi_{11} \quad \psi_{i1} \quad \psi_{ij}] = [1 \quad 0 \quad 1 \quad 1]$.

$$\overrightarrow{S_{HC_{\psi 1}}} = \left| \begin{array}{cccc} [N\psi_{10} & N\psi_{11} & N\psi_{12} & N\psi_{13}] \\ \hline [\psi_{10} & \psi_{11} & \psi_{12} & \psi_{13}] \end{array} \right| = \left| \begin{array}{cccc} [1 & 0 & 1 & 1] \\ \hline [1 & 0 & 1 & 1] \end{array} \right|$$

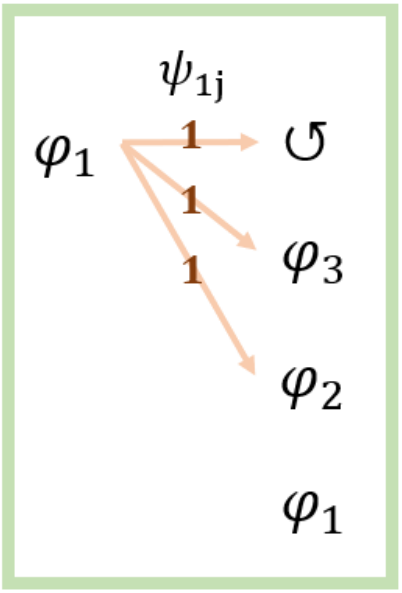


Figure 3. 7: Ramification mapping of the plant's φ_1

We can represent the links between the physiological ages of the plant through the fig 3. 7. The physiological age is linked with the physiological age 2 with a phytomere capable of ramification (with an axillary bud of φ_1), plus a phytomere and with no ramification (no axillary bud).

Now, we add the other two physiological ages (since we considered $max\psi = 4 \Rightarrow max\varphi = 3$:

$\overrightarrow{\Phi_2}(1 \times 4) = [1 \quad 0 \quad 1 \quad 1]$, $\overrightarrow{\Psi_2}(1 \times 4) = [1 \quad 0 \quad 0 \quad 2]$.

$\overrightarrow{\Phi_3}(1 \times 4) = [1 \quad 0 \quad 0 \quad 0]$, $\overrightarrow{\Psi_3}(1 \times 4) = [1 \quad 0 \quad 0 \quad 0]$.

Giving the following matrix:

$$\overrightarrow{S_{HC}} = \left| \begin{array}{c|c|c} [1 \quad 0 \quad 1 \quad 1] & [1 \quad 0 \quad 1 \quad 1] & [1 \quad 0 \quad 0 \quad 0] \\ \hline [1 \quad 0 \quad 1 \quad 1] & [1 \quad 0 \quad 0 \quad 2] & [1 \quad 0 \quad 0 \quad 0] \end{array} \right|$$

We represent the relationships between the different physiological ages with the following map:

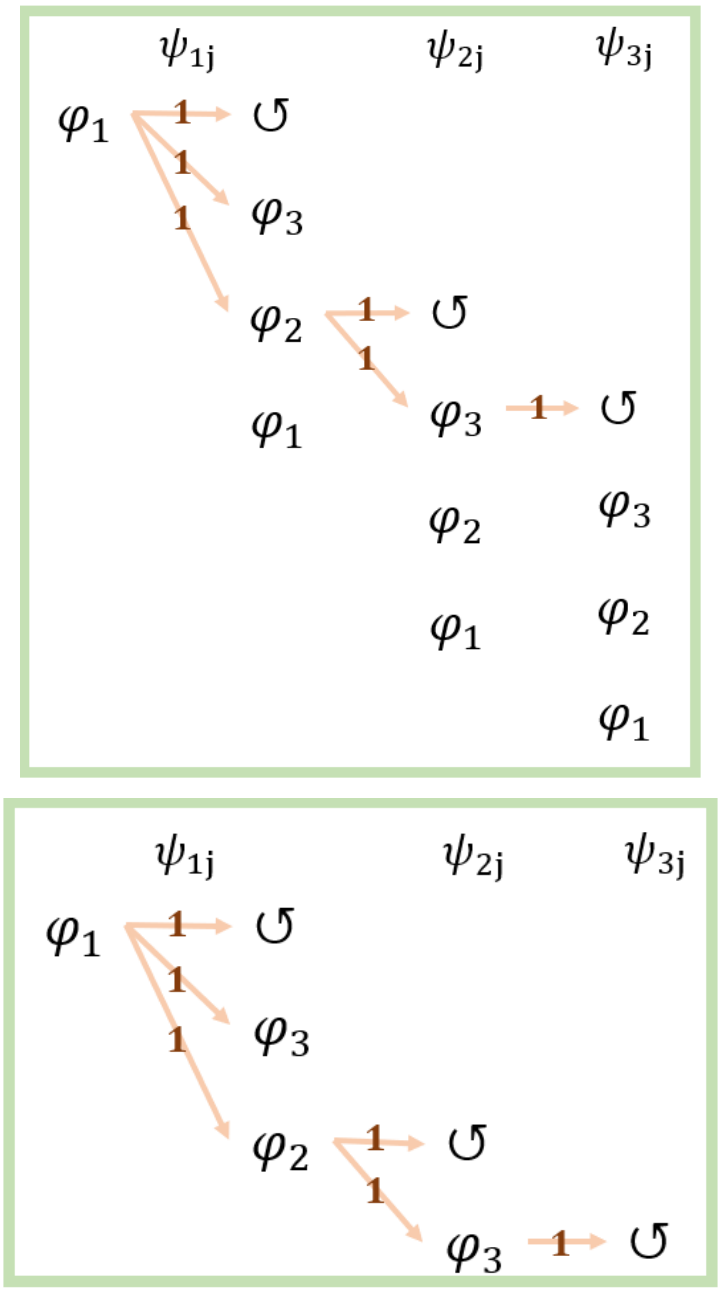


Figure 3. 8: Ramification mapping of the plant. Full representation (upper), simplified representation (below)

This representation illustrates the various branching pathways of the plant structure. Each occurrence of the symbol ↺ signifies a return to the same physiological age, indicating that development resumes from that specific stage. The diagram is bidirectional in its interpretability: when read from right to left, it reveals the developmental progression of the plant, whereas reading from left to right allows for the identification of the supporting structures' physiological age (bearers) associated with each phytomere corresponding to a given physiological age. Thus, this approach provides a more refined criterion for defining cohorts, incorporating enhanced spatial information into the variable.

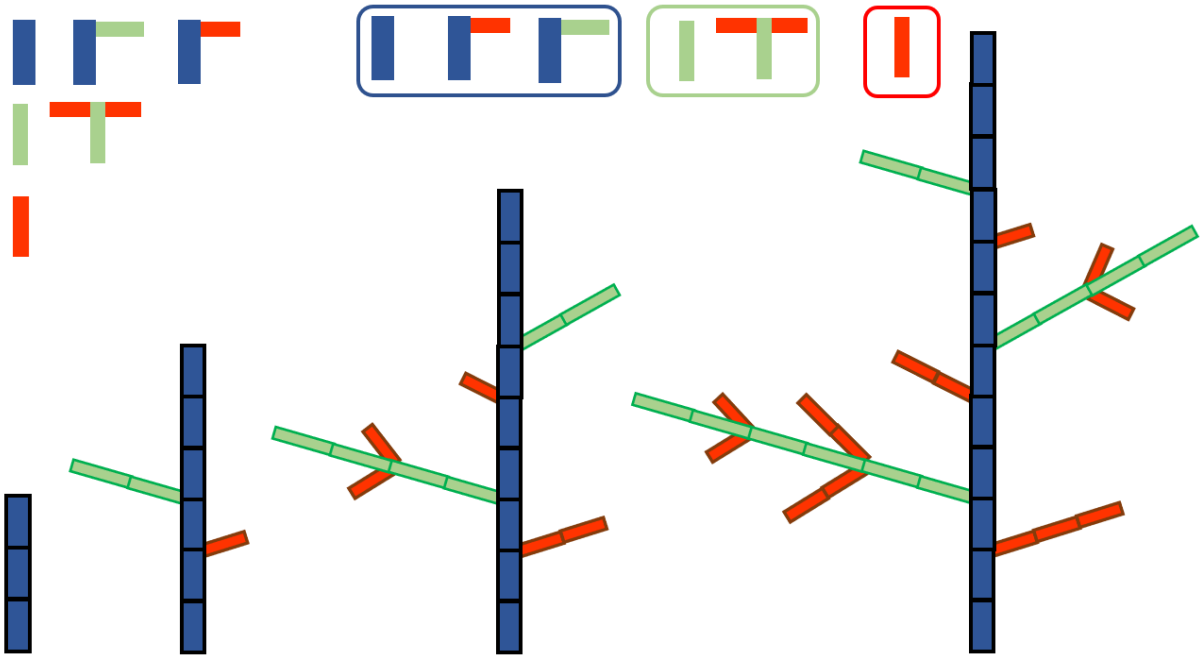


Figure 3. 9: Representation of the structure of the plant presented in the application after 4 growth cycles, and with every possible phytomere established

New cohort definition

To align with the new definition of the phytomere and, we introduce a revised cohort definition in the following format:

$$HC = (GC_k,\ \varphi_i, (GC_{k-N},\ \varphi_j))$$

Where $GC_k$is the occurrence's age of the cohort at the growth cycle k and physiological age φ_i.

GC_{k-j} is the occurrence's age of the carrier cohort that appeared N cycles ago of physiological age φ_j.

This formulation defines a Phytomere Cohort, grouping plant organs (internodes, leaves, and fruits) by position and function. The framework identifies each phytomere's bearer and structures branching processes. This hierarchy improves understanding of plant architecture and helps predict how stress (pests, diseases, or damage) spreads through the plant.

Development operator

The classical development operator (see 5.0) can now be extended to our new cohort definition. We can introduce the development of each axe of the plant, using the automaton matrix $\overrightarrow{S_{HC}}$. Let us consider the development vector of the plant axis $\vec{U}$:

$$\vec{U}(1 \times max\varphi) = [u_1\ \ u_2\ \ \dots\ \ u_N]^T$$

In order to integrate the development factor in the construction of the plant, we multiply (scalar) $\vec{U}$ with $\overrightarrow{S_{\mathrm{HC1}}}$. This results in:

$$\overrightarrow{US_{\mathrm{HC1}}} = \left[u_1.\vec{\Phi}_1 \quad u_2.\vec{\Phi}_2 \quad \dots \quad u_N.\vec{\Phi}_N\right]$$

Ramification operator

A similar approach is applied to the ramification process. To achieve this, we extend the ramification operator to the ramification vector of the plant axis, denoted as $\vec{M}$

$$\vec{M}(max\varphi \times 1) = [\overrightarrow{m_1} \quad \overrightarrow{m_2} \dots \overrightarrow{m_N}]^T$$

Where $\overrightarrow{m_N}\,(max\varphi + 1 \times 1)$ is the vector containing all the ramifications probabilities associated with the i^{th} plant axe and a reiteration probability.

To incorporate the ramification factor into the plant's structural construction, we apply a scalar multiplication between $\vec{M}$ with $\overrightarrow{S_{HC}}$ second row, ensuring that the ramifications are properly integrated within the model.

$$\overrightarrow{M\Psi_1} = \left[\overrightarrow{m_1}.\overrightarrow{\Psi_1} \quad \overrightarrow{m_2}.\overrightarrow{\Psi_2} \quad \dots \quad \overrightarrow{m_N}.\overrightarrow{\Psi_N}\right]$$

Application

Taking the same example as before:

$$\overrightarrow{S_{HC}} = \left|\begin{array}{c|c|c} [1 \;\; 0 \;\; 1 \;\; 1] & [1 \;\; 0 \;\; 1 \;\; 1] & [1 \;\; 0 \;\; 0 \;\; 0] \\ \hline [1 \;\; 0 \;\; 1 \;\; 1] & [1 \;\; 0 \;\; 0 \;\; 2] & [1 \;\; 0 \;\; 0 \;\; 0] \end{array}\right|$$

We will estimate the plant structure and development with $\vec{U} = [0{,}9 \;\; 0{,}9 \;\; 1]^T$. The ramification probability is $\vec{M} = [[\,1 \;\; 0 \;\; 1 \;\; 0{,}8\;\;][\,1 \;\; 0 \;\; 0 \;\; 0{,}7\,][1 \;\; 0 \;\; 0 \;\; 0]]$

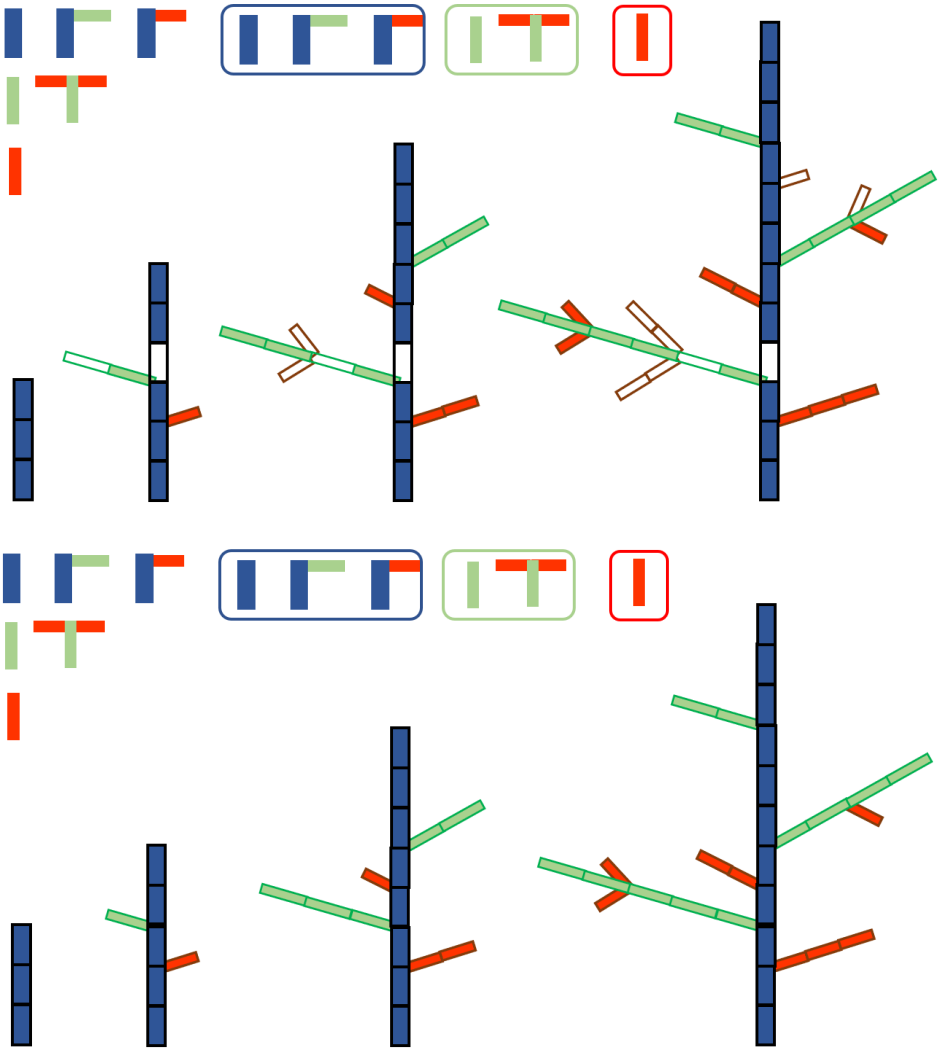


Figure 3. 10: Plant's structure representation with stochastic parameters after 4 growth cycles. Chronological representation of the plant structure (upper), Topologic representation (below)

11.Plant function

11.1. Reminders

Light interception and biomass production

Positioned between traditional individual-based plant models and large-scale crop models, GreenLab incorporates key agronomic simplifications derived from experimental studies. These include the assumption of a common biomass pool, the use of net photosynthesis calculations, and biomass estimation based on **Beer's Law**. Such simplifications eliminate the need for an explicit topological structure in biomass production computations, enhancing the model's efficiency and applicability to diverse cropping systems.

The biomass accumulation process in GreenLab is adapted from the classical crop model equation, ensuring its applicability at the individual plant scale. The fundamental equation is expressed as:

$$Q = LUE \cdot PAR \cdot Sp \cdot (1 - e^{-\frac{kSf}{Sp}})$$

where $\boldsymbol{Q}$ represents the increase in plant biomass during a growth cycle, $\boldsymbol{S_f}$ denotes the plant's total leaf area, and $\boldsymbol{S_p}$ is a surface-related parameter. The parameter $\boldsymbol{S_p}$ ensures the equation remains valid even under low-density canopy conditions. In high-density stands, where the canopy is uniform, $\boldsymbol{S_p}$ adheres to the relation:

$$Sp = \frac{1}{d}$$

where $\boldsymbol{d}$ represents plant density. This formulation allows GreenLab to effectively simulate plant growth across varying stand densities while maintaining computational efficiency.

Assuming that the leaf area remains constant during a growth cycle, the GreenLab model defines fresh biomass production using the following equation:

$$Q(n) = \frac{E(n)S_p}{r}\left(1 - \exp\left(-k\frac{S(n)}{S_p}\right)\right) \quad equation\ (Q)$$

where:

- $Q(n)$ is the fresh biomass produced at the cycle n,
- $E(n)$ is an aggregate variable representing environmental resource conditions, including Light Use Efficiency (LUE) and Photosynthetically Active Radiation (PAR)
- r represents the water resource availability, proportional to the inverse of Water Use Efficiency (WUE),
- k is the Beer's Law extinction coefficient determining the light attenuation ratio within the canopy,
- Sp stands for the projection area, which defines the reference area for biomass production,
- $S(n)$ represents the total functional leaf area at cycle n

The total functioning Leaf area leaf area is computed as follows:

$$S(n) = \frac{1}{e}\left(\sum_{i=1;T_b} P_b \frac{Q(n-i-1)}{D(n-i)}\right) \qquad equation\ (S)$$

- P_b stands for the leaf blade sink function at age j
- T_b is the number of cycles before the leaf gets senescent (the number of functional cycles)
- e is the blade thickness

Biomass partitioning (sink/sources)

In the GreenLab model, dry matter production is systematically allocated to distinct organ cohorts, including leaves, stems, roots, and fruits. These compartments function as biomass sinks, storing the assimilated dry matter based on their physiological demand. While certain organs, such as leaves and seeds, act as biomass sources through photosynthesis and carbon assimilation, others, including internodes and fruits, primarily function as sinks, consuming and storing the allocated biomass.

Organ biomass demand, for its expansion, beta law

Biomass partitioning among organ cohorts is dynamic and governed by competition, rather than a fixed process. Within a given cohort, all organs are of the same type, such as leaves, internodes, or flowers, and share identical properties and developmental trajectories. The GreenLab model incorporates this assumption by estimating biomass demand and consumption based on a single representative organ per cohort, with the total demand scaled by the number of organs within that cohort.

Organs within their respective cohorts compete for biomass to support their growth. The capacity of an individual organ to accumulate biomass is defined by its sink strength, which is quantified over a specific period corresponding to its expansion time. The set of sink values throughout this period determines the organ's sink strength function, which represents its capacity to attract biomass at different stages of development.

The sink strength function must be expressed with organ expansion, meaning it is age-dependent. Because all organs within a given cohort follow the same developmental trajectory, they share the same sink strength value at any given time. This allows for a coherent integration of sink strength into the cohort-based modeling approach. Beta laws are frequently employed to describe sink functions, offering a flexible mathematical framework that can represent various growth patterns using only two parameters.

$$P_{o,\varphi}(i) = P_{o,\varphi} * F_e(\frac{t}{T_e})$$

Where $P_{o,\varphi}$ is the sink strength, and $F_e(\frac{t}{T_e})$ is the expansion function evaluated over chronological time t, relative to its expansion duration T_e.

Considering now the period of a growing cycle n, the biomass allocated to a single organ o, of physiological age φ, can be written as follows:

$$q_{o,p}(n) = \quad P_{o,\varphi}(i) \,.\, Q(n-1)/D(n)$$

Where:
i stands for the organs' age, since the beginning of the expansion
$P_{o,\varphi}(i)$ stands for the organ o sink value at physiological age φ and ontogenic age i
D(n) represents the biomass demand of the plant.
Q(n-1) the available biomass at previous cycle

Plant Demand

All organs within the same cohort and of the same type share identical physiological states, allowing for an efficient factorization of biomass demand calculations. This simplification enables the total plant demand, denoted as D(n), at a given growth cycle n, to be computed as the sum of the demands of all organ cohorts.

We have three level of demands:

- Organ: $d_o(f_n) = p.\beta(f_n)$, where p is the sink strength and $\beta(n)$ is the variation of the sink expressed as a beta law,
- Cohort: $D_c(n) = d_o(n) * N_{oc}$, the demand of the cohort is the demand of all the organ in a cohort C

The plant demand function is expressed as:

$$D(n) = \sum_{t1=1}^{1} D_c(n)$$

$$D(n) = \sum_{o,p} \sum_{t1=n-l}^{n} N_{o,\varphi}(t1)\mathrm{P}_{\mathrm{o},\varphi}(t1 - n + l)$$

where:

- n is the current growth cycle,
- o denotes the organ type (e.g., internode, leaf, fruit, root),
- p represents the physiological age of the organ,
- $t1$ refers to the cycle in which a given cohort first appeared,
- $t1 - n + l$ indicates the organ's age within the range $[0, l]$
- $N_{o,\varphi}(t1)$ is the number of organs that appeared at cycle $t1$,
- $\varphi_(o, p)\ \ (t1 - n + l)$ is the sink strength function of the organ.

By aggregating demand across all cohorts, this formulation provides a structured and computationally efficient approach to modeling biomass partitioning in the GreenLab framework.

12.Tuning GreenLab for wide-use interactions (Arts and Crafts for interaction)

Principles

The enhancements made to the plant model aim to maintain its hierarchical organisation while allowing for the integration of new interaction levels. Several key principles guide these developments.

First, the model preserves the core assumptions of the GreenLab framework while introducing additional parameters. This added flexibility enables the modeling of more complex interactions, primarily through the management module and the incorporation of regulatory parameters that influence these interaction effects.

Second, the architecture of the model supports the integration of interactions at multiple scales, encompassing the whole-plant level as well as individual organs. This multi-scale approach results in a more detailed representation of biomass allocation and organ expansion.

Third, despite these enhancements, the model remains fully compatible with the original GreenLab structure. This compatibility ensures continuity in the use of existing parameters and simulation procedures, making it easier to integrate with both previous and ongoing modeling efforts.

Finally, the modifications are developed within an internally consistent mathematical framework, with careful attention to maintaining numerical stability throughout the simulations.

At the plant level

At the whole plant level, various theoretical adjustments could be made to refine biomass allocation and growth prediction. However, not all potential modifications are implemented in this study. The $E(n)$ and r are not considered in this thesis. Since they work as inputs for the plant model, we don't need to instantiate a variation within the equations.

Nevertheless, several model components can be regulated to simulate damage or an improvement in the plant's functioning. The demand, for instance, can increase or decrease depending on the stress applied to the plant, either due to an attack of a disease that parasites some organ of the plant and depletes the biomass, which can be translated into an additional demand for the plant. In the general equation, the influence will be on the level of $S(n)$.

To represent such modifications, a regulatory coefficient, C_s is introduced. This coefficient can be applied at two different structural levels of the model:

Global level

To model a global impact on functional leaf area the coefficient is incorporated as follow, starting from equation (Q):

$$Q(n) = \frac{E(n)S_p}{r} . \ (1 - \exp\left(-k \frac{(S(n) - C_s * S(n))}{S_p}\right)$$

Rewritten using exponential properties leads to:

$$Q(n) = \frac{E(n)S_p}{r} . (1 - \frac{\exp\left(-k * \frac{S(n)}{Sp}\right)}{\exp\left(-k * \frac{C_s S(n)}{Sp}\right)})$$

This new formulation allows us to determine how much of the incoming resource is contributing to the production of biomass by distinguishing between the “healthy” leaves and the “sick” ones. This form introduces the effect as a ratio between the light extinction of all leaves (ignoring their health status) and a virtual light extinction corresponding to the unfunctional leaf area

An alternate form is

$$Q(n) = \frac{E(n)S_p}{r}.(1 - \exp\left(-k\frac{S(n)}{S_p}\right)^{Csh})$$

Where $Csh = (1 - Cs)$ coefficient is this time standing for the ratio of functional area

In both cases, the coefficient works as a ponderation factor modulating the productivity of the leaf area, resulting in a long linear effect in the light interception at the full plant level. On this basis, such a model is easy to compare to Process-Based models, since the same approach can be straightforwardly applied to the LAI in these, without referring explicitly to any chronological or leaf ages.

Local level

A more refined approach can be proposed by introducing a coefficient C_m directly into the definition of S(n), in equation (S). This allows consideration of a generalised reduction in functional efficiency that uniformly affects the entire canopy. This reflects scenarios in which stressors alter leaf functionality systemically rather than targeting specific cohorts.

$$S(n) = \frac{C_m}{e}(\sum_{i=1;T_b} P_b \frac{Q(n-i-1)}{D(n-i)})$$

Mathematically, the overall effect is similar to the previous formulation, it allows however to analyse a potentially link the coefficient to the history of the plant production on demand ratio, during the overall leaf functional duration (the Tb cycles). Pushing the Cm coefficient in the functional cycle summation results in introducing the effect at the Organ level, as proposed here under.

Organ level

A more effective strategy involves managing the problem through groups of leaves, as well as taking into account other relevant plant structures. This cohort-based approach provides a clearer and more biologically relevant representation of growth dynamics, allowing for the tracking of how different stressors affect various developmental stages.

At the organ level, improvements focus on refining the mechanisms for biomass allocation. One key enhancement involves adjusting the coefficients that determine the sink strength of each organ. For instance, the demand for biomass by leaf cohorts is now represented as:

$$D_l = N_l(n) C_l P_{leaf}$$

Where C_l is a regulation coefficient (default value = 1), used to simulate influences or stress effects that modify the leaves' demand.

Applying this redefined formulation extended to the entire plant (i.e., all types of organs), the new expression of the demand is:

$$D(n) = N_l(n) C_l P_{leaf} + N_e(n) C_i P_{intrenoeud} + N_f(n) C_f P_{fruit} + C_r P_{root}$$

Note that, when introducing a constant C_l value for leaves and no effective coefficient for all other organs (Co =1), the formulation leads to the local level formulation, with $C_l = C_m^{-1}$

The introduction of the organ demand coefficient makes it possible to adjust the response of organs to different types of stress and can also be used reversely to incorporate more complex behaviours such as prioritising a certain type of organ for damage recovery or prioritising reproduction.

New specific organs

Introducing specialised organs for biomass capture and distribution offers a way to introduce a regulating element for the plant. In the case of an infection by disease of a specific organ, let's say a contaminated organ, or "ghost organ", $HGhC$, standing as a reproduction of the leaf cohort (that is fully contaminated) with the same cohort elements values. This new organ can reproduce the capture of biomass by the disease, which is also the lost biomass due to it [Kang et all, 2022].

We propose to define these new organ cohorts as:

$$HGhC = (GC_k, \varphi_i, (GC_{k-N}, \varphi_j))$$

Where $GC_k$is the occurrence's age of the cohort at the growth cycle k and physiological age φ_i. GC_{k-j} is the occurrence's age of the carrier's cohort that appeared N cycles ago of physiological age φ_j.

Integrating the Ghost Organ (HGhC) into the model achieves several important objectives. Firstly, it allows us to quantify biomass loss due to parasitism or disease in a dynamic and timely manner, capturing the effects of infection as they evolve. Secondly, the HGC facilitates the simulation of disease progression across different organ cohorts while maintaining the integrity of the core biomass allocation equations. This means the model can track the impacts of disease without requiring a complete overhaul of the underlying allocation mechanisms.

Additionally, the HGC enables stress feedback, allowing the host plant to adjust its biomass allocation in response to the diversion of resources caused by a pathogen for instance. Finally, the introduction of the HGC enhances the model's modularity and reusability; this concept

can be extended to simulate a wide range of biotic interactions, including infections in other organs (such as leaves or fruits) or different pathogens, such as root parasites or fruit diseases.

13.Discussion

In the context of integrating interactions into a plant growth model, we distinguish two types of interactions that play different roles at various levels of the model. The first type operates similarly to a crop model, encompassing broader, generalised effects that influence the model's overall behaviour. These interactions act at a higher level, capturing global, system-wide influences on plant growth. For example, environmental factors (denoted as *E*) and soil nutrient content (*r*) can exert global effects on plant growth and can be modelled as noise in the input of the system.

These interactions are crucial for understanding large-scale dynamics, such as yield potential, resource allocation, and the general growth trajectory of the plant during a growing season. The effects of these interactions are represented at the level of the overall equation *Q(n)*, providing a comprehensive picture of plant performance without delving into the detailed processes at the organ level.

In contrast, the second type of interaction focuses on finer details, particularly at the organ level, and is more sensitive to changes in local conditions. These interactions capture physiological and biochemical processes occurring in specific organs, such as leaves, stems, and roots. They are often characterised by a greater sensitivity to small variations in environmental or internal factors. At this level, the model simulates how local factors influence particular organs, thereby impacting the overall development of the plant. These interactions are essential for capturing fine-scale dynamics that the broader plant-level models may overlook. For instance, the impact of leaf surface area on photosynthesis, which can be reduced by pests or diseases, is a crucial component of organ-level interactions that significantly affect plant performance. The sensitivity of these interactions enables the model to make more accurate predictions of plant responses to varying environmental conditions, resource availability, and internal processes.

Integrating these two levels of interaction—overall and organ-specific—into a unified model offers a more comprehensive representation of plant growth. The broader interactions at the overall level provide the necessary framework for understanding large-scale, system-wide effects, while the detailed organ-level interactions capture the complexity and sensitivity of plant development. This integration enhances the model's ability to simulate how plants respond to external environmental stresses and internal physiological processes. Consequently, it improves the model's predictive power, enabling more accurate simulations of plant growth under varying conditions. Ultimately, this approach provides valuable insights into the mechanisms of plant development, which can be used to optimise agricultural practices, improve crop management, and inform climate change adaptation strategies.

14. Implementation

Plant Model Hierarchy

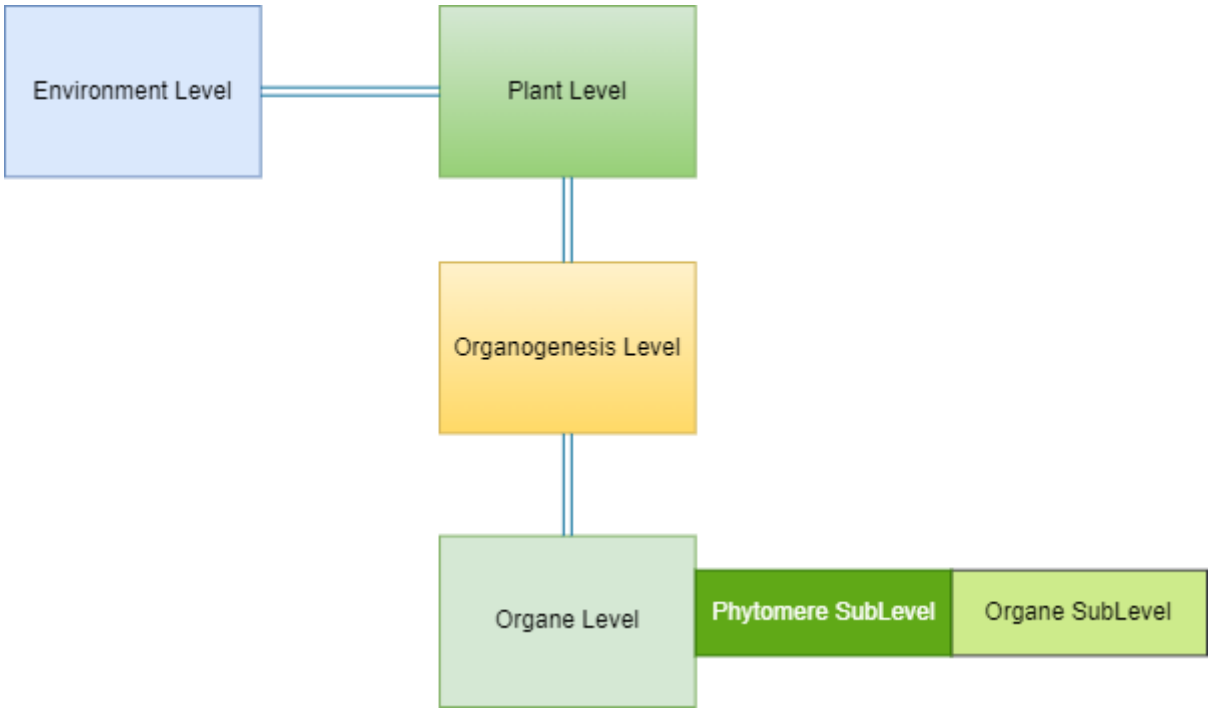


Figure 3. 11: Hierarchy of modules that define the plant model. Each level contains a structure modelled as an object

The modules in Figure 3.11 represent the following levels:

Interaction with the Environment Level

- This level encapsulates plant characteristics for interacting with the environment, including parameters like water-use efficiency, Lambert-Beer's extinction coefficient, and leaf thickness. These parameters define the plant's ability to exploit external resources for growth.
- It also contains state variables of the plant interacting with environmental conditions, separating external conditions (e.g., water and light availability) from the plant's internal model. All these elements are contained in a numerical object: **M_Environement**

1.1 Plant Level

- This level defines the dynamics of plant growth, including its initial state. The **M_Plant** structure is a numerical object that includes the plant's life cycle, initial biomass, seed decomposition rates, and the common resource pool.
- The **M_Plant** object simulates plant development over multiple cycles, considering resource allocation, gradual changes in growth conditions, and the biomass common pool reserve.

Organogenesis Level

- Organogenesis is the process by which new organs form throughout the plant's life cycle. This process is modelled by the numerical object M_Organogenesis, which includes variables such as the microstate of phytomeres, branching probabilities, and the final age of organogenesis. These parameters incorporate stochastic development rules, determining the likelihood of forming new organs based on environmental and internal factors.

Organ Level

- Plant organs are modelled as cohorts. Each organ cohort is defined by its physiological properties (age, organ type, biomass, leaf area) and development dynamics (expansion, function, lifespan). In the object
- Relationships between organs (internodes, leaves, fruits) are hierarchically structured through a Phytomere Cohort, grouping organs based on their position and function. This hierarchy identifies primary and secondary growth axes, organises branching processes, and synchronises organ development based on their location and role in the plant's metabolism.

Integrating Organ Health

The health of plant organs is a fundamental aspect of modeling as it directly influences plant growth, longevity, and productivity. In this model, organ health is represented by physiological properties such as biomass, lifespan, and functional status.

Mechanisms integrated to track and simulate organ health evolution over the growth cycles include:

- Dynamic monitoring of organ performance.
- Linking biomass to organ health.
- Regulating leaf area and biomass.

Health Parameters at the Organ Cohort Level

- Each set of organs sharing the same physiological chronological ages and history is represented by a cohort, including attributes related to health and development. Parameters like "Expansion Duration," "Functioning Duration," and "Lifespan" define the active growth period, useful functioning period, and total lifespan of the organ, respectively. These durations adjust based on the organ's physiological age and stress conditions.

- SinkValue and SourceValue relate respectively to biomass demand and production capacity for each organ. Fluctuations in these values, depending on organ age and resource allocation, indicate organ health degradation or improvement.

Managing Organ Status

- Managing organ status is essential for representing the dynamics of growth and degradation under variable conditions. The organ cohort status is a Boolean parameter indicating whether the organ is functioning optimally. Stress (attacks, resource shortages, water stress) can change this parameter, signalling organ health degradation.

- Fruits, internodes, and other organs also undergo biomass adjustments based on health status. For example, a poorly maintained fruit will have reduced biomass, and its demand capabilities may vary (higher or lower).

- When reaching a status of “stress” with no functioning capabilities, the dead organ is still considered in the simulation. This will allow us to have the history of the plant in its growth process.

Regulating Leaf Area and Biomass

- Regulating leaf area and biomass is crucial for understanding the effects of external stresses on plant performance. Reductions in leaf area (due to biomass loss) indicate biotic aggressor attacks and resource stress directly affecting photosynthesis efficiency and biomass production capacity.

Plant Representation

This module visualises the spatial arrangement and development of plant organs, such as internodes, leaves, and fruits, based on their physiological age. The code is structured to distinguish organs by type, age, and establishment status, using a specific palette of colours and shapes for each organ type. This approach provides a clear visualisation of the plant and its components over time.

Geometric shapes (rectangles, ellipses, circles) differentiate organ types. The size of these shapes is proportional to organ attributes (e.g., biomass or relative size), ensuring a biologically consistent representation of the plant's structure.

Visualisation Function Inputs

The plant visualisation function takes three input parameters:

1. **Sscale**: Visualization scale, used to adjust the size of the plant and its components in the graphical rendering.
2. **OrganCohorts**: List of the plant's organ cohorts.
3. **PhysAge**: Target physiological age, used to filter organs based on this age.

Organs are depicted using geometric shapes, with sizes and colours varying according to organ type and developmental status.

Organ Types and Graphical Representation

- **Internodes**: **Established organs**: Active internodes are represented by black rectangles for the base. The interior colour (brown or beige) depends on whether the organ's relative age is defined.
- **Unestablished organs**: Internodes not yet established are shown in grey.
- **Leaves**: **Mature leaves**: Leaves with positive biomass and matching the specified physiological age are drawn as ellipses. Their colour (green or yellow) varies with the relative age of the leaf.
- **Unestablished leaves**: These are represented as standard grey ellipses.
- **Fruits**: **Mature fruits**: Healthy fruits are displayed as circles coloured red or brown.
- **Unestablished fruits**: These are also shown in grey.

Management of Physiological Age

The **PhysAge** parameter filters the organs to be displayed, ensuring the model can focus on specific plant developmental stages.

Colour Palette

A predefined colour palette distinguishes organ states:

- **Black**: Internode base.
- **Brown and beige**: Internode interior.
- **Green and yellow**: Mature leaves by relative age.
- **Red and brown**: Fruits by health status.
- **Grey**: Unestablished organs.

This approach offers a flexible and intuitive method to observe the growth dynamics of plants across developmental stages.

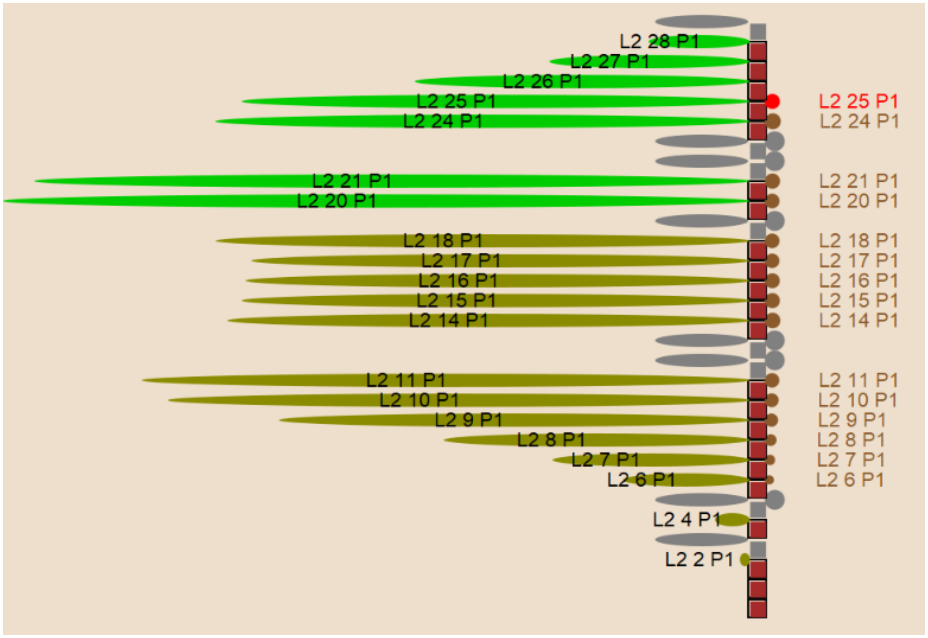


Figure 3. 12: 2D plant representation of stem growth, using Ugandan Robust coffee tree development parameters over 30 growth cycles.

15.References

Abel, D.J., Kilby, P.J., Davis, J.R., 1994. The systems integration problem. Int. J. Geogr. Inf. Syst. 8, 1–12. https://doi.org/10.1080/02693799408901984

Aggarwal, P.K., Kalra, N., Chander, S., Pathak, H., 2006. InfoCrop: A dynamic simulation model for the assessment of crop yields, losses due to pests, and environmental impact of agro-ecosystems in tropical environments. I. Model description. Agric. Syst. 89, 1–25. https://doi.org/10.1016/j.agsy.2005.08.001

Argent, R.M., Voinov, A., Maxwell, T., Cuddy, S.M., Rahman, J.M., Seaton, S., Vertessy, R.A., Braddock, R.D., 2006. Comparing modeling frameworks – A workshop approach. Environ. Model. Softw. 21, 895–910. https://doi.org/10.1016/j.envsoft.2005.05.004

Aristizábal, L.F., Jiménez, M., Bustillo, A.E., Trujillo, H.I., Arthurs, S.P., 2015. Monitoring Coffee Berry Borer, *Hypothenemus hampei* (Coleoptera: Curculionidae), Populations with Alcoholbaited Funnel Traps in Coffee Farms in Colombia. Fla. Entomol. 98, 381–383. https://doi.org/10.1653/024.098.0165

Avelino, J., Barboza, B., Araya, J., Fonseca, C., Davrieux, F., Guyot, B., Cilas, C., 2005. Effects of slope exposure, altitude and yield on coffee quality in two altitude terroirs of Costa Rica, Orosi and Santa María de Dota. J. Sci. Food Agric. 85, 1869–1876. https://doi.org/10.1002/jsfa.2188

Bale, J., Masters, G., Hodkinson, I., Awmack, C., Bezemer, T. m, Brown, V., Butterfield, J., Buse, A., Coulson, J., Farrar, J., Good, J., Harrington, R., Hartley, S., Jones, T., Lindroth, R., Press, M., Symrnioudis, I., Watt, A., Whittaker, J., 2002. Herbivory in global climate change research: Direct effects of rising temperature on insect herbivores. Glob. Change Biol. 8, 1–16. https://doi.org/10.1046/j.1365-2486.2002.00451.x

Barthélémy, D., Caraglio, Y., 2007. Plant Architecture: A Dynamic, Multilevel and Comprehensive Approach to Plant Form, Structure and Ontogeny. Ann. Bot. 99, 375–407. https://doi.org/10.1093/aob/mcl260

Bar-Yam, Y., 2002. General Features of Complex Systems. UNESCO Encycl. Life Support Syst.

Ben-Kiki, O., Evans, C., n.d. YAML Ain't Markup Language (YAML™) Version 1.2.

Bergez, J.-E., Chabrier, P., Gary, C., Jeuffroy, M.H., Makowski, D., Quesnel, G., Ramat, E., Raynal, H., Rousse, N., Wallach, D., Debaeke, P., Durand, P., Duru, M., Dury, J., Faverdin, P., Gascuel-Odoux, C., Garcia, F., 2013. An open platform to build, evaluate and simulate integrated models of farming and agro-ecosystems. Environ. Model. Softw., Thematic Issue on the Future of Integrated Modeling Science and Technology 39, 39–49. https://doi.org/10.1016/j.envsoft.2012.03.011

Bezanson, J., Edelman, A., Karpinski, S., Shah, V.B., 2017. Julia: A Fresh Approach to Numerical Computing. SIAM Rev. 59, 65–98. https://doi.org/10.1137/141000671

Bolker, B.M., 2008. Ecological Models and Data in R. Princeton University Press. https://doi.org/10.2307/j.ctvcm4g37

Bondad, J., Harrison, M.T., Whish, J., Sprague, S., Barry, K., 2023. Integrated crop-disease models: New frontiers in systems thinking. Farming Syst. 1, 100004. https://doi.org/10.1016/j.farsys.2023.100004

Bouchet, P.J., Peterson, A.T., Zurell, D., Dormann, C.F., Schoeman, D., Ross, R.E., Snelgrove, P., Sequeira, A.M.M., Whittingham, M.J., Wang, L., Rapacciuolo, G., Oppel, S., Mellin, C., Lauria, V., Krishnakumar, P.K., Jones, A.R., Heinänen, S., Heikkinen, R.K., Gregr, E.J., Fielding, A.H., Caley, M.J., Barbosa, A.M., Bamford, A.J., Lozano-Montes, H.,

Parnell, S., Wenger, S., Yates, K.L., 2019. Better Model Transfers Require Knowledge of Mechanisms. Trends Ecol. Evol. 34, 489–490. https://doi.org/10.1016/j.tree.2019.04.006

Bouman, B.A.M., van Keulen, H., van Laar, H.H., Rabbinge, R., 1996. The 'School of de Wit' crop growth simulation models: A pedigree and historical overview. Agric. Syst. 52, 171–198. https://doi.org/10.1016/0308-521X(96)00011-X

Brandmeyer, J.E., Karimi, H.A., 2000. Coupling methodologies for environmental models. Environ. Model. Softw. 15, 479–488. https://doi.org/10.1016/S1364-8152(00)00027-X

Buddie, A.G., Crozier, J., Rutherford, M.A., Flood, J., Bridge, P.D., 2015. Population development within the coffee wilt pathogen Gibberella xylarioides reflects host-related divergence. Eur. J. Plant Pathol. 142, 291–304. https://doi.org/10.1007/s10658-015-0613-z

Buis, R., Barthou, H., Frezouls, M., 1987. Relations dimensionnelles inter-feuilles: Mise en évidence d'actions locales et à distance. Bull. Société Bot. Fr. Lett. Bot. 134, 107–114. https://doi.org/10.1080/01811797.1987.10824734

Cerda, R., Avelino, J., Gary, C., Tixier, P., Lechevallier, E., Allinne, C., 2017. Primary and Secondary Yield Losses Caused by Pests and Diseases: Assessment and Modeling in Coffee. PLOS ONE 12, e0169133. https://doi.org/10.1371/journal.pone.0169133

Chabrier, P., Garcia, F., Martin-Clouaire, R., Quesnel, G., Raynal, H., 2007. Toward a simulation modeling platform for studying cropping systems management: the record project, in: International Congress on Modeling and Simulation, International Society for Computer Simulation. Citeseer, pp. 10–13.

Cournède, P.-H., Guyard, T., Bayol, B., Griffon, S., de Coligny, F., Borianne, P., Jaeger, M., de Reffye, P., 2009. A Forest Growth Simulator Based on Functional-Structural Modeling of Individual Trees, in: 2009 Third International Symposium on Plant Growth Modeling, Simulation, Visualization and Applications. Presented at the 2009 Third International Symposium on Plant Growth Modeling, Simulation, Visualization and Applications, pp. 34–41. https://doi.org/10.1109/PMA.2009.55

Cournède, P.-H., Kang, M.-Z., Mathieu, A., Barczi, J.-F., Yan, H.-P., Hu, B.-G., de Reffye, P., 2006. Structural Factorization of Plants to Compute Their Functional and Architectural Growth. SIMULATION 82, 427–438. https://doi.org/10.1177/0037549706069341

Daane, K.M., Malakar-Kuenen, R.D., Walton, V.M., 2004. Temperature-dependent development of *Anagyrus pseudococci* (Hymenoptera: Encyrtidae) as a parasitoid of the vine mealybug, *Planococcus ficus* (Homoptera: Pseudococcidae). Biol. Control 31, 123–132. https://doi.org/10.1016/j.biocontrol.2004.04.010

Damon, A., 2000. A review of the biology and control of the coffee berry borer, *Hypothenemus hampei* (Coleoptera: Scolytidae). Bull. Entomol. Res. 90, 453–465. https://doi.org/10.1017/S0007485300000584

de REFFYE, P., n.d. Etude du fonctionnement des méristèmes et de la croissance des axes végétatifs.

de Reffye, P., Heuvelink, E., Guo, Y., Hu, B.-G., Zhang, B.-G., 2009. Coupling Process-Based Models and Plant Architectural Models: A Key Issue for Simulating Crop Production, in: Cao, W., White, J.W., Wang, E. (Eds.), Crop Modeling and Decision Support. Springer, Berlin, Heidelberg, pp. 130–147. https://doi.org/10.1007/978-3-642-01132-0_15

de Reffye, P., Hu, B., Kang, M., Letort, V., Jaeger, M., 2021. Two decades of research with the GreenLab model in Agronomy. Ann. Bot. 127, 281–295. https://doi.org/10.1093/aob/mcaa172

De Reffye, P., Jaeger, M., 2013. Modèles mathématiques du développement et de la croissance de l'architecture des plantes. Le cas du modèle GreenLab - Agritrop, in: Modéliser & Simuler. pp. 625–658.

De Reffye, P., Snoeck, J., 1976. Modèle mathématique de base pour l'étude et la simulation de la croissance et de l'architecture du Coffea robusta. Café Cacao Thé.

Donatelli, M., Magarey, R.D., Bregaglio, S., Willocquet, L., Whish, J.P.M., Savary, S., 2017. Modeling the impacts of pests and diseases on agricultural systems. Agric. Syst. 155, 213–224. https://doi.org/10.1016/j.agsy.2017.01.019

Dufour, B.P., Diman, C., De San Mateo, A., Mouttet, R., 2022. Le scolyte des fruits du caféier, *Hypothenemus hampei* (Ferr.) détecté en Guadeloupe. Cah. Agric. 31, 10. https://doi.org/10.1051/cagri/2022008

Dufour, B.P., Frérot, B., 2008. Optimization of coffee berry borer, *Hypothenemus hampei* Ferrari (Col., Scolytidae), mass trapping with an attractant mixture. J. Appl. Entomol. 132, 591–600. https://doi.org/10.1111/j.1439-0418.2008.01291.x

Dufour, B.P., Kerana, I.W., Ribeyre, F., 2021. Population dynamics of Hypothenemus hampei (Ferrari) according to the phenology of Coffea arabica L. in equatorial conditions of North Sumatra. Crop Prot. 146, 105639. https://doi.org/10.1016/j.cropro.2021.105639

Gaitán, A.L., Cristancho, M.A., Castro Caicedo, B.L., Rivillas, C.A., Gómez, G.C., 2016a. PART I: Infectious Diseases, in: Bertha, L.C.C., Marco, A.C., Gabriel, C.G., Carlos, A.R., Alvaro, L.G. (Eds.), Compendium of Coffee Diseases and Pests, Diseases and Pests Compendium Series. The American Phytopathological Society, pp. 3–44. https://doi.org/10.1094/9780890544723.002

Gaitán, A.L., Cristancho, M.A., Castro Caicedo, B.L., Rivillas, C.A., Gómez, G.C., 2016b. PART II: Pests, in: Bertha, L.C.C., Carlos, A.R., Marco, A.C., Alvaro, L.G., Gabriel, C.G. (Eds.), Compendium of Coffee Diseases and Pests, Diseases and Pests Compendium Series. The American Phytopathological Society, pp. 45–60. https://doi.org/10.1094/9780890544723.003

Gaitán, A.L., Cristancho, M.A., Castro Caicedo, B.L., Rivillas, C.A., Gómez, G.C., 2016c. PART III: Abiotic and Physiological Disorders, in: Marco, A.C., Carlos, A.R., Gabriel, C.G., Bertha, L.C.C., Alvaro, L.G. (Eds.), Compendium of Coffee Diseases and Pests, Diseases and Pests Compendium Series. The American Phytopathological Society, pp. 61–66. https://doi.org/10.1094/9780890544723.004

Gamma, E., Helm, R., Johnson, R., Vlissides, J., 1994. Design Patterns: Elements of Reusable Object-Oriented Software. Pearson Education.

Garin, G., Fournier, C., Andrieu, B., Houlès, V., Robert, C., Pradal, C., 2014. A modeling framework to simulate foliar fungal epidemics using functional–structural plant models. Ann. Bot. 114, 795–812. https://doi.org/10.1093/aob/mcu101

Gaudio, N., Louarn, G., Barillot, R., Meunier, C., Vezy, R., Launay, M., 2022. Exploring complementarities between modeling approaches that enable upscaling from plant community functioning to ecosystem services as a way to support agroecological transition. Silico Plants 4, diab037. https://doi.org/10.1093/insilicoplants/diab037

Gaunt, R.E., 1995. The Relationship Between Plant Disease Severity and Yield. Annu. Rev. Phytopathol. 33, 119–144. https://doi.org/10.1146/annurev.py.33.090195.001003

Gignoux, J., Davies, I.D., Flint, S.R., 2022. 3Worlds, a simulation platform for ecosystem modeling. Ecol. Model. 473, 110121. https://doi.org/10.1016/j.ecolmodel.2022.110121
Giordanengo, P., Brun, L.O., Frerot, B., 1993. Evidence for allelochemical attraction of the coffee berry borer,Hypothenemus hampei, by coffee berries. J. Chem. Ecol. 19, 763–769. https://doi.org/10.1007/BF00985007
Greco, E.B., Wright, M.G., 2015. Ecology, Biology, and Management of Xylosandrus compactus (Coleoptera: Curculionidae: Scolytinae) with Emphasis on Coffee in Hawaii. J. Integr. Pest Manag. 6, 7–7. https://doi.org/10.1093/jipm/pmv007
Guo, Y., Fourcaud, T., Jaeger, M., Zhang, X., Li, B., 2011. Plant growth and architectural modeling and its applications. Ann. Bot. 107, 723–727. https://doi.org/10.1093/aob/mcr073
Hallé, F., 2017. Des données récentes sur les arbres 48.
Hallé, F., Oldeman, R., 1970. Essai sur l'architecture et la dynamique de croissance des arbres tropicaux, Collection de monographies de botanique et de biologie végétale. Masson et Cie, Paris.
Hallé, F., Oldeman, R.A.A., Tomlinson, P.B., 1978. Tropical Trees and Forests. Springer, Berlin, Heidelberg. https://doi.org/10.1007/978-3-642-81190-6
Hamilton, L.J., Hollingsworth, R.G., Sabado-Halpern, M., Manoukis, N.C., Follett, P.A., Johnson, M.A., 2019. Coffee berry borer (Hypothenemus hampei) (Coleoptera: Curculionidae) development across an elevational gradient on Hawai'i Island: Applying laboratory degree-day predictions to natural field populations. PLoS ONE 14, e0218321. https://doi.org/10.1371/journal.pone.0218321
Henke, M., Kurth, W., Buck-Sorlin, G.H., 2016. FSPM-P: towards a general functional-structural plant model for robust and comprehensive model development. Front. Comput. Sci. 10, 1103–1117. https://doi.org/10.1007/s11704-015-4472-8
Heuvelink, E., 1996. Dry Matter Partitioning in Tomato: Validation of a Dynamic Simulation Model. Ann. Bot. 77, 71–80. https://doi.org/10.1006/anbo.1996.0009
Hultman, C., 2016. Black coffee twig borer, Xylosandrus compactus (Eichhoff) on robusta coffee in Uganda [WWW Document]. URL https://stud.epsilon.slu.se/9580/ (accessed 5.5.25).
Jaramillo, J., Chabi-olaye, A., Borgemeister, C., 2010. Temperature-Dependent Development and Emergence Pattern of <I>Hypothenemus hampei</I> (Coleoptera: Curculionidae: Scolytinae) From Coffee Berries. J. Econ. Entomol. 103, 1159–1165. https://doi.org/10.1603/EC09408
Jaramillo, J., Chabi-Olaye, A., Kamonjo, C., Jaramillo, A., Vega, F.E., Poehling, H.-M., Borgemeister, C., 2009. Thermal Tolerance of the Coffee Berry Borer Hypothenemus hampei: Predictions of Climate Change Impact on a Tropical Insect Pest. PLoS ONE 4, e6487. https://doi.org/10.1371/journal.pone.0006487
Johnson, M.A., Manoukis, N.C., 2021. Influence of seasonal and climatic variables on coffee berry borer (Hypothenemus hampei Ferrari) flight activity in Hawaii. PLOS ONE 16, e0257861. https://doi.org/10.1371/journal.pone.0257861
Kagezi, G., Kucel, P., Egonyu, J.P., Kyamanywa, S., Karungi, J.T., Pinard, F., Jaramillo, J., Van Asten, P.J.A., Wagoire, W.W., Ngabirano, H., 2015. A review of the status and progress in management research of the black coffee twig borer, Xylosandrus compactus (Eichhoff) in Uganda [WWW Document]. Proc. 25th Int. Conf. Coffee Sci. URL https://agritrop.cirad.fr/579968/ (accessed 2.27.23).

Kang, M., Hua, J., de Reffye, P., Jaeger, M., 2016. Parameter identification of plant growth models with stochastic development, in: 2016 IEEE International Conference on Functional-Structural Plant Growth Modeling, Simulation, Visualization and Applications (FSPMA). Presented at the 2016 IEEE International Conference on Functional-Structural Plant Growth Modeling, Simulation, Visualization and Applications (FSPMA), pp. 98–105. https://doi.org/10.1109/FSPMA.2016.7818294

Kang, M., Hua, J., Wang, X., de Reffye, P., Jaeger, M., Akaffou, S., 2018. Estimating Sink Parameters of Stochastic Functional-Structural Plant Models Using Organic Series-Continuous and Rhythmic Development. Front. Plant Sci. 9, 1688. https://doi.org/10.3389/fpls.2018.01688

Kang, M.Z., Cournède, P.H., de Reffye, P., Auclair, D., Hu, B.G., 2008. Analytical study of a stochastic plant growth model: Application to the GreenLab model. Math. Comput. Simul. 78, 57–75. https://doi.org/10.1016/j.matcom.2007.06.003

Khan, J., Rio, L.E.D., Nelson, R., Rivera-Varas, V., Secor, G.A., Khan, M.F.R., 2008. Survival, Dispersal, and Primary Infection Site for Cercospora beticola in Sugar Beet. Plant Dis. 92, 741–745. https://doi.org/10.1094/PDIS-92-5-0741

Kirkeby, C., Brookes, V.J., Ward, M.P., Dürr, S., Halasa, T., 2021. A Practical Introduction to Mechanistic Modeling of Disease Transmission in Veterinary Science. Front. Vet. Sci. 7, 546651. https://doi.org/10.3389/fvets.2020.546651

Kropff, M.J., Teng, P.S., Rabbinge, R., 1995. The challenge of linking pest and crop models. Agric. Syst., Agricultural Systems Applications Through an International Consortium, ICASA 49, 413–434. https://doi.org/10.1016/0308-521X(95)00034-3

Lasso, E., Motisi, N., Avelino, J., Corrales, J.C., 2021. FramePests: A Comprehensive Framework for Crop Pests Modeling and Forecasting. IEEE Access 9, 115579–115598. https://doi.org/10.1109/ACCESS.2021.3104537

Le Chevalier, V., Jaeger, M., Mei, X., Cournède, P.-H., 2007. Simulation and Visualisation of Functional Landscapes: Effects of the Water Resource Competition Between Plants. J. Comput. Sci. Technol. 22, 835–845. https://doi.org/10.1007/s11390-007-9105-8

Leclerc, G., Bommel, P., Motisi, N., Vezy, R., Treminio, E., Avelino, J., 2021. Coffee leaf rust (Hemeleia vastatrix) risk management in Central America: contribution of remote interactive simulations. Agron. Environ. Sociétés 11. https://doi.org/10.54800/roc535

Lessler, J., Cummings, D.A.T., 2016. Mechanistic Models of Infectious Disease and Their Impact on Public Health. Am. J. Epidemiol. 183, 415–422. https://doi.org/10.1093/aje/kww021

Letort, V., Sabatier, S., Okoma, M.P., Jaeger, M., de Reffye, P., 2020. Internal trophic pressure, a regulator of plant development? Insights from a stochastic functional–structural plant growth model applied to Coffea trees. Ann. Bot. 126, 687–699. https://doi.org/10.1093/aob/mcaa023

Loi, C., Cournède, P., Françon, J., 2010. A symbolic method to compute the probability distribution of the number of pattern occurences in random texts generated by stochastic 0L-systems. Discrete Math. Theor. Comput. Sci.

Loi, C., Cournède, P.-H., Françon, J., 2014. A Symbolic Method to Analyse Patterns in Plant Structure. Comb. Probab. Comput. 23, 842–860. https://doi.org/10.1017/S0963548314000108

Lorenz, E.N., 1963. Deterministic Nonperiodic Flow. J. Atmospheric Sci. 20, 130–141. https://doi.org/10.1175/1520-0469(1963)020<0130:DNF>2.0.CO;2

Louarn, G., Song, Y., 2020. Two decades of functional–structural plant modeling: now addressing fundamental questions in systems biology and predictive ecology. Ann. Bot. 126, 501–509. https://doi.org/10.1093/aob/mcaa143

Luzinda, H., Nelima, M., Wabomba, A., Kangire, A., Musoli, P., Musebe, R., 2016. Farmer awareness, coping mechanisms and economic implications of coffee leaf rust disease in Uganda. Uganda J. Agric. Sci. 16, 207. https://doi.org/10.4314/ujas.v16i2.6

Ma, Y., Li, B., Zhan, Z., Guo, Y., Luquet, D., de Reffye, P., Dingkuhn, M., 2007. Parameter Stability of the Functional–Structural Plant Model GREENLAB as Affected by Variation within Populations, among Seasons and among Growth Stages. Ann. Bot. 99, 61–73. https://doi.org/10.1093/aob/mcl245

Mathieu, A., Cournède, P.H., Letort, V., Barthélémy, D., de Reffye, P., 2009. A dynamic model of plant growth with interactions between development and functional mechanisms to study plant structural plasticity related to trophic competition. Ann. Bot. 103, 1173–1186. https://doi.org/10.1093/aob/mcp054

Matovu, R., Kangire, A., Phiri, N., Hakiza, G., Kagezi, G., Musoli, P., 2013. Ecological factors influencing incidence and severity of Coffee Leaf Rust and Coffee Berry Disease in major Arabica coffee growing districts of Uganda. Uganda J. Agric. Sci.

Merle, I., Tixier, P., Virginio Filho, E. de M., Cilas, C., Avelino, J., 2020. Forecast models of coffee leaf rust symptoms and signs based on identified microclimatic combinations in coffee-based agroforestry systems in Costa Rica. Crop Prot. 130, 105046. https://doi.org/10.1016/j.cropro.2019.105046

Mora, J.R.M., n.d. Resposta Da Broca - Do - Cafe, Hypothenemus hampel, A Estimulos Visuais E Semioquimicos. INIAP Archivo Historico.

Motisi, N., Bommel, P., Leclerc, G., Robin, M.-H., Aubertot, J.-N., Butron, A.A., Merle, I., Treminio, E., Avelino, J., 2022. Improved forecasting of coffee leaf rust by qualitative modeling: Design and expert validation of the ExpeRoya model. Agric. Syst. 197, 103352. https://doi.org/10.1016/j.agsy.2021.103352

Motisi, N., Ribeyre, F., Poggi, S., 2019. Coffee tree architecture and its interactions with microclimates drive the dynamics of coffee berry disease in coffee trees. Sci. Rep. 9, 2544. https://doi.org/10.1038/s41598-019-38775-5

Nanjego, W., Kagezi, G., Kyamanywa, S., Ronald, S., Kobusinge, J., Arinaitwe, G., 2024. Population Dynamics of the Black Coffee Twig Borer Xylosandrus compactus (Eichhoff) in Robusta Coffee Coffea canephora. Indian J. Entomol. https://doi.org/10.55446/IJE.2024.2046

Nelson, S.C., 2008. Cercospora Leaf Spot and Berry Blotch of Coffee.

Okoma, P., Akaffou, S., De Reffye, P., Hamon, P., Hamon, S., Konan, O., Kouassi, K.H., Legnate, H., Letort, V., Sabatier, S., 2018. Estimation of stem and leaf dry biomass using a non-destructive method applied to African Coffea species. Agrofor. Syst. 92, 667–675. https://doi.org/10.1007/s10457-016-0031-z

Papastamati, K., Welham, S.J., Fitt, B.D.L., Gladders, P., 2001. Modeling the progress of light leaf spot (Pyrenopeziza brassicae) on winter oilseed rape (Brassica napus) in relation to leaf wetness and temperature. Plant Pathol. 50, 154–164. https://doi.org/10.1046/j.1365-3059.2001.00551.x

Parmesan, C., Hanley, M.E., 2015. Plants and climate change: complexities and surprises. Ann. Bot. 116, 849–864. https://doi.org/10.1093/aob/mcv169

Peck, L.D., Boa, E., 2024. Coffee wilt disease: The forgotten threat to coffee. Plant Pathol. 73, 506–521. https://doi.org/10.1111/ppa.13833

Perkel, J.M., 2019. Julia: come for the syntax, stay for the speed. Nature 572, 141–142. https://doi.org/10.1038/d41586-019-02310-3

Pham, Y., Reardon-Smith, K., Mushtaq, S., Cockfield, G., 2019. The impact of climate change and variability on coffee production: a systematic review. Clim. Change 156, 609–630. https://doi.org/10.1007/s10584-019-02538-y

Piao, S., Liu, Q., Chen, A., Janssens, I.A., Fu, Y., Dai, J., Liu, L., Lian, X., Shen, M., Zhu, X., 2019. Plant phenology and global climate change: Current progresses and challenges. Glob. Change Biol. 25, 1922–1940. https://doi.org/10.1111/gcb.14619

Pinard, F., Makune, S.E., Campagne, P., Mwangi, J., 2016. Spatial Distribution of Coffee Wilt Disease Under Roguing and Replanting Conditions: A Case Study from Kaweri Estate in Uganda. Phytopathology® 106, 1291–1299. https://doi.org/10.1094/PHYTO-04-15-0097-R

Pradal, C., Dufour-Kowalski, S., Boudon, F., Donès, N., 2007. The architecture of OpenAlea: A visual programming and component based software for plant modeling.

Pradal, C., Dufour-Kowalski, S., Boudon, F., Fournier, C., Godin, C., 2008. OpenAlea: a visual programming and component-based software platform for plant modeling. Funct. Plant Biol. 35, 751–760. https://doi.org/10.1071/FP08084

Qi, R., Cournède, P.-H., de Reffye, P., 2009a. Tri-trophic Ecosystem Oil Palm-Pests-Auxiliaries: II. Sensitivity Analysis, Parameter Identification and Control, in: 2009 Third International Symposium on Plant Growth Modeling, Simulation, Visualization and Applications. Presented at the 2009 Third International Symposium on Plant Growth Modeling, Simulation, Visualization and Applications, pp. 327–333. https://doi.org/10.1109/PMA.2009.49

Qi, R., Cournède, P.-H., Lecoustre, R., de Reffye, P., 2009b. Tri-trophic Ecosystem Oil Palm-Pests-Auxiliaries: I. Modeling and Simulation, in: Proceedings of the 2009 Plant Growth Modeling, Simulation, Visualization, and Applications, PMA '09. IEEE Computer Society, USA, pp. 87–94. https://doi.org/10.1109/PMA.2009.48

Reffye, P. de, Hu, B.G., 2003. Relevant Qualitative and Quantitative choices for building an efficient dynamic plant growth model : Greenlab Case. Presented at the International Symposium on Plant Growth Modeling, Simulation, Visualization and their Applications - PMA'03, Springer and Tsinghua University Press, p. 87.

Ribeyre, F., Avelino, J., 2012. Impact of field pests and diseases on coffee quality. pp. 151–176.

Rivals, P., 1965. Essai sur la croissance des arbres et sur leurs systèmes de floraison (application aux espèces fruitières). J. Agric. Tradit. Bot. Appliquée 12, 655–686. https://doi.org/10.3406/jatba.1965.2856

ROBUST | Capacity4dev [WWW Document], n.d. URL https://capacity4dev.europa.eu/projects/desira/info/robust_en (accessed 5.13.25).

Rodríguez, D., Cure, J.R., Cotes, J.M., Gutierrez, A.P., Cantor, F., 2011. A coffee agroecosystem model: I. Growth and development of the coffee plant. Ecol. Model. 222, 3626–3639. https://doi.org/10.1016/j.ecolmodel.2011.08.003

Rodríguez, D., Cure, J.R., Gutierrez, A.P., Cotes, J.M., Cantor, F., 2013a. A coffee agroecosystem model: II. Dynamics of coffee berry borer. Ecol. Model. 248, 203–214. https://doi.org/10.1016/j.ecolmodel.2012.09.015

Rodríguez, D., Cure, J.R., Gutierrez, A.P., Cotes, J.M., Cantor, F., 2013b. A coffee agroecosystem model: II. Dynamics of coffee berry borer. Ecol. Model. 248, 203–214. https://doi.org/10.1016/j.ecolmodel.2012.09.015

Royama, T., 1992. Analytical population dynamics. London ; New York : Chapman & Hall.
Rutherford, M.A., 2006. Current Knowledge of Coffee Wilt Disease, a Major Constraint to Coffee Production in Africa. Phytopathology® 96, 663–666. https://doi.org/10.1094/PHYTO-96-0663
Savary, S., Nelson, A., Djurle, A., Esker, P.D., Sparks, A., Amorim, L., Filho, A.B., Caffi, T., Castilla, N., Garrett, K., Mcroberts, N., Rossi, V., Yuen, J., Willocquet, L., 2018. Concepts, approaches, and avenues for modeling crop health and crop losses. Eur. J. Agron. 15 p. https://doi.org/10.1016/j.eja.2018.04.003
Savary, S., Teng, P.S., Willocquet, L., Nutter, F.W., 2006. Quantification and Modeling of Crop Losses: A Review of Purposes. Annu. Rev. Phytopathol. 44, 89–112. https://doi.org/10.1146/annurev.phyto.44.070505.143342
Sedgwick, P., 2014. Retrospective cohort studies: advantages and disadvantages. BMJ 348, g1072. https://doi.org/10.1136/bmj.g1072
Siad, S.M., Iacobellis, V., Zdruli, P., Gioia, A., Stavi, I., Hoogenboom, G., 2019. A review of coupled hydrologic and crop growth models. Agric. Water Manag. 224, 105746. https://doi.org/10.1016/j.agwat.2019.105746
Sievänen, R., Perttunen, J., Nikinmaa, E., Posada, J.M., 2009. Invited Talk: Functional Structural Plant Models - Case LIGNUM, in: 2009 Third International Symposium on Plant Growth Modeling, Simulation, Visualization and Applications. Presented at the 2009 Third International Symposium on Plant Growth Modeling, Simulation, Visualization and Applications (PMA), IEEE, Beijing, China, pp. 3–9. https://doi.org/10.1109/PMA.2009.64
Soualiou, S., Wang, Z., Sun, W., de Reffye, P., Collins, B., Louarn, G., Song, Y., 2021. Functional–Structural Plant Models Mission in Advancing Crop Science: Opportunities and Prospects. Front. Plant Sci. 12, 747142. https://doi.org/10.3389/fpls.2021.747142
Souza, A.G.C., Rodrigues, F.Á., Maffia, L.A., Mizubuti, E.S.G., 2011. Infection Process of Cercospora coffeicola on Coffee Leaf: Infection Process of Cercospora coffeicola on Coffee Leaf. J. Phytopathol. 159, 6–11. https://doi.org/10.1111/j.1439-0434.2010.01710.x
Tan, M., Gou, F., Stomph, T.J., Wang, J., Yin, W., Zhang, L., Chai, Q., van der Werf, W., 2020. Dynamic process-based modeling of crop growth and competitive water extraction in relay strip intercropping: Model development and application to wheat-maize intercropping. Field Crops Res. 246, 107613. https://doi.org/10.1016/j.fcr.2019.107613
Tendeloo, Y.V., Vangheluwe, H., 2018. DISCRETE EVENT SYSTEM SPECIFICATION MODELING AND SIMULATION, in: 2018 Winter Simulation Conference (WSC). Presented at the 2018 Winter Simulation Conference (WSC), IEEE, Gothenburg, Sweden, pp. 162–176. https://doi.org/10.1109/WSC.2018.8632372
Túler, A., Valbon, W., de Souza Rodrigues, H., Noia, L., Santos, L., Fogaça, I., Rondelli, V., Filho, A., 2019. Black twig borer, Xylosandrus compactus (Eichhoff), a potential threat to coffee production. Rev. Cienc. Agríc. 36. https://doi.org/10.22267/rcia.1936E.102
Vezy, R., le Maire, G., Christina, M., Georgiou, S., Imbach, P., Hidalgo, H.G., Alfaro, E.J., Blitz-Frayret, C., Charbonnier, F., Lehner, P., Loustau, D., Roupsard, O., 2020. DynACof: A process-based model to study growth, yield and ecosystem services of coffee agroforestry systems. Environ. Model. Softw. 124, 104609. https://doi.org/10.1016/j.envsoft.2019.104609

Wang, N., Jassogne, L., van Asten, P.J.A., Mukasa, D., Wanyama, I., Kagezi, G., Giller, K.E., 2015. Evaluating coffee yield gaps and important biotic, abiotic, and management factors limiting coffee production in Uganda. Eur. J. Agron. 63, 1–11. https://doi.org/10.1016/j.eja.2014.11.003

Whish, J.P.M., Herrmann, N.I., White, N.A., Moore, A.D., Kriticos, D.J., 2015. Integrating pest population models with biophysical crop models to better represent the farming system. Environ. Model. Softw. 72, 418–425. https://doi.org/10.1016/j.envsoft.2014.10.010

Willmott, C.J., 1981. On the Validation of Models. Phys. Geogr. 2, 184–194. https://doi.org/10.1080/02723646.1981.10642213

Willocquet, L., Savary, S., Fernandez, L., Elazegui, F.A., Castilla, N., Zhu, D., Tang, Q., Huang, S., Lin, X., Singh, H.M., Srivastava, R.K., 2002. Structure and validation of RICEPEST, a production situation-driven, crop growth model simulating rice yield response to multiple pest injuries for tropical Asia. Ecol. Model. 153, 247–268. https://doi.org/10.1016/S0304-3800(02)00014-5

Wit, C.T. de, 1982. Simulation of living systems, in: Simulation of Plant Growth and Crop Production. Pudoc, pp. 3–8.

Wit, C.T. de, Vries, F.W.T.P. de, 1982. L'analyse des systemes de production primaire, in: La productivite des paturages Saheliens. Pudoc, pp. 20–23.

Yan, H., de Reffye, P., Pan, C., Hu, B., 2003. Fast construction of plant architectural models based on substructure decomposition. J. Comput. Sci. Technol. 18, 780–787. https://doi.org/10.1007/BF02945467

Yates, K.L., Bouchet, P.J., Caley, M.J., Mengersen, K., Randin, C.F., Parnell, S., Fielding, A.H., Bamford, A.J., Ban, S., Barbosa, A.M., Dormann, C.F., Elith, J., Embling, C.B., Ervin, G.N., Fisher, R., Gould, S., Graf, R.F., Gregr, E.J., Halpin, P.N., Heikkinen, R.K., Heinänen, S., Jones, A.R., Krishnakumar, P.K., Lauria, V., Lozano-Montes, H., Mannocci, L., Mellin, C., Mesgaran, M.B., Moreno-Amat, E., Mormede, S., Novaczek, E., Oppel, S., Ortuño Crespo, G., Peterson, A.T., Rapacciuolo, G., Roberts, J.J., Ross, R.E., Scales, K.L., Schoeman, D., Snelgrove, P., Sundblad, G., Thuiller, W., Torres, L.G., Verbruggen, H., Wang, L., Wenger, S., Whittingham, M.J., Zharikov, Y., Zurell, D., Sequeira, A.M.M., 2018. Outstanding Challenges in the Transferability of Ecological Models. Trends Ecol. Evol. 33, 790–802. https://doi.org/10.1016/j.tree.2018.08.001

Yin, X., 2003. A Flexible Sigmoid Function of Determinate Growth. Ann. Bot. 91, 361–371. https://doi.org/10.1093/aob/mcg029

Zeigler, B.P., 1989. DEVS representation of dynamical systems: event-based intelligent control. Proc. IEEE 77, 72–80. https://doi.org/10.1109/5.21071

Zeigler, B.P., Muzy, A., 2017. From Discrete Event Simulation to Discrete Event Specified Systems (DEVS). IFAC-Pap., 20th IFAC World Congress 50, 3039–3044. https://doi.org/10.1016/j.ifacol.2017.08.672

Zhao, X., De Reffye, P., Houllier, F., Hu, B.-G., 2003. Interactive simulation of plant architecture based on a dual-scale automaton model.

Chapter 4: Field Protocols, Data Collection, and Model Parameterisation

1. Introduction

This chapter outlines the methodology employed in the field experiments, including tree and plot selection, experimental design, and the measurement protocols implemented throughout the project. It details the approaches used to monitor the physiological development of coffee trees as well as the progression of pest and disease infections. The chapter concludes with a description of the data recording and management strategies adopted to ensure accuracy and reproducibility. The data collection process was carried out with the assistance of a research assistant, Hafashimana Davis (NACORI), who was hired using project funds. The protocol and datasheets for data collection are available at [].

2. Field protocol

Site and Clone Selection

The study and observations were conducted at the CAFNET trial site, which provides an ideal context for evaluating Robusta coffee under different environmental and biotic stress conditions. Two Robusta clones were selected for this study based on their distinct agronomic characteristics, including phenology. Clone L2 (J24/13/20/4) consists of 67 trees within the trial site, while clone L3 (MFCT1) comprises 57 trees. These clones were chosen based on their distribution, susceptibility to pest and disease attacks, and historical health status. Clone L2 is known to be more impacted by Red Blister Disease (RBD), whereas Clone L3 has shown higher resistance. **[Git Repository:** https://github.com/Houssem-Triki/RobustaFieldProtocols.git**]**

Tree and Plot Selection Criteria

All trees were required to be of similar age and, when possible, of comparable past health status, with preference given to those that had not experienced significant pest or disease damage during the previous season. The experimental plot was divided into blocks selected to ensure uniform environmental conditions—particularly in terms of soil characteristics and topography—with shading as the only intentionally varying factor. The plot was well-maintained, easily accessible, and actively in production. Importantly, branches were not pruned, and all phytosanitary interventions were controlled and systematically recorded. The maintenance history of the plot and individual blocks was documented to account for background variables that could influence tree performance.

Experimental Design

The experimental design incorporated multiple factors to explore the dynamics of coffee tree physiology and pest interactions. The factors considered include clone (L2 or L3), shading (shaded or unshaded), and sanitary status (healthy or affected by BTB, RBD, or CBB). Trees

were grouped into experimental categories accordingly. Each tree received a unique identifier and was mapped on a plot plan. Specific branches on each tree were marked for consistent monitoring over time.

A total of 154 trees were selected, including 10 trees per clone and shade level for each of the healthy, BTB, and RBD categories, with smaller numbers for the RBD category. Destructive sampling was planned for four trees (one per clone per shading condition).

Tree architecture (TA)

The TA experiment aimed to evaluate growth patterns. Trees from all experiments were included, along with those previously measured in earlier campaigns. Branches at levels 16, 17, and 18 were tagged at the beginning of the observations for detailed measurement of internode number, leaf count, and cluster development.

A crown architecture analysis is conducted by examining the spatial and developmental organisation of branches along the main axis. Observations proceeded from the apical tip toward the base, where the chronological age of branches increases with rank. This revealed that, within a given axis typology, multiple developmental stages coexist, highlighting the inherent stochastic nature of tree architecture.

Crown architecture analysis is based on a probabilistic framework defined by three parameters: w, b_1, and b_2. The parameter w represents the rhythm ratio, indicating the relative developmental pace of lateral branches compared to the main axis, which is normalized to w = 1. The parameter b_1 defines a Bernoulli process that governs the occurrence of phytomers along the main axis, while b_2 regulates the probability of branching from these phytomers.

Contamination and Physiology (C&P)

This experiment focused on physiological responses to infection and attacks. Four branches per tree were tagged—two near level 10 and two near level 20. Each pair included one attacked and one healthy branch. Detailed cluster-level data were collected on internodes, fruit count, infection status, and accompanying symptoms.

Pest monitoring were planned on a three-week cycle, but due to time constraints, it was conducted less frequently in years 2 and 3.

In RBD-infected trees, assessments included lesion type and location on fruits and leaves. Visual symptoms (e.g., fungal lesions, discolouration) were characterised. For shaded trees, where RBD development is suspected to be suppressed due to low light availability, a smaller number of trees were studied in order to verify this hypothesis.

In BCTB-affected trees, the number and location of entry holes, leaf discolouration, and signs of dieback were noted. The same parameters were recorded for the corresponding healthy branches to enable comparative analysis.

In CBB-affected trees, the number and age category of berries per node, including both healthy and attacked ones, were noted. The same parameters were recorded for the corresponding healthy branches to enable comparative analysis.

To prevent cross-contamination, technicians were instructed to follow a pest-specific monitoring schedule, work on only one pest per day, and sanitise tools between measurements.

Pest Interaction Experiment (P&I)

Building upon the same trees used in the C&P experiment, this study focused on monitoring the entire tree. The experiment tracked the four major pests (BTB, RBD, CBB) under both shaded and unshaded conditions, employing a balanced design. Each clone (L2, L3) consisted of 20 trees, with an equal distribution of 10 shaded and 10 unshaded trees. Data collection encompassed the presence or absence of pests on each branch, branch tagging status, and associated symptoms.

Harvest Weight Tracking (HWT)

Fruit harvests were conducted according to a standard procedure across all experimental trees. The harvest focused exclusively on red, fully ripe fruits. In experiments P&I and C&P, all previously marked branches were harvested. Data included the overall fruit weight and number of red fruits, recorded by clone and branch position. For total tree-level harvests, both total red fruit weight and the weight of floating (potentially CBB-infected) fruits were recorded. Floating fruits were separated using water and noted for disease analysis. Fruit harvest monitoring involved weighing the fruits from previously marked branches.

This allowed for comparisons between healthy and infected trees in terms of fruit yield and development.

3. Data Overview, Dynamics and Analytical Insights

3.1. Pest Interaction Experiment (P&I)

An analysis of pest and disease (P&D) interaction data across tree architecture levels reveals clear vertical stratification in their distribution patterns (Fig. 4.1). The branching position, represented as levels from the top of the tree downward, provides a spatial framework to assess the susceptibility of different parts of the crown.

A striking feature in the data is the concentration of **healthy branches** at the uppermost levels of the canopy. These branches, typically younger and less structurally developed, are often free of fruiting structures. Since pests like the **Coffee Berry Borer (CBB)** and **Red Berry Disease (RBD)** primarily target fruit-bearing nodes, their absence in these apical regions may explain

the reduced infestation. This observation aligns with phenological development, where reproductive organs emerge later and lower in the architectural sequence.

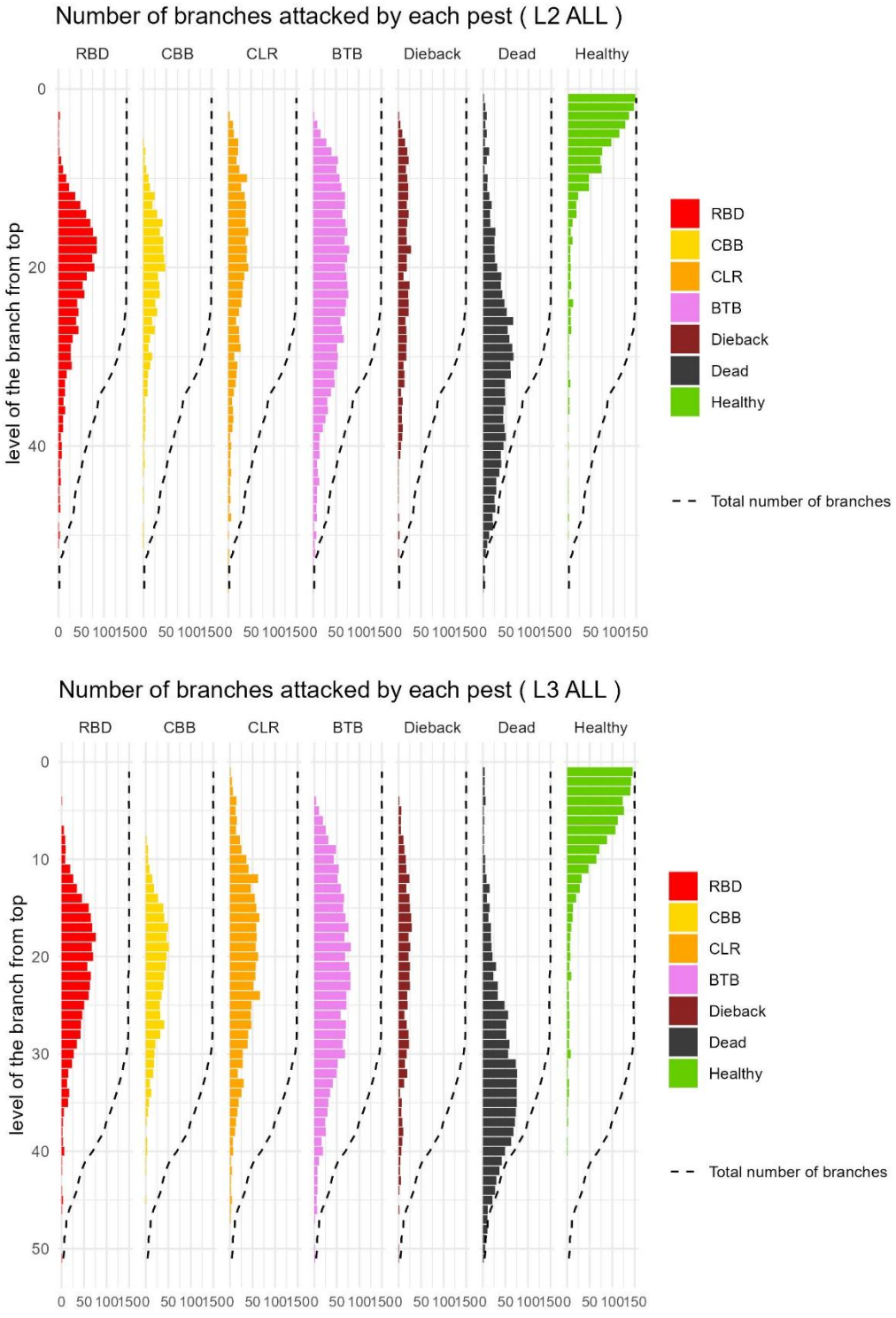


Figure 4. 1: Presence and absence of pests and diseases on the observed trees in their different ranks (branching level)

Descending the tree profile, there is a marked increase in the occurrence of various P&Ds. Mid to lower crown levels show elevated frequencies of infestation by **CBB**, **CLR (Coffee Leaf Rust)**, and **BCTB (Black Coffee Twig Borer)**. Each of these follows a unique vertical pattern:

- **CBB** and **RBD** both concentrate below the top 10–15 branch levels, consistent with their dependency on fruit presence.
- **CLR** shows a broader vertical distribution but is densest in mid-levels, potentially reflecting favourable microclimatic conditions and mature leaf abundance.
- **BCTB** exhibits a slightly deeper distribution, extending further downward, which may reflect a preference for older, more lignified branches, as well as the persistence of symptoms over several years.

The presence of **dieback** and **dead branches** increases notably toward the base. These categories likely result from accumulated pest pressure, ageing, and physiological decline. The transition from live infestation to necrosis provides insight into the long-term impact of unchecked P&D presence.

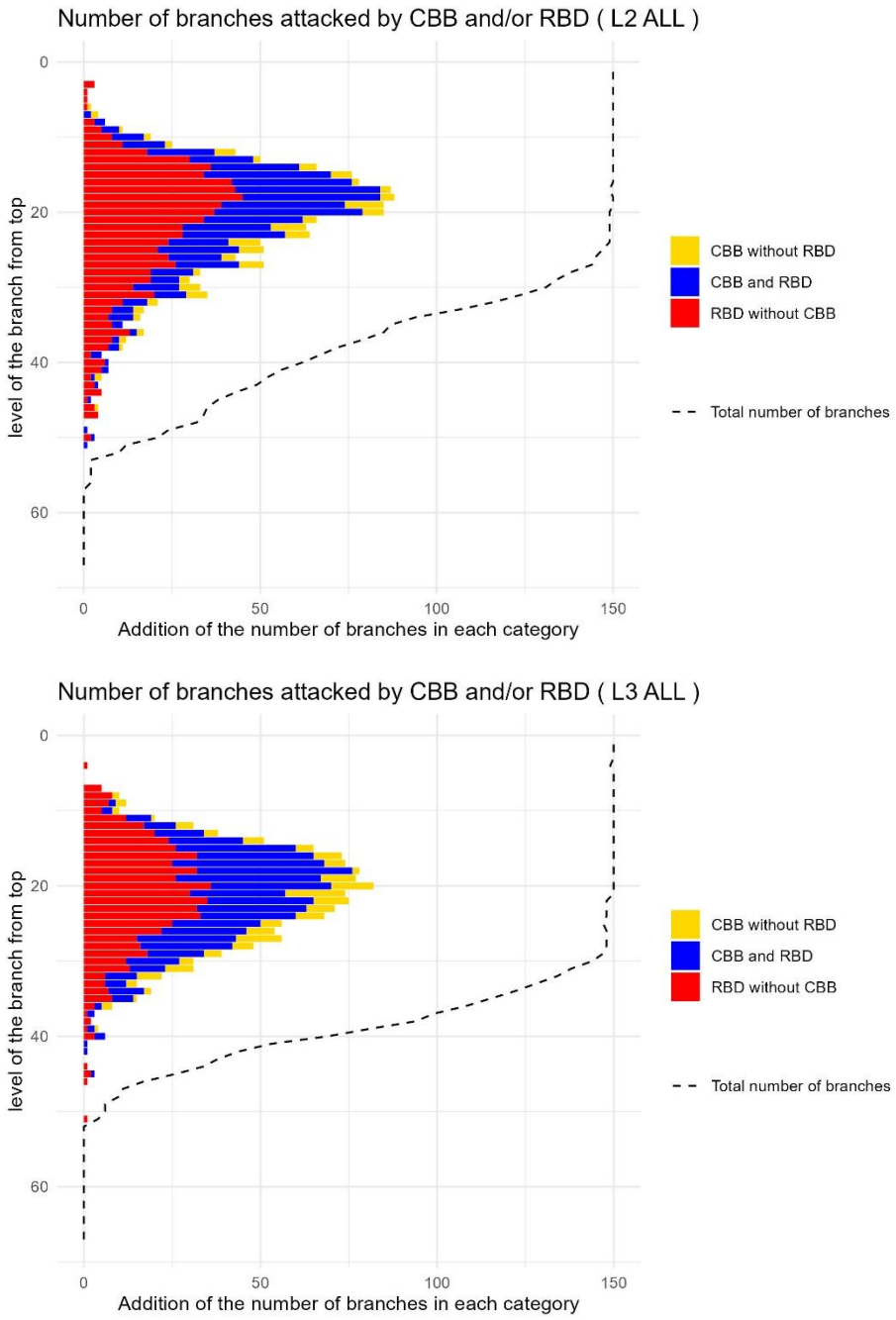


Figure 4. 2: RBD and CBB presence observations on trees' different ranks (L2 and L3)

To further explore pest interaction patterns, we focus specifically on the relationship between RBD and CBB, two pests that target the same organ type: the fruit. The distribution shown in Fig. 4.2 presents a rougher view of their co-occurrence across branching levels.

The figure reveals a predominant overlap in the presence of the two pests. A significant proportion of infested branches host both CBB and RBD simultaneously (blue bars), particularly in the middle section of the crown (ranks 10–30). In contrast, occurrences of CBB without RBD (yellow bars) are relatively rare, suggesting that CBB infestation may frequently occur on branches already colonised by RBD

Meanwhile, RBD without CBB (red bars) appears more frequently, indicating that RBD can establish independently and possibly earlier than CBB in the infection sequence. This asymmetry in co-occurrence suggests a non-random interaction, possibly indicative of a facilitative relationship whereby the presence of RBD increases branch susceptibility to CBB colonisation, either through physiological weakening of the fruit, increased attractiveness due to RBD-induced premature ripening, or by facilitating entry through surface deformation of the fruit.

Moreover, the absence of these pests at uppermost levels once again aligns with fruit availability and maturation gradients. These findings raise the possibility that RBD may act as a gateway pest, paving the way for CBB invasion under certain conditions. Future work should investigate the temporal sequence of infestations and test for statistical dependency between pest occurrences. These interactions underscore the importance of integrating multiple pest models with the plant model through MIMIC, offering a more nuanced and comprehensive understanding of pest–plant dynamics.

3.2. Contamination and Physiology (C&P)

Figure 4.3 provides insight into the dynamics of Coffee Berry Borer (CBB) attacks in relation to fruiting patterns across two coffee clones, L2 and L3, over time. The dotted lines indicate the number of fruit-bearing clusters, while the solid lines represent the number of clusters attacked by CBB.

The patterns observed confirm a tight physiological dependency between fruit availability and pest activity. Comparing the two clones reveals clone-specific dynamics.

In the L3 clone, a decline in the number of fruiting clusters corresponds with a sharp decrease in CBB attacks, particularly noticeable between April and July. This temporal synchronisation underscores the phenological sensitivity of the CBB: its infestation peaks during periods of high fruit availability and diminishes as fruit becomes scarce.

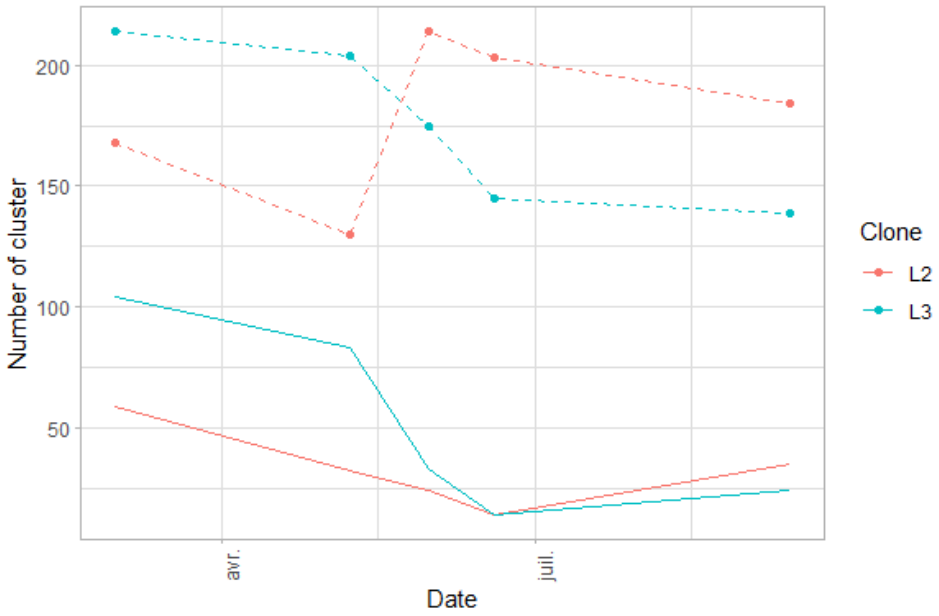


Figure 4. 3: CBB attack dynamics on both Coffee tree clones. Clusters with fruits (dotted) and attacked by CBB (solid) per clone.

The fruiting dynamics of L2 differ from those of L3, with the number of fruiting clusters in L2 increasing when those of L3 decrease, particularly in July. L2 consistently produces fewer fruiting clusters than L3. We also observed lower overall levels of CBB infestation in L2, along with a distinct pattern: during periods of higher fruit production in L2 (e.g., July), a delayed increase in CBB infestations is noted. This temporal shift in fruiting may help explain the observed pattern of CBB attacks, suggesting that the variation in infestation levels is primarily linked to the timing of fruiting.

Figure 4.4 presents the temporal evolution of Black Twig Borer (BTB) attacks across 10 monitored trees per clone (L2 and L3), based on the number of entry holes observed on four designated branches per tree. Each line represents the progression of hole counts for an individual tree from February to December 2023.

In this study, a new hole corresponds to a newly established BTB colony, typically initiated by a female insect boring into a suitable branch to create a gallery. Occasionally, a single colony may produce multiple holes: additional exit holes allow for the dispersal of emerging beetles to colonise new branches. Thus, rising hole counts reflect ongoing colonisation pressure and pest persistence.

Decreases in the number of holes often indicate branch mortality caused by severe BCTB infestation. When a branch dies, it is removed from the study and replaced by a new, healthy branch to maintain observations, resulting in an artificial drop in the recorded hole count.

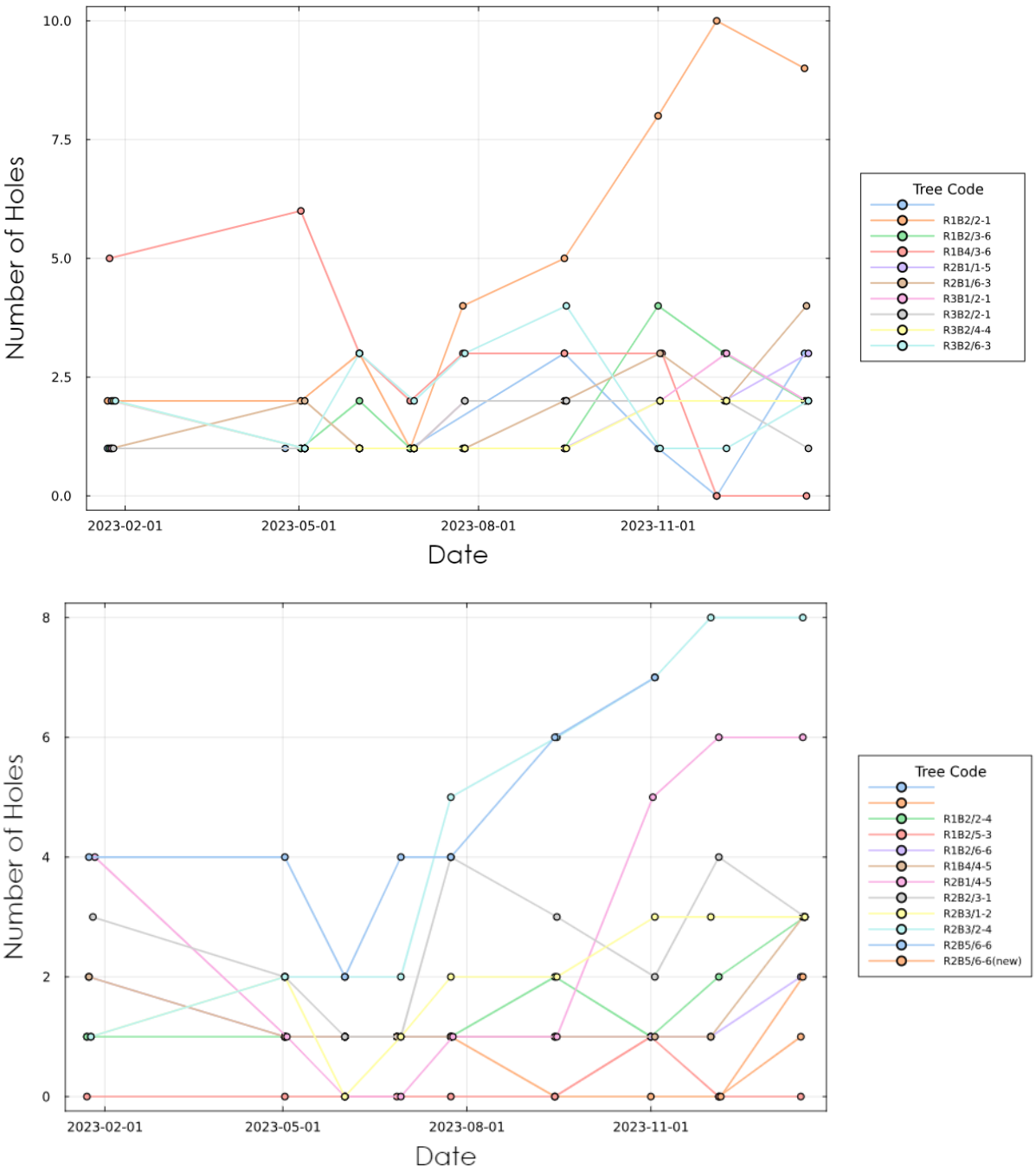


Figure 4. 4: Dynamics of Black Twig Borer (BTB) Infestation in Coffee Tree Clones L2 (top) and L3 (bottom). The new branch R2B5/6-6 was selected after the death of a previously marked branch.

In the upper panel (L2 clone), two trees exhibit distinct infestation patterns: one with high infestation levels at the beginning of the period (R1B4/3-6), and another with elevated levels towards the end (R3B2/6-5). The remaining trees maintain relatively stable or low infestation levels, though frequent drops in hole count may suggest repeated episodes of branch mortality.

In contrast, the lower panel (L3 clone) shows more consistent and gradual increases in infestation. Some trees (e.g., R1B2/7-4 and R2B2/5-4) display sustained rises in hole count

throughout the year. Overall, L3 trees tend to exhibit lower maximum infestation levels compared to those of L2.

Interestingly, both clones show a period during which hole counts stabilise or decrease across all trees, occurring earlier in L2 than in L3. This pattern may indicate a phase of reduced branch attractiveness or increased susceptibility to mortality, potentially linked to physiological changes in the host trees.

These trends may reflect clone-specific differences in structural resistance, wood density, or physiological traits influencing the success of pest colonisation. Further statistical analysis is needed to assess whether a clone provides a measurable resistance advantage under comparable field conditions

3.3. Tree Architecture (TA)

Crown analysis allowed for the extraction of key developmental parameters describing the growth rhythms and branching structure of the two studied coffee tree clones (**L2** and **L3**). Using the modeling framework based on phytomer development and branch initiation probabilities, we estimated the parameters $\mathbf{b_1}$, $\mathbf{b_2}$, and **w**, which respectively represent the Bernoulli process for phytomer initiation on the main axis, the branching process on lateral axes, and the rhythm ratio relative to the main axis.

Table 4.1. Development parameters of the coffee trees L2 and L3

Clone	b1	b2	w	Branching probability
L2	0.72	0.88	0.92	0.2778
L3	0.77	0.92	0.86	0.384

Clone L3 exhibits higher values for both b_1 and b_2, indicating a greater likelihood of both phytomer and branch development. Additionally, its branching probability is noticeably higher than that of L2, implying a denser and potentially more complex crown structure. Conversely, L2, while slightly more regular in rhythm (w = 0.92), has a lower overall architectural complexity.

These architectural traits have meaningful implications for pest dynamics and physiological performance. A more branched structure, such as that of L3, could provide more microhabitats for pests like the Coffee Berry Borer (CBB).

Ultimately, these results reinforce the importance of tree architecture in shaping both ecological interactions and agronomic performance. Incorporating architectural modeling into pest management strategies could enable trait-based selection of clones that balance yield and resistance.

3.4. Harvest Weight Tracking (HWT)

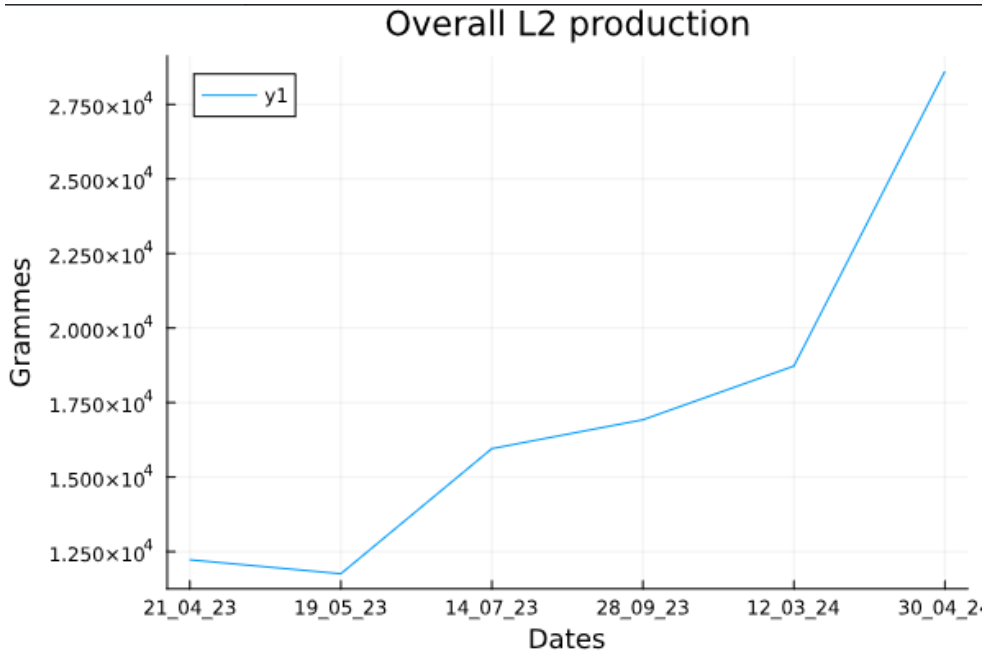


Figure 4. 5: Weight of Ripe Fruit Produced by Clone L2 (in grams)

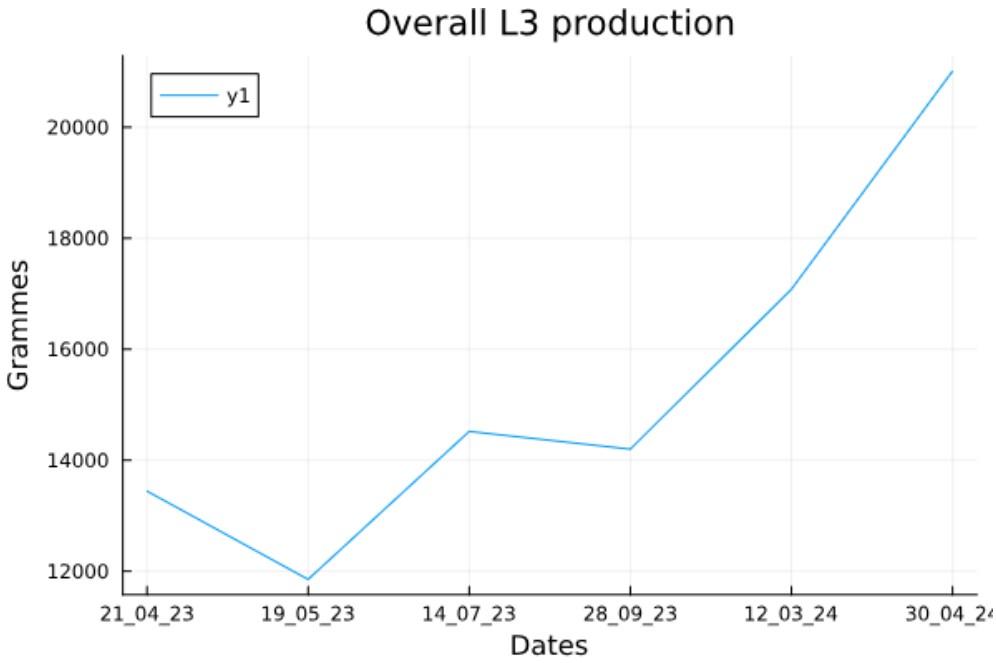


Figure 4. 6: Weight of Ripe Fruit Produced by Clone L3 (in grams)

Figures 4.5 and 4.6 illustrate the temporal evolution of fruit production (in grams) for clones L2 and L3, respectively, as recorded in the Harvest Weight Tracking (HWT) experiment. This analysis summarises yield data across sequential harvests from April 2023 to April 2024.

Clone L2 shows a progressive increase in total fruit yield over time, with a sharp rise observed in the final harvest (April 2024), where the total production surpasses 27,500 grams on 4 branches from 10 trees. After a slight dip in May 2023, yield levels steadily climb through each subsequent harvest. The most significant jump occurs between March and April 2024, suggesting a possible delayed but robust fruiting cycle or the influence of favourable seasonal or physiological conditions.

Clone L3 follows a similar upward trend but with a more moderate overall yield profile compared to L2. The initial decline in May 2023 is followed by a gradual recovery and sustained growth, peaking at just over 21,000 grams in April 2024. Unlike L2, Clone L3 displays a more evenly distributed production curve over time, with fewer abrupt fluctuations in ripe fruit yield.

While both clones exhibit increasing productivity during the year, L2 ultimately outperforms L3 in terms of total harvest weight. However, the yield acceleration in L2 appears more episodic, with pronounced surges, whereas L3's output is more stable and steadier. These differences may be attributed to clone-specific traits such as flowering synchronicity, branch architecture, or pest tolerance, all of which can influence fruit maturation and retention.

L2 and L3 exhibit distinct fruiting dynamics, phenological patterns, and pest infestation profiles. Further integrated analyses combining pest pressure data with physiological monitoring are warranted to better understand the underlying interactions.

4. Data-based parameter estimation for the CBB model

While the previous sections focused on data collected specifically within the framework of this PhD research, centred on Robusta coffee clones and their interactions with pests, this final section introduces a complementary dataset obtained through collaboration with colleagues working on Arabica coffee systems in Indonesia. These external data were not part of the core experimental design but were essential for parameterising and validating a generalised Coffee Berry Borer (CBB) model. Their inclusion enables the extrapolation of findings beyond the Robusta context and supports the broader objective of developing a predictive tool for CBB infestation dynamics across diverse agroecological settings.

To support the development and validation of the CBB behavioural model, field data were collected to estimate attraction parameters and assess model accuracy under real-world conditions. The experimental setup involved two consecutive years of monitoring in Simalungun province, North Sumatra, Indonesia, focusing on Arabica coffee plants that received no chemical treatments against CBB.

Each year, six distinct plots were selected. In each plot, 15 coffee plants were monitored, with six branches per plant observed over the course of one full year. This setup yielded a robust dataset across multiple environmental and biological conditions.

Observations were conducted every three weeks, focusing on fruit availability and status across all fruit-bearing nodes on the selected branches. Importantly, only berries considered

attractive to CBB—those larger than 0.5 mm in diameter—were included in the counts. Fruits were classified into four categories:

1. Healthy unripe berries (green/yellow)
2. Attacked unripe berries
3. Healthy ripe berries
4. Attacked ripe berries

Following each observation, ripe berries, both healthy and attacked, were harvested to prevent confounding effects due to overripe or decaying fruit.

The first year's dataset was used to estimate key model parameters, specifically those associated with the "*Host interaction*" elements of the simulation. These components govern the probability of a fruit becoming a target for infestation as a function of its physiological status and the surrounding pest pressure.

The second year's data served as an independent dataset for model validation, enabling a quantitative assessment of the model's predictive capacity under similar but distinct field conditions.

This structured approach provided both calibration and validation phases, essential for ensuring model robustness and transferability across time and space. The empirical basis ensures that simulated infestation dynamics are grounded in realistic pest-fruit interaction patterns, strengthening the model's applicability to decision support and integrated pest management.

To model the association between the number of new pest attacks and a set of explanatory variables derived from model-based hypotheses, we used Boosted Regression Trees (BRT). BRT is a machine learning technique well-suited for capturing complex, non-linear interactions without requiring pre-specification of the functional form. The BRT model was used to estimate the marginal effect of each explanatory variable while holding the others constant at their mean values. To facilitate interpretation of the partial dependence plots, a locally estimated scatterplot smoothing (LOESS) curve was superimposed

The response variable was defined as the number of new attacks occurring between two consecutive observation dates. It was computed as the difference between the total number of attacks observed on both mature and non-mature fruits at time d, and the number of attacks recorded on non-mature fruits at the preceding time point. This approach accounted for the systematic removal of mature fruits between sampling dates.

Explanatory variables were formulated to reflect biologically motivated assumptions. Trees with a higher number of available fruits are more attractive to pests. Clusters with a higher proportion of ripe fruits are more attractive. The number of previously attacked fruits influences the likelihood of new attacks.

Accordingly, the selected explanatory variables included: the number of available fruits on the focal tree and within the cluster, the proportion of ripe fruits on the focal tree and within the

cluster, the number of previously attacked fruits and the number of ripe fruits harvested at the previous date.

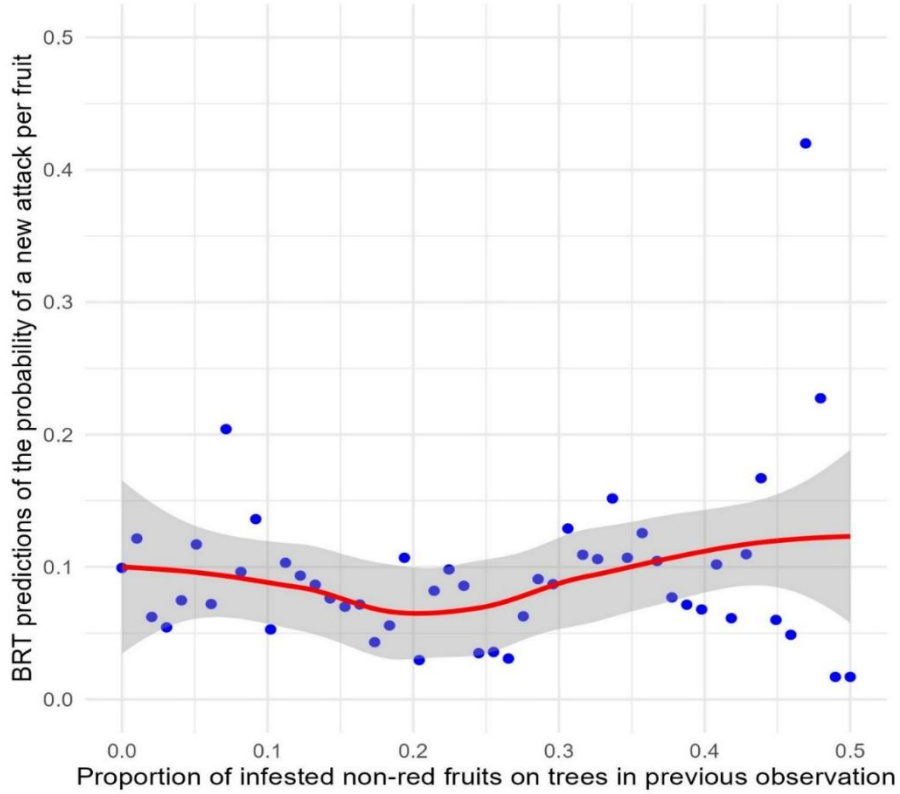


Figure 4. 7: Relationship Between Non-Red Fruit Proportion and Attack Probability (Year 1). Predictions are derived from a Boosted Regression Tree (BRT) model, with individual observations shown as blue dots, the fitted trend as a red line, and the 95% confidence (grey).

To estimate the attractiveness parameter associated with the “Attractive” fruit category in the CBB model (H4), we analysed the relationship between the proportion of infested non-red fruits observed in the previous count and the probability of new attacks per fruit in the subsequent observation.

The fitted trend curve from the Boosted Regression Tree (BRT) model in Figure 4.7 indicates a modestly increasing relationship: as the proportion of previously infested non-red fruits rises, the probability of a new fruit becoming infested also tends to slightly increase. This suggests that local infestation history plays a role in influencing subsequent attack likelihood, possibly due to residual beetle activity or localised host-marking effects. These dynamics inform the parameterisation of the “Attractive” category by quantifying how fruit status modulates attack pressure across time steps in the simulation, here around 0.1.

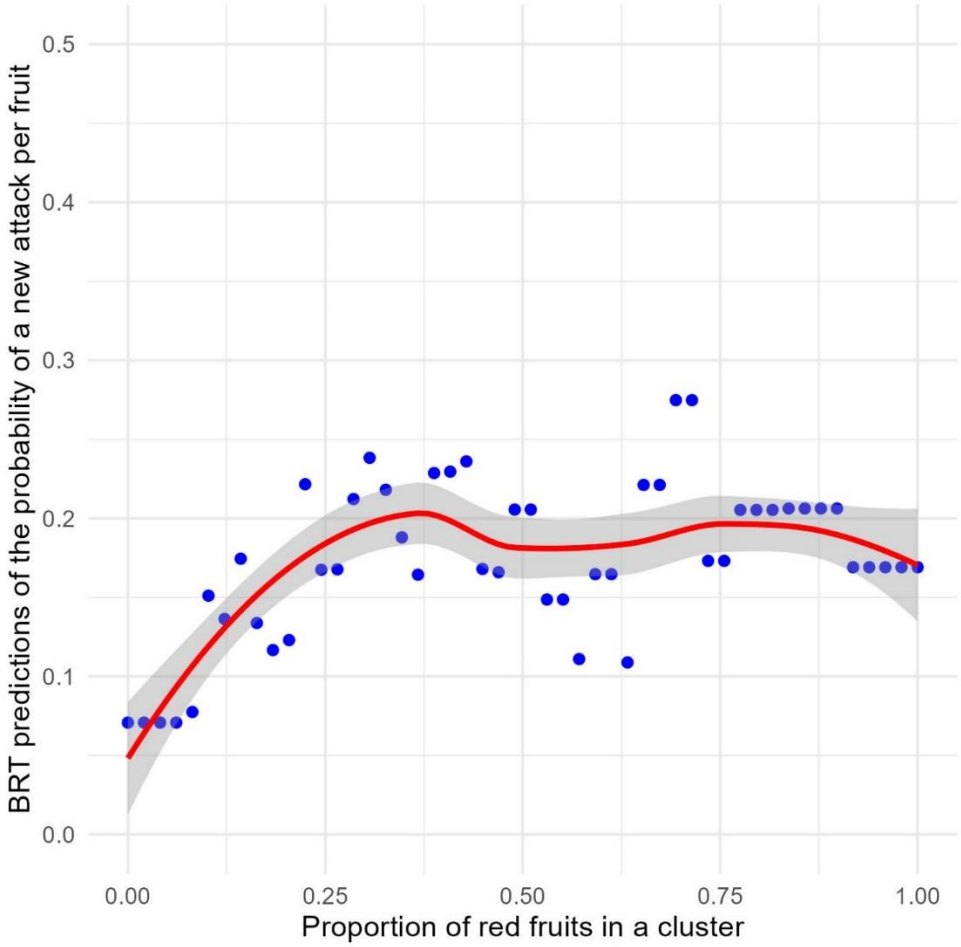


Figure 4. 8: Relationship Between Proportion of Red Fruits in a Cluster and Attack Probability (Year 1). Predictions are derived from a Boosted Regression Tree (BRT) model, with individual observations shown as blue dots, the fitted trend as a red line, and the 95%

To calibrate the “Very Attractive” category in the CBB model, we examined the relationship between the proportion of red fruits within a fruit cluster and the probability of a new CBB attack per fruit during the same observational window (H2) using the BRT prediction in Figure 4.8.

The analysis reveals that the probability of attack increases rapidly as the proportion of red fruits rises from 0 to approximately 0.25, after which it stabilises around a mean attack probability of 0.2. This plateau suggests that even a relatively small presence of red fruits can trigger a high attractiveness signal to CBB females, beyond which additional ripening confers little further increase in colonisation likelihood.

This behaviour supports the parameterisation of the “Very Attractive” category in the model, reflecting a threshold-based response: once a minimum density of mature fruits is present in a cluster, the site becomes highly attractive for infestation. These empirical estimates inform key model elements governing spatial host selection and attack probability as a function of fruit maturity.

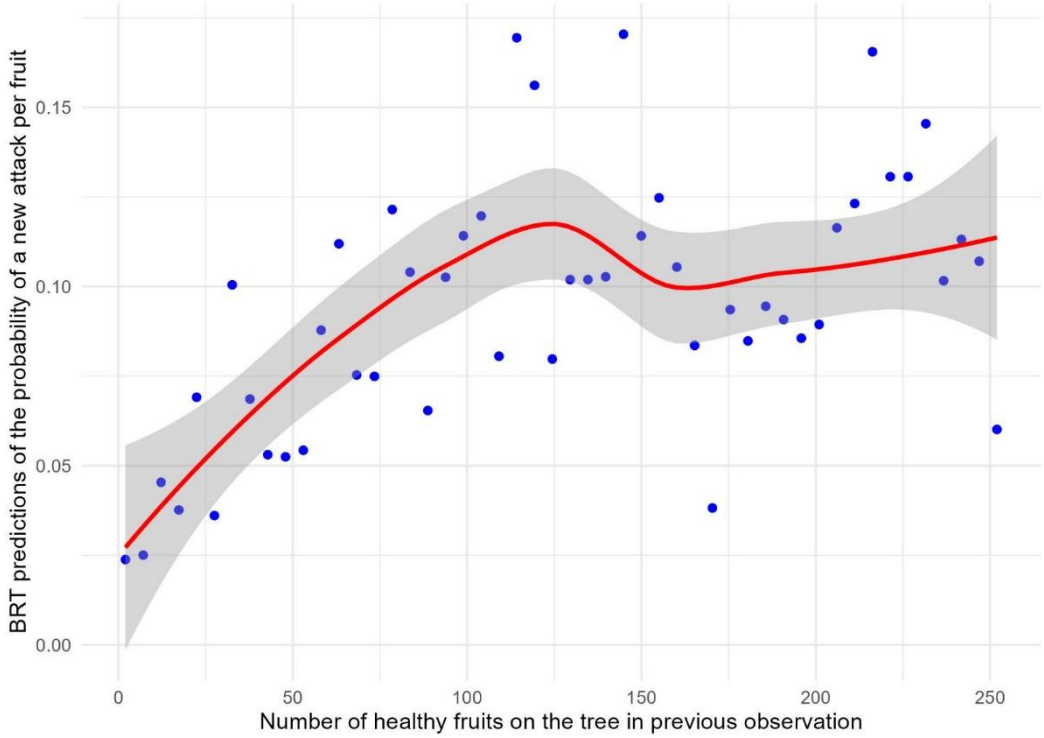


Figure 4. 9: Influence of Tree-Level Fruit Load on CBB Attack Probability (Year 1). Predictions are derived from a Boosted Regression Tree (BRT) model, with individual observations shown as blue dots, the fitted trend as a red line, and the 95% confidence interval

To estimate the ω (omega) parameter in the CBB model, which captures the saturation threshold beyond which increased fruit availability no longer proportionally raises attack probability, we examined the effect of the total number of healthy fruits per tree in the previous observation on the probability of a new attack per fruit (Fig. 4.9).

The relationship is nonlinear and saturating. Attack probability increases sharply with rising fruit abundance up to approximately 100–120 healthy fruits per tree, where it reaches a maximum probability of ~0.12–0.13. Beyond this point, the response plateaus and even dips slightly, suggesting potential local resource dilution effects, where an abundance of hosts may reduce the likelihood of any individual fruit being targeted.

This saturation point was used to parameterise the ω value in the model, setting the threshold at which the fruit load no longer increases per-fruit attack probability. Accurately capturing this density threshold is critical for simulating realistic pest pressure in trees with varying fruit loads and for modeling the diminishing returns of fruit abundance on CBB colonisation success.

5. Discussion and conclusion

This chapter presented a comprehensive methodology for studying coffee tree physiology and pest dynamics under field conditions, with an emphasis on balancing experimental rigour and ecological realism. The original protocol was designed before entering the CAFNET field site, drawing on theoretical knowledge and previous studies. However, once fieldwork commenced, it became clear that adjustments were necessary to accommodate the complex realities observed on-site, especially the co-existence of multiple pests, heterogeneous environmental conditions, and ongoing human intervention in the experimental plots.

Originally, the experimental design assumed clearly defined treatment conditions—e.g., healthy vs. infested trees, shaded vs. unshaded environments. However, once data collection began, it was evident that:

- **Multiple pest species (CBB, RBD, BTB, CLR)** were present simultaneously across most plots, often co-infesting the same trees or branches.
- **Shading conditions were not homogeneous**, as anticipated. Canopy cover varied within and between plots due to surrounding vegetation and management practices, requiring a more flexible interpretation of "shaded" conditions as a gradient rather than a strict category.
- Despite applying **fungicides and attempting physical isolation**, it was **nearly impossible to establish true control trees** that represented uninfluenced physiological development. Infestations were spatially diffuse and dynamically changing, which blurred the boundaries between treatment groups.

Rather than invalidating the protocol, these conditions prompted its evolution, reinforcing the need for context-responsive methodology in field-based agricultural research.

Another key factor influencing results was the active presence of farmers and technicians in the trial plots. These individuals performed tasks such as pruning, harvesting, and routine maintenance, which introduced both risks and benefits to the integrity of the experimental system:

- On the one hand, human activity may have facilitated passive pest transmission (e.g., via contaminated tools or handling of infected branches).
- On the other hand, such activity also mimicked real-world farming conditions and contributed to passive pest control, especially through the removal of visibly damaged or dying branches, which reduced pathogen and pest spread.

This dual role highlights the value of studying pest dynamics within a functional agroecosystem, where biotic interactions and human decisions co-shape outcomes.

Several important insights emerged from the data collected:

Vertical stratification in pest presence was clear. As shown in Section 3.1.1, healthy branches dominated the upper canopy, where fruiting was rare, while pest presence increased in mid-to-lower levels, coinciding with fruit availability and wood maturity.

- CBB and RBD were most abundant between branch levels 10–30, where fruit clusters are concentrated.
- BTB was found deeper in the canopy, favouring older, woody tissue, while CLR peaked in mid-levels, likely influenced by microclimatic conditions.

Pest co-occurrence patterns suggest facilitative interactions. Section 3.1.2 showed that CBB was more likely to appear where RBD was already present, hinting that RBD may weaken fruit or create favourable conditions for subsequent CBB infestation.

Further analyses are needed to investigate the relationships between fruiting patterns, branching architecture, pest and disease dynamics, and shading conditions.

To move beyond clone-specific or site-specific findings, the final part of this chapter incorporates external data collected from Arabica coffee plantations in Sumatra. These data were used to parameterise and validate a generalised Coffee Berry Borer (CBB) model, offering a broader, more transferable understanding of pest dynamics across different coffee systems.

One key advantage of the Sumatra dataset is that it was collected from untreated plants, allowing for the observation of natural CBB infestation patterns without chemical interference. Additionally, the data come from an equatorial region, where coffee trees fruit continuously throughout the year. This contrasts with the more seasonal fruiting patterns observed in the CAFNET Robusta trial and enables the analysis of CBB behaviour under conditions of constant host availability, which is critical for understanding pest pressure in tropical lowland systems.

Moreover, this dataset provided the necessary empirical basis for estimating several critical model parameters. It allowed the quantification of fruit attractiveness through the observed relationships between infestation probability and the proportion of non-red and red fruits in a cluster (Figures 4.6 and 4.7). These estimates were used to define the “Attractive” and “Very Attractive” categories in the model. In addition, a saturation threshold was identified (Figure 4.8), informing the calibration of the ω value—the point at which increasing fruit abundance no longer leads to a proportional increase in attack probability.

By incorporating these empirically derived relationships, the model gains a realistic and biologically grounded structure that reflects both tree-level fruit conditions and temporal dynamics of pest pressure. This strengthens its ability to simulate CBB behaviour across diverse contexts and contributes to its potential as a decision-support tool in pest management.

This chapter documents the evolution of a flexible and ecologically grounded methodology for studying coffee tree–pest interactions under field conditions. While the original protocol aimed for controlled comparisons, the realities of the CAFNET trial, including overlapping pest

presence, inconsistent shading, and ongoing human intervention, necessitated methodological adaptation.

These adjustments not only reflect good experimental practice but also strengthen the relevance and applicability of the findings to real-world agroecosystems. The resulting data provided meaningful insights into tree architecture, pest behaviour, and yield dynamics, while also feeding into a generalised CBB model capable of operating across environments and coffee species.

By combining detailed field experimentation with complementary external datasets, this chapter establishes a solid foundation for modeling CBB dynamics across different coffee production systems. The integration of empirical observations from both Robusta and Arabica systems enhances the model's relevance and supports its potential application in a variety of agroecological contexts. In doing so, it provides a framework for developing more informed, context-sensitive strategies for pest monitoring and management.

Chapter 5: Simulating Plant Pest Interactions: Evaluation and Validation

1. Introduction

This chapter presents the implementation and evaluation of the simulation models developed in the previous stages. Two main components are examined: the plant growth model, which simulates coffee tree development under varying conditions, and the generalised Coffee Berry Borer (CBB) model, which predicts pest dynamics in response to host availability and environmental factors.

The first section focuses on the simulation of plant architectural and physiological development, using parameters derived from field data. These results are assessed against observed growth patterns to evaluate the model's accuracy in representing coffee tree structure and dynamics under both optimal and stress conditions.

2. Results of the Plant Model

2.1. Healthy plant (Stable case)

This simulation presents the results of the plant growth model using parameters calibrated for the so-called clone L3 (Table 4.1), one of the two Robusta genotypes studied in our partner fields.

The outputs are shown over 42 growth cycles, where each cycle represents a timestep corresponding to phenological or architectural events (e.g., leaf expansion, internode initiation). The results are summarised across eight metrics, grouped into functional and structural dynamics:

Plant Demand and Biomass Allocation

The top row displays the incremental plant demand (left) and accumulated demand (right). We observe that plant demand rapidly increases during the initial 5–10 cycles and then stabilises, oscillating around a consistent range. This plateau suggests a transition from vegetative establishment to a more stable growth phase, where the number of active organs remains relatively constant.

Correspondingly, biomass allocation shows a similar trend. The incremental biomass plot (second row, left) demonstrates an S-curve: a lag phase in early cycles (low biomass allocation), followed by a steep rise, and finally a plateau as the plant reaches a state of functional maturity. The cumulative biomass graph (second row, right) reflects this, showing a steady linear accumulation once the initial establishment phase concludes around cycle 15.

Leaf Area Dynamics

The third-row tracks leaf blade area increments and cumulative leaf area, key indicators of photosynthetic potential. The model predicts a marked increase in leaf area in the first 10–15 cycles, mirroring the early vegetative phase. Afterwards, the blade area increment stabilises, supporting the assumption of architectural equilibrium in later cycles.

The cumulative area continues to rise linearly, consistent with the continued initiation of new leaves. This suggests that while the per-cycle contribution levels off, the photosynthetic surface area keeps expanding as the plant develops further cohorts.

Net Biomass Production

The bottom row focuses on net biomass, which accounts for both organ allocation and source–sink balance. The accumulated net biomass curve shows a continuous upward trend, affirming that the plant maintains a positive carbon balance throughout the simulation period.

Notably, the net biomass per cycle plot reveals a steep increase in early cycles, reaching a maximum by around cycle 12, after which production remains stable. This result aligns with the earlier trends: after a critical developmental threshold, the system enters a quasi-steady state, maintaining productivity without major fluctuations in demand or resource allocation.

These simulation results demonstrate that the model correctly reproduces a biologically plausible growth trajectory for a coffee tree with L3-like characteristics. Early growth is dominated by resource allocation to structural expansion (leaves, internodes), followed by stabilisation as functional equilibrium is reached. This is particularly important in the context of coupling with P&D dynamics, where the timing of biomass availability and organ vulnerability plays a critical role in pest exposure and resource-mediated resistance.

The regularity of increment curves and the stability in net biomass from mid-simulation onward indicate that the model achieves internal consistency and is suitable for integration with external modules (e.g., pest models), which require temporally resolved input data on host dynamics.

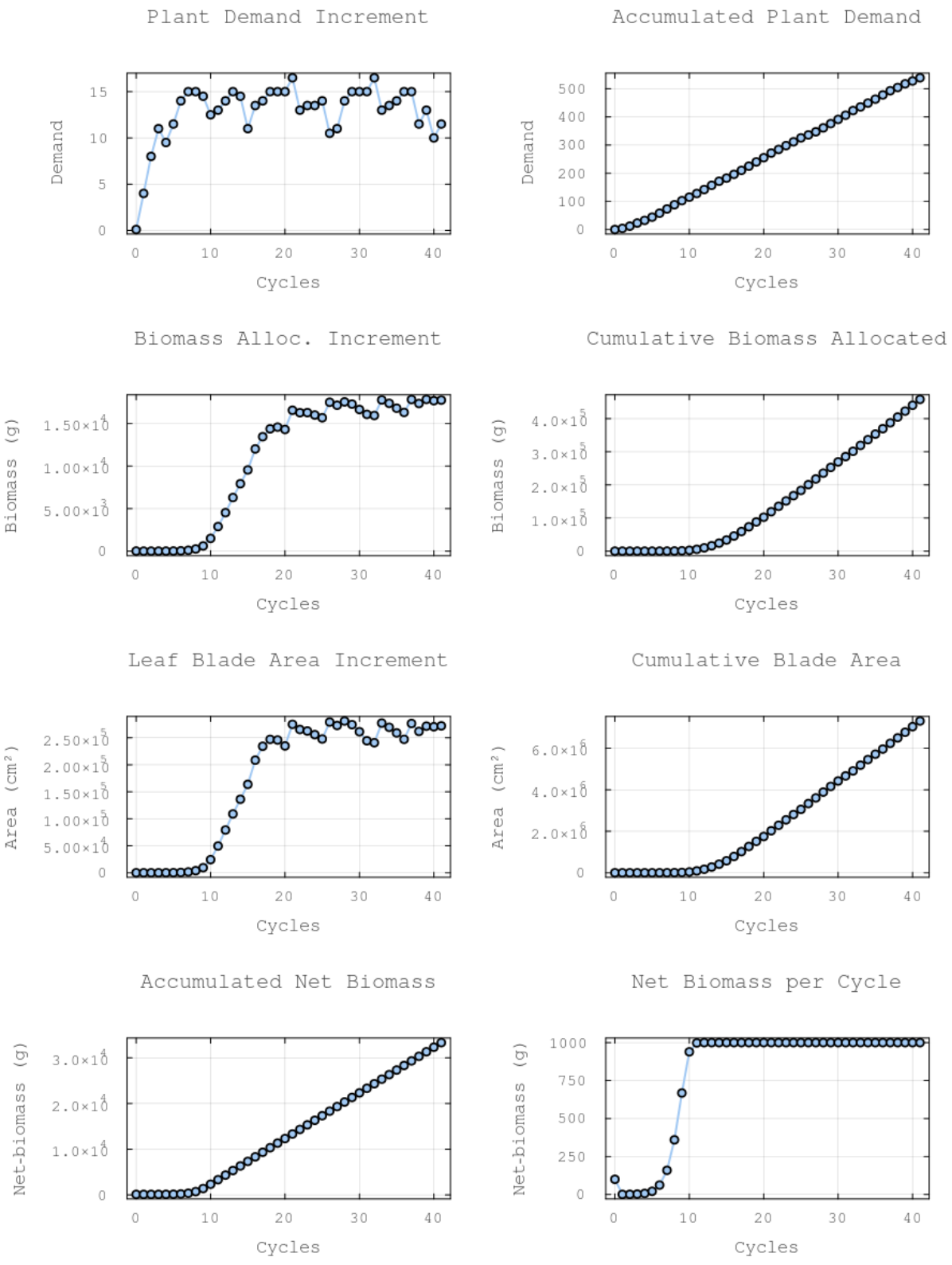


Figure 5. 1: Simulated dynamics of Growth, Demand, and Biomass Allocation in clone L3 arabica Coffee tree over 42 growth cycles

Structural Visualisation of the Plant: Physiological Age

To improve interpretability and clarity in representing plant architecture, we mobilized the visualization tools we did developed (see description end chapter 3).

The Figure 5.2 provides a simplified simulation output depiction of all cohorts belonging to physiological age 2 (PA2). In this representation, cohorts that share identical functional parameters, aside from co-physiological age, have been grouped and visualised as single entities. Their biomass values were aggregated to maintain quantitative coherence and offer a more legible overview of the plant's functional structure. The left-hand side (L2) shows leaf cohorts of 2 organs, while the right-hand side (L10) displays fruit cohorts of 10 organs, both organised by their internode position along the stem.

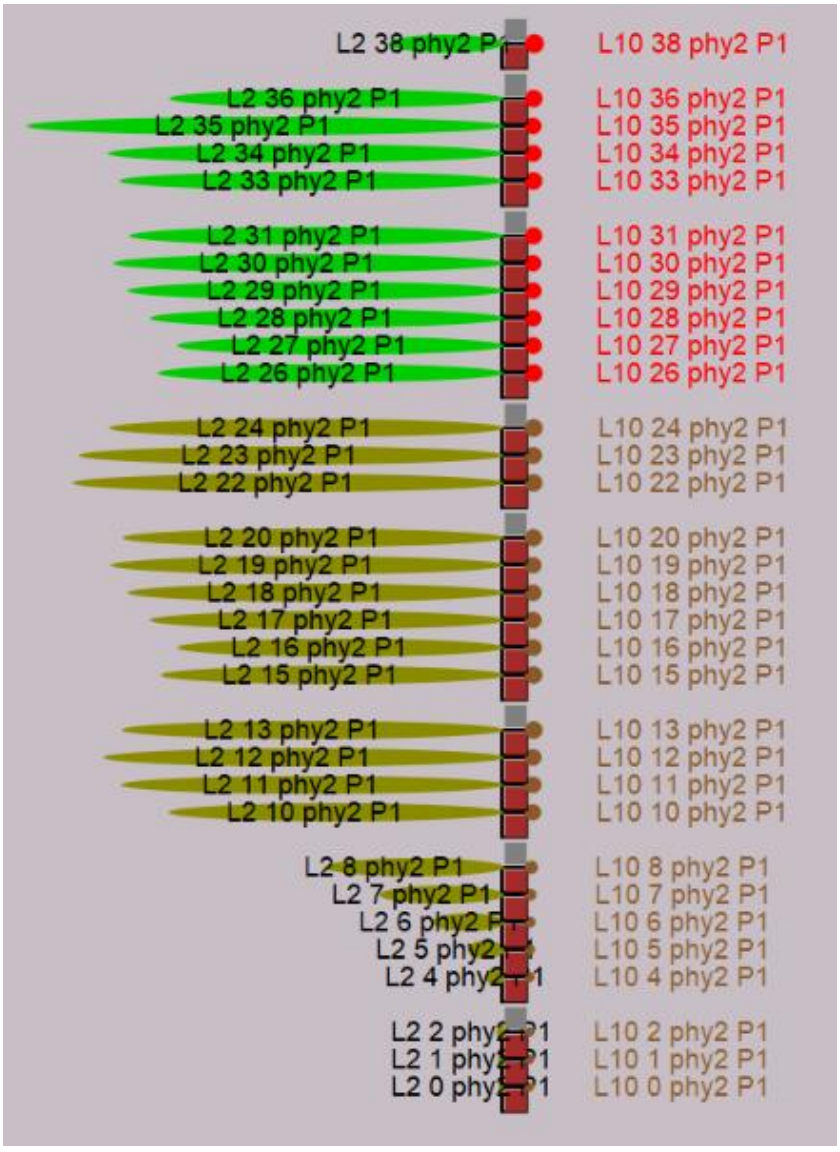


Figure 5. 2: Structural representation of the simulated L3 coffee tree physiological age 2 in a stable growth (39 growth cycles). Grey internodes stand for development pauses on the trunk

This simplified view serves two visualization purposes.

- Reducing visual redundancy: many cohorts exhibit near-identical behaviour in terms of growth, development stage, and resource allocation. Clusters help to highlight structural regularities without losing critical information.
- Enhancing functional understanding: aggregating biomass and parameter groups illustrates the cumulative impact of organ cohorts on overall plant functioning, particularly in terms of photosynthetic surface (leaves), demand generation, and assimilate use.

In this figure, each horizontal element represents a leaf-bearing axis of PA2, with the length corresponding to leaf blade area or other associated organ properties. The colour-coding distinguishes different aspects of physiological status or cohort identity (e.g., green for active cohorts, brown

This visualisation complements the quantitative dynamics presented earlier (e.g., biomass allocation, demand increment), offering an intuitive understanding of the spatial distribution of growth and function within the tree. By aggregating cohorts in this way, the model facilitates comparisons between simulated architecture and observed field structures, improving both validation and interpretation in the context of coupled plant–pest simulations.

2.2. Non-healthy plant (Stable case)

To evaluate the effects of biotic stress on plant physiological performance, a second simulation was conducted introducing a controlled leaf-level damage. This simulation was built upon the same baseline as the healthy L3 clone simulation, but included a targeted attack on the photosynthetic organs. Specifically, a surface loss of 0.75% was applied to each leaf between the 10th and 24th internode of physiological age 2 (PA2), simulating the impact of pest or disease infestation over a defined structural region of the plant.

As one can see in Figure 5.3 curves, the consequences of this relatively small but strategically located attack are immediately apparent:

- Plant demand increment increases markedly during the attack window, peaking around cycles 28–30. This suggests that the plant compensates for the lost assimilate supply by increasing sink strength or resource mobilisation elsewhere.
- Biomass allocation shows a sharp dip following this demand surge, reflecting an internal imbalance between the demand and available photosynthate. This indicates that the loss of functional leaf area had a measurable impact on the plant's ability to meet its growth requirements.
- Leaf blade area increment declines significantly during the same period, consistent with a physiological slowdown, before rebounding as new leaves emerge to replace lost function.
- Cumulative blade area shows a noticeable inflexion point, a clear indicator of the structural disruption introduced by the attack. The plant eventually resumes growth, but the curve reflects a delay in expansion compared to the healthy baseline.
- Net biomass per cycle remains relatively stable, suggesting the plant maintains its carbon balance overall. However, the temporary suppression in cumulative metrics implies a reallocation of resources and a growth penalty during the affected period.

Overall, this simulation illustrates how even a modest loss in photosynthetic area, when strategically distributed across actively functioning cohorts, can generate system-wide adjustments in biomass allocation and demand regulation. Importantly, the plant recovers without collapse, reaffirming that the model can capture resilience and compensatory behaviour, which are critical features in agroecological systems exposed to intermittent pest pressure like the Cafnet trial.

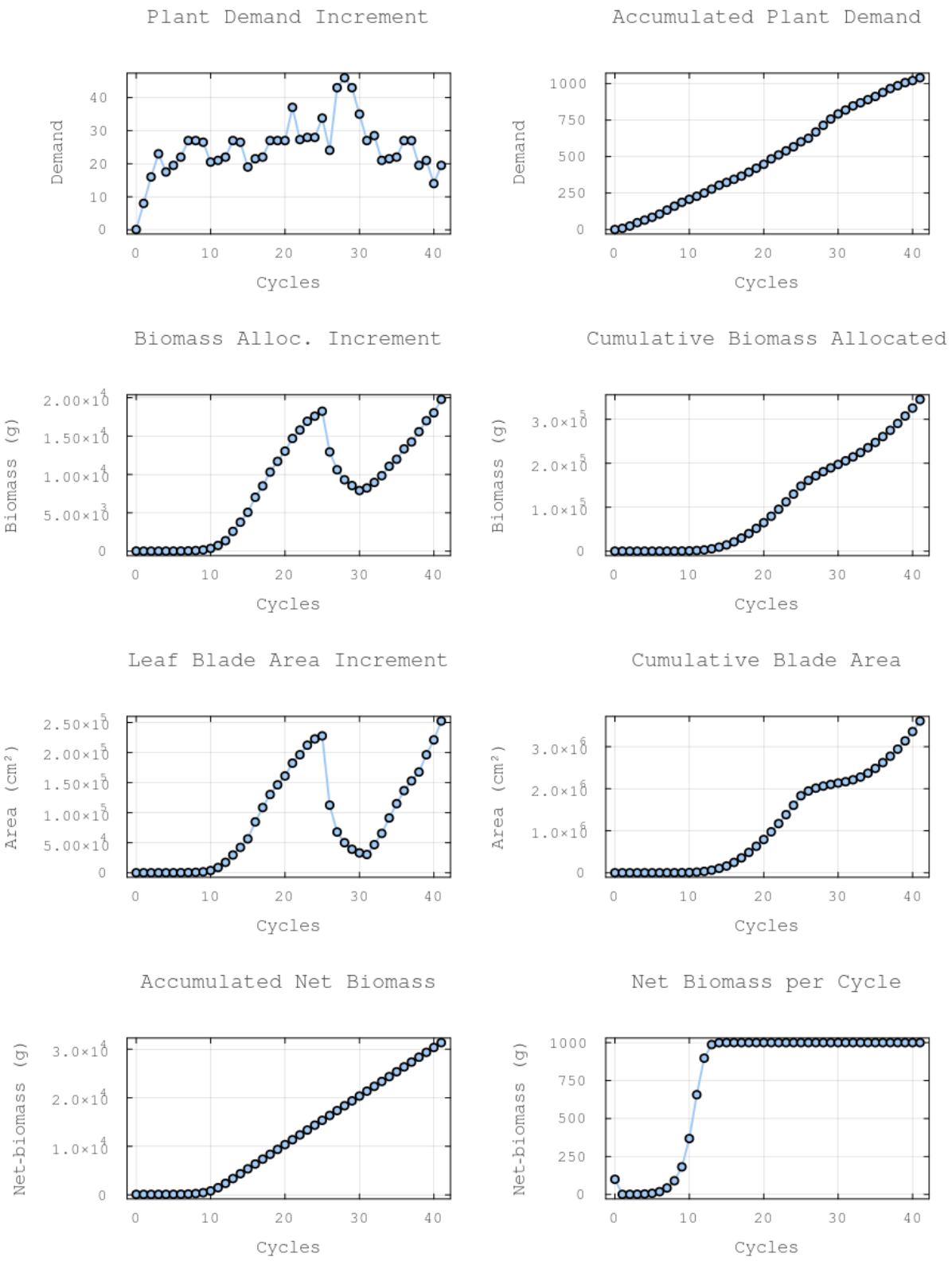


Figure 5. 3: Simulated dynamics of Growth, Demand, and Biomass Allocation in clone L3 Coffee tree over 42 growth cycles, under limited leaf attacks.

Structural Visualisation of the Plant: Physiological Age

Similarly, we illustrate in Figure 5.4 the simulated simplified architectural visualisation of the L3 clone plant after the simulated pest-induced leaf surface reduction between internodes 10 and 24 of physiological age 2 (PA2).

In this simulation, a pest-like disturbance was imposed by reducing 0.75% of the surface area of leaves located between internodes 10 and 24. These affected cohorts are visible in the diagram: in the L2 column, the horizontal green bars representing leaf blades are visibly shorter within that range, denoting their reduced area. This reduction is consistent across the impacted segment, accurately reflecting the input condition used to simulate localised biotic stress. The L10 side (fruit representation) shows no structural disruption, as fruit cohorts were not targeted in this simulation. Their regular and uninterrupted appearance across the axis reinforces that the damage was restricted to photosynthetic organs only.

This figure complements the temporal graphs of blade area, demand, and biomass shown previously by offering a cohort-level anatomical perspective. It visualises how the leaf damage was both localised and quantifiable, while also revealing the plant's ability to maintain structural integrity and continue reproductive development despite partial loss of functional leaf surface.

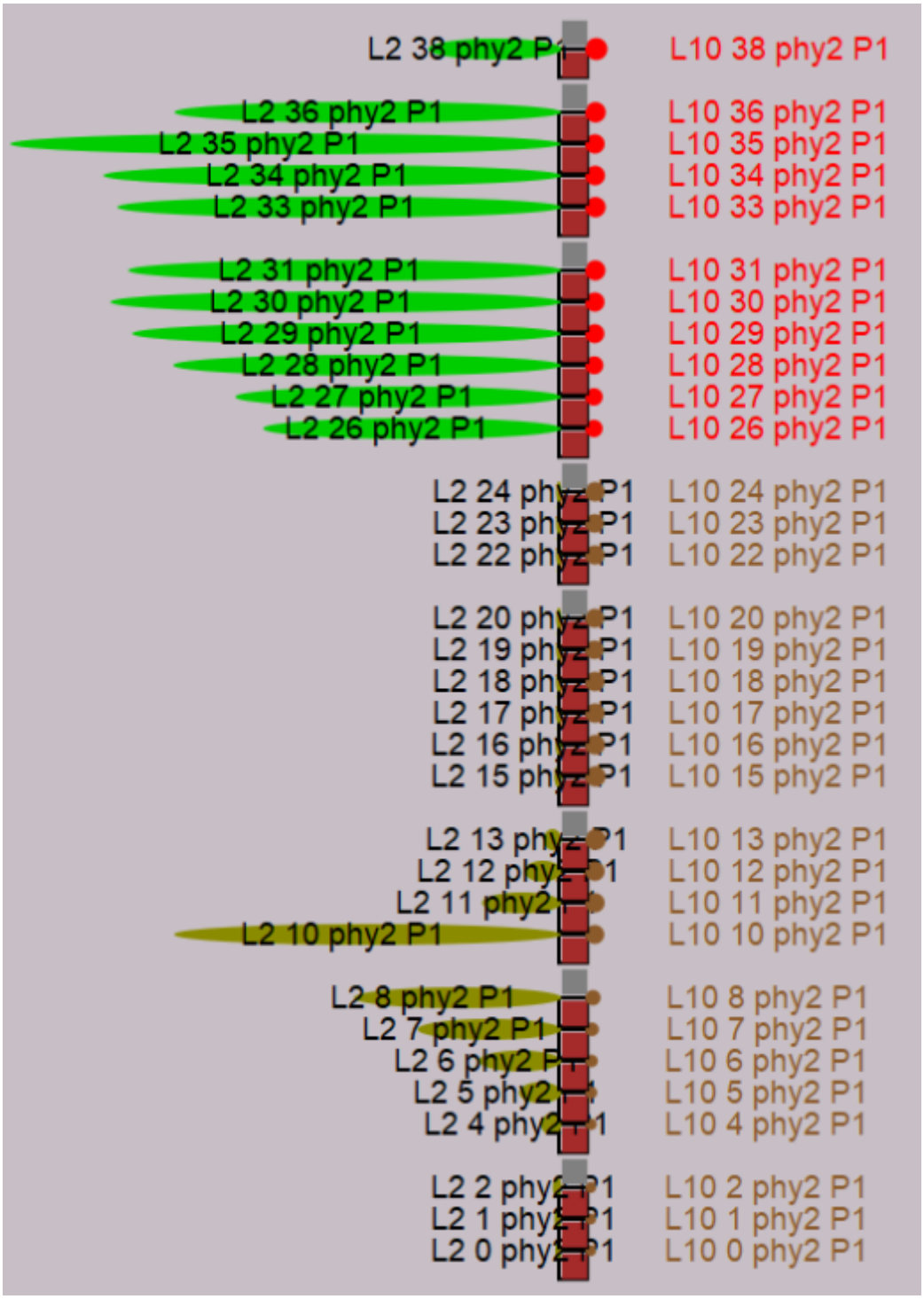


Figure 5. 4: Structural representation of the simulated L3 coffee tree physiological age 2. Reduced leaf blade length between internodes 10–24 reflects simulated surface loss due to pest damage. To compare with Fig. 5.2, standing for the healthy “reference” plant.

3. Results of the generalised model CBB version

3.1. Predictions of the model

To evaluate the ability of the generalised Coffee Berry Borer (CBB) model to reproduce real-world infestation dynamics, we first analysed the fruit production patterns of 90 coffee trees observed over time with the Sumatra plant dataset in the second year. These trees displayed a wide range of temporal fruiting behaviours. Using the Calinski-Harabasz clustering criteria based on the temporal standardised distribution of attacks on red fruits using the ratio of attacked red fruits per date to the total number of attacked red fruits for each tree., seven distinct classes were identified, labelled A through G, each representing a typical fruiting trajectory Fig. 5.5. This classification forms the foundation for testing the model's sensitivity to host availability and its capacity to simulate corresponding pest dynamics.

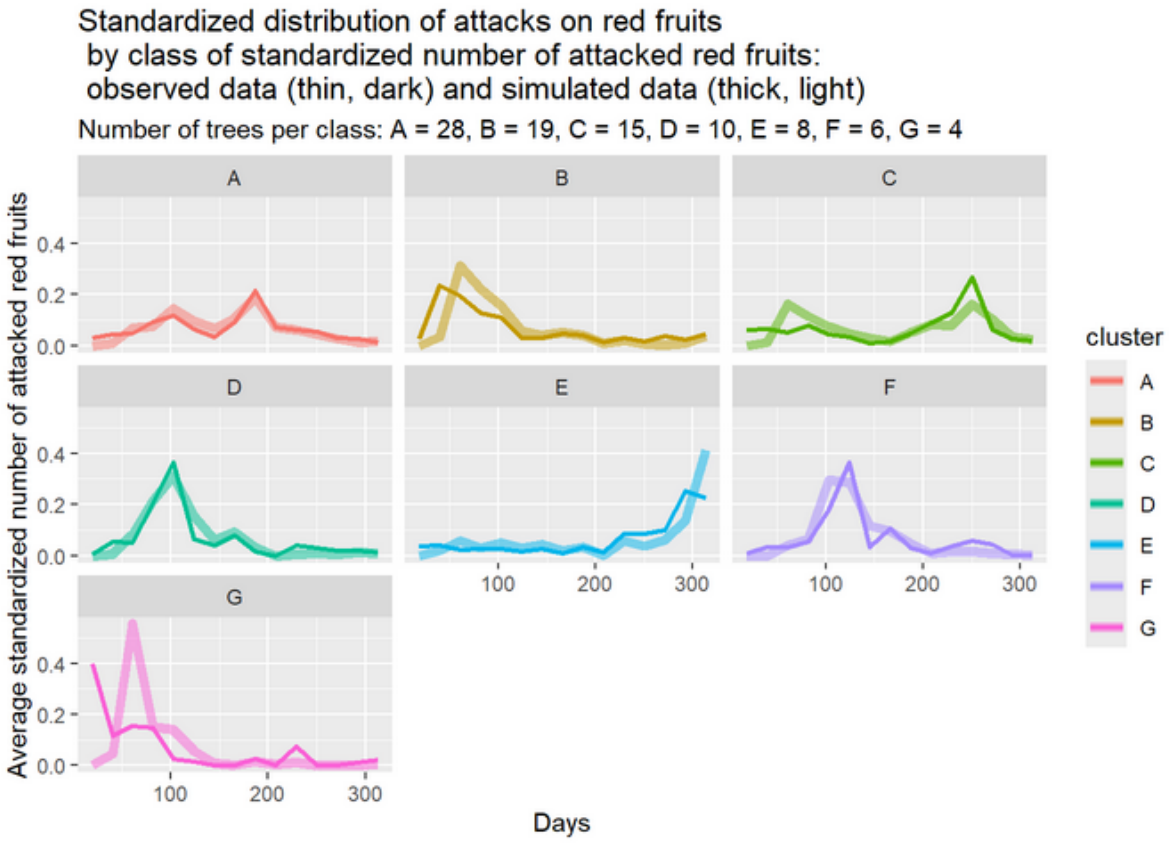


Figure 5. 5: Standardised distribution of attacks on red fruits by class of standardised number of attacked red fruits.

The table below lists the tree identifiers affiliated with each class, forming the basis for the comparative simulations that follow.

Table: Affiliation of each tree to its respective class, established through observed data clustering.

Class	Trees
A	C16 C18 C23 C27 C29 C32 C36 C37 C39 C40 C41 C43 C44 C46 C48 C49 C50 C59 C6 C60 C62 C64 C69 C70 C72 C75 C8 C83
B	C1 C12 C24 C26 C31 C33 C34 C35 C42 C58 C73 C76 C77 C78 C84 C85 C86 C88 C89
C	C14 C22 C38 C4 C47 C5 C51 C52 C53 C54 C55 C56 C57 C67 C9
D	C17 C2 C21 C28 C3 C45 C68 C81 C82 C87
E	C19 C30 C61 C63 C65 C7 C79 C80
F	C10 C11 C13 C15 C20 C25
G	C66 C71 C74 C90

To assess the generalisation and predictive capacity of the CBB model, simulations were performed using the same parameter set derived from first-year data, applied across a new set of trees observed in year two. The goal was to evaluate how well the model performs when exposed to previously unseen data with varying fruiting profiles and total fruit production.

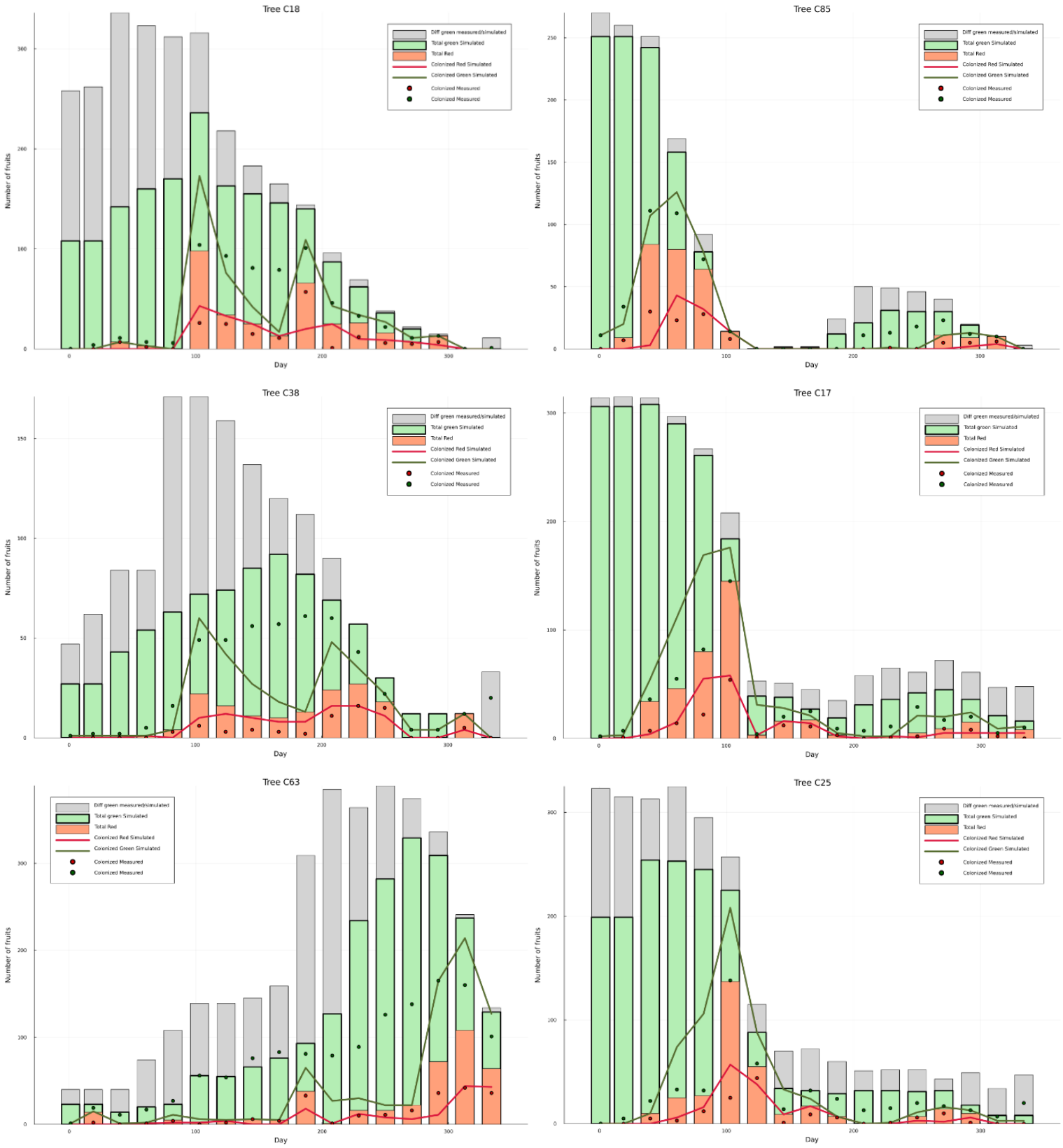


Figure 5. 6: Simulation results compared to observed data for six representative trees: C18 (Class A), C85 (Class B), C38 (Class C), C17 (Class D), C63 (Class E), and C25 (Class F).

Dots on each plot of Figure 5.6, represent the observed number of colonised fruits harvested from six fruiting branches. The solid lines indicate the corresponding simulation outputs. Bars represent the total fruits harvested over time, green for healthy fruits, red for colonised ones and grey for the difference between observed and simulated green fruits.

The model successfully captured the overall colonisation dynamics across the distinct fruiting profiles:

- **C18 and C85 (Classes A and B)** had high early-season fruit loads, leading to early colonisation peaks. The model followed these dynamics closely, though with minor deviations in the declining phases.
- **C38 (Class C)** maintained a sustained fruiting pattern, allowing colonisation to persist moderately over time. The simulation reproduced this continuous pressure effectively.
- **C17 (Class D)** had a later fruiting onset, mirrored by delayed colonisation. The model tracked both the onset and intensity of the infestation with good fidelity.
- **C63 (Class E)**, with moderate fruit numbers and a mid-season peak, experienced infestation concentrated over a narrower window. The model matched this window accurately, albeit with a slight underestimation during the decline.
- **C25 (Class F)** displayed a focus in fruiting pattern with an early peak followed by late-season activity. The model captured both phases, demonstrating its ability to reflect temporally discontinuous dynamics.

3.2. Validation of the simulation results

To validate the model, we used the second-year data, which were not used to build the model. We aimed to validate both the quantities and the temporal distribution of attacks. Therefore, we used two criteria to compare the model results to field data: one based on the number of red and total attacked fruits per date. The other, used previously to analyse and cluster the fruits' dynamics in the previous section.

To compare quantities, we used the concordance index (IA), a metric introduced by (Willmott, 1981) to quantify the agreement between observed (Oi) and predicted (Pi) values:

$$IA = 1 - \frac{\sum(P_i - O_i)^2}{\sum(|P_i - \bar{o}| - |O_i - \bar{o}|)^2}$$

The index ranges from 0 (no agreement) to 1 (perfect agreement) and accounts for both systematic errors (bias) and differences in variability (variance). It provides a more comprehensive assessment of model performance than simple correlation-based measures. IA was calculated for both attacked red fruits and total attacked fruits.

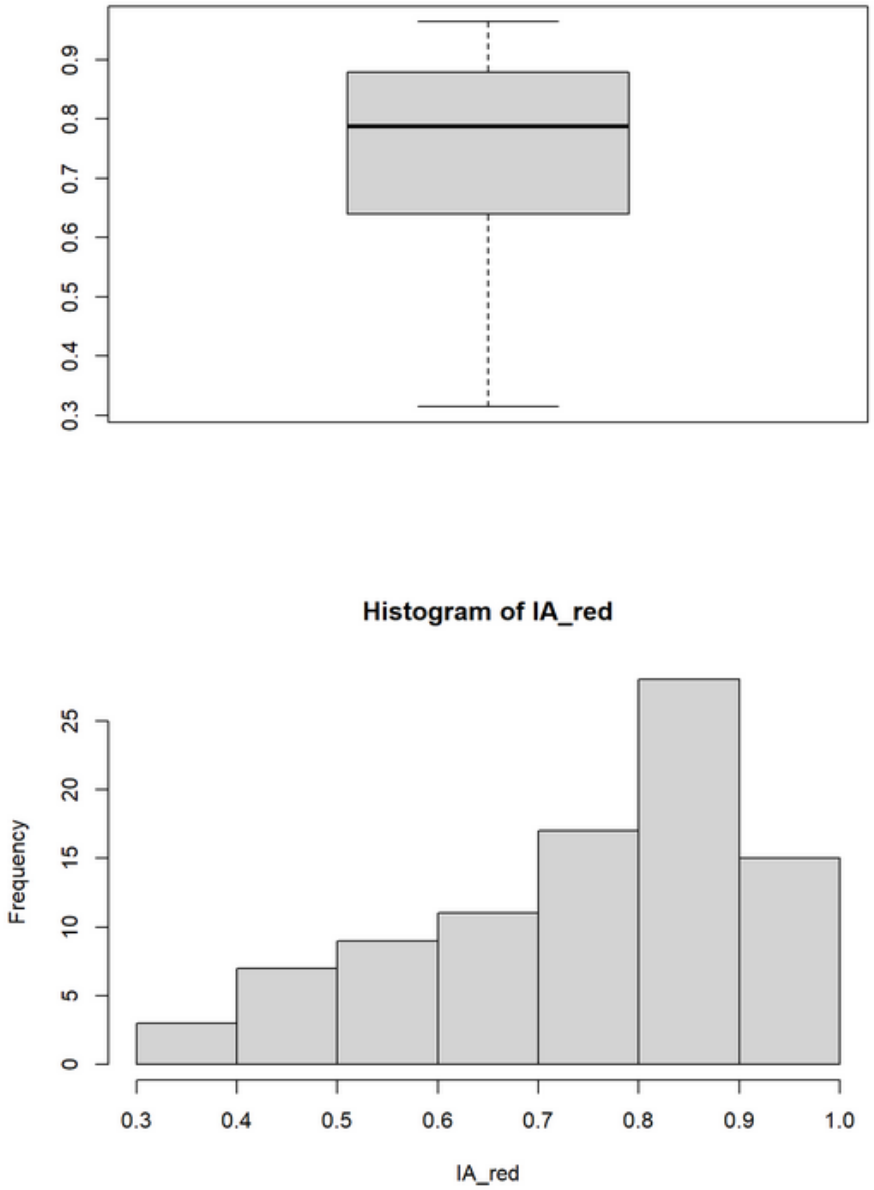


Figure 5. 7: Distribution of the Index of Agreement (IA_red) for Red Fruit Colonisation Predictions. *Top: Boxplot showing the variability and central tendency of IA_red across trees. Bottom: Histogram representing the frequency distribution of IA_red values.*

The IA values for red fruits (IA_red) were generally high across trees, with a median of 0.79, a mean of 0.74, and a third quartile of 0.88, indicating strong agreement between predictions and observations (Figure 5.7). The histogram of IA_red showed a right-skewed distribution, with most values above 0.7, confirming that the model captured the temporal patterns of red fruit colonisation well.

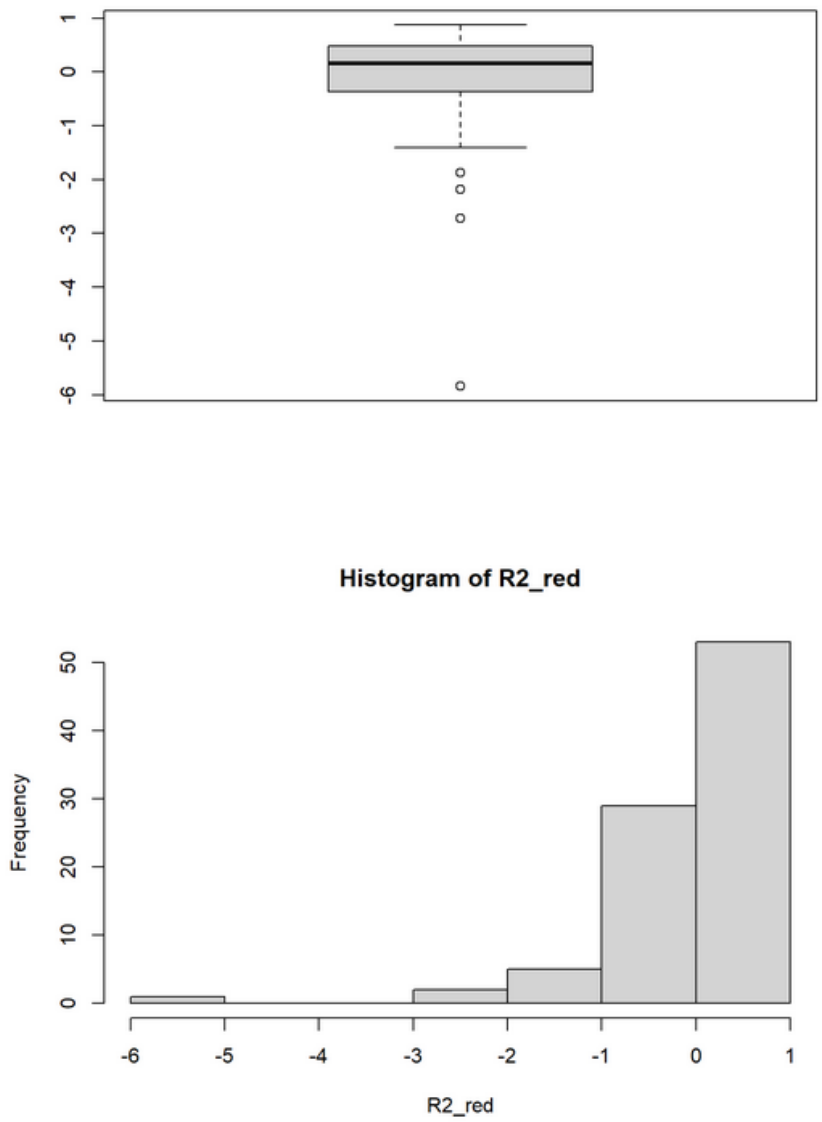


Figure 5. 8: Distribution of R^2 Values (R2_red) for Red Fruit Colonisation Predictions. *Top: Boxplot highlighting the spread and outliers in R^2 values. Bottom: Histogram showing the frequency distribution, illustrating variability and prevalence of near-zero or negative values.*

However, R^2 values (Fig. 5.8) for red fruits showed greater variability: although some trees achieved high scores (max = 0.87), the mean R^2 was slightly negative (-0.06), and 25% of the trees had R^2 values below -0.36, indicating that for some cases, the model performed worse than a simple mean predictor. This discrepancy highlights the sensitivity of R^2 to data noise and variance, particularly when the magnitude of variation in observations is small.

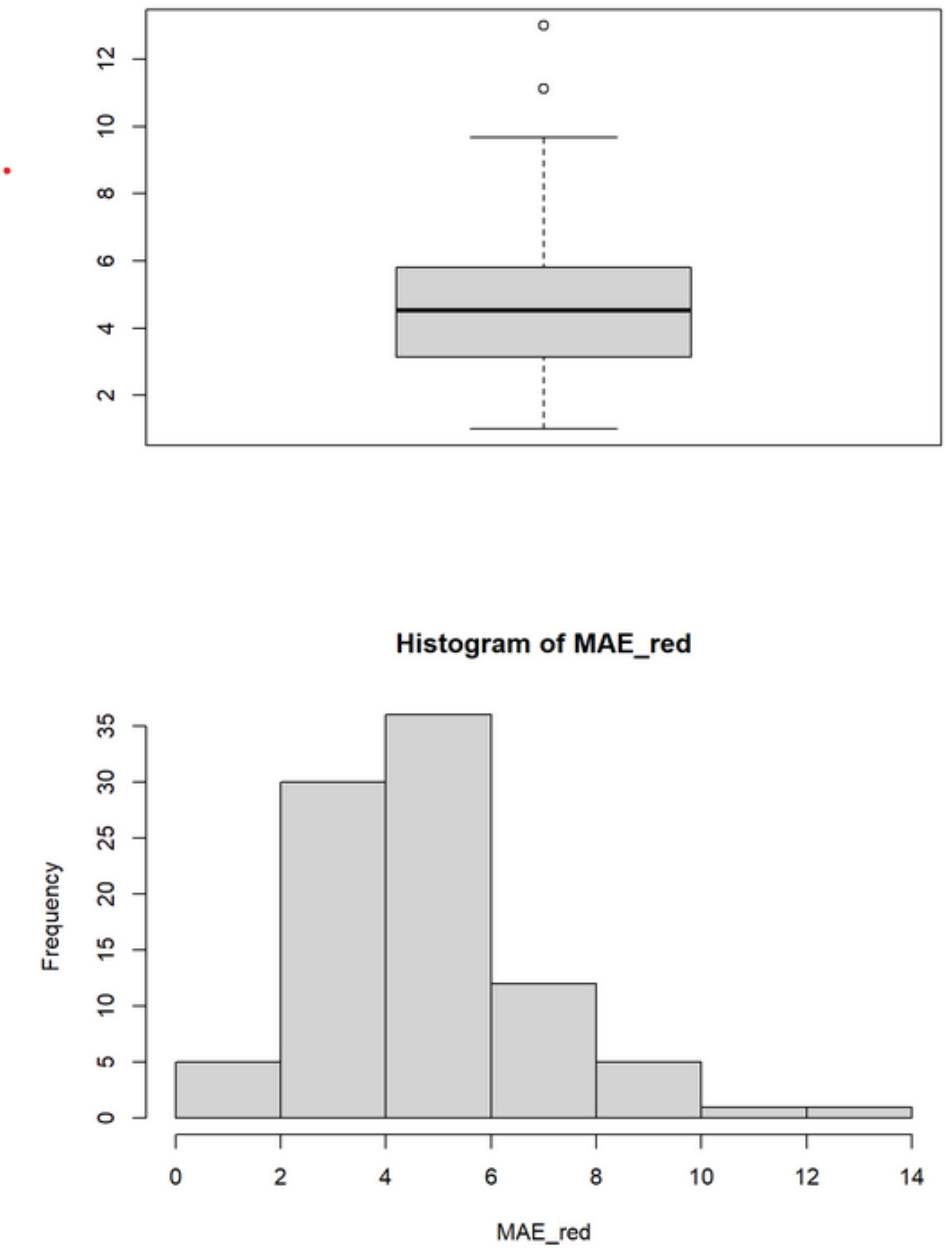


Figure 5. 9: Distribution of Mean Absolute Error (MAE_red) for Red Fruit Colonisation. *Top: Boxplot showing central tendency and outliers in MAE values. Bottom: Histogram of MAE_red across all simulated trees, reflecting overall prediction accuracy.*

The MAE results (MAE_red) further support the model's utility in practical terms: the average error across trees was 4.8 fruits, with most values ranging between 3 and 6 fruits. This relatively low error reinforces that, despite some noise in variance-based metrics like R^2, the model produced accurate point estimates of colonised fruit counts.

Total-Attacked Fruits

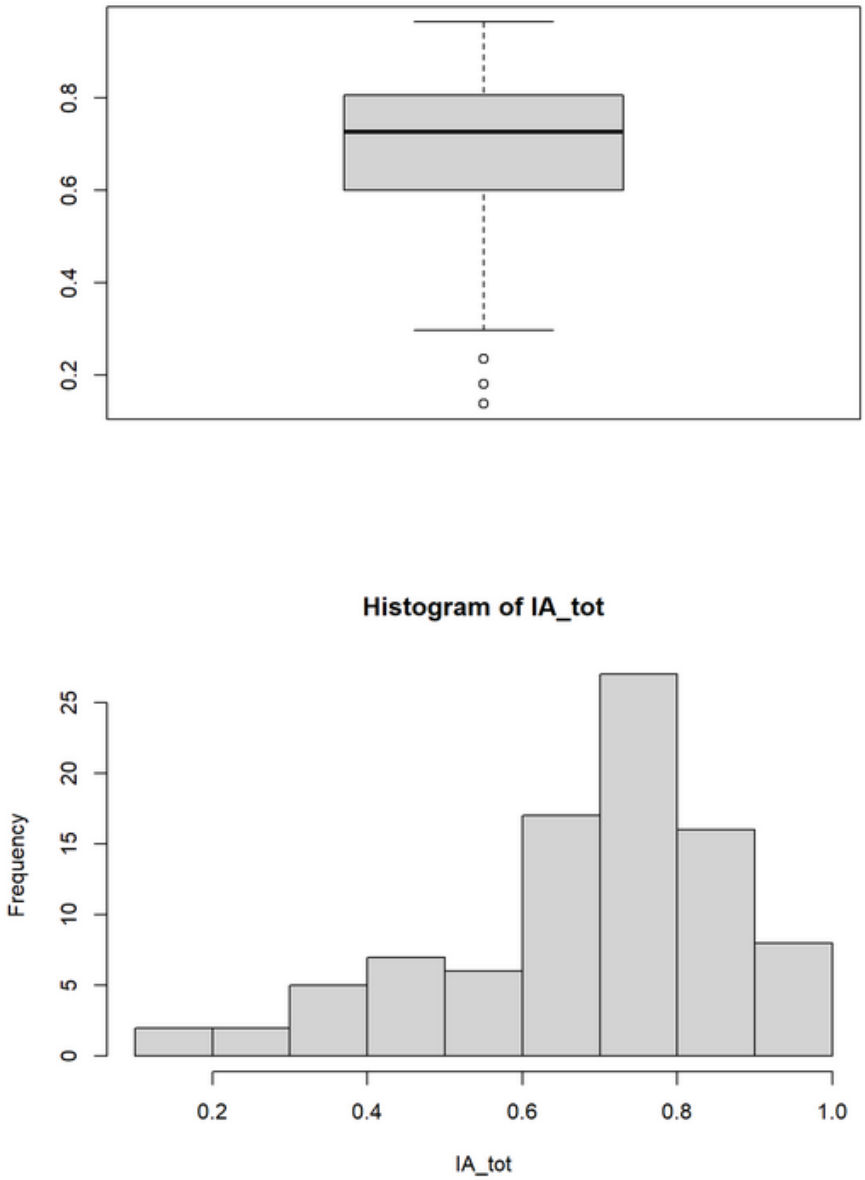


Figure 5. 10: Distribution of Index of Agreement (IA_tot) for Total Fruit Colonisation Predictions. *Top: Boxplot illustrating the range, median, and outliers of IA_tot across all trees. Bottom: Histogram showing the frequency distribution of IA_tot values, with most simulations achieving moderate to high agreement between predicted and observed total attacks.*

In contrast, the model's performance in predicting total attacked fruits (IA_tot, R2_tot, MAE_tot) showed more inconsistencies. While IA values remained reasonably high (median = 0.73, mean = 0.68), suggesting that the general shape and timing of total attacks were captured, the R^2 distribution revealed substantial issues.

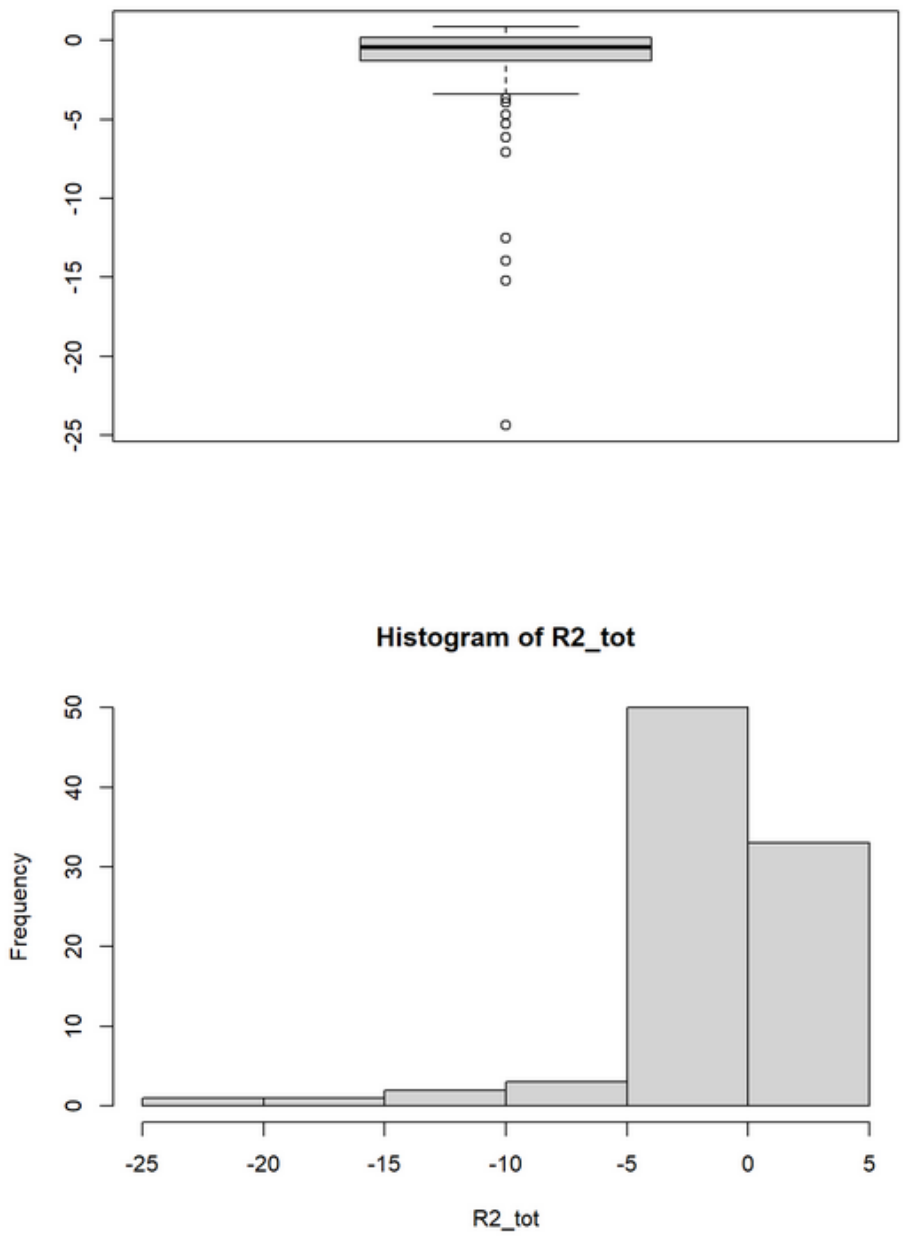


Figure 5. 11: Distribution of R^2 Values (R2_tot) for Total Fruit Colonisation Predictions. *Top: Boxplot revealing wide variance and negative outliers in R^2 values. Bottom: Histogram showing a skewed distribution of R2_tot, highlighting limitations in explaining total infestation variance.*

Specifically, R2_tot values were predominantly negative, with a mean of -1.48, a median of -0.42, and a minimum reaching -24.39. This suggests that the model frequently failed to explain the observed variance in total attacks, likely due to high noise in total fruit measurements, differences in attack dynamics not captured by the model, or inter-tree variability in unmeasured factors (e.g., microclimate, pruning, or nearby infestation sources).

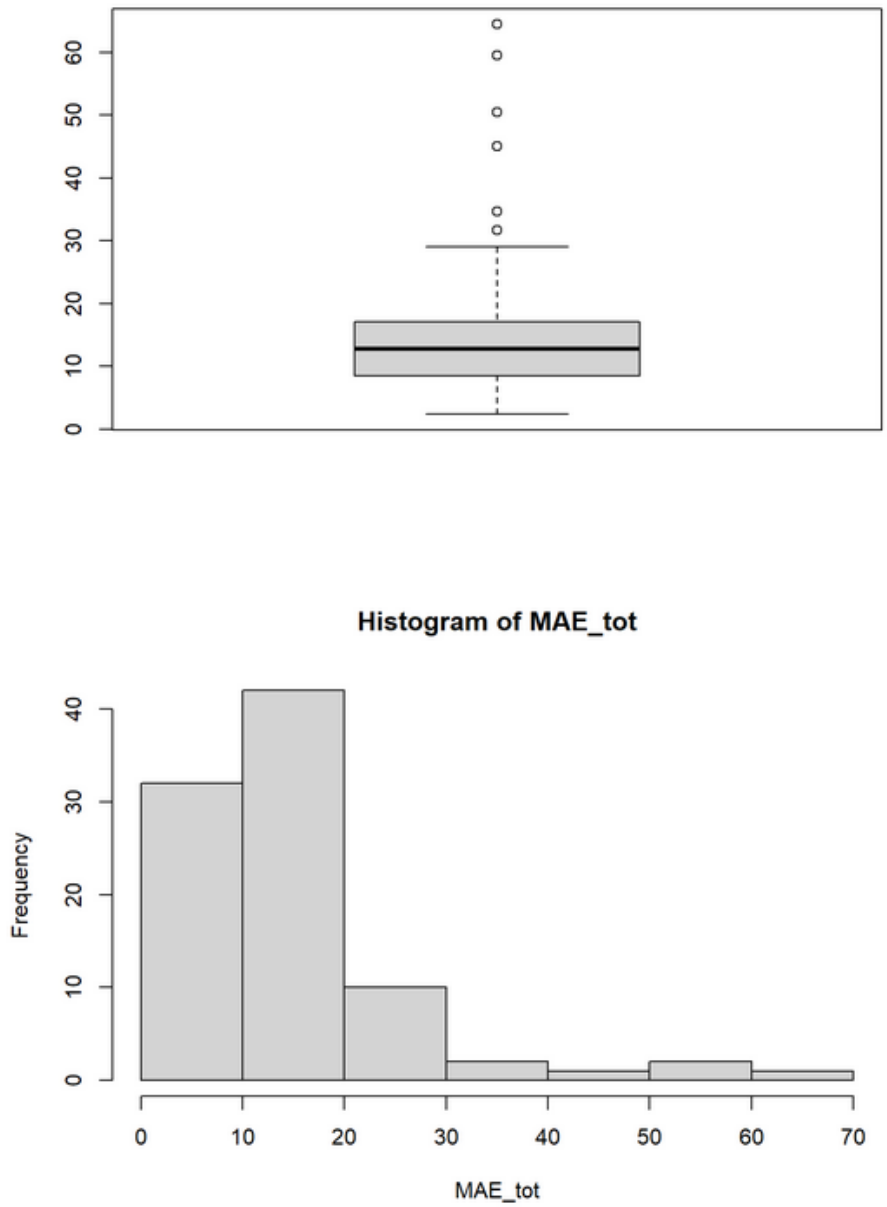


Figure 5. 12: Distribution of Mean Absolute Error (MAE_tot) for total Fruit Colonisation. *Top: Boxplot illustrating the range, median, and outliers of* MAE_tot *across all trees. Bottom: Histogram showing the frequency distribution of* MAE_tot *values, with most simulations achieving moderate to high agreement between predicted and observed total attacks.*

Figure 5.8: Distribution of R^2 Values (R2_tot) for Total Fruit Colonisation Predictions.

The MAE for total attacks (MAE_tot) also reflected this: while the majority of trees showed errors between 8 and 17 fruits, some outliers exceeded 60 fruits, indicating severe mismatches in a few trees. Nevertheless, the median MAE of 12.8 fruits and IQR between 8.6 and 17.1 show that for many trees, the model still achieved reasonable prediction accuracy.

Overall, these validation results indicate that the CBB model performs robustly when predicting red fruit colonisation, with high agreement and low average errors across a diverse range of tree dynamics. The model was able to generalise well to new, unseen trees, even when faced with varying fruiting intensities and temporal patterns, supporting its use in simulating pest pressure under heterogeneous field conditions. The prediction of total attacks, while capturing broad patterns, remains more variable and sensitive to individual tree dynamics. Nonetheless, these results confirm that the model offers a solid foundation for simulating CBB colonisation across heterogeneous coffee plots under varying fruiting conditions.

Discussion

Framing the Problem: Towards Integrated Plant–Pest Modeling

In agroecological systems, the relationship between crop development and pest or disease pressure is not merely sequential but deeply intertwined. Pest infestations affect plant physiology, which in turn alters pest habitat availability, colonisation success, and population dynamics. Despite this interdependence, plant and pest models are still often developed in isolation, lacking the capacity to communicate dynamically or simulate reciprocal feedbacks. This PhD addresses this modeling gap by proposing and implementing an integrated framework that couples detailed plant growth with flexible pest and disease (P&D) models, grounded in field data and calibrated through empirical interaction dynamics.

The thesis is built on the foundational recognition that modeling such systems requires both theoretical and practical adaptability. Models must be biologically realistic, computationally efficient, and flexible enough to respond to diverse and changing field conditions. To this end, this work introduced a cohort-based coupling approach, implemented through the MIMIC platform, and validated it through the simulation of coffee–CBB (Coffee Berry Borer) interactions across multiple seasons and growing systems.

A Cohort-Based Framework for Coupled Models (Chapter One)

The first chapter laid the formal and computational groundwork for this thesis by introducing a generalisable methodology for coupling models of plant growth and pest dynamics. The core innovation is using cohorts as the unit of interaction, enabling models with inherently different time steps, spatial assumptions, or biological granularity to interface cleanly. Unlike embedded systems that require direct modification of model internals, the MIMIC framework uses a lightweight parser and external interaction rules (UIM and ISS components) to handle feedbacks and variable exchanges dynamically.

This structure offers several advantages. Cohorts' abstract complexity by grouping organs or pest individuals by shared attributes (e.g., age, developmental stage), enabling scalable simulations without sacrificing biological fidelity. In plants, cohorts can be extracted from organogenesis or architectural data; in pest models, cohorts correspond to developmental stages or oviposition events. This consistency supports synchronous feedback, thereby making the system highly modular and robust to models' evolution over time, as well as to the injection of changes across multiple models.

Furthermore, MIMIC's ability to support cohort-based models and its implementation with the high-performance Julia language (Morales, A. et al. 2025) make it both powerful and accessible, since Julia's syntax is close to R, Python and MATLAB. This architecture allows researchers to construct and simulate coupled systems without writing monolithic code or facing exponential increases in interaction complexity. In short, the first chapter establishes a structural logic and computational feasibility proposal of integrated plant–pest simulation.

A Modular Pest and Disease Model for General Application (Chapter Two)

In the second chapter, we developed a generic and modular P&D model, designed to represent a broad range of pest dynamics while remaining tuneable to specific cases. The model separates maturation processes (e.g., development, mortality) from interaction processes (e.g., host selection, colonisation), a design both biologically sound and practically useful. Each module, covering processes like reproduction, dispersal, or survival, can be activated or suppressed depending on data availability, making the model suitable for both data-rich and data-poor systems.

The Coffee Berry Borer (CBB) served as the primary case study. Here, key assumptions, such as fruit attractiveness determined by thermal age, categorisation into “attractive” and “very attractive,” and cohort-based pest emergence, were implemented and tested. These abstractions allowed the model to simulate realistic colonisation waves while retaining a level of generality suitable for other pests. Mortality was modelled in distinct phases (pre- and post-emergence), and environmental conditions (temperature, humidity, rainfall) were used as drivers for pest development and host availability.

A key strength of the model is its integration of empirical relationships with modular flexibility. When data were available, the model produced tightly calibrated simulations; when data were limited, expert-derived rules and default parameters still enabled biologically meaningful results. This modularity is critical in agricultural research, where consistent data across spatial and temporal scales is rarely available.

The future integration of this pest model into MIMIC further enabled real-time coupling with plant models, simulating dynamic, reciprocal feedbacks. For instance, infestation could reduce fruit biomass or alter plant development, while changing fruit phenology would, in turn, affect pest behaviour, moving the model beyond simple overlays of plant and pest outputs.

Modeling Plant Growth and Interaction Sensitivity (Chapter Three)

The third chapter focused on the plant system, proposing a mechanistic model of coffee tree architecture and physiology based on the GreenLab formalism. A key contribution here was the recognition and modeling of two levels of interaction.

System-wide interactions, comparable to those used in crop modeling, capture the plant’s global response to environmental factors such as climate, resource availability, and systemic stress. In the model, these interactions are formalised at the level of the global production equation at cycle n, Q(n), which governs biomass production and partitioning during each growth cycle. This abstraction provides a macroscopic view of plant function, yield potential, vegetative growth, and overall resource allocation, without delving into organ-level detail. As such, regulation on Q(n) serves as the structural backbone of the model, enabling efficient simulation of the plant’s developmental trajectory and performance across seasons and environmental conditions. This approach functions as a simplified analogue to the regulatory

logic proposed in the work of Letort (Letort. V. et al. 2020), where internal trophic balance (production on plant demand Q/D) plays a similar role in modulating development. Although it does not capture fine-scale physiological processes, this level is essential for representing broad dynamics and supporting scalable applications.

Organ-level interactions captured fine-scale responses, such as how leaf damage reduces photosynthetic area. These interactions allowed local stressors (e.g., pest feeding) to ripple through the system, affecting overall development and fruiting potential.

By tracking structural history and regulating feedbacks through organ-level rules, the model was able to simulate how damage or resource limitation at one point in time influences future growth through the accumulated biomass and the plant demand.



Figure D. 1: Dieback (dark parts) caused by a black twig borer colony inside it. Presence of a hole (entrance of the colony) at the right part of the branch.

The introduction of the *Cophysiological age* component in the definition of organ cohorts enhances the structural realism of the model, particularly in how it captures damage propagation. This addition enables the simulation of dieback phenomena (Fig.D.1) induced by stress or pest and disease (P&D) attacks, such as those caused by BTB and RBD in our study. Structurally, this enriched cohort definition aligns closely with the “signal propagation” logic found in context-sensitive L-systems for plant development (Prusinkiewicz & Lindenmayer, 1990), allowing the model to dynamically reconstruct architecture over time. Moreover, it enables the integration of stress-related structural changes, in line with approaches like growth grammars that incorporate local variables and sensitivity to environmental conditions, leading also to functional aspects (Kurth & Sloboda, 1997).

Field Experimentation and Real-World Complexity (Chapter Four)

We then addressed the design and application of a field protocol to collect high-resolution data on coffee growth and pest pressure at the CAFNET trial site in Uganda. Initially based on standard experimental logic (treatment/control, shaded/unshaded), the protocol required substantial adaptation to field realities, including:

- Co-infestation by multiple pests (CBB, RBD, BTB, CLR)
- Heterogeneous shading conditions
- Ongoing farmer activity (pruning, harvesting)

Rather than undermining the research, these conditions enhanced its ecological relevance. The inability to isolate perfect controls reflected the complexity of real farms and emphasised the need for models that can simulate systems under flux.

Key biological insights emerged: pest vertical stratification, clone-specific responses, co-occurrence and facilitation (e.g., RBD enhances susceptibility to fruit attacks by CBB), and phenology-driven infestation waves. Yield data revealed variability in production between coffee trees, with some cases exhibiting high levels of pest attacks yet maintaining relatively high yields. This suggests differences in resilience among clones and across environmental conditions, which could be further explored through simulations.

The integration of external Arabica data from Sumatra was pivotal. It facilitates parameterisation, particularly for fruit attractiveness and pest saturation effects, thanks to continuous fruiting that prevents population fluctuations linked to host absence. We validated its applicability in an equatorial system with continuous fruiting. The estimated parameters should be robust and serve as a good starting point for other systems, although the model allows users to refine them. This parameterisation aims to support broader application of the pest model beyond the original trial context in other equatorial systems and tropical regions, including the more seasonal Robusta system in Uganda.

Simulation Results and Model Evaluation (Chapter Five)

The fifth chapter presented the implementation and evaluation of both the plant and pest simulation frameworks. The aim was to show how the plant model responds to a simulated attack on leaves. And for the CBB-oriented generalised pest model to predict infestation dynamics.

Plant-Level Dynamics: Healthy Versus Stressed Simulations

The plant model was used to simulate physiological responses under both healthy and pest-affected scenarios, offering insight into how localised perturbations cascade into systemic functional changes. The healthy simulation, based on clone L3, demonstrated a stable developmental trajectory: regular biomass allocation, stable photosynthetic demand, and

consistent leaf area expansion. The system was able to reach quasi-steady state. Hence, enabling the comparison between the outputs of this simulation and the “non-healthy” case.

The results of the “non-healthy” simulation revealed the consequences of a simulated attack on growth dynamics, both at the moment of the disturbance and in the subsequent developmental cycles. Plant demand patterns fluctuated more sharply, biomass allocation and leaf blade area increment showed temporary reductions, and key cumulative indicators, such as total blade surface and net biomass accumulation, exhibited distinct inflexion points. Crucially, the model also captured the plant’s compensatory behaviour in later cycles, as newly emerged leaves contributed to restoring lost function. This highlights the system's resilience and plasticity in its ability to re-establish a steady state. The immediate effects of the attack can be analysed by observing the shifts in dynamics during the attack period, while the longer-term impact on plant growth can be quantified as the difference between the steady states of the healthy and non-healthy simulations.

These simulations illustrate the model’s ability to account for both the direct effects of localised damage and the subsequent structural adjustments in plant development. The results suggest that even relatively small perturbations can lead to measurable deviations in growth trajectories.

To complement functional indicators, a cohort-level architectural visualisation was produced, showing the spatial manifestation of simulated damage. The affected leaf cohorts (L2) were visibly reduced in blade size, while the fruit cohorts (L10), unaffected in the scenario, maintained normal structure and distribution. This visualisation demonstrated the model’s capacity to spatially localise stress, preserving the integrity of unaffected structures and offering a clearer interpretation of how pest damage physically unfolds in plant form. This type of representation bridges the gap between data-driven metrics and biological intuition, enhancing the interpretability of model outputs for agronomists and field practitioners alike.

Evaluation of Pest Model Predictions

The CBB model was then evaluated across seven fruiting dynamic classes, derived from a clustering analysis of 90 trees. These classes represented a spectrum of temporal fruiting profiles and were used to test the model's robustness under varied phenological conditions. When simulating red fruit colonisation, a direct and observable indicator of pest presence, which can be relevant for the producer, the model performed strongly. Overall trend capture was reliable in most cases, both at the class level and globally, as reflected by the Index of Agreement (IA), even though the details of the variations were not always well captured, as indicated by the highly variable R^2

Predicting total fruit attacks (including both red and green fruits) proved more challenging. IA and MAE scores were more variable, and R^2 values were often negative, reflecting the increased noise inherent in real-world fruiting and pest data. Contributing factors include unobserved early-stage infestations, variable pruning practices, local microclimatic conditions, and clustering effects in fruit distribution. Another important factor was the

initialisation of fruit number and age in the fruit model, which was based on biased observations and subject to potential counting errors. This limitation could be addressed in future versions of the model by integrating the plant growth model with MIMIC to provide a more realistic and consistent fruiting pattern. Nonetheless, the model successfully reproduced major infestation peaks and captured the saturation effect associated with fruit abundance, providing a solid functional approximation even in the presence of ecological complexity.

These results highlight both the potential and limitations of the pest models. While perfect accuracy is difficult under field conditions, the model's ability to generalise well across structural profiles (the order of the modules) and predict biologically plausible dynamics makes it a valuable tool for pest forecasting and simulation-based intervention design.

Limitations

While this thesis presents a new proposal in integrated modeling of plant–pest interactions, several limitations must be acknowledged. These span across model structure, data availability, implementation choices, and real-world complexity.

A necessary trade-off in any modeling effort lies between biological realism and operational simplicity. Both the plant and pest models developed in this work rely on structural simplifications, cohort aggregation, parameter homogeneity, and stage-based development rules, which, while biologically grounded, abstract away certain micro-level dynamics. For instance, spatial heterogeneity within trees (e.g., leaf orientation, microclimatic gradients) and among trees (e.g., edge effects, wind exposure) is not explicitly modelled. Similarly, CBB behaviour is described probabilistically without capturing all behavioural nuances (e.g., selective oviposition, pest development stages).

Moreover, certain ecological interactions, such as predators or the role of microbial antagonists, are outside the scope of the current framework. These may play non-negligible roles in real-world dynamics and merit future inclusion as additional modules.

A major limitation of this work lies in the partial validation of the modeling framework. While individual components, the plant growth model and the pest dynamics model, were calibrated and showed behaviourally plausible outputs, neither underwent full formal validation in isolation, nor was their coupled interaction exhaustively tested. As a result, while the simulations are informative and biologically consistent, their predictive reliability in broader contexts remains to be rigorously assessed.

Model calibration depended largely on field data collected under real agroecological conditions. These datasets, while rich, were affected by several constraints typical of field research. Environmental variability, logistical challenges, and incomplete observations limited the precision of parameter estimation. In particular, estimating CBB infestation on green fruits or tracking internal colonisation stages.

Moreover, the dynamic nature of field conditions introduced additional noise. Irregular pruning, harvesting by technicians, and human interventions such as the removal of diseased branches introduced uncontrolled variables into the system. These actions, while reflective of

real-world farming practices, complicated the process of simulation validation and made it difficult.

Together, these limitations underscore the need for future work to focus on targeted experimental designs, improved pest monitoring (e.g., non-destructive tracking, controlled environment), and formal validation protocols for each model and their interactions. Only then can the model's full potential as a decision-support tool be confidently realised.

Despite careful parameterisation, the models contain uncertainties in key variables, such as fruit attractiveness coefficients, developmental thresholds, or environmental mortality modifiers. These uncertainties can propagate and lead to divergence in long-term simulations. Moreover, a more formal quantification of uncertainty propagation (e.g., through Monte Carlo methods or Bayesian frameworks) could strengthen confidence in model robustness, especially under extrapolation.

While the MIMIC framework enabled efficient coupling without direct code entanglement, it currently assumes synchronous time progression and simplified feedback formats. As such, the framework may not yet fully support high-resolution temporal dynamics (e.g., hourly weather data or fast pest emergence) or asynchronous behaviours (e.g., lagged physiological responses). In future applications, this could limit precision in systems with rapid or highly reactive processes.

Additionally, while the use of Julia allows fast computation, certain aspects, such as visualisation routines or external interface development, remain less developed than in larger ecosystems like R or Python, potentially limiting user accessibility for non-programmers.

References:

Kurth, W., Sloboda, B., 1997. Growth grammars simulating trees – an extension of L-systems incorporating local variables and sensitivity. Silva Fenn. 31. https://doi.org/10.14214/sf.a8527

Prusinkiewicz, P., Lindenmayer, A., 1990. Graphical modeling using L-systems, in: Prusinkiewicz, P., Lindenmayer, A. (Eds.), The Algorithmic Beauty of Plants. Springer, New York, NY, pp. 1–50. https://doi.org/10.1007/978-1-4613-8476-2_1

Letort, V., Sabatier, S., Okoma, M.P., Jaeger, M., de Reffye, P., 2020. Internal trophic pressure, a regulator of plant development? Insights from a stochastic functional–structural plant growth model applied to Coffea trees. Annals of Botany 126, 687–699. https://doi.org/10.1093/aob/mcaa023

Morales, A., Kottelenberg, D.B., Ernst, A., Vezy, R., Evers, J.B., 2025. The Virtual Plant Laboratory: a modern plant modeling framework in Julia. in silico Plants diaf005. https://doi.org/10.1093/insilicoplants/diaf005

Conclusion

This thesis presented a comprehensive approach to model the dynamic interactions between coffee plant development and pest infestation, with a focus on the Coffee Berry Borer (CBB). Recognising that plant and pest dynamics are deeply interdependent yet often modelled in isolation, this work introduced a novel, cohort-based framework for coupling mechanistic plant growth and pest population models in a modular and biologically interpretable way.

The modeling framework developed in this thesis, called MIMIC, enables real-time, in-memory interaction between independently constructed models. It provides a flexible and lightweight alternative to tightly integrated or hard-coded systems. MIMIC allows for the arrangement of multiple models while facilitating the integration of explicit interaction hypotheses between them. This architecture ensures consistency across simulations without requiring the models to be merged into a single monolithic system. Moreover, the models can share common inputs, such as environmental data in our case, while maintaining their structural independence.

The plant model, developed using the GreenLab formalism, includes several improvements aimed at integrating the effects of stress at multiple levels. One key enhancement is the introduction of an interaction coefficient within the plant's functioning equation, allowing the model to account for external biotic stressors. Additionally, the updated definition of organ cohorts enables recursive structural calculations and the simulation of damage propagation to neighbouring organs. These modifications facilitate coupling with pest and disease models that exert spatially distributed effects on the plant architecture.

The generic modular pest model was designed with scalability, adaptability, and empirical calibration in mind. Its structure allows the life cycle to be customised to match the biology of a specific pest, while observational data can be incorporated to simulate its population dynamics. Using the coffee/CBB system as a case study, the model provides a robust basis for simulating the dynamics of both the Coffee Berry Borer (CBB) and the Black Twig Borer (BTB).

Fieldwork conducted at the CAFNET trial site in Uganda provided rich biological data that captured real-world complexity, including multiple pests, heterogeneous environmental conditions, and active human management. These data informed the parameterisation and testing of both presented models.

Simulation results demonstrated the ability of the coupled system to accurately reproduce red fruit colonisation patterns, simulate plant physiological responses under stress, and reflect compensatory growth mechanisms following pest-induced organ loss.

The integration of external data from Arabica coffee in Sumatra further validated the generality of the approach and enabled the estimation of key model parameters under continuous fruiting conditions, extending the relevance of the model across agroecological zones. Simulation tests illustrate that even localised disruptions in plant structure, such as minor leaf damage, can have systemic impacts, reinforcing the value of organ-level modeling in capturing emergent crop responses. The architectural visualisations developed alongside

the simulations added a critical interpretive layer, helping to bridge simulated outputs with real-world plant behaviour.

While limitations remain in data resolution, ecological scope, and modeling assumptions, the work lays a strong foundation for future research and practical applications. The models and methods developed here are designed for integration into decision-support tools, exploration of climate-resilient management strategies, and the study of multi-pest or plant–pathogen interactions.

Ultimately, this thesis contributes both a coupling framework and a generic point of view that together highlight the potential benefits of integrating plant development and pest dynamics in a unified system. While further refinement, validation, and expansion are needed, especially for broader applications or policy integration, the work tends to make a step toward more responsive and ecologically informed tools for understanding plant–pest interactions. By emphasising modularity, empirical grounding, and structural coherence, it opens pathways for future research that can better reflect the complexity of agroecosystems and support more adaptive approaches to crop and pest management.

Figures Table

Figure 1: Interactions between P&D dynamics and coffee phenology. . _____ 2
Figure 2: A typical process-based model application. _____ 4
Figure 3: Roux architectural model representation _____ 5

Figure 2. 1: Pests and disease damage in coffee trees (C. canephora) _____ 38
Figure 2. 2: Life cycles of the CBB/BTB (Bottom), and RBD (top) _____ 44
Figure 2. 3: Structure of the Cercospora pathogen model. _____ 47
Figure 2. 4: Architecture of the generalised pest model, inspired by bark beetles' life cycle conceptualisation _ 49
Figure 2. 5: CBB model modules, distributed between two main blocks. _____ 51

Figure 3. 1The leafy axis (Drawing D. Barthelemy, Cirad) (Barthélémy and Caraglio, 2007)_____ 74
Figure 3. 2:The latest list of architectural models (Hallé, 2017). _____ 76
Figure 3. 3:Representation of a structural simulation of a rhythmic plant of chronological age 3. _____ 78
Figure 3. 4: A set of macro states standing for Figure 3.3 _____ 79
Figure 3. 5: The proposed frame structure of the plant model. _____ 85
Figure 3. 6: Representation of the structure of the plant presented in the application after 4 growth cycles___ 88
Figure 3. 7: Ramification mapping of the plant's $\varphi 1$ _____ 92
Figure 3. 8: Ramification mapping of the plant. Full representation (upper), simplified representation (below) 93
Figure 3. 9: Representation of the structure of the plant presented in the application after 4 growth cycles___ 94
Figure 3. 10: Plant's structure representation with stochastic parameters after 4 growth cycles. _____ 96
Figure 3. 11: Hierarchy of modules that define the plant model. _____ 104
Figure 3. 12: 2D plant representation of stem growth, using Ugandan Robust coffee tree development_____ 108

Figure 4. 1: Presence and absence of pests and diseases on the observed trees in their different ranks_____ 122
Figure 4. 2: RBD and CBB presence observations on trees' different ranks (L2 and L3) _____ 124
Figure 4. 3: CBB attack dynamics on both Coffee tree clones _____ 126
Figure 4. 4: Dynamics of Black Twig Borer (BTB) Infestation in Coffee Tree . _____ 127
Figure 4. 5: Weight of Ripe Fruit Produced by Clone L2 (in grams) _____ 129
Figure 4. 6: Weight of Ripe Fruit Produced by Clone L3 (in grams) _____ 129
Figure 4. 7: Relationship Between Non-Red Fruit Proportion and Attack Probability (Year 1). _____ 132
Figure 4. 8: Relationship Between Proportion of Red Fruits in a Cluster and Attack Probability (Year 1) _____ 133
Figure 4. 9: Influence of Tree-Level Fruit Load on CBB Attack Probability (Year 1). _____ 134

Figure 5. 1: Simulated dynamics of Growth, Demand, and Biomass Allocation in clone L3 arabica Coffee tree 141
Figure 5. 2: Structural representation of the simulated L3 coffee tree physiological age 2 in a stable growth_ 142
Figure 5. 3: Simulated dynamics of Growth, Demand, and Biomass Allocation in clone L3 Coffee tree. _____ 145
Figure 5. 4: Structural representation of the simulated L3 coffee tree physiological._____ 147
Figure 5. 5: Standardised distribution of attacks on red by class of standardised number of attacked fruits. _ 148
Figure 5. 6: Simulation results compared to observed data for six representative trees._____ 150
Figure 5. 7: Distribution of the Index of Agreement (IA_red) for Red Fruit Colonisation Predictions. . _____ 152
Figure 5. 8: Distribution of R^2 Values (R2_red) for Red Fruit Colonisation Predictions. _____ 153
Figure 5. 9: Distribution of Mean Absolute Error (MAE_red) for Red Fruit Colonisation. _____ 154
Figure 5. 10: Distribution of Index of Agreement (IA_tot) for Total Fruit Colonisation Predictions._____ 155
Figure 5. 11: Distribution of R^2 Values (R2_tot) for Total Fruit Colonisation Predictions._____ 156
Figure 5. 12: Distribution of Mean Absolute Error (MAE_tot) for total Fruit Colonisation. _____ 157

Figure D. 1: Dieback (dark parts) caused by a black twig borer colony inside it. branch._____ 162